



TRANSMITTAL LETTER

TO:

DATE: February 12, 1996

Our Ref. No.: 953-2908

Dan Ramey
BHP-Copper
Resource Development Technology Group
7400 North Oracle Rd., Suite 162
Tucson, AZ 85704

SENT VIA: Hand Delivered

QUANTITY	ITEM	DESCRIPTION
2	Copies	Analytical Interpretation of Hydraulic Tests at the Florence Mine Site

Per Amado Guzman

Analytical Interpretation of
Hydraulic Tests at the Florence Mine Site
for
Magma Copper Company
Florence In Situ Leaching Project

Prepared for:

Magma Copper Company
Resource and Development Group
7400 N. Oracle Road, Suite 162
Tucson, Arizona 85704

Prepared by:

Golder Associates Inc.
4700 N. Oracle Road, Suite 210
Tucson, Arizona 85704

Distribution:

2 Copies - Dan Ramey, Magma Copper Company
2 Copies - Golder Associates

February 1996

DRAFT

TABLE OF CONTENTS

1.0	INTRODUCTION	1
1.1	Background	2
2.0	INTERPRETATION METHODS	4
2.1	Analysis of Drawdown Period	5
2.2	Analysis of Shut-in (Recovery) Period	6
3.0	TEST INTERPRETATION RESULTS	10
	Aquifer Test in M1-GL	13
	Aquifer Test in M2-GU	14
	Aquifer Test in M3-GL	14
	Aquifer Test in M4-O	15
	Aquifer Tests in M10-GU and M11-GL	17
	Aquifer Test in M12-O	17
	Aquifer Test in M14-GL	18
	Aquifer Test in M15-GU	19
	Aquifer Test in M18-GU	19
	Aquifer Test in P5-O	20
	Aquifer Test in PW1-1	21
	Aquifer Test in PW2-1	22
	Aquifer Test in PW2-2	23
	Aquifer Test in PW3-1	24
	Aquifer Test in PW4-1 (Test 1)	24
	Aquifer Test in PW4-1 (Test 2)	25

Aquifer Test in PW7-1	25
Aquifer Test in P8.1-O	26
Aquifer Test in P8-GU	27
Aquifer Test in P12-O	28
Aquifer Test in P13.1-O	30
Aquifer Test on P15-O	30
Aquifer Test on P19.1-O	32
Aquifer Test on P28-GL	33
Aquifer Test on P28.1-O (Test #1)	35
Aquifer Test on P28.1-O (Test #2)	36
Aquifer Test on P39-O	39
Aquifer Test on P49-O	40
Regional Aquifer Test WW-3	41
 4.0 DISCUSSION	 46
 5.0 RECOMMENDATIONS	 50

LIST OF TABLES AND FIGURES

FIGURES and TABLES

Figure 1	Test Locations
Table 1	Summary of Available Hydraulic Test Data
Table 2	Hydraulic Conductivity and Storage Estimates
Table 3	Summary of Aquifer Test Coordinates and Screen Intervals
Table 4	Summary of Aquifer Parameters Derived from the Regional Aquifer Test.

Appendix A, Semi-Log Aquifer Test Plots, FlowDim™ Analysis Summaries, and FlowDim™ or Aqtesolv™ Log-Log Plots of Well Response Data and Modeled Response

Figure 1A	M1-GL	Semi-Log Aquifer Test Plot
B	M1-GL	Aqtesolv™ Analysis Log-Log Plot
C	M1-GL (3D)	FlowDim™ Analysis Summary
D	M1-GL (3D)	FlowDim™ Analysis Log-Log Plot
Figure 2A	M2-GU	Semi-Log Aquifer Test Plot
Figure 3A	M3-GL	Semi-Log Aquifer Test Plot
B	M3-GL	Aqtesolv™ Analysis Log-Log Plot
C	M3-GL (3D)	FlowDim™ Analysis Summary
D	M3-GL(3D)	FlowDim™ Analysis Log-Log Plot
Figure 4A	M4-O	Semi-Log Aquifer Test Plot
B1,B2,B3	M4-O	Aqtesolv™ Analysis Log-Log Plot
C	M4-O (3D)	FlowDim™ Analysis Summary
D	M4-O (3D)	FlowDim™ Analysis Log-Log Plot
E	<i>M3-GL (3D)</i>	FlowDim™ Analysis Summary
F	<i>M3-GL (3D)</i>	FlowDim™ Analysis Log-Log Plot
Figure 5A	M10-GU	Semi-Log Aquifer Test Plot
Figure 6A	M11-GL	Semi-Log Aquifer Test Plot
Figure 7A	M12-O	Semi-Log Aquifer Test Plot

	B	M12-O	Aqtesolv™ Analysis Log-Log Plot
	C	M12-O	FlowDim™ Analysis Summary
	D	M12-O	FlowDim™ Analysis Log-Log Plot
Figure 8A		M14-GL	Semi-Log Aquifer Test Plot
	B	M14-GL (3D)	FlowDim™ Analysis Summary
	C	M14-GL (3D)	FlowDim™ Analysis Log-Log Plot
Figure 9A		M15-GU	Semi-Log Aquifer Test Plot
	B	M15-GU	Aqtesolv™ Analysis Log-Log Plot
	C	M15-GU	FlowDim™ Analysis Summary
	D	M15-GU	FlowDim™ Analysis Log-Log Plot
Figure 10A		M18-GU	Semi-Log Aquifer Test Plot
	B	M18-GU	Aqtesolv™ Analysis Log-Log Plot
	C	M18-GU	FlowDim™ Analysis Summary
	D	M18-GU	FlowDim™ Analysis Log-Log Plot
Figure 11A		P5-O	Semi-Log Aquifer Test Plot
	B	P5-O	FlowDim™ Analysis Summary
	C	P5-O	FlowDim™ Analysis Log-Log Plot
	D	O5.2-O	FlowDim™ Analysis Summary
	E	O5.2-O	FlowDim™ Analysis Log-Log Plot
Figure 12A		PW1-1	Semi-Log Aquifer Test Plot
	B	PW1-1	Aqtesolv™ Analysis Log-Log Plot
	C	PW1-1	Aqtesolv™ Analysis Log-Log Plot
	D	OB1-1	Aqtesolv™ Analysis Log-Log Plot
	E	523MCC	Aqtesolv™ Analysis Log-Log Plot
	F	PW1-1 (3D)	FlowDim™ Analysis Summary
	G	PW1-1 (3D)	FlowDim™ Analysis Log-Log Plot
	H	OB1-1 (3D)	FlowDim™ Analysis Summary
	I	OB1-1 (3D)	FlowDim™ Analysis Log-Log Plot
	J	523MCC (3D)	FlowDim™ Analysis Summary
	K	523MCC (3D)	FlowDim™ Analysis Log-Log Plot
Figure 13A		PW2-1	Semi-Log Aquifer Test Plot
	B	PW2-1	Aqtesolv™ Analysis Log-Log Plot
	C	OB2-1	Aqtesolv™ Analysis Log-Log Plot
Figure 14A		PW2-2	Semi-Log Aquifer Test Plot

	B	PW2-2	Aqtesolv™ Analysis Log-Log Plot
	C	OB2-2	Aqtesolv™ Analysis Log-Log Plot
Figure 15A	PW3-1		Semi-Log Aquifer Test Plot
	B	PW3-1	Aqtesolv™ Analysis Log-Log Plot
	C	OB3-1	Aqtesolv™ Analysis Log-Log Plot
Figure 16A	PW4-1 (Test 1)		Semi-Log Aquifer Test Plot
	B	PW4-1 (Test 1)	Aqtesolv™ Analysis Log-Log Plot
	C	PW4-1 (Test 1) (3D)	FlowDim™ Analysis Summary
	D	PW4-1 (Test 1) (3D)	FlowDim™ Analysis Log-Log Plot
Figure 17A	PW4-1 (Test 2)		Semi-Log Aquifer Test Plot
Figure 18A	PW7-1		Semi-Log Aquifer Test Plot
	B	PW7-1	FlowDim™ Analysis Summary
	C	PW7-1	FlowDim™ Analysis Log-Log Plot
	D	OB7-1	FlowDim™ Analysis Summary
	E	OB7-1	FlowDim™ Analysis Log-Log Plot
Figure 19A	P8.1-O		Semi-Log Aquifer Test Plot
	B	P8.1-O (3D)	FlowDim™ Analysis Summary
	C	P8.1-O (3D)	FlowDim™ Analysis Log-Log Plot
Figure 20A	P8-GU		Semi-Log Aquifer Test Plot
	B	P8-GU	FlowDim™ Analysis Summary
	C	P8-GU	FlowDim™ Analysis Log-Log Plot
Figure 21A	P12-O		Semi-Log Aquifer Test Plot
	B	P12-O	FlowDim™ Analysis Summary
	C	P12-O	FlowDim™ Analysis Log-Log Plot
	D	O12-O	FlowDim™ Analysis Summary
	E	O12-O	FlowDim™ Analysis Log-Log Plot
Figure 22A	P13.1-O		Semi-Log Aquifer Test Plot
	B	P13.1-O (3D)	FlowDim™ Analysis Summary
	C	P13.1-O (3D)	FlowDim™ Analysis Log-Log Plot
	D	P13.2-O (3D)	FlowDim™ Analysis Summary
	E	P13.2-O (3D)	FlowDim™ Analysis Log-Log Plot
Figure 23A	P15-O		Semi-Log Aquifer Test Plot

B	P15-O	FlowDim™ Analysis Summary
C	P15-O	FlowDim™ Analysis Log-Log Plot
D	<i>O15-O (3D)</i>	FlowDim™ Analysis Summary
E	<i>O15-O (3D)</i>	FlowDim™ Analysis Log-Log Plot
Figure 24A	P19.1-O	Semi-Log Aquifer Test Plot
B	P19.1-O (3D)	FlowDim™ Analysis Summary
C	P19.1-O (3D)	FlowDim™ Analysis Log-Log Plot
D	<i>O19-O (3D)</i>	FlowDim™ Analysis Summary
E	<i>O19-O (3D)</i>	FlowDim™ Analysis Log-Log Plot
F	<i>P19.2-O (3D)</i>	FlowDim™ Analysis Summary
G	<i>P19.2-O (3D)</i>	FlowDim™ Analysis Log-Log Plot
H	<i>O19-GL (3D)</i>	FlowDim™ Analysis Summary
I	<i>O19-GL (3D)</i>	FlowDim™ Analysis Log-Log Plot
Figure 25A	P28-GL	Semi-Log Aquifer Test Plot
B	P28-GL (3D)	FlowDim™ Analysis Summary
C	P28-GL (3D)	FlowDim™ Analysis Log-Log Plot
D	<i>O28-GL (3D)</i>	FlowDim™ Analysis Summary
E	<i>O28-GL (3D)</i>	FlowDim™ Analysis Log-Log Plot
F	<i>P28.2-O (3D)</i>	FlowDim™ Analysis Summary
G	<i>P28.2-O (3D)</i>	FlowDim™ Analysis Log-Log Plot
H	<i>O28.1-O (3D)</i>	FlowDim™ Analysis Summary
I	<i>O28.1-O (3D)</i>	FlowDim™ Analysis Log-Log Plot
J	<i>O28.2-S (3D)</i>	FlowDim™ Analysis Summary
K	<i>O28.2-S (3D)</i>	FlowDim™ Analysis Log-Log Plot
Figure 26A	P28.1-O (Test 1)	Semi-Log Aquifer Test Plot
B	P28.1-O	FlowDim™ Analysis Summary
C	P28.1-O	FlowDim™ Analysis Log-Log Plot
Figure 27A	P28.1-O (Test 2)	Semi-Log Aquifer Test Plot
B	P28.1-O	FlowDim™ Analysis Summary
C	P28.1-O	FlowDim™ Analysis Log-Log Plot
D	<i>P28.2-O</i>	FlowDim™ Analysis Summary
E	<i>P28.2-O</i>	FlowDim™ Analysis Log-Log Plot
F	<i>O28.1-O (3D)</i>	FlowDim™ Analysis Summary
G	<i>O28.1-O (3D)</i>	FlowDim™ Analysis Log-Log Plot
H	<i>P28-GL (3D)</i>	FlowDim™ Analysis Summary
I	<i>P28-GL (3D)</i>	FlowDim™ Analysis Log-Log Plot

J	<i>O28-GL (3D)</i>	FlowDim™ Analysis Summary
K	<i>O28-GL (3D)</i>	FlowDim™ Analysis Log-Log Plot
Figure 28A	P28.2-O	Semi-Log Aquifer Test Plot
B	P28.2-O	FlowDim™ Analysis Summary
C	P28.2-O	FlowDim™ Analysis Log-Log Plot
D	<i>O28.1-O</i>	FlowDim™ Analysis Summary
E	<i>O28.1-O</i>	FlowDim™ Analysis Log-Log Plot
F	<i>P28-GL</i>	FlowDim™ Analysis Summary
G	<i>P28-GL</i>	FlowDim™ Analysis Log-Log Plot
H	<i>O28-GL</i>	FlowDim™ Analysis Summary
I	<i>O28-GL</i>	FlowDim™ Analysis Log-Log Plot
J	<i>O28.2-S</i>	FlowDim™ Analysis Summary
K	<i>O28.2-S</i>	FlowDim™ Analysis Log-Log Plot
Figure 29A	P39-O	Semi-Log Aquifer Test Plot
B	P39-O	FlowDim™ Analysis Summary
C	P39-O	FlowDim™ Analysis Log-Log Plot
D	<i>O39-O</i>	FlowDim™ Analysis Summary
E	<i>O39-O</i>	FlowDim™ Analysis Log-Log Plot
Figure 30A	P49-O	Semi-Log Aquifer Test Plot
B	P49-O (3D)	FlowDim™ Analysis Summary
C	P49-O (3D)	FlowDim™ Analysis Log-Log Plot
D	<i>O49-O</i>	FlowDim™ Analysis Summary
E	<i>O49-O</i>	FlowDim™ Analysis Log-Log Plot

Regional Aquifer Test

Figure 31A	WW-3 Observation Wells	Semi-Log Aquifer Test Plot, page 1
B	WW-3 Observation Wells	Semi-Log Aquifer Test Plot, page 2
C	WW-3 Observation Wells	Semi-Log Aquifer Test Plot, page 3
D	WW-3 Observation Wells	Semi-Log Aquifer Test Plot, page 4
E	<i>P28.1-O</i>	FlowDim™ Analysis Summary
F	<i>P28.1-O</i>	FlowDim™ Analysis Log-Log Plot
G	<i>P28.2-O</i>	FlowDim™ Analysis Summary
H	<i>P28.2-O</i>	FlowDim™ Analysis Log-Log Plot
I	<i>O28.1-O</i>	FlowDim™ Analysis Summary
J	<i>O28.1-O</i>	FlowDim™ Analysis Log-Log Plot
K	<i>O28-GL</i>	FlowDim™ Analysis Summary
L	<i>O28-GL</i>	FlowDim™ Analysis Log-Log Plot
M	<i>P15-O (3D)</i>	FlowDim™ Analysis Summary

Figure 31N	<i>P15-O (3D)</i>	FlowDim™ Analysis Log-Log Plot
O	<i>O15-O (3D)</i>	FlowDim™ Analysis Summary
P	<i>O15-O (3D)</i>	FlowDim™ Analysis Log-Log Plot
Q	<i>P15-GL</i>	FlowDim™ Analysis Summary
R	<i>P15-GL</i>	FlowDim™ Analysis Log-Log Plot
S	<i>O12-O (3D)</i>	FlowDim™ Analysis Summary
T	<i>O12-O (3D)</i>	FlowDim™ Analysis Log-Log Plot
U	<i>O12-GL (3D)</i>	FlowDim™ Analysis Summary
V	<i>O12-GL (3D)</i>	FlowDim™ Analysis Log-Log Plot
W	<i>O3-GL (3D)</i>	FlowDim™ Analysis Summary
X	<i>O3-GL (3D)</i>	FlowDim™ Analysis Log-Log Plot
Y	<i>M14-GL (3D)</i>	FlowDim™ Analysis Summary
Z	<i>M14-GL (3D)</i>	FlowDim™ Analysis Log-Log Plot
AA	<i>O19-O (3D)</i>	FlowDim™ Analysis Summary
BB	<i>O19-O (3D)</i>	FlowDim™ Analysis Log-Log Plot
CC	<i>O19-GL (3D)</i>	FlowDim™ Analysis Summary
DD	<i>O19-GL (3D)</i>	FlowDim™ Analysis Log-Log Plot
EE	<i>AIR SHAFT (3D)</i>	FlowDim™ Analysis Summary
FF	<i>AIR SHAFT (3D)</i>	FlowDim™ Analysis Log-Log Plot

1.0 INTRODUCTION

This report summarizes the analytical interpretation of hydraulic tests for Magma Copper Company's (Magma) in-situ mining project near Florence, Arizona. The purpose of this report is to provide estimates of hydraulic conductivity and storage, in support of Magma's site characterization. This report supersedes a previous submittal entitled "Data Report for the Initial Hydraulic Tests Interpretation" by Golder Associates (1995).

The analyses presented in this report are based on standard methods developed in the water well and oil and gas industries. These methods are applied to data collected and provided by Brown and Caldwell as part of the Aquifer Protection Permit application on behalf of Magma. A number of tests performed by Magma personnel during early 1994, as part of the prefeasibility study, are also interpreted. Interpretation of the field data is performed with FLOWDIM™ (Golder Associates, 1993) and AQTESOLV™ software (Geraghty & Miller, 1995).

This report is divided into four major sections. First, Chapter 2 provides a brief description of the analysis techniques used in this study, Golder (1995) presents a detailed account of the theoretical background of these analytical techniques. Second, a discussion of each aquifer test and its results is presented in Chapter 3. Chapter 4 presents a summary of findings, and Chapter 5 presents recommendations for future characterization studies at the Florence Site. Tables summarizing relevant test information for these analyses are provided after Chapter 5.

1.1 Background

Magma has undertaken field studies to characterize the hydrogeologic conditions near its proposed in-situ mining site in the Poston Butte porphyry copper deposit. The proposed mine site is located in the Basin and Range physiographic province of southern Arizona, in the Eloy sub-basin of the Pinal Active Management Area (AMA). The site is about one mile southwest of Poston Butte and two miles northwest of the town of Florence, Arizona, on the margins of the floodplain of the Gila river.

The rock units in the study area range in age from Precambrian to Quaternary. The floodplain alluvium is Quaternary in age and consists mainly of unconsolidated silt, sand, gravel and boulders. The Cenozoic basin fill deposits have been divided into three major units; the Upper Basin Fill Unit (UBFU), Middle Fine Grained Unit (MFGU), and Lower Basin Fill Unit (LBFU). The UBFU is composed of unconsolidated to weakly cemented, interbedded clay, silt, sand, gravel and boulders. Its thickness ranges from 200 ft to about 500 ft in the vicinity of the mine site. The MFGU is a discontinuous layer composed of silt and clay that varies in thickness from zero to about 80 ft. Weakly to moderately cemented boulders, gravel, sand, silt and clay constitute the LBFU. The thickness of this latter unit varies from less than 50 ft on the east to about 800 ft on the west of the mine site. The bedrock complex consists of quartz monzonite and granodiorite porphyry, diabase, basalt and other volcanic rocks. The bedrock is subdivided into an upper oxide zone and a lower sulfide zone depending on copper mineralization (Brown and Caldwell, 1995).

Brown and Caldwell has installed forty six (46) monitoring wells and seventeen (17) test wells around the site (Figure 1). Eight (8) wells are completed within the UBFU, seventeen (17) within the LBFU and thirty eight (38) within the bedrock complex. Magma requested that Golder Associates assist Brown and Caldwell with the design and interpretation of the hydraulic tests. Magma Copper conducted seven (7) aquifer tests as part of their prefeasibility study during early 1994. To date, Brown and Caldwell has conducted twenty six (26) aquifer tests which include

monitoring, observation and pumping wells. These tests result in forty nine (49) aquifer test locations and 121 data sets from pumping and observation wells. These locations cover a wide range of hydrogeologic conditions throughout the site.

The objective of these tests was to determine the hydraulic properties of the geologic materials in the vicinity of the Poston Butte copper deposit. Specific questions related to the flow character and potential interaction between fluids of the different geologic units were addressed in the field characterization effort. Chief among these questions were: (1) Differentiation between porous media flow and flow dominated by discrete geologic features such as faults and fractures, and (2) Determination of the degree and mode of hydraulic communication between the basin fill deposits and the oxide zone. The following sections present a brief description of the analytical models used, methods of interpretation applied, and the results of this parameter estimation study.

2.0 INTERPRETATION METHODS

Aquifer testing through wells provides a means of estimating the properties of geologic formations. In the process of a well test, a known signal (usually a change in flow rate) is applied to the formation and the resulting output signal or response is measured (usually in terms of a change in pressure). Well test interpretation is therefore an inverse problem, in that the formation parameters are inferred by comparing a simulated model response to the measured response. The formation parameters are derived by adjusting the flow model parameters to obtain a simulation response that matches the measured data. There can be significant ambiguity and non-uniqueness involved in this process as more than one flow model with different physical assumptions and attributes may match the data.

The overall methodology for the well test analysis of the Florence Project data is summarized as follows:

- the data set was divided into its major components, such as the drawdown period and the shut-in or recovery period;
- appropriate parts were then analyzed separately, with different methods of analysis for flow periods and shut-in periods;
- the analyses of the different periods were checked for consistency.

A hydraulic test analysis involves the selection of an appropriate flow model. These models are generally divided into three basic components:

- inner boundary conditions (i.e., wellbore storage and skin effects, and fracture flow effects);

- formation flow component (i.e., homogeneous formation, dual porosity, and composite model);
- outer boundary conditions (i.e., infinite extent condition, no flow or constant pressure conditions).

In practice, recognition of a suitable model is performed using diagnostic plots. The data are plotted in different coordinate systems (such as, log-log plots, semi-log Horner plots, etc.) to help the analyst identify the appropriate model from the shape of the data. One key diagnostic plot is the derivative plot where the derivative of the pressure with respect to the natural logarithm of elapsed time is plotted against the log of time. The pressure derivative is extremely sensitive to the shape of the pressure data and, as such, constitutes one of the most useful tool for diagnostic purposes (Bourdet et al, 1983). For example, a horizontal line on a derivative plot indicates infinite-acting radial flow behavior whereas a minus one-half slope indicates three dimensional flow.

It is worth noting that, while the different flow dimensions are easily detected through the pressure derivative approach, identification of the physical conditions which yield such dimensionality is typically not straight forward. For example, three-dimensional flow may result from partial penetration, semiconfined conditions or from a highly interconnected fracture network. In order to discriminate among these possibilities, detailed hydraulic testing may need to be conducted. The following paragraphs present a brief summary of the data interpretation methodology and techniques applied to the field data from the Florence Site.

2.1 Analysis of Drawdown Period

Most of the tests conducted to date were designed as constant, single discharge tests. In some tests the discharge rate oscillated around a stable value. When a well defined drawdown was achieved

during the pumping period, the available data from the Florence Site were analyzed assuming a constant discharge test. Otherwise, the data were not used in the interpretation.

In an analysis of the main flow period, the source signal is assumed to be in the form of an instantaneous pressure change from undisturbed static conditions. The data for this flow period is the measured hydraulic head decrease that results from fluid being extracted from the formation. The analysis used a simple set of type curves which correspond to a single interpretation model with:

- inner boundary condition: wellbore storage and skin;
- formation: homogeneous; and
- outer boundary condition: infinite lateral extent.

Only one of two parameter sets can be determined from this analysis: either hydraulic conductivity and wellbore skin (the static water level being an input parameter for this analysis), or hydraulic conductivity and porosity. The best fit of the data to the type curves, therefore, corresponds to finding the optimum set of the two output parameters. For a more detailed description of the theory and methodology of well test analysis, the reader is referred to "Data Report for the Initial Hydraulic Tests Interpretation," Golder (1995).

2.2 Analysis of Shut-in (Recovery) Period

The analysis of recovery or shut-in periods is usually based on the assumption that the shut-in period corresponds to an event of no pumping where water levels are allowed to return to their pre-stressed level. If the flow rate history prior to the shut-in period is variable, then this flow history can be

included in the analysis by using the superposition of a number of different but constant flow rates of different durations.

Data from shut-in periods are examined in both log-log and semi-log diagnostic plots. This approach allows the analyst to review the characteristics of the shut-in period. For example, when the effects of the pre-test injection/extraction flows during drilling are significant, the shut-in pressure data reach a peak, and decline at late time. This form of data is referred to as a 'rollover' and can be easily diagnosed on the log-log and semi-log plots. The log-log and the semi-log diagnostic plots are also used to fit selected portions of the shut-in data with appropriate straight lines and obtain initial estimates of formation parameters.

After the flow model has been selected, the quality of the fit of the data to the model response (called 'type curve') can be adjusted by using automated regression methods. During this stage of the analysis, the entire data set from the selected shut-in period is considered. However, during the final regression stages, emphasis is always placed on the fit of the type curve to specific portions of the data. Judgment of the relative goodness of fit to specific portions of the shut-in data comprises one of the most important aspects of the automated data fitting procedure. Once a suitable and consistent fit between the drawdown data and the type curve is obtained, the fit is reviewed by plotting the drawdown derivative and improving the match.

After the flow model has been selected and a consistent set of analysis results obtained, a sensitivity analysis can be conducted. This exercise is designed to quantify the likely uncertainty in the estimated hydraulic conductivity. When carried out, as in the case of some of our AQTESOLV interpretations, it helps to determine the range of the parameter within which, a reasonably good fit is retained between the model response and the data. As shown in a latter section, the range of this parameter reflects large uncertainty in the AQTESOLV analyses.

2.3 Analytical Models

Two different models were used for interpreting the hydraulic tests at the Florence Site; (1) FLOWDIM, a homogeneous confined aquifer model which accounts for flow dimensionality (2D or 3D) and borehole storage effects, and (2) a two-dimensional, semiconfined aquifer model which accounts for storage in the semiconfining layers (leaky aquifer) and borehole storage. This latter model is one of many choices in the commercial package AQTESOLV.

It is important to note that the analytical approach taken by these two software packages is significantly different. FLOWDIM uses curve matching techniques which rely heavily on the pressure derivative approach (Bourdet et al, 1983), whereas AQTESOLV relies on a more traditional curve matching approach which uses only the drawdown versus time data. Although the FLOWDIM approach significantly improves parameter resolution and reduces the non-uniqueness of the estimation, the number of aquifer models and outer boundary conditions implemented within FLOWDIM is currently limited.

The leaky aquifer model of Moench (1985) was fitted with AQTESOLV to several data sets. This model utilizes four aquifer parameters: transmissivity (T), storage coefficient (S), a dimensionless parameter that accounts for the leakance from semi-confining layers above and below the tested interval (β), and a "leakance factor" (r/B). At the Florence site this semiconfining condition may result from the MFGU separating the UBFU from the LBFU. For the pumping well, the leaky aquifer model includes the effect of wellbore storage, using two additional parameters; wellbore storage (α), and skin factor (S_w).

The drawdown data from several aquifer tests were modeled as a confined aquifer using FLOWDIM. Available geologic information for the site indicates that the local aquifer may vary from confined, to semiconfined to confined depending on the interaction between the basin fill deposits and the oxide zone. However, in cases where drawdown is small relative to the saturated thickness, the

aquifer response of an unconfined aquifer model can be closely approximated by that from a confined aquifer model. Many of these tests were performed in wells whose screen length is small relative to the saturated thickness, a condition known as partial penetration, causing the drawdown to resemble that from a three-dimensional flow model. This interpretation accounts for vertical, as well as horizontal flow into the wellbore, but still assumes a homogeneous and isotropic porous media. It is our opinion that, in cases where the geologic information is inconclusive with regard to aquifer conditions, and due to the significant influence of nearby pumping, the "best" conceptual model for the aquifer can not be established with certainty given the present field data. It is important to recognize, however, that three-dimensional flow may be induced by geologic structure controls, aquifer heterogeneity and the spatial arrangement of the wells.

As discussed in Chapter 3.0, due to the method of interpretation used by AQTESOLV, the resulting parameter estimates are strongly non-unique. Also, based on the parsimony principle, a two-parameter model that explains the field data and results in realistic parameter estimates, should be preferred over a six-parameter model that equally reproduces the data. Several data sets are interpreted with both AQTESOLV and FLOWDIM, while some others are subject to multiple AQTESOLV interpretations. Whenever possible, based on geologic information, the parameter set that is thought to best represent the field setting is selected. Although in some cases the semiconfined model may be appropriate, non-uniqueness in the parameter estimate renders the AQTESOLV interpretation uncertain. As shown in a later section, FLOWDIM and AQTESOLV estimates of hydraulic conductivity are sometimes close to each other. It is our contention that for a given data set, FLOWDIM analysis yields a unique set of parameters, while the AQTESOLV parameters are strongly non-unique. Combination of the pressure derivative approach with the semiconfining model will significantly enhance the parameter estimation process.

3.0 TEST INTERPRETATION RESULTS

This section provides a description of the conditions during each aquifer test, general comments on the quality of the data, and estimates of hydraulic parameters resulting from the analytical interpretation. Two critical pieces of information during any hydraulic test program are; (a) the behavior of the static water levels before the test is started, and (b) the location of nearby active wells and their pumping rates and duration of pumping periods. In most cases, neither of these data are available for the Florence aquifer tests. A precise interpretation aquifer tests which show the effect of agricultural pumping may not be possible. Depending on the pumping rate of these wells, their stage on the drawdown cycle, and their proximity to the observation wells, their effect on the hydraulic parameter estimates may be significant.

In some cases, aquifer heterogeneity, abrupt changes in the pumped well discharge rate, and the effect of nearby agricultural wells, complicated the interpretation of the drawdown and recovery data. To the extent permitted by the data, an attempt was made to distinguish between effects produced by geologic controls and those produced by the cycling of nearby agricultural wells. The available information about the hydraulic tests conducted at the Florence Site to date is summarized in Table 1. Included in this table are the name designations of the wells participating in a given test, starting and ending date of the test, and available information regarding geologic formation tested, location of screened interval and the availability of drawdown and discharge rate data during the test.

Table 2 presents a summary of the hydraulic conductivity and storage and specific storage estimates resulting from our interpretation. Also included in this table is the name of the formation tested, and comments and qualifiers on the conductivity estimates. The available data are classified into three different categories; poor, fair, and good. A poor data set is one that fits the type curve only in a general sense. These tests indicate strong effects of agricultural wells cycling and/or displayed a noisy signal resulting from other un-identify conditions. The estimated hydraulic conductivity

interpreted from these tests should be used with caution. A fair data set represents a test with some uncertainty, mainly due to nearby pumping. A good data set results in a hydraulic conductivity that is deemed to be a close representation of the formation conductivity.

In the case that the drawdown due to nearby pumping is significant, the analytical interpretation of the field data will underestimate the formation hydraulic parameters. Conversely, if the agricultural pumping has recently ceased, and the rate of recovery of its drawdown cone is significant in comparison to the drawdown rate produced by a particular test, the analytical interpretation will overestimate the hydraulic parameters of the hydrogeologic units.

Table 3 summarizes the state plane coordinates and elevations above mean sea level (AMSL) of the forty-nine (49) unique well locations for which hydraulic conductivity estimates were obtained. It also includes the elevation AMSL of the screen interval mid-point, as well as, the screen length.

Interpretation results from FLOWDIM analyses are presented in two figures, the first summarizes relevant test information, and provides the value of hydraulic conductivity, and the second presents a log-log plot displaying the match between the field data and the analytical model (circles), and the match between the derivative of the field data and that from the analytical model (triangles). Results from AQTESOLV interpretations are presented in a single figure which includes both a log-log diagram of the data and the analytical model selected, a summary of relevant test information, and the parameter values for the particular model.

The following paragraphs offer a cursory description of test conditions and hydraulic parameter estimates for each test. A number of these tests had no usable drawdown data and are so noted in the text. The tests are discussed in alphabetical order using the pumping well identification and starting with tests conducted on the monitoring wells. The first few tests are discussed in detail to provide the reader with a basis for understanding the remaining test interpretations. Detailed discussion for unique and interesting tests is given as warranted by test response.

Aquifer Test in M1-GL

This constant rate test involved a single well, located just southwest of the proposed in-situ mine area, with a discharge of 10 gallons per minute (gpm). Well M1-GL is a borehole completed within the lower basin fill unit (LBFU) in an area where the MFGU is thought to occur (Brown and Caldwell, 1995). The screen interval is located between depth 315 ft and 355 ft from the surface. Top of the oxide zone in the vicinity of well M1-GL is reported to be about 1,000 ft below ground surface (bgs). Nearby agricultural wells BIA-9 and BIA-10B were reported to have been active during the test. The test response shows a slight "recovery" of the hydraulic head (after about 10 minutes) during the test (Figure 1A). Final recovery of the hydraulic head resulted in a water elevation higher than the elevation reported at the beginning of the test, indicating that the observed hydraulic response maybe a superposition of more than one stress on the aquifer (namely, the transient effects from wells BIA-9 and BIA-10B).

AQTESOLV was used to interpret the data from this test. Figure 1B shows the log of drawdown versus the log of time and the dimensionless type curve of a leaky aquifer model with wellbore storage. This figure shows the transient effects produced by nearby pumping, as indicated by the poor match between data and type curve just before drawdown stabilization. The hydraulic conductivity estimate is 3.6 ft/day based on a screened interval of 40 ft. The aquifer storage coefficient estimate for this test is 1.3×10^{-3} . Also shown in Figure 1B are the r/B , β , $S\omega$, and α parameters.

FLOWDIM analysis (Figure 1D) of these data indicates that a homogeneous, isotropic aquifer model under three-dimensional flow may also reproduce the observed behavior. Note, however, that at about 9 minutes into the test (see Figure 1A) the drawdown starts to decrease, as indicated by the sharp drop in the pressure derivative (triangles). The estimated hydraulic conductivity in this analysis is 7.3 ft/day with a specific storage of 1.8×10^{-4} 1/ft (Figure 1C). Clearly from the log-log plot, the pressure derivative shows that the data collected after 0.15 hours is affected by nearby

pumping and that the reliability of this test is low. In contrast, when only the drawdown is considered, as in the AQTESOLV approach (Figure 1B), one may be misled to accept this otherwise poor data set. The overall fit of the type curve is poor, rendering these estimates uncertain.

Aquifer Test in M2-GU

As is evident in the semi-log plot of drawdown versus time (Figure 2A), although the test lasted more than 1,000 minutes, none of the data sets recorded are usable.

Aquifer Test in M3-GL

Aquifer tests in monitoring well M3-GL (Figure 3A) involved wells M2-GU, M4-O and M5-S as observation points. These wells are located about 1,700 ft southeast of the proposed in-situ mine area. Average discharge from M3-GL during this test was reported at 10 gpm. Well M3-GL is completed in the Lower Basin Fill Unit, while M2-GU and M4-O are completed in the UBFU and the oxide zone, respectively. Irrigation Well ENGLAND #3 was on during the test but no information regarding its pumping rate is available. Observation wells M2-GU and M5-S showed recovery after 100 minutes into the test (Figure 3A). The hydraulic response for wells M2-GU and M4-O is minimal and quite erratic. This small response between M2-GU, M3-GL and M4-O may indicate a limited hydraulic connection between the Lower and Upper Basin Fill Unit and the oxide zone in this area. After shut in of well M3-GL, observation wells M2-GU and M4-O, and M3-GL itself, showed a slight recovery and then began to drop off again which may be the effect of cycling of agricultural pumping. The hydraulic response of well M5-S appears completely independent of pumping on well M3-GL. Due to these conditions, the response from the observation wells was not interpreted.

Data interpretation for the drawdown data from this test was accomplished by means of a 2D homogeneous model using the leaky aquifer model. Only the drawdown data were used for this interpretation. The overall fit of the data to the selected type curve is relatively good (Figure 3B). However, the early data are poorly represented. The estimated hydraulic conductivity from this test for the Lower Basin Fill Unit is 16.7 ft/day, for a screen interval of 40 ft, and a storage coefficient of 8.4×10^{-6} .

A FLOWDIM interpretation using a confined, three dimensional model is presented in Figures 3C and 3D. The drawdown data are closely reproduced by the model, however, the pressure derivative of these data show significant discrepancies from the analytical model at late time (beyond 1 hour into the test) resulting in fair estimates of the hydraulic parameters. The hydraulic conductivity estimate is 6.9 ft/day and the specific storage 2.8×10^{-4} .

Aquifer Test in M4-O

The aquifer test in monitoring well M4-O involved wells M2-GU, M3-GL and M5-S as observation points. Average discharge from M4-O during this test was reported at 15 gpm. Irrigation Well ENGLAND #3 was on during the test but no information is available regarding its pumping rate history. Little or no drawdown was seen in any of the observation wells (Figure 4A). However, at about 550 minutes into the test, the hydraulic head in M2-GU and M3-GL shows a sharp decrease. After turning the pump off in well M4-O, the observation wells in the unconsolidated unit showed some partial recovery, and at about 1,900 minutes, a sharp drawdown was observed. The hydraulic connection between the oxide zone and the unconsolidated units above seems limited at this location. A similar condition was observed in the M3-GL test (above) which may indicate the influence of the MFGU, and may offer some justification for the use of a leaky aquifer model. Observation well M5-S (completed in the sulfide zone) did not show any drawdown, but instead recovered throughout the test. Due to these conditions, the test response from the observation wells M2-GU and M5-S was

considered unsuitable for interpretation.

AQTESOLV interpretation of the drawdown data for pumping well (M4-O) results in a good match (Figure 4B1) between the type curve of a leaky aquifer model and the field data. The hydraulic conductivity estimate is 0.3 ft/day using a screened interval of about 60 ft. However, this value is deemed uncertain due to the effect of pumping well ENGLAND #3. The storage coefficient for the oxide zone is estimated from this test to be 3.5×10^{-2} . To explore the uncertainty of the parameter estimates from a seemingly good data set, three AQTESOLV interpretations were performed (See figures 4B1, 4B2, and 4B3). As shown in these plots the goodness of fit is almost identical for these alternative parameter sets. However, the hydraulic parameters show significant variability. For instance, hydraulic conductivity varies from 0.1 to 0.3 ft/day and storativity varies from 0.0045 to 0.096. The other four parameters show a variation of over two orders of magnitude.

Interpretation of these data with a homogeneous three-dimensional flow model using FLOWDIM, results in a relatively good fit with the drawdown data (Figures 4C and 4D). The estimated hydraulic conductivity is 0.2 ft/day and the specific storage is 6.4×10^{-6} 1/ft. Given the reported thickness of the oxide (about 200 ft) in the vicinity of this monitoring cluster a three-dimensional model may adequately represent the effect of partial penetration.

FLOWDIM interpretation of drawdown data in observation well M3-GL using a 3D model resulted in a hydraulic conductivity estimate for the LBFU of 5.7 ft/day and a specific storage of 7.6×10^{-6} 1/ft. The summary for this interpretation and the type curve match are presented in Figure 4E and 4F, respectively. Note that after about one hour into the test, a significant increase in drawdown was observed. Only data before this time was used in the analysis. This estimated hydraulic conductivity for the LBFU is most likely an underestimation of the actual conductivity of the since our approach assumes an equivalent continuum to represent this two-layer system.

Aquifer Tests in M10-GU and M11-GL

Semi-log plots for these tests are presented in Figures 5 A and 6 A. In spite the duration of the pumping period (about 900 minutes) these figures clearly show that these test yielded no interpretable information.

Aquifer Test in M12-O

Well M12-O was tested under a constant discharge of about 15 gpm. The well was completed in the oxide zone. Three observation wells (M10-GU, M11-GL, and M13-S) were used for this test, however, none of these produced usable data (Figure 7A). All four wells are located in the east central portion of the proposed in-situ mine area. Irrigation wells BIA-10B and England #3 were pumping during portions of the test, but no information is available regarding their flow rate history. Drawdown data for pumping well M12-O appear reasonably interpretable. These data show significant drawdown during the late time recovery period. This is likely caused by the superposition of the effects of M12-O and the drawdown from some other well. Well M12-O is screened from about 420 ft to about 480 ft bgs within the oxide layer. The top of the oxide is reported at about 800 ft bgs with a thickness of about 500 ft. Given the geologic setting around this well, either a semiconfined or a confined aquifer model with partial penetration may be used for data interpretation.

A 2D leaky aquifer model with well-bore storage was used to interpret hydraulic parameters for M12-O (Figure 7 B). The transmissivity estimate using this model is 149.9 ft²/day. With a screened interval of 60 ft, this produces a hydraulic conductivity of 2.5 ft/day. The estimated storage coefficient is 1.6×10^{-4} .

Interpretation of data from this well by means of FLOWDIM homogeneous, isotropic, three-dimensional model is presented in Figures 7C and 7D. The early data shows a very good match

with the type curve. However, at about 0.8 hours into the test, the pressure derivative of the data deviates significantly from the analytical model. The hydraulic conductivity is estimated at 2.5 ft/day, and the specific storage at 6.3×10^{-6} 1/ft. Note that the hydraulic conductivity is identical to that obtained with the semiconfined model, however, the FLOWDIM estimate of K is unique. As previously discussed, appealing to the principle of parsimony, the simplest 3D model is preferred over the more complex, six-parameter model.

Aquifer Test in M14-GL

Well M14-GL was tested under a constant discharge of 10.5 gpm. This well is completed within the Lower Basin Fill Unit. Well M15-GU, in the Upper Basin Fill Unit, served as an observation well. Both of these wells are located southwest of the proposed in-situ mine area. Irrigation Wells BIA-9 and BIA-10B were on during the test but no information is available regarding their pumping rate history. Additionally, M1-GL was pumping during the test period. There was very little drawdown in observation well M15-GU (Figure 8A), however, a sharp increase in hydraulic head was observed at about 1,000 minutes after pumping in M14-GL ceased. Recovery in the pumping well went beyond initial reported static water level. It is suspected that one or both of the pumping and recovery periods on the agricultural wells may be responsible for these effects. Field data from the observation well was not considered suitable for interpretation.

Analyses of these data using a 3D model (Figures 8B and 8C) shows a satisfactory fit for both pressure and pressure derivative. Given the relatively short length of the screened interval (40 ft), as compared to the thickness of the Lower Basin Fill Unit in that location (about 1,000 ft), it is not surprising that the test response suggests 3D flow, typical of a partially penetrating well. The hydraulic conductivity estimate from this interpretation is 0.9 ft/day and the specific storage 1.3×10^{-5} 1/ft.

Aquifer Test in M15-GU

This constant rate test involved a single pumping well (M15-GU) discharging at 10 gpm from the Basin Fill Unit and one observation well (M14-GL) which was completed in the Lower Basin Fill Unit. The test is similar to the previous test (M14-GL) with the pumping and observation wells swapping roles. Irrigation Wells BIA-9 and BIA-10B were on during the test but no information is available regarding their pumping rate history. The hydraulic head on the pumping well rose above the static water level during recovery (Figure 9A). This behavior may be produced by one or both of the irrigation wells being shut off during testing. Due to these effects the data from the observation well are not interpretable. Only the drawdown data for M15-GU was analyzed.

This test was analyzed with AQTESOLV and modeled as a 2D leaky aquifer with wellbore storage. Only the drawdown data was analyzed and, as shown in the log-log plot (Figure 9B), the match between the data and the type curve is fair. The hydraulic conductivity of the UBFU estimated for this test is 0.7 ft/day with a storage coefficient of 1.2×10^{-4} .

A FLOWDIM interpretation of these data is presented on Figures 9C and 9D. This latter figure shows that only the early data fits the model properly. The decrease in the drawdown at about six minutes prevents an adequate match with later portions of the test. The estimated hydraulic conductivity is, however, identical (0.9 ft/day) to that obtained from testing well M14-GL. The specific storage is 4.4×10^{-7} . Because of agreement between the hydraulic conductivity estimates, the 3D model is deemed a better representation of the field conditions at this location.

Aquifer Test in M18-GU

This constant rate test consisted of pumping a single monitoring well (M18-GU) with a flow rate of 10 gpm from the Upper Basin Fill Unit (UBFU). The well is located south of the proposed in-situ

mine area. This was a short duration test (100 minutes) with no observation wells. The data set is amenable to interpretation (Figure 10A). Well M18-GU is screened over 40 ft, within the 300 ft thick UBFU. Under these conditions, three-dimensional flow as resulting from partial penetration is very likely. The drawdown data for M18-GU was interpreted using the 2D semiconfined model resulting in an estimate for the UBFU hydraulic conductivity of 4.0 ft/day. However, as shown in the log-log plot (Figure 10B), the match between the data and the type curve is relatively poor. The estimate for the storage coefficient is 2.6×10^{-3} . A similar hydraulic conductivity estimate (5.2 ft/day) is obtained from the three-dimensional FLOWDIM interpretation (Figure 10C and 10D). The specific storage is estimated at 3.5×10^{-6} 1/ft using this model. Because this well is clearly a partially penetrating well, the FLOWDIM three-dimensional interpretation is preferred.

Aquifer Test in P5-O

This constant pumping rate test utilized well P5-O as the pumping well (discharge at 66.5 gpm) and O5.1-O and O5.2-O as observations wells. All three wells were completed in the oxide zone and they are located in the southeastern part of the proposed in-situ mine area between the Sidewinder and the Party Line Faults. The length of the screened intervals for the observation wells is 158 ft and 59 ft for O5.1-O and O5.2-O respectively. Pumping well P5-O is screened at multiple sections between 414 ft and 720 ft bgs. The total open area represents 238 ft out of these 356 ft. The oxide zone in this area is about 400 ft thick, and is overlain by 80 ft of LBFU. The drawdown curves (Figure 11A) for these wells show pronounced effects of other pumping wells (BIA-9 and BIA-10). In addition, the transducer in O5.1-O was not functioning for most of the test and digital drawdown data had to be supplemented with hand written notes. In spite of these problems, an attempt was made to interpret these data.

An interpretation of the P5-O and O5.2-O drawdown data using a FLOWDIM two-dimensional model (Figures 11B through 11E) results in an estimate of hydraulic conductivity of 1.3 and 2.2

ft/day and storage coefficients of 8.3×10^{-3} and 2.3×10^{-2} , respectively. The overall fit to the type curves is fair. FLOWDIM interpretations for drawdown data from observation well O5.1-0 was not possible due to the low quality of the data. Noisy drawdown data results in erratic behavior of the derivative and prevents correct application of this interpretation method. According to this conceptual model, the oxide zone behaves as a confined unit without any interaction with the LBFU. A similar lack of connection between the oxide zone and the alluvial deposits was observed in the hydraulic tests of nearby wells M3-GL and M2-GU, southeast of well-cluster five.

Aquifer Test in PW1-1

This constant rate test, conducted by Magma personnel during February 1994, involved a single pumping well (PW1-1 pumping at 32.5 gpm) and three observation wells (OB1-1, 523MCC, and OB-6) all in the oxide zone. These wells are located in the north-central part of the proposed in-situ mine area. The drawdown data for PW1-1, OB1-1, and 523MCC were analyzed, but, the data for 523MCC were very noisy (Figure 12A). Although well OB-6 is halfway between PW1-1 and 523MCC, drawdown in it shows only a small variation throughout the test and was therefore not interpreted. No completion data was available for this well, so its lack of response can not be explained at this time.

This aquifer test lasted 6,000 minutes and resulted in a complete data set -the three typical stages in a theoretical response are represented. Late time data show a stabilized hydraulic head typical of an infinite-acting formation. This test provides a good opportunity to compare the two competing conceptual models (leaky and confined) and to assess the uncertainty associated with the resulting parameters.

Figures 12B and 12C show two alternative interpretations of the drawdown data for PW1-1 using the semiconfined model by Moench (1983). Clearly, either of these analyses provides a good match

to the experimental data. Note, however, the significant difference between parameter values. Transmissivity estimates differ by a factor of two, while the other five parameters estimates differ by up to an order of magnitude. Given the strong variability of hydraulic parameters observed throughout the site, selection of the appropriate parameter set using this six-parameter model is not straight forward. Although a reasonable match (Figures 12 D and 12 E) is obtained with the semiconfined aquifer model for the observation wells (OB1-1 and 523 MCC), it is our opinion that due to uncertainty in the parameter estimates, the interpretation of these data is best accomplished by the confined aquifer (two parameter) model.

Interpretation of the drawdown data by means of a confined aquifer model provides a consistent set of aquifer parameters (Figures 12 F through 12 K). The hydraulic conductivity estimates are 0.1, 0.3, and 0.1 ft/day, with specific storage equal to 1.2×10^{-7} , 9.6×10^{-8} and 9.6×10^{-8} 1/ft, for wells PW1-1, OB1-1 AND 523MCC, respectively.

Early drawdown data from both observation wells show an interesting behavior. The early data from OB1-1 shows a surprisingly 1:1 slope, typical of borehole storage whereas the early data from 523MCC show an 1:0.5 slope characteristic of fracture-dominated flow. The available geological information is not sufficient to determine whether fracture flow is indeed occurring at this location, but it may be related to the sidewinder fault zone.

Aquifer Test in PW2-1

This constant rate test, also conducted by Magma personnel during March 1994, was located in the north-central part of the proposed in-situ mine area and involved a single pumping well (PW2-1) with a discharge of about 50 gpm and one observation well (OB2-1), both in the oxide zone. Both of these wells are surrounded by the old underground workings. The screened length on these wells is 220 ft and the thickness of the oxide zone in this area is reported to be more than 200 ft. The

drawdown data for both PW2-1 and OB2-1 (Figure 13A) were analyzed.

The best match to these data was obtained with a type curve corresponding to a 2D, homogeneous flow model that assumes a leaky aquifer with wellbore storage. As shown in the log-log plot (Figure 13B), the match between the data and the type curve is good. The hydraulic conductivity estimate is 0.7 ft/day. The estimated storage coefficient for the oxide zone is 2.2×10^{-4} .

The same model was used to interpret the drawdown data for OB2-1 (Figure 13C). The resulting hydraulic conductivity estimate is 1.0 ft/day with a storage coefficient of 1.7×10^{-5} . No sufficient geologic evidence exists to determine whether this semiconfined model is appropriate for this portion of the aquifer system.

An attempt to interpret these data using FLOWDIM results in a flow dimension of 2.5 (!) which indicates that the flow system in the area may be controlled by discrete features. A number of fault zones are reported in the vicinity of wells PW2-1 and OB-2-1.

Aquifer Test in PW2-2

This constant rate test, conducted by Magma's personnel during April 1994, involved a single pumping well (PW2-2 pumping at 45 gpm) and one observation well (OB2-2). These wells are located in the east-central portion of the proposed in-situ mine area and are completed in the oxide zone. Both of these wells have a screen length of 300 ft. The thickness of the oxide is about 420 ft in this area of the site. The drawdown data for both PW2-2 and OB2-2 (Figure 14A) were analyzed, however, the OB2-2 data shows an erratic response despite a relatively constant flow rate. At about 900 minutes into the test the drawdown on both of these wells starts to decrease without an apparent reason.

These aquifer tests were interpreted using a 2D leaky aquifer model with wellbore storage (Figures 14B-14C). Based on this interpretation, the estimated hydraulic conductivity for pumping well PW2-2 is 0.3 ft/day, and its estimated storage coefficient is 3.4×10^{-5} . Data from OB2-2 yield a poor match to the analytical model. The hydraulic conductivity estimate for OB2-2 is 1.1 ft/day and the estimated storage coefficient is 2.7×10^{-4} . In view of the noise in the drawdown data for OB2-2, these estimates are not considered reliable.

Aquifer Test in PW3-1

This constant rate test, performed by Magma personnel during late March, 1994 involved a single pumping well (PW3-1) with a discharge of 58 gpm and one observation well (OB3-1), both in the oxide zone. The wells are located in the northwest quadrant of the proposed in-situ mine area on the hanging wall of the sidewinder fault, where the thickness of both the oxide and the unconsolidated sediments increase sharply. These wells are screened over a 280 ft length. The thickness of the oxide zone is reported at about 800 ft. The drawdown data for both PW3-1 and OB3-1 was analyzed, however, the OB3-1 data show significant amount of noise (Figure 15A).

These aquifer tests were interpreted using a 2D leaky aquifer model with wellbore storage (Figures 15B-15C). Based on this 2D interpretation, the estimated hydraulic conductivity for pumping well PW3-1 is 0.9 ft/day and its estimated storage coefficient is 1.2×10^{-3} . The hydraulic conductivity estimate for OB3-1 is 0.5 ft/day, and the estimated storage coefficient is 1.6×10^{-4} . However, in view of the noise in the drawdown data for OB3-1, these estimates are not considered reliable.

Aquifer Test in PW4-1 (Test 1)

This constant rate test involved a single pumping well (PW4-1 pumping at 71 gpm) and one

observation well OB4-1. These wells are located in the west central part of the proposed in-situ mine area where the thickness of the oxide zone is more than 900 ft. Both wells were completed with 340 ft of perforated casing, which most likely induces three-dimensional flow as a result of partial penetration. Because of significant noise in the drawdown data from well OB4-1, only the drawdown data for PW4-1 was analyzed (Figure 16A).

The type curves used to interpret PW4-1 assumed a 2D homogeneous, leaky aquifer with wellbore storage. Only the drawdown data was used and, as shown in the log-log plot (Figure 16B), the match between the data and the type curve is good. The hydraulic conductivity estimated for the oxide zone based on this test is 3.7 ft/day and the estimate for the storage coefficient is 3.0×10^{-2} . A FLOWDIM interpretation of the drawdown data from this well is presented on Figures 16C and 16D. Although the drawdown data is matched closely by the model, the derivative plot shows significant discrepancy between the type curve and the data for elapsed time larger than about 3 hours. The hydraulic conductivity estimate is 1.8 ft/day and the specific storage is 3.1×10^{-7} 1/ft. Given the small penetration of well PW4-1, the three-dimensional model is appropriate for interpreting this test.

Aquifer Test in PW4-1 (Test 2)

Drawdown data for test #2 on pumping well PW4-1 and observation well OB4-1 were not interpreted. The test lasted 2,000 minutes, but no drawdown was observed in the pumping well. Data from the observation well show an erratic behavior (Figure 17A).

Aquifer Test in PW7-1

This constant rate test involved a single pumping well (PW7-1) with a discharge of 38 gpm from the

oxide zone. Two observation wells OB7-1 and OB-1, also completed in the oxide zone, and an observation well O3-GL completed along the interface between the basin fill deposits and the oxide were used as drawdown monitoring locations. All four wells are located near the center of the proposed in-situ mine area. Irrigation wells BIA-10B and WW-3 were on during testing and appear to have had some effect on the data, as shown by the change of slope in the drawdown curve at about 200 minutes into the test (Figure 18A). However, early data from PW7-1 and OB7-1 are reasonably well behaved and suitable for analysis. On the other hand, data from observation wells O3-GL and OB-1 show very little response to pumping. The thickness of the oxide zone is reported at about 600 ft. Wells PW 7-1 and OB7-1 have a screened interval of 340 ft which results in partial penetration.

FLOWDIM was used to interpret drawdown data from well PW7-1. The selected type curve for this analysis corresponds to a 2D, homogeneous flow model, with a $C_D e^{2s}$ parameter equal to 100. This value results in a skin coefficient of -2.1 (Figure 18B), which indicates enhanced hydraulic conductivity near the well. This enhanced conductivity could be natural, resulting from nearby fractures, or it could be due to the drilling and well development process. As shown in the log-log plot (Figure 18C), and in spite of the transient effects produced by nearby pumping, the match between the early data and the type curve is good. The hydraulic conductivity estimate is 0.2 ft/day and the storage coefficient is 1.9×10^{-3} .

The selected type curve for the observation well data (OB7-1) corresponds to a 2D, homogeneous flow model. As shown in this log-log plot (Figure 18E), and due to the transient effects produced by nearby pumping, the match between the data and the type curve is fair. The hydraulic conductivity estimate is 0.1 ft/day and the estimate for the storage coefficient is 1.3×10^{-4} . Despite the relatively short length of the screened interval in these wells, and the fact that these wells are completed near known fault zones, the early data from this test follow a two-dimensional model.

Aquifer Test in P8.1-O

Aquifer test on P8.1-O consisted of a constant pumping rate of 12 gpm from the oxide zone. Two observations wells were monitored in the oxide zone (P8.2-O and O8-O) and two in the upper basin fill unit (P8-GU and O8-GU). All five wells are located in the northern portion of the proposed in-situ mine area. The thickness of the oxide zone in this area is about 200 ft and that of the MFGU ranges from 30 to 40 ft. Wells P8.1-O and O8-O are screened within a fault zone. The screened interval for the oxide wells is 180 ft. Irrigation well BIA-9 was on during the test, but no information is available regarding its pumping rate. The drawdown data for P8-GU and O8-GU show a small response (Figure 19A).

The transducer in P8.1-O looks like it went dry after one minute into the test. Interpretation of the drawdown data from the pumping well was not attempted. Drawdown data for P8.2-O and O8-O have obvious effects of other pumping superimposed upon the drawdown caused by P8.1-O.

The overall data set is marginal, however, the superposition principle combined with a three-dimensional model was applied to the recovery data. The resulting hydraulic conductivity estimate is 0.4 ft/day and specific storage is 1.1×10^{-5} 1/ft (Figure 19B). The overall fit to these data is relatively poor as shown in Figure 19C.

Aquifer Test in P8-GU

This aquifer test involved a single pumping well (P8-GU) with a discharge of 85 gpm from the Upper Basin Fill Unit (UBFU). Four observations wells (P8.1-O, P8.2-O, O8-O, and O8-GU) were monitored. This test used the same wells as the test in well P8.1-O (above). Irrigation wells BIA-9 and BIA-10B were on during the test but no information is available regarding their pumping rate history. Additionally, irrigation well WW-3 was turned on briefly for sampling toward the beginning of this test, and P28-GL also pumped during this test. The effect of these wells is apparent as shown by drawdown measurements in the observation wells. Note that the head in all observation

wells continues to decline even after the pumping in P8-GU ceased at about 3,200 minutes into the test (Figure 20A). Also, the recovery in the pumping well did not reach static water level, indicating that observations in the pumping well are also affected by nearby pumping. Under these circumstances, the derived hydraulic parameters are uncertain and most likely underestimate the conductivity of the UBFU.

According to the data from this test, pumping on the UBFU produces a drawdown on the oxide wells of a magnitude similar to that observed in the pumping well. This may result from the larger discharge rate used during this test (85 gpm as opposed to 12 gpm when testing P8.1-O) or more likely due to the effect of nearby pumping (BIA-9 and BIA-10B). The results from testing P8.1-O seem to indicate a limited hydraulic connection between the basin fill deposits and the oxide zone. In contrast, hydraulic head in observation well O8-GU (less than 20 ft away from the pumping well) changes by less than one foot throughout the duration of the test. Because of the uncertainty associated with the conditions existing during this test, only the data from the pumping well were interpreted.

A FLOWDIM interpretation was attempted for the drawdown data from P8-GU using a 2D homogeneous flow model, with a C_{De}^{2s} parameter equal to 1.0×10^6 . This value, in turn, results in a skin coefficient of 0.9 (Figure 20B) indicating, perhaps, minor formation clogging near the well face. As shown in the log-log plot (Figure 20C), the match between the data and the type curve is poor. The hydraulic conductivity estimate is 61.3 ft/day and the estimate for the storage coefficient is 3.2×10^{-6} . This hydraulic conductivity is too large when compared with the other estimates on the UBFU.

Aquifer Test in P12-O

This constant rate test involved a single pumping well (P12-O) with a discharge of 64 gpm from the

oxide zone. Observation well O12-O was also completed in the oxide zone, whereas observation well O12-GL was completed within the LBFU just above the contact between these two units. These wells are located in the south-central part of the proposed in-situ mine area. The length of screen installed in the oxide wells is 500 ft which almost completely penetrates the oxide zone. About one-fourth of this screened interval is in contact with the Sidewinder Fault. The data appear to show superposition of multiple pumping and recovery effects (Figure 21A). Drawdown increased at approximately 300 minutes into the test, recovery was observed at 3,000 minutes, an additional drawdown period was seen at 7,000 minutes, and still another recovery period was observed after 9,000 minutes. Irrigation well WW-3 was also pumping through the duration of the test. Large drawdown variations were also recorded in the observation wells. Due to the above effects, this test is considered marginal for interpretation, and only the first 3,000 minutes of data were used. Note also that the maximum drawdown in pumping well was 30 ft, whereas that reported O12-GL was more than 70 ft. Obviously the data from the latter well were affected by nearby pumping.

The selected type curve for the pumping well data (P12-O) corresponds to a 2D homogeneous flow model, with a $C_D e^{2s}$ parameter equal to 3.0. This value, in turn, results in a skin coefficient of -4.3 which indicates enhanced hydraulic conductivity near the well which may result from presence of the Sidewinder Fault (Figure 21B). As shown in the log-log plot (Figure 21C), the match between the data and the type curve is poor. The hydraulic conductivity estimate is 0.4 ft/day and the storage coefficient is 4.2×10^{-1} .

The selected type curve for observation well data (O12-O) corresponds to a 2D homogeneous flow model. As shown in this log-log plot (Figure 21E), the match between the data and the type curve is fair. The hydraulic conductivity estimate is 0.8 ft/day and the estimate for the storage coefficient is 9.6×10^{-4} (Figure 21E). Drawdown data for O12-GL is erratic and no interpretation was attempted. As indicated above, the overall quality of this data set is poor and can not be used to derive information about the hydraulic connection between the basin fill sediments and the oxide zone.

Aquifer Test in P13.1-O

This constant rate test involved a single pumping well (P13.1-O) with a discharge of 46 gpm. All irrigation wells are reported to be off during the test. Observation well P13-GL data show some irregularity, but seem to indicate no hydraulic connection between the basin fill deposits and the oxide zone. The pumping well and observation well P13.2-O data appear suitable for analysis (Figure 22A). Observation well O13-O showed no drawdown during this test. These four wells are located in the northwest corner of the proposed in-situ mine area in an area west of the Sidewinder Fault. The MFGU is thought to be thin or missing in this area (Brown and Caldwell, 1995). The thickness of the oxide zone is reported at more than 900 ft, while the overlain unconsolidated sediments are about 600 ft thick. Total saturated thickness is about 1,350 ft. Wells P13.1-0 and P13.2-0 have a screened interval of about 680 ft and 600 ft, respectively.

The drawdown data for P13.1-O was interpreted using a 3D homogeneous flow model. As shown in the log-log plot (Figure 22C), there is a good match between the data and the type curve however, the pressure derivative of the data after 20 hours becomes erratic. This effect is also seen in data from observation well P13.2-O. The hydraulic conductivity estimate is 0.2 ft/day which is a typical value for the oxide zone and the specific storage estimate is 1.2×10^{-7} 1/ft (Figure 22B).

The hydraulic response for observation well P13.2-O shows a clear 3D response (Figure 22E). Analyses of these data result in a hydraulic conductivity of 0.3 ft/day and a specific storage of 5.5×10^{-7} 1/ft (Figure 22D). Most likely, the three-dimensional response of these wells results from the fact that they are partially penetrating.

Aquifer Test on P15-O

This constant rate test involved a single pumping well (P15-O) with a discharge of 59 gpm. Irrigation Wells BIA-9 and BIA-10B were on during the test but no information is available regarding their pumping rates. These wells did affect observation wells (P15-GL and O15-O) as evidenced by the sudden change in drawdown near the end of the test (Figure 23A). From the available pumping rate records, the discharge on well P15-O was fairly constant throughout the test. The sudden change in drawdown is superimposed upon the drawdown due to P15-O and is difficult to separate without the rate history from the agricultural wells. Data for P15-GL shows no response to P15-O pumping for more than 3,000 minutes suggesting that hydraulic connection between the oxide and the LBFU is limited. Data from P15-O and O15-O show a small interference from nearby pumping before 3,000 minutes into the test, and a significant interference after that. These wells are located near the western edge within the proposed in-situ mine area. The thickness of the oxide on this area is reported to reach about 800 ft, geologic cross-section D-D' (Brown and Caldwell, 1995) indicates that the wells in cluster 15 are located on the hanging wall of the Sidewinder Fault, where a number of other faults have been mapped. Wells P15-O and O15-O are screened over a length of 680 ft and 600 ft, respectively.

Interpretation of drawdown data from well P15-O was done by means of a 2D homogeneous flow model with a $C_D e^{2s}$ parameter equal to 100. This value results in a skin coefficient of -5.0 indicating enhanced hydraulic conductivity near the well (Figure 23B). As shown in the log-log plot (Figure 23C), there is a fair match between the data and the type curve, despite the complications introduced by additional pumping wells (BIA-9 and BIA-10B). The hydraulic conductivity estimate is 0.5 ft/day which is a typical value for the oxide zone and the storage coefficient estimate is 1.3×10^{-2} .

Observation well O15-O data indicates three-dimensional flow in the vicinity of this well. A log-log plot of the drawdown data for this well is shown in Figure 23E. As seen in this figure, the match between the analytical model and the data is relatively poor. Interpretation of these data resulted in a hydraulic conductivity estimate of 0.5 ft/day and a specific storage coefficient estimate of 9.7×10^{-7} .

1/ft.

Aquifer Test on P19.1-O

This constant rate test involved a single pumping well (P19.1-O) with a discharge of 24 gpm pumping from the oxide zone. Observation wells P19-O and P19.2-O were also completed in the oxide zone. Two additional observation wells were also monitored during this test (O19-GL and Well 138). The data from well O19-GL were strongly affected by pumping on irrigation wells BIA-10B and WW-3 at times greater than 1,000 minutes from the start of the test. (Figure 24A). Well 138 shows no response to pumping on P19.1-O. These wells are located just outside the northwest quadrant of the proposed in-situ mine area. The three oxide wells are completed within the Sidewinder fault zone and the screened interval in these wells is about 200 ft. This area is characterized by a thickening of the basin fill deposits towards the west, away from the fault zone. The oxide zone is reported to be about 400 ft thick at the location of these wells. Observation well O19-GL is completed within the LBFU just west of the contact between this unit and the oxide zone. Well completion information for Well 138 is not available.

Drawdown data from well P19.1-O was interpreted using a 3D homogeneous flow model. The hydraulic conductivity estimate is 0.2 ft/day and the estimate for the specific storage coefficient is 1.1×10^{-7} 1/ft (Figure 24B). As shown in the log-log plot (Figure 24C), the match between the data and the type curve is good.

Drawdown data for observation well O19-O was interpreted with a 3D homogeneous flow model. The hydraulic conductivity estimate is 0.2 ft/day and the estimate for the specific storage coefficient is 3.8×10^{-7} 1/ft (Figure 24D). As shown in the log-log plot (Figure 24E), the match between the data and the type curve is fair.

Note that as indicated by the decrease in drawdown at late time, the drawdown cycles from nearby wells strongly affected this test. Interpretation of data from observation well P19.2-O was also based on a 3D homogeneous flow model. The hydraulic conductivity estimate is 0.1 ft/day and the estimate for the specific storage coefficient is 4.4×10^{-8} 1/ft (Figure 24F). As shown in this log-log plot (Figure 24G), the match between the data and the type curve is fair up to about 3 hours into the test.

Hydraulic response for observation well O19-GL is strongly affected by nearby wells (See Figure 24A) at times beyond 540 minutes. The early data was interpreted with a 3D model resulting in a hydraulic conductivity estimate of 0.4 ft/day and a specific storage coefficient estimate is 1.3×10^{-8} . (Figure 24H). As seen in Figure 24I, the field data closely matches the proposed model until about 9 hours, at which time the effects from the nearby wells becomes dominant. Note that this estimate of hydraulic conductivity is smaller than reported for the other tests on the LBFU. This may result from the continuum approach used to interpret the heterogeneous geology. Under this concept, the estimated conductivity value represents an average of both the conductivity of the LBFU and the that of the oxide zone.

Aquifer Test on P28-GL

This constant rate test involved a single pumping well (P28-GL) with a discharge of 75 gpm from the Lower Basin Fill Unit. Observation well O28-GL was completed in the Lower Basin Fill Unit and observation wells P28.1-O, P28.2-O and O28.1-O were completed in the oxide zone, while observation well O28.2-S was completed in the sulfide zone. The top of the oxide zone is at a depth of about 360 ft bgs and its thickness varies from 120 to 220 ft towards the west near these wells. The screen length of P28-GL is 30 ft and that for O28-GL is 30.1 ft. The thickness of the LBFU is about 110 ft, which renders these wells partially penetrating. The screen lengths of P28.1-O, P28.2-O and O28.1-O are 98.7 ft, 100 ft, and 99 ft respectively. These oxide wells appear to penetrate most of

the oxide zone. This well cluster was specifically constructed to test the hydraulic conductivity of the Party Line Fault. Observation well O28.2-S has a screen length of 38.9 ft in the sulfide zone.

These wells are located outside the eastern boundary of the proposed in-situ mine area. Traces of the MFGU have been observed in this area (Brown and Caldwell, 1995). Irrigation Wells BIA-9 and BIA-10B were on during the test but no information is available regarding their pumping rate history. Additionally, irrigation wells ENGLAND #3 and WW-3 were on briefly for sampling toward the beginning of the test, and test well P8-GU was also pumping during this test. The observed drawdown records appear good and suitable for analysis (Figure 25A).

The screen interval of well P28-GL is located approximately 100 to 120 ft above the screen of the oxide and the sulfide well. As seen in Figure 25A, the maximum drawdown observed in the pumping well is about 120 ft, while that in well O28-GL is close to 20 ft. The drawdown in the oxide and sulfide wells reaches a maximum of about 12 ft. Given the spatial arrangement of these wells, a drawdown measurement in the oxide and sulfide well(s) indicates three-dimensional flow. Apparently, there is a good hydraulic connection between the LBFU and the bedrock. This aquifer response could also be partially explained by the MFGU acting as an aquitard.

The selected type curve for the pumping well data (P28-GL) corresponds to a 3D homogeneous flow model. The hydraulic conductivity estimate is 3.4 ft/day and the estimate for the specific storage is 1.9×10^{-4} 1/ft (Figure 25B). As shown in the log-log plot (Figure 25C), and in spite of the transient effects produced by nearby pumping, the match between the drawdown data and the type curve is good. The pressure derivative of the data, however, deviates somewhat from the type curve at times greater than 10 hours. The hydraulic conductivity estimate is 3.4 ft/day and the specific storage is 1.9×10^{-4} 1/ft (Figure 25B).

Figures 25D and 25E show the data interpretation for the observation well O28-GL. This well is located at the same elevation of pumping well P28-GL on the LBFU. The drawdown data appear to fit a 3D homogeneous model. The hydraulic conductivity estimate is 0.8 ft/day. The estimate for

the specific storage is 3.8×10^{-9} 1/ft.

A 3D interpretation was made for observation wells P28.2-O, O28.1-O, and O28.2-S using FLOWDIM (Figures 25F-25K). The response of these wells to pumping well P28-GL is uniform indicating, perhaps similar hydraulic properties between the oxide and the sulfide. Note that well O28.2S is completed just below the interface between the oxide and sulfide zones. The hydraulic conductivity estimates for the oxide aquifer based on data from these wells are 1.5, 1.2, and 0.8 ft/day respectively. The specific storage based on these interpretations are 5.2×10^{-7} , 1.2×10^{-8} , and 2.0×10^{-8} 1/ft, respectively.

Aquifer Test on P28.1-O (Test #1)

This constant rate test involved a single pumping well (P28.1-O) with a discharge of 28.5 gpm from the oxide zone. Observation wells P28-GL and O28-GL were completed in the LBFU and observation wells P28.2-O and O28.1-O were completed in the oxide zone. The thickness of the LBFU and oxide and screen lengths for these wells were described in the section "Aquifer Test on P28-GL." Irrigation Well England #3 was on during the test but no information is available regarding its pumping rate history. Hydraulic head during recovery in these wells went beyond the static water level reported just before pumping started in P28.1-O (Figure 26A). Due to this anomalous drawdown behavior, and because a second test at a higher rate was conducted at the same location, only the information from well P28.1-O was interpreted.

The selected type curve for the pumping well data (P28.1-O) corresponds to a 2D, homogeneous flow model, with a $C_D e^{2s}$ parameter equal to 10. This value results in a skin coefficient of -6.7 which indicates enhanced hydraulic conductivity near the well (Figure 26B) perhaps resulting from the effect Party Line Fault. As shown in the log-log plot (Figure 26C), and due to the transient effects produced by nearby pumping, the match between the data and the type curve is only fair. The

hydraulic conductivity estimate is 7.7 ft/day. The estimate for the storage coefficient is 5.2 which is clearly unreasonable. It is our opinion that this impossible estimate results from the superposition of pumping on well P28.1-O and recovery of one of the agricultural wells (which pump at rates of 1,800 gpm or higher). Also, as discussed in the next paragraph, a second test (with a large discharge rate) on this same location results in a similar value of hydraulic conductivity and a reasonable storage coefficient.

Aquifer Test on P28.1-O (Test #2)

This constant rate test involved a single pumping well (P28.1-O) with a discharge of 86 gpm from the oxide zone. The observation wells were those described for the earlier test (P28.1-O; test #1). The depths and screen length for these wells are as described in that section. Irrigation Well BIA-9 was on during testing, as was well P8.1-O. However, the data appear well-behaved and suitable for analysis (Figure 27A).

The selected type curve for the pumping well data (P28.1-O) corresponds to a 2D homogeneous flow model, with a $C_D e^{2s}$ parameter equal to 10 (Figure 27B). This value results in a skin coefficient of -4.2 which indicates enhanced hydraulic conductivity near the well or the effect of the party line fault. As shown in the log-log plot (Figure 27C), and in spite of the transient effects produced by nearby pumping, the match between the data and the type curve is good. The hydraulic conductivity estimate is 3.6 ft/day and the estimate for the storage coefficient is 3.4×10^{-2} . It has been argued (Barker, 1988) that flow through a fractured medium may result in flow geometry other than integer values (i.e., 1D, 2D, 3D). This fractal dimension depends on the degree of interconnectivity of the fracture network; a highly connected network produces a flow system that closely resembles a 3D continuum. As the connectivity decreases the flow "dimension" decreases. The lower limit, of course, is a flow dimension of unity. The pressure response of well P28.1-O (Figure 27C) can be closely represented by a fractal flow model of dimension 1.8. Although, the practical significance

of this fractal dimension is not yet well understood it may provide clues as to the potential effect of discrete features such as faults or fractures.

The selected type curve for the observation well data (P28.2-O) corresponds to a 2D homogeneous flow model, with a $C_D e^{2s}$ parameter equal to 2.0 (Figure 27D). As shown in this log-log plot (Figure 27E), and in spite of the transient effects produced by nearby pumping, the match between the data and the type curve is fair. The hydraulic conductivity estimate is 2.7 ft/day. The estimate for the storage coefficient is 2.9×10^{-4} . This two-dimensional behavior is surprising, since well P28.2-O is screened along the party line fault. On the other hand, the thickness of the oxide zone decreases towards the east with the LBFU and the sulfide zone as its upper and lower boundary, respectively. As this thickness decreases, the presence of the sulfide zone may force the flow lines to remain horizontal.

Interpretation of the drawdown data from well O28.1-O, completed on the oxide zone, used a three-dimensional model and resulted in a hydraulic conductivity value of 0.5 ft/day and a specific storage of 6.8×10^{-8} 1/ft (Figure 27F). The log-log plot of the pressure derivative data shows a typical one-half slope for the first 4 hours of the test which causes a derivation of the field data from the proposed analytical model. This one-half slope is indicated by the straight line in figure 27G. According to this interpretation, the presence of the Party Line Fault has a significant impact on the cross-hole response during this test.

Hydraulic response of the LBFU wells (P28-GL and O28-GL) to pumping on the oxide zone is very similar to that described for well O28.1-O. However, maximum drawdown on the oxide well is larger than that observed on the LBFU wells. (See Figure 27I and 27K). Once again, the effect of the Party Line Fault is clearly seen in the early time pressure derivative data. The estimated hydraulic conductivity is 1.5 and 2.0 ft/day, and the specific storage is 6.4×10^{-7} and 8.4×10^{-6} 1/ft (Figures 27H and 27J) for wells P28-GL and O28-GL.

Aquifer Test on P28.2-O

This constant rate test was the fourth test ran on well cluster 28. It involved pumping well P28.2-O at a constant discharge of 76 gpm. Several observation wells were monitored during this test; P28-GL and O28-GL completed in the LBFU, wells O28.1-O and P28.1-O completed in the oxide zone, and well O28.2-S completed in the sulfide zone. The depths and screen lengths for these wells were described in a previous section "Aquifer Test on P28-GL." Irrigation Wells BIA-9 and BIA10-B were on during the test but no information is available regarding their pumping rate history. These wells did affect the data in all observation wells as evidenced by decrease in the drawdown at times greater than 3,000 minutes wells (Figure 28A). Also, the recovery in all the wells went beyond static water level. The exact impact of well interference on the hydraulic parameters is difficult to quantify.

The selected type curve for the pumping well data (P28.2-O) corresponds to a 2D, homogeneous flow model, with a $C_D e^{2s}$ parameter equal to 10 (Figure 28B). This value results in a skin coefficient of -6.5 which indicates enhanced hydraulic conductivity near the well. This may be attributed to the presence of the Party Line Fault. As shown in the log-log plot (Figure 28C), and due to the transient effects produced by nearby pumping, the match between the data and the type curve is only fair and the drawdown data is very erratic during the first 18 minutes of the test. The hydraulic conductivity estimate is 3.1 ft/day. The estimate for the storage coefficient turns out to be 3.8 which is clearly unreasonable. This unreasonable storage coefficient estimate results, most likely, from the effect of structural control imposed by the fault or to the effects of drawdown and recovery cycles from wells BIA-9 and BIA 10-B.

The type curve selected for interpreting the observation well data from O28.1-O corresponds to a 3D homogeneous flow model. The hydraulic conductivity estimate is 0.4 ft/day and the specific storage is 1.1×10^{-8} 1/ft (Figure 28D). Note that the derivative of the drawdown shows two typical stages of flow in a fracture controlled reservoir; the early slope is one-half, indicating linear flow (as

that resulting from a high conductivity fracture), and later on, it follows the slope of the three dimensional model. The data beyond 3,000 minutes was not used during this analysis. This one-half slope (as indicated by the straight line in Figure 28E) was also observed on the previous tests on well cluster 28. Drawdown data from one of the two oxide observation wells was not collected as a result of pressure transducer problems.

Test data for two observation wells in the LBFU were available. Interpretation of field data from well P28-GL results in a estimated hydraulic conductivity of 1.8 ft/day and a specific storage of 4.8×10^{-6} 1/ft as reported in Figure 28F. The log-log plot of the field data and the three dimensional type curve (Figure 28G) shows that the first seven hours of the test are strongly controlled by a highly conductive fracture-like response similar to the one described for observation well O28.1-O. Drawdown data from the other LBFU observation wells results in an estimated hydraulic conductivity of 0.6 ft/day and specific storage of 1.7×10^{-8} 1/ft (Figure 28H). The log-log plot shows a one-half slope for at least the first seven hours of the test (Figure 28I).

Observation well O28.2-S is completed within the sulfide, near the interface between oxide and sulfide, and close to the active well in this test. The pressure response of this test shows a behavior which is similar to that of the other observation wells. The interpretation of these data results in a hydraulic conductivity of 0.4 ft/day and a specific storage of 3.4×10^{-8} 1/ft (Figures 28J and 28K). It is interesting to note, that the one-half slope occurs over a longer period of time on the LBFU and sulfide observation wells than in the oxide wells. An explanation for this pressure behavior is not evident.

Aquifer Test on P39-O

This constant rate test involved a single pumping well (P39-O) with a discharge of 56 gpm pumping from the oxide zone. It had a single observation well (O39-O) which was also completed in the

oxide zone. These wells are located on the southeast end of the proposed mine area. The top of the oxide zone is about 700 ft bgs in this location and the MFGU appears to be about 20 ft thick (Brown and Caldwell, 1995). The screen length of P39-O is 355 ft and the screen length for O39-O is 415 ft. The data appears to be good and suitable for analysis (Figure 29A). In fact, this data set is one of the best sets available from the Florence site.

The type curve selected for interpreting the pumping well data (P39-O) corresponds to a 2D homogeneous flow model, with a $C_D e^{2s}$ parameter equal to 100. This value results in a skin coefficient of -1.8 (Figure 29B). As shown in the log-log plot (Figure 29C), the match between the data and the type curve is good. The hydraulic conductivity estimate is 0.3 ft/day and the estimate for the storage coefficient is 9.6×10^{-4} .

The type curve analysis for the data from observation well O39-O corresponds to a 2D homogeneous flow model, with a $C_D e^{2s}$ parameter equal to 2.0 (Figure 29D). As shown in this log-log plot (Figure 29E), the match between the data and the type curve is good. The hydraulic conductivity estimate is 0.3 ft/day and the estimate for the storage coefficient is 4.3×10^{-4} . Although the oxide zone is overlain by more than 300 ft of basin fill sediments, the flow lines resulting from pumping P39-O seem to remain confined within the oxide zone and no effects of 3D flow or leakance are observed.

Aquifer Test on P49-O

The aquifer test conducted on well P49-O consisted of a constant discharge of about 40 gpm. Two observation wells were monitored during this test; well O49-O, completed in the oxide zone, and well O49-GL completed in the Lower Basin Fill Unit. These wells are located on the southwest corner of the proposed mine area. The oxide zone in this location ranges in depth from about 400 ft to 600 ft bgs and has a thickness which varies from 500 to 300 ft towards the west. (Brown and Caldwell, 1995). P49-O and O49-O have screen lengths of 415 ft and 395.6 ft respectively, which

were designed to penetrate nearly all of the oxide zone. Depending on the interconnection between the LBFU and oxide zone, pumping on P49-O may produce a hydraulic response typical of partial penetration. Well O49-GL is located near well O49-O, however its screened interval (60 ft) is about 200 ft above the top of the screen of the oxide well. More than 180 ft of drawdown in the pumping well rendered the pressure transducer dry (Figure 30A). Pressure response on the observation wells was relatively clean, with well O49-O showing a drawdown of about 95 ft, and O49-GL showing about 0.5 ft. The hydraulic connection between the oxide zone and the LBFU seems fairly limited in this location. No other wells were reported in operation during this test, so the quality of the data is good. As mentioned before, only partial data was collected during drawdown in the pumping well, so the hydraulic conductivity for this test was estimated from the shut in data.

The log-log plot (Figure 30C) for the pumping well P49-O shows that a 3D model represents the observed data quite well. This type curve match results in a hydraulic conductivity of 0.1 ft/day and a specific storage of 2.3×10^{-6} 1/ft (Figure 30B). Observation well O49-O, on the oxide zone, shows a drawdown versus time curve which can be represented by a three-dimensional model. Interpretation with this model yields a hydraulic conductivity of 0.1 /ft/day and a specific storage of 5.4×10^{-8} 1/ft (Figures 30D and 30E). The data set collected from observation well O49.-GL is too short, so a unique set of parameters can not be defined.

Regional Aquifer Test WW-3

Two regional tests were conducted, one with BIA-9 as the pumping well and the other with WW-3. However, the data from the BIA-9 test was not analyzed as it was strongly affected by pumping in nearby wells. The regional aquifer test with well WW-3 was conducted at an average pumping rate of about 1,984 gpm. The well was screened mostly in the oxide zone with a small fraction extending into the basin fill unit. Sixteen observation wells were used during the test. Eight of these (P28.1-O, P28.2-O, O28.1-O, P15-O, O15-O, O12-O, OB7-1, and O19-O) were completed in the oxide zone.

Six observation wells (O28-GL, P15-GL, O12-GL, O3-GL, M14-GL, and O19-GL) were completed in the Lower Basin Fill Unit and one (M15-GU) was completed in the Upper Basin Fill Unit. The mine air shaft was also used as an observation well, however, completion information for this well is not available. The screen length on the other wells varies for about 30 ft on O28-GL to more than 700 ft on P15-O, while the thickness of the aquifer layer containing the wells varies from about 100 ft to 1,000 ft. The oxide zone contains various fault zones which may have a significant effect on the hydraulic conductivity.

With the exception of OB7-1 and M15-GU, the data recorded in the observation wells is fair to good (Figures 31A-31D). The pressure transducer in OB7-1 was reported to be malfunctioning during the test and no pressure response for this observation well was observed. The pressure data for M15-GU is noisy and appears to have been affected by nearby pumping, although, no wells were reported to be operating during the test other than well WW-3. Drawdown in the observation wells ranged from about two ft in wells P28.1-O, P28.2-O, O28.1-O, and O28-GL to about 33 ft in P15-O. M15-GU showed about 100 ft of drawdown, but, as previously mentioned, the drawdown in this well appears to have been affected by a nearby pumping well. No drawdown data was recorded in the pumping well WW-3.

Well cluster 28 is the farthest from the pumping well at a distance of about 3,000 ft and shows drawdown of about 2 ft. As expected, the response of P28.1-O, P28.2-O and O28.1, which are all screened in oxide is similar. However, it is worth noting that O28-GL shows an almost identical response, despite being screened in LBFU. This indicates that either (a) the LBFU and oxide are hydraulically connected at this location or (b) the conductivity of LBFU and that of oxide interspersed with faults are comparable. Another important observation from drawdown data for this well cluster is that the recovery of all of the wells went beyond the static water level. Since no other well was reported pumping during this test, it is not clear what caused this behavior.

The Log-log plot for P28.1-O (Figure 31F) shows a poor fit of the data to the type curve. The 2D

interpretation results in a hydraulic conductivity of 29.9 ft/day (Figure 31E) and an estimated storage coefficient of 4.0×10^{-3} . These values represent the properties of the quartz monzonite and granodiorite into the fault zones. Drawdown data for P28.2-O is poorly fitted by the analytical model. The Log-log plot of these data (Figure 31H) and the associated 2D interpretation gives a hydraulic conductivity value of 40.5 ft/day and a storage coefficient estimate of 3.0×10^{-3} . Observation well O28.1-O shows a similarly poor fit to the type curve as the previous wells in this cluster. The Log-log plot (Figure 31J) was interpreted with a 2D model which resulted in a hydraulic conductivity value of 35.3 ft/day (Figure 31I) and an estimate for the storage coefficient of 3.4×10^{-3} . Observation data from well O28-GL results in a similar fit to the analytical model. The Log-log plot and associated 2D interpretation are shown in Figure 31L. The resulting hydraulic conductivity estimate is 38.8 ft/day and the storage coefficient estimate is 4.0×10^{-3} .

Well cluster 15 is the closest to the pumping well at a distance of about 500 ft and shows drawdown of about 30 ft in oxide and 8 ft in the LBFU. It appears that the two layers are not hydraulically connected at this location.

Drawdown data for observation well P15-O is good (Figure 31N). A 3D interpretation of these data yielded a hydraulic conductivity estimate at this well of 1.4 ft/day and a specific storage estimate of 9.3×10^{-5} 1/ft. According to the geologic cross-sectional maps, these values represent the properties of quartz monzonite and granodiorite with minimal effect of fault zone. The hydraulic conductivity at observation well O15-O is estimated to be 1.3 ft/day (Figure 31O) based on a 3D interpretation for a cylindrical sink. Drawdown data for observation well P15-GL is good. The Log-log plot and associated 2D interpretation (Figure 31R) shows an acceptable match between the data and the 2D model response. The hydraulic conductivity estimated from these data is 17.2 ft/day and the storage coefficient estimate is 1.1×10^{-2} . As seen from the cross-sectional maps, these values represent average properties of the sand, silt and clay layer and the sand, gravel, and boulder layer of the LBFU.

Wells cluster 12 is at about 1,000 ft southwest from the pumping well. Both O12-O and O12-GL show drawdown of similar order, in spite of being screened in different units.

Observation well O12-O shows good drawdown data. The Log-log plot and associated 3D interpretation (Figure 31T) shows a fair match between the data and modeled response. The hydraulic conductivity is estimated to be 0.8 ft/day and the specific storage estimate is 8.5×10^{-10} 1/ft, which represent the quartz monozonite porphyry. Observation well O12-GL shows good drawdown data on the Log-log plot (Figure 31V). A 3D interpretation was made of these data which resulted in a hydraulic conductivity estimate of 1.0 ft/day and a specific storage coefficient estimate of 1.4×10^{-9} 1/ft, representing the sand, silt and clay layer of the LBFU.

The drawdown data for observation well O3-GL is good. The log-log plot and associated 3D interpretation is shown in Figure 31X. The estimated hydraulic conductivity is 1.8 ft/day and the specific storage estimate is 2.7×10^{-9} 1/ft. These values represent the sand, silt and clay layer of the LBFU.

Observation well M14-GL has good drawdown data. A 3D model was used to interpret these data (Figure 31Z) which gave an estimate for hydraulic conductivity at this site of 1.4 ft/day and an estimated specific storage of 1.1×10^{-9} 1/ft.

Well cluster 19 is about 2,000 ft from the pumping well and shows drawdown of about 6 ft. Drawdown data and a 3D interpretation for observation well O19-O are shown in Figure 31BB. The results of this interpretation give a hydraulic conductivity estimate of 2.0 ft/day and a specific storage of 6.2×10^{-10} 1/ft. Observation well O19-GL has good drawdown data from which a 3D interpretation was made (Figure 31DD). The hydraulic conductivity estimated at this well was 2.4 ft/day and the specific storage was estimated to be 3.01×10^{-10} 1/ft. These values represent the sand and gravel layer of the LBFU.

The drawdown data for the air shaft is acceptable. The log-log plot and associated 3D interpretation is shown in Figure 31FF. This 3D model resulted in a hydraulic conductivity estimate of 1.9 ft/day and an estimated specific storage of 1.3×10^{-9} 1/ft.

The Table 4 summarizes the hydraulic conductivity estimates calculated from the regional aquifer test. Observation wells are grouped into the Basin Fill Unit and Oxide zone. The hydraulic conductivity ranges from 1.0 to 38.8 ft/day in the Basin Fill Unit and 0.8 to 40.5 ft/day in the Oxide zone.

4.0 DISCUSSION

The hydraulic conductivity estimates from aquifer tests in the basin fill are quite variable (Table 2) and range from 0.9 to 61.3 ft/day, whereas those for the oxide zone vary from 0.1 to 3.6 ft/day. As expected, the basin fill deposits are about an order of magnitude more conductive than the oxide zone. Despite difficulties during data collection, the majority of hydraulic conductivity estimates in the basin fill and oxide zone are reasonable. A large variation in storativity is observed and two of these estimates are unrealistically large. As commonly found in most field tests, and also indicated by the Florence data, test analyses in observation wells tend to give more reasonable storativity estimates than analyses of pumping well data.

The hydraulic conductivity values estimated through the analytical approach are reported in Figure 1. The values reported in this figure were selected from Table 1 in such a way that both the pumping well and the observation well test the same "unit," (basin fill or oxide). For locations with multiple hydraulic conductivity values, the arithmetic average was used. This procedure resulted in eight (8) spatial locations with conductivity estimates for the basin fill units (UBFU and LBFU), and thirty three (33) for the oxide.

Based on the information derived from the local tests (including only wells in a particular well cluster) the following statements can be made:

- ▶ the overall quality of the data is poor due mostly to the influence of nearby irrigation well pumping. However, the estimated hydraulic conductivity for both the basin fill deposits and the oxide are consistent and of the order of magnitude expected for such geologic materials;
- ▶ although there is some evidence of fracture dominated flow near cluster 28 (near the Party Line Fault), interpretation of the available aquifer test data was accomplished by means of analytical models which rely on the continuum approach. This indicates that simulation of

flow with a code such as Modflow is appropriate at the scale of the proposed in-situ leaching area;

- ▶ hydraulic responses from well clusters 12, 19, and 39, located near the Sidewinder Fault, do not show any indication of discrete-feature dominated flow. Their conductivity estimates are in fact on the low end of the range for the oxide wells;
- ▶ hydraulic conductivity of the basin fill deposits, as expected, decreases with depth (see for example monitoring wells M14-GL and M15-GU);
- ▶ hydraulic connection between the UBFU and the LBFU is not well characterized by the available test data. No data are available to quantify this connection beyond the west margin of the proposed in-situ leaching area;
- ▶ hydraulic connection between the basin fill deposits and the oxide zone seems limited to non-existent in the vicinity of the proposed in-situ leaching area, except near cluster 28 where this connection has been identified in the analysis;

Combining the small-scale data with the regional test interpretations yields hydraulic conductivity estimates that varies over a wider range, from about 0.1 ft/day to over 60 ft/day. The results obtained from most small-scale pumping tests, as noted before, are strongly affected by nearby pumping and are therefore given less weight in the following summary.

Separation of the aquifer into basin fill units, and oxide and sulfide zones adequately represents the hydraulic characteristics of the aquifer. However other factors, for example the grain size distribution, the degree of consolidation, presence of faults and fractures (at some locations), considerably alter the hydraulic conductivity. Based on the interpretation of the aquifer tests, hydraulic conductivity of 1 ft/day to 60 ft/day was obtained for the sand, silt and clay portion of the

basin fill unit. Higher values are associated with the upper unconsolidated part whereas lower values occur near the interface with the oxide zone. The conductivity of the sand, gravel and boulder portion could not be estimated separately from the available tests but is expected to be near the same order of magnitude. A value of 17 ft/day was obtained for a region of the aquifer containing sand, silt, clay, gravel and boulders. The hydraulic conductivity of the quartz monzonite and granodiorite was estimated as 1 ft/day to 2 ft/day (Table 4). The presence of fault zones and associated fracture networks increases the effective conductivity of the oxide zone to about 40 ft/day over a length scale of about 3,000 ft (Cluster 28). This value, however, is based on the observations in a single cluster of wells and needs further verification with carefully planned tests.

It should also be noted that data from cluster 28 show hydraulic head recovery beyond the static head level therefore parameter estimates from these data may not be reliable. Surprisingly, most of the small-scale tests show a decrease in the hydraulic conductivity of the oxide zone when faults are present at or near the test area, except cluster 28. This decrease, however, was not that significant when compared to the range of conductivity (0.1 to 1.4 ft/day) for the local tests, and may be due to the influence of other wells pumping nearby.

Analyses of many of the tests described above show the effects from multiple pumping wells with unknown pumping rate histories. The actual effect of irrigation pumping on the magnitude of the estimated hydraulic parameters is not well understood. It would depend on whether a particular well is pumping or shut in after some period of pumping. When a nearby irrigation well is pumping, the test estimates would probably underestimate the actual aquifer parameters. When that well is recovering interpretation of the data yield overestimates of the actual parameters. The true effect, however, needs to be evaluated through analytical studies that simulate typical conditions observed in the field.

Several of the hydraulic responses for the tests analyzed in this report seem to be represented better by assuming a 3D flow geometry, possibly due to the partial penetration of wells. Geologic data and

hydrologic information from the regional test show that the overall behavior of the aquifer, at the scale of the proposed in-situ mine area, is better represented by a two-dimensional layered model. However, for some of the local tests, the flow behavior near the well is better represented by a 3D model.

Of paramount importance for in-situ mining operations and for environmental protection, is the distinction between porous media flow and flow resulting from discrete hydrologic features. So far, the available field data indicate that flow at the Florence Site can be generally characterized by a porous media approach, however, a particular location (cluster 28) shows strong fault controlled flow, which may result in preferential flow paths. These faults zones can be zones of high permeability or low permeability depending on the amount of fault gouge present and the age of the fault. Fractures can also show extreme variation in their permeability depending on whether or not clays and oxide minerals have been deposited in them. Heterogeneities such as these may be responsible for some of the peculiar behavior observed in some of the Florence aquifer tests. Existence of such features should be expected when consideration is given to the geology of the area.

5.0 RECOMMENDATIONS

Additional aquifer tests should be conducted in such a way to avoid the complicating factors like pumping from nearby wells. Since the pumping rate of the irrigation wells is much larger than that used for the tests, even the wells located far from the irrigation wells show a significant drawdown due to these wells. Whenever feasible, the irrigation should remain inactive during the test period. Field data collection should include at least the following: (a) hydraulic head measurement should be monitored at least one day prior and one day after the test is executed, (b) a detailed report, in electronic form if possible, on the pumping rates of all the well active during a test should be obtained, (c) field data should be processed as gathered to determine anomalous conditions and also to define when a test should be terminated, and (d) data collection should be continued until complete recovery to the static water is achieved.

The available field data seems to indicate that the hydraulic connection between the basin fill deposits and the oxide zone is limited. Not much information is available, however, regarding the interconnection between the UBFU and LBFU. If necessary, this information could be collected from several of the existing monitoring well clusters, for example, M6-GU and M7-GL, and M16-GU and M17-GL on the west margin of the in-situ mine area, M18-GU and M1-GL to the site of this area, and M10-GU and M11-GL on the east-central portion of this area.

As evidence by the data from the local and regional tests, the hydraulic data produced by these two types of tests are significantly different. Local tests produce information that is relevant to the operation of a particular in-situ leaching cluster, whereas the regional tests provide information related to overall behavior of the system. These latter data should be helpful in determining our ability to intercept and control migration of fluids away from a leaching cluster. It is our opinion that more regional tests are needed. The drawdown data should be collected for a sufficiently long time after the end of pumping, especially in observation wells far from the pumping well. Geologic features, such as the major faults should be monitored closely to determine their ability to move

fluids in all directions. If possible, it would be preferable to pump from well that is screened over a single zone. This would help in determining the nature and extent of hydraulic connection between the basin fill unit and the oxide zone, and the effect of discrete features. Also, these large scale tests should be supplemented with more detailed hydrologic evaluation of the local heterogeneity, such as spinner logger or heat pulse flow meter logs to determine the vertical distribution of the conductive zones.

6.0 REFERENCES

- Barker, J. A., A generalized radial flow model for hydraulic tests in fractured rock, *Water Resour. Res.*, 24, 1796, 1988.
- Brown and Caldwell, 1995, *Preliminary Site Characterization Report, Magma Florence In-Situ Project*, Brown and Caldwell, Phoenix, Arizona, December, 1995.
- Bourdet, D., Whittle, T.M., Douglas, A.A., and Pirard, Y.M., 1983, *A New Set of Type Curves Simplifies Well Test Analysis*, World Oil, May 1983, pp.95-1-6.
- Geraghty and Miller, 1995, *User manual for AQTESOLV, Aquifer Test Solver, Ver. 2.01*, Geraghty and Miller, Inc., Reston, Virginia, February, 1995.
- Golder Associates, 1993, *User manual for FLOWDIM, Ver. 2.0*, Golder Associates (UK), Ltd, Nottingham, U.K., September 1993.
- Golder Associates, 1995, *Data Report for the Initial Hydraulic Tests Interpretation for Magma Copper Company, Aquifer Protection Permit, Florence In Situ Leaching Project (Draft)*, Golder Associates Inc., Tucson, Arizona, November, 1995.
- Moench, A.F., 1985, *Transient Flow to a Large-Diameter Well in An aquifer With Storative Semiconfining Layers*, Water Resources Research, Vol. 21, No. 8, pp. 1121-1131.

TABLE 1 SUMMARY OF AVAILABLE HYDRAULIC TEST DATA

Active Well	Observation Wells	Start Date	End Date	Well Location	Screen Location	Drawdown Data	Rate (gpm)	Summary Sheet
M1-GL		11-Aug-95	13-Aug-95	X	X	X	10	X
	none							
M2-GU		25-Jul-95	26-Jul-95	X	X	X	10	X
	M3-GL			X	X	X		X
	M4-O			X	X	X		X
	M5-S			X	?	X		X
M3-GL		26-Jul-95	27-Jul-95	X	X	X	10	X
	M2-GU			X	X	X		X
	M4-O			X	X	X		X
	M5-S			X	X	X		X
M4-O		28-Jul-95	29-Jul-95	X	X	X	15	X
	M2-GU			X	X	X		X
	M3-GL			X	X	X		X
	M5-S			X	?	X		X
M10-GU		25-Jul-95	26-Jul-95	X	X	X	15	X
	M11-GL			X	X	X		X
	M12-O			X	X	X		X
	M13-S			X	X	X		X
M11-GL		29-Jul-95	30-Jul-95	X	X	X	14	X
	M10-GU			X	X	X		X
	M12-O			X	X	X		X
	M13-S			X	X	X		X
M12-O		31-Jul-95	1-Aug-95	X	X	X	15	X
	M10-GU			X	X	X		X
	M11-GL			X	X	X		X
	M13-S			X	?	X		X
M14-GL		11-Aug-95	13-Aug-95	X	X	X	10.5	X
	M15-GU			X	X	X		X
M15-GU		8-Aug-95	11-Aug-95	X	X	X	10	X
	M14-GL			X	X	X		X
M18-GU		8-Aug-95	11-Aug-95	X	X	X	10	X
	none							
P5-O (Modified)		18-Oct-95	24-Oct-95	X	X	X	66.5	X
	O5.1-O			X	X	X		X
	O5.2-O			X	X	X		X
PW1-1		7-Feb-94	14-Feb-94	X	X	X	33	N/A
	OB1-1			X	X	X		
	523MCC			X	X	X		
	OB-6			X	N/A	X		
PW2-1		8-Mar-94	21-Mar-94	X	X	X	50	N/A
	OB2-1			X	X			
PW2-2		20-Apr-94	2-May-94	X	X	X	45	N/A
	OB2-2			X	X	X		
PW3-1		24-Mar-94	1-Apr-94	X	X	X	58	N/A
	OB3-1			X	X	X		

Active Well	Observation Wells	Start Date	End Date	Well Location	Screen Location	Drawdown Data	Rate (gpm)	Summary Sheet
PW4-1	(Test 1)	19-May-94	?	X	X	X	71	N/A
	OB4-1			X	X	X		
PW4-1	(Test 2)	23-May-94	31-May-94	X	X	X	72	N/A
	OB4-1			X	X			
PW7-1		16-Jun-95	21-Jun-95	X	X	X	38	X
	OB7-1			X	X	X		X
	O3-GL			X	X	X		X
	OB-1			X	X	X		X
P8.2-O		?	?	X	X	?	?	?
(Test 3?)	P8-GL			X	X	?		
	P8.1-O			X	X	?		
	O8-O			X	X	?		
	O8-GL			X	X	?		
P8.1-O		8-Sep-95	11-Sep-95	X	X	X	12	X
(Test 1)	P8-GU			X	X	X		X
	P8.2-O			X	X	X		X
	O8-O			X	X	X		X
	O8-GU			X	X	X		X
P8-GU		18-Sep-95	22-Sep-95	X	X	X	85	X
(Test 2)	P8.1-O			X	X	X		X
	P8.2-O			X	X	X		X
	O8-O			X	X	X		X
	O8-GU			X	X	X		X
P12-O		1-Jun-95	7-Jun-95	X	X	X	64.5	X
	O12-O			X	X	X		X
	O12-GL			X	X	X		X
P13.1-O		9-Oct-95	16-Oct-95	X	X	X	46	X
	P13-GL			X	X	X		X
	P13.2-O			X	X	X		X
	O13-O			X	X	X		X
P15-O		29-Sep-95	5-Oct-95	X	X	X	59	X
	P15-GL			X	X	X		X
	O15-O			X	X	X		X
	WW3			?	?	?		X
	BIA-9			?	?	?		X
P19.1-O		3-Jul-95	6-Jul-95	X	X	X	24	X
	O19-O			X	X	X		X
	P19.2-O			X	X	X		X
	O19-GL			X	X	X		X
	138			X	X	X		X
P28-GL		20-Sep-95	25-Sep-95	X	X	X	75	X
	P28.1-O			X	X	No Data		
	P28.2-O			X	X	X		X
	O28-GL			X	X	X		X
	O28.1-O			X	X	X		X
	O28.2-S			X	X	X		X

Active Well	Observation Wells	Start Date	End Date	Well Location	Screen Location	Drawdown Data	Rate (gpm)	Summary Sheet
P28.1-O		15-Aug-95	18-Aug-95	X	X	X	28.5	X
(Test 1)	P28.2-O			X	X	X		X
	P28-GL			X	X	X		X
	O28-GL			X	X	X		X
	O28.1-O			X	X	X		X
	O28.2-S			X	X	No Data		
P28.1-O		8-Sep-95	11-Sep-95	X	X	X	86	X
(Test 2)	P28.2-O			X	X	X		X
	P28-GL			X	X	X		X
	O28-GL			X	X	X		X
	O28.1-O			X	X	X		X
	O28.2-S			X	X	No Data		
P28.2-O		2-Oct-95	5-Oct-95	X	X	X	76	X
	P28-GL			X	X	X		X
	P28.1-O			X	X	X		X
	O28.1-O			X	X	X		X
	O28-GL			X	X	X		X
	O28.2-S			X	X	X		X
P39-O		19-May-95	20-May-95	X	X	X	56	X
	O39-O			X	X	X		X
P49-O		11-Oct-95	16-Oct-95	X	X	X	41	X
	O49-O			X	X	X		X
	O49-GL			X	X	X		X

Regional Test

PMW-3		23-Aug-96	26-Aug-96	X	X	X	2,000	X
	O28-GL			X	X	X		X
	P15-GL			X	X	X		X
	O12-GL			X	X	X		X
	O3-GL			X	X	X		X
	M14-GL			X	X	X		X
	M15-GL			X	X	X		X
	O19-GL			X	X	X		X
	OB7-1			X	X	X		X
	P28.1-O			X	X	X		X
	P28.2-O			X	X	X		X
	O28.1-O			X	X	X		X
	P15-O			X	X	X		X
	O15-O			X	X	X		X
	O12-O			X	X	X		X
	O19-O			X	X	X		X
	Air Shaft			X	X	X		X

Well	Active/Observation	K (ft/day)	Ss (1/ft)	Comments	Model	Date
3-Dimensional Analyses						
LBFU						
M1-GL	Active	7.3	1.8E-4	(1), (2); Fair	Confined w/ WBS	11-Aug-95
M3-GL	Active	6.9	2.8E-5	(1), (3); Fair	Confined w/ WBS	26-Jul-95
M3-GL	Observation (M4-O)	5.7	7.6E-6	(1), (3); Fair	Confined	28-Jul-95
M14-GL	Active	0.9	1.3E-5	(1), (2); Fair	Confined w/ WBS	11-Aug-95
O19-GL	Observation (P19.1-O)	0.4	1.3E-8	(1),(2),(3);Fair	Confined	3-Jul-95
P28-GL	Active	3.4	1.9E-4	(1), (3); Fair	Confined w/ WBS	20-Sep-95
P28-GL	Observation (P28.1-O,2)	1.5	6.4E-7	(1); Good	Confined	8-Sep-95
O28-GL	Observation (P28.1-O,2)	2.0	8.4E-6	(1); Good	Confined	8-Sep-95
P28-GL	Observation (P28.2-O)	1.8	4.8E-6	(1), (2), (3) Fair	Confined	2-Oct-95
O28-GL	Observation (P28.2-O)	0.6	1.7E-8	(1), (2), (3) Fair	Confined	3-Oct-95
UBFU						
M15-GU	Active	0.9	4.4E-7	(1), (2), (3); Poor	Confined w/ WBS	8-Aug-95
M18-GU	Active	5.2	3.5E-6	(2); Poor	Confined w/WBS	8-Aug-95
OXIDE						
M4-O	Active	0.2	6.4E-6	(1), (3); Fair	Confined w/ WBS	28-Jul-95
M12-O	Active	2.5	6.3E-6	(1), (3); Fair	Confined w/ WBS	31-Jul-95
P8.1-O	Active/Recovery	0.4	1.1E-5	(1), (2), (3); Poor	Confined w/ WBS	8-Sep-95
P13.1-O	Active	0.2	1.2E-7	Good	Confined w/ WBS	9-Oct-95
P13.2-O	Observation (P13.1-O)	0.3	5.5E-7	Good	Confined	9-Oct-95
O15-O	Observation (P15-O)	0.5	9.7E-7	(1), (3); Fair	Confined	29-Sep-95
P19.1-O	Active	0.2	1.1E-7	(1), (2), (3); Fair	Confined w/ WBS	3-Jul-95
O19-O	Observation (P19.1-O)	0.2	3.8E-7	(1), (2), (3); Fair	Confined	3-Jul-95
P19.2-O	Observation (P19.1-O)	0.1	4.4E-8	(1), (2), (3); Fair	Confined	3-Jul-95
P28.2-O	Observation (P28-GL)	1.5	5.2E-7	(1), (3); Fair	Confined	20-Sep-95
O28.1-O	Observation (P28-GL)	1.2	1.2E-8	(1), (3); Fair	Confined	20-Sep-95
O28.2-S	Observation (P28-GL)	0.8	2.1E-8	(1), (3); Good	Confined	20-Sep-95
O28.1-O	Observation (P28.1-O,2)	0.5	6.8E-8	(1); Fair	Confined	8-Sep-95
O28.1-O	Observation (P28.2-O)	0.4	1.1E-8	(1), (2), (3); Fair	Confined	2-Oct-95
O28.2-S	Observation (P28.2-O)	0.4	3.4E-8	(1), (2), (3); Fair	Confined	2-Oct-95
P49-O	Active/Recovery Data	0.1	2.3E-6	Good	Confined w/ WBS	11-Oct-95
O49-O	Observation (P49-O)	0.1	5.4E-8	Good	Confined	11-Oct-95
PW1-1	Active	0.1	1.2E-7	Good	Confined w/WBS	7-Feb-94
OB1-1	Observation (PW1-1)	0.3	9.6E-8	Good	Confined	7-Feb-94
523MCC	Observation (PW1-1)	0.1	9.6E-8	Poor	Confined	7-Feb-94
PW4-1 (#1)	Active	1.8	3.7E-7	Good	Confined w/ WBS	19-May-94
Comments						
(1)	Other wells were pumping during this test at an unknown rate					
(2)	Data indicates recovery over the initial "static" water table					
(3)	Observation wells show effects of recovery or drawdown					
	produced by other wells					
Qualifiers Description						
Good	The reported K value is a good indication of the formation hydraulic conductivity					
Fair	The reported K value is most likely an under-estimation of the formation conductivity					
Poor	The reported K value has a large uncertainty due to conditions during test					
WBS	Well Borehole Storage effects considered					

Well	Active/Observation	K (ft/day)	S	Comments	Model	Date
2-Dimensional Analyses						
UBFU						
P8-GU	Active	61.3	3.2E-6	(1), (3); Poor	Confined w/ WBS	18-Sep-95
OXIDE						
P5-O	Active	1.3	8.3E-3	(1), (2), (3); Fair	Confined w/WBS	18-Oct-95
O5.2-O	Observation (P5-O)	2.2	2.3E-2	(1), (2), (3); Fair	Confined	18-Oct-95
PW2-1	Active	0.7	2.2E-3	Good	Leaky w/WBS	8-Mar-94
OB2-1	Observation (PW2-1)	1.0	1.6E-5	Good	Leaky	8-Mar-94
PW2-2	Active	0.3	3.4E-5	(1), (2), (3); Fair	Leaky w/WBS	20-Apr-94
OB2-2	Observation (PW2-2)	1.1	2.7E-4	(1), (2), (3); Poor	Leaky	20-Apr-94
PW3-1	Active	0.9	1.2E-3	(1), (2), (3); Fair	Leaky w/WBS	24-Mar-94
OB3-1	Observation (PW3-1)	0.5	1.6E-4	(1), (2), (3); Poor	Leaky	24-Mar-94
PW7-1	Active	0.2	1.9E-3	(1), (3); Fair	Confined w/ WBS	16-Jun-95
OB7-1	Observation (PW7-1)	0.1	1.3E-4	(1), (3); Fair	Confined	16-Jun-95
P12-O	Active	0.4	4.2E-1	(1), (2), (3); Poor	Confined w/ WBS	1-Jun-95
O12-O	Observation (P12-O)	0.8	9.6E-4	(1), (3); Poor	Confined	1-Jun-95
P39-O	Active	0.3	1.0E-3	Good	Confined w/ WBS	19-May-95
O39-O	Observation (P39-O)	0.3	4.3E-4	Good	Confined	19-May-95
P28.1-O (1)	Active	7.7	N/A	(1), (2), (3); Poor	Confined w/ WBS	15-Aug-95
P28.1-O (2)	Active	3.6	3.5E-2	(1); Good	Confined w/ WBS	8-Sep-95
P28.2 -O	Observation (P28.1-O,2)	2.7	2.9E-4	(1); Fair	Confined	8-Sep-95
P28.2-O	Active	3.1	N/A	(1), (3); Poor	Confined w/ WBS	2-Oct-95
P15-O	Active	0.5	1.3E-2	(1), (3); Fair	Confined w/ WBS	29-Sep-95
Comments						
(1)	Other wells were pumping during this test at an unknown rate					
(2)	Data indicates recovery over the initial "static" water table					
(3)	Observation wells show effects of recovery or drawdown					
	produced by other wells					
Qualifiers						
Description						
Good	The reported K value is a good indication of the formation hydraulic conductivity					
Fair	The reported K value is most likely an under-estimation of the formation conductivity					
Poor	The reported K value has a large uncertainty due to conditions during test					
WBS	Well Borehole Storage effects considered					

TABLE 3. SUMMARY OF AQUIFER TEST COORDINATES AND SCREEN INTERVALS

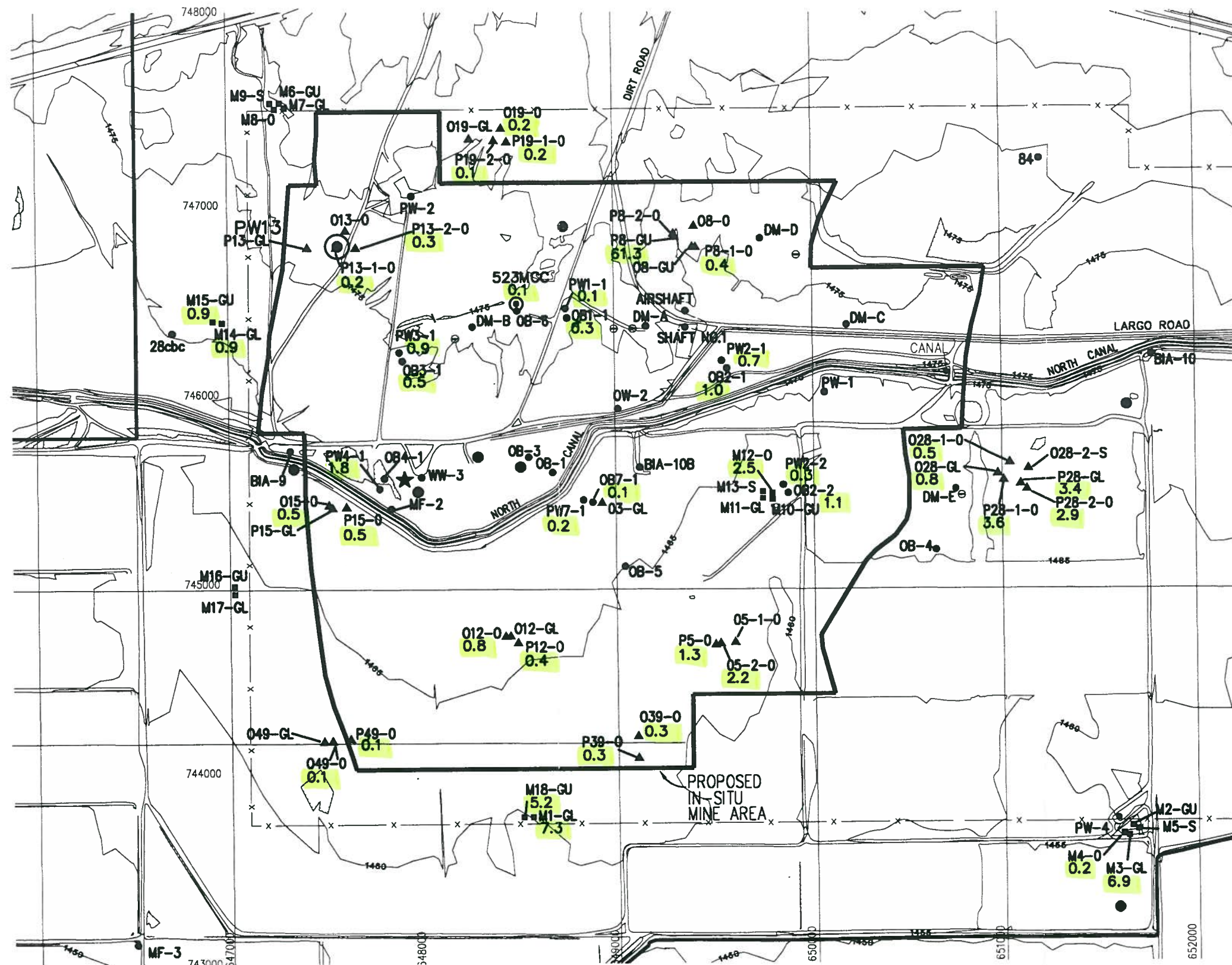
(All Vaules Are In Feet)

Well	Active/Observation	Screened Formation	Coordinates		Surface Elevation	Mid Elevation of Screen Interval	Top	Bottom	Screen Length
			Easting	Northing					
M1-GL	Active	LBFU	648501.52	743800.82	1461.1	1126.1	315.00	355.00	40.00
M3-GL	Active/Observation	LBFU	651636.79	743685.56	1458.8	1141.2	297.60	337.70	40.10
M14-GL	Active	LBFU	646964.20	746414.71	1472.8	665.0	777.90	837.80	59.90
M15-GU	Active	UBFU	646908.14	746418.02	1472.6	898.5	554.20	594.10	39.90
M18-GU	Active	LBFU	648550.02	743799.85	1461.0	1263.4	177.60	217.60	40.00
O12-GL	Observation	LBFU	648411.82	744745.55	1466.5	1121.5	325.00	365.00	40.00
O19-GL	Observation	LBFU	648233.62	747359.29	1481.7	1076.7	375.00	435.10	60.10
O28-GL	Observation	LBFU	650966.70	745592.65	1464.8	1173.1	276.70	306.80	30.10
O49-GL	Observation	LBFU	647477.36	744193.98	1461.2	770.6	660.58	720.62	60.04
P8-GU	Active	UBFU	649293.48	746846.80	1479.8	1291.5	128.20	248.40	120.20
O8-GU	Observation (P8-GU)	UBFU	649386.23	746792.74	1479.8	1287.7	132.80	251.40	118.60
P28-GL	Active/Observation	LBFU	651085.74	745535.76	1464.0	1170.0	279.00	309.00	30.00
M4-O	Active	Oxide	651635.22	743717.36	1458.9	1024.4	404.80	464.20	59.40
M12-O	Active	Oxide	649798.24	745506.14	1464.3	1014.5	419.50	480.10	60.60
PW1-1	Active	Oxide	648742.16	746476.50	1477.0	927.0	360.00	740.00	380.00
OBI-1	Observation (PW1-1)	Oxide	648750.08	746428.25	1476.5	926.5	360.00	740.00	380.00
523MCC	Observation (PW1-1)	Oxide	648476.00	746502.00			320.00	690.00	370.00
PW2-1	Active	Oxide	649536.12	746250.70	1471.0	961.0	400.00	620.00	220.00
OB2-1	Observation (PW2-1)	Oxide	649563.89	746157.89	1471.6	961.6	400.00	620.00	220.00
PW2-2	Active	Oxide	649854.34	745543.15	1464.3	854.3	460.00	760.00	300.00
OB2-2	Observation (PW2-2)	Oxide	649879.13	745500.70	1464.0	854.0	460.00	760.00	300.00
PW3-1	Active	Oxide	647873.55	746250.70	1475.5	835.5	500.00	780.00	280.00
OB3-1	Observation (PW3-1)	Oxide	647890.16	746204.02	1475.8	835.8	500.00	780.00	280.00
PW4-1	Active	Oxide	647769.65	745530.80	1471.8	861.8	440.00	780.00	340.00
PW7-1	Active	Oxide	648823.52	745467.86	1468.6	758.6	540.00	880.00	340.00
OB7-1	Observation (PW7-1)	Oxide	648872.17	745455.55	1468.3	758.3	540.00	880.00	340.00
P5-O	Active	Oxide	649499.22	744696.96	1462.4	870.4	414.00	770.00	356.00
O5.1-O	Observation (P5-O)	Oxide	649599.80	744708.01	1462.2	709.2	674.00	832.00	158.00
O5.2-O	Observation (P5-O)	Oxide	649524.74	744701.23	1462.2	720.7	712.00	771.00	59.00
P8.1-O	Active	Oxide	649403.82	746793.36	1478.9	989.3	399.50	579.60	180.10
P8.2-O	Observation	Oxide	649289.85	746863.66	1479.7	993.5	396.10	576.30	180.20
O8-O	Observation	Oxide	649393.30	746903.12	1481.3	991.0	401.50	579.20	177.70
P12-O	Active	Oxide	648473.26	744708.35	1466.0	776.0	440.00	940.00	500.00
O12-O	Observation (P12-O)	Oxide	648436.70	744739.89	1466.2	784.9	433.80	928.80	495.00
P13.1-O	Active	Oxide	647551.22	746799.40	1478.5	368.2	771.70	1448.85	677.15
P13.2-O	Observation (P13.1-O)	Oxide	647653.82	746807.64	1479.2	399.2	780.66	1379.35	598.69
P15-O	Active	Oxide	647596.44	745428.58	1468.0	527.8	580.00	1300.50	720.50
O15-O	Observation (P15-O)	Oxide	647508.44	745376.92	1467.5	503.6	632.20	1295.60	663.40
P19.1-O	Active	Oxide	648427.94	747345.78	1483.0	981.6	402.45	600.45	198.00
O19-O	Observation (P19.1-O)	Oxide	648359.48	747350.40	1482.7	974.0	409.80	607.60	197.80
P19.2-O	Observation (P19.1-O)	Oxide	648397.07	747413.63	1482.6	979.4	404.50	602.00	197.50
P28.1-O	Active	Oxide	650998.32	745558.54	1464.9	1114.9	300.00	400.00	100.00
P28.2-O	Active/Observation	Oxide	651118.23	745516.17	1465.4	1017.8	398.30	497.00	98.70
O28.1-O	Observation	Oxide	651027.87	745652.04	1464.6	1020.4	394.70	493.70	99.00
O28.2-S	Observation	Oxide	651123.95	745621.06	1464.8	991.0	454.40	493.30	38.90
P39-O	Active	Oxide	649102.65	744102.51	1461.7	813.2	471.00	826.00	355.00
O39-O	Observation (P39-O)	Oxide	649098.12	744220.52	1463.1	781.1	474.00	890.00	416.00
P49-O	Active (Recovery Data)	Oxide	647611.87	744202.71	1461.8	446.6	808.11	1222.30	414.19
O49-O	Observation (P49-O)	Oxide	647517.19	744195.29	1461.8	431.2	832.80	1228.40	395.60

Golder Associates

Table 4 Summary of Aquifer Parameters Derived
from the Regional Aquifer Test.

Well	S	K
Identification		(feet/day)
<i>2-D Interpretations</i>		
Basin Fill Deposits		
O28-GL	4.0E-03	38.8
P15-GL	1.1E-02	17.2
Oxide		
P28.1-O	4.0E-03	29.9
P28.2-O	3.0E-03	40.5
O28.1-O	3.4E-03	35.3
Well	Ss	K
Identification	(1/ft)	(feet/day)
<i>3-D Interpretations</i>		
Basin Fill Deposits		
O12-GL	1.4E-09	1.0
O3-GL	2.7E-09	1.8
M14-GL	1.1E-09	1.4
O19-GL	3.0E-10	2.4
Oxide		
P15-O	9.3E-09	1.4
O15-O	7.4E-09	1.3
O12-O	8.5E-10	0.8
O19-O	6.2E-10	2.0
Air Shaft	1.3E-09	1.9



EXPLANATION:

▲ P28-2-0 WELL IDENTIFIER

2.9 HYDRAULIC CONDUCTIVITY

DRAFT



- NOTE:
1. HYDRAULIC CONDUCTIVITY (K) VALUES ARE IN FT/DAY.
 2. TEST LOCATIONS AND TOPOGRAPHIC INFORMATION OBTAINED FROM BROWN AND CALDWELL, 1995



Golder Associates

Tucson, Arizona

CLIENT/PROJECT

MAGMA / FLORENCE

TITLE

TEST LOCATIONS AND HYDRAULIC CONDUCTIVITY ESTIMATES

DRAWN	MST	DATE	FEB 1996	JOB NO.	953-2908
CHECKED	WJE	SCALE	1" = 600'	DWG. NO./REV. NO.	0001
REVIEWED		FILE NO.	2908D001	FIGURE NO.	1

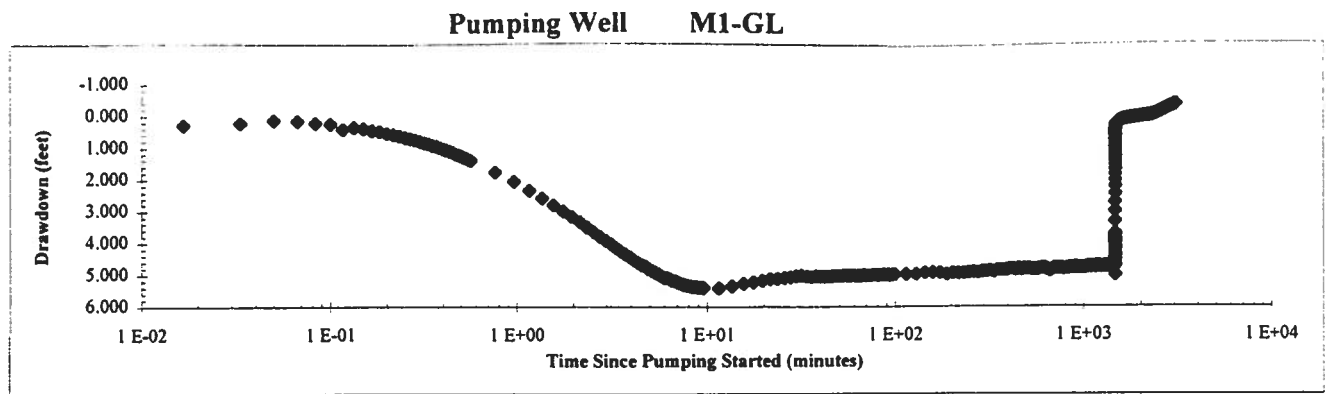
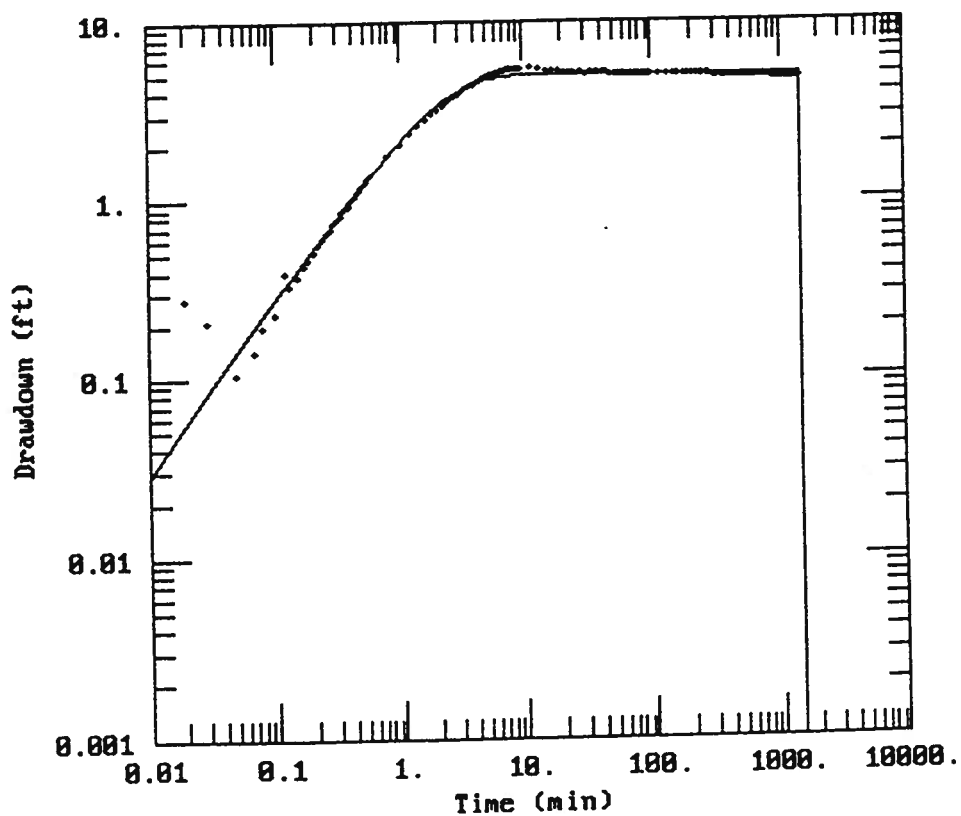


Figure 1A M1-GL Semi-Log Aquifer Test Plot



DATA SET:
M1-GL.DAT
01/05/96

AQUIFER MODEL:
Leaky

SOLUTION METHOD:
Moench

TEST DATA:
Q = 10. gal/min
r = 0. ft
r_c = 0.200 ft
r_w = 0.200 ft
b = 400. ft

PARAMETER ESTIMATES:
T = 142.6 ft²/day
S = 0.001304
r/B = 0.1189
B = 1.E-05
S_w = 0.
α = 0.0003807

Figure 1B M1-GL Aqtesolv™ Analysis Log-Log Plot

Hydraulic Conductivity Calculation for a Cylindrical Source

Well Name:	M1-GL
Sink Radius:	6.35E-02 m
Sink Screened Interval:	12.19 m
Pseudo-Transmissivity:	3.00E-05 m ² /sec
Pseudo-Storage:	6.91E-04
Anisotropy Ratio:	1.00

Pseudo-Spherical Radius:

 $r_{sw} = 1.16 \text{ m}$ Hydraulic Conductivity: $2.59\text{E-}05 \text{ m/sec} = 7.34 \text{ ft/day}$ Specific Storage: $5.96\text{E-}04 \text{ 1/m} = 1.82\text{E-}04 \text{ 1/ft}$ **Figure 1C M1-GL (3D) FlowDim™ Analysis Summary**

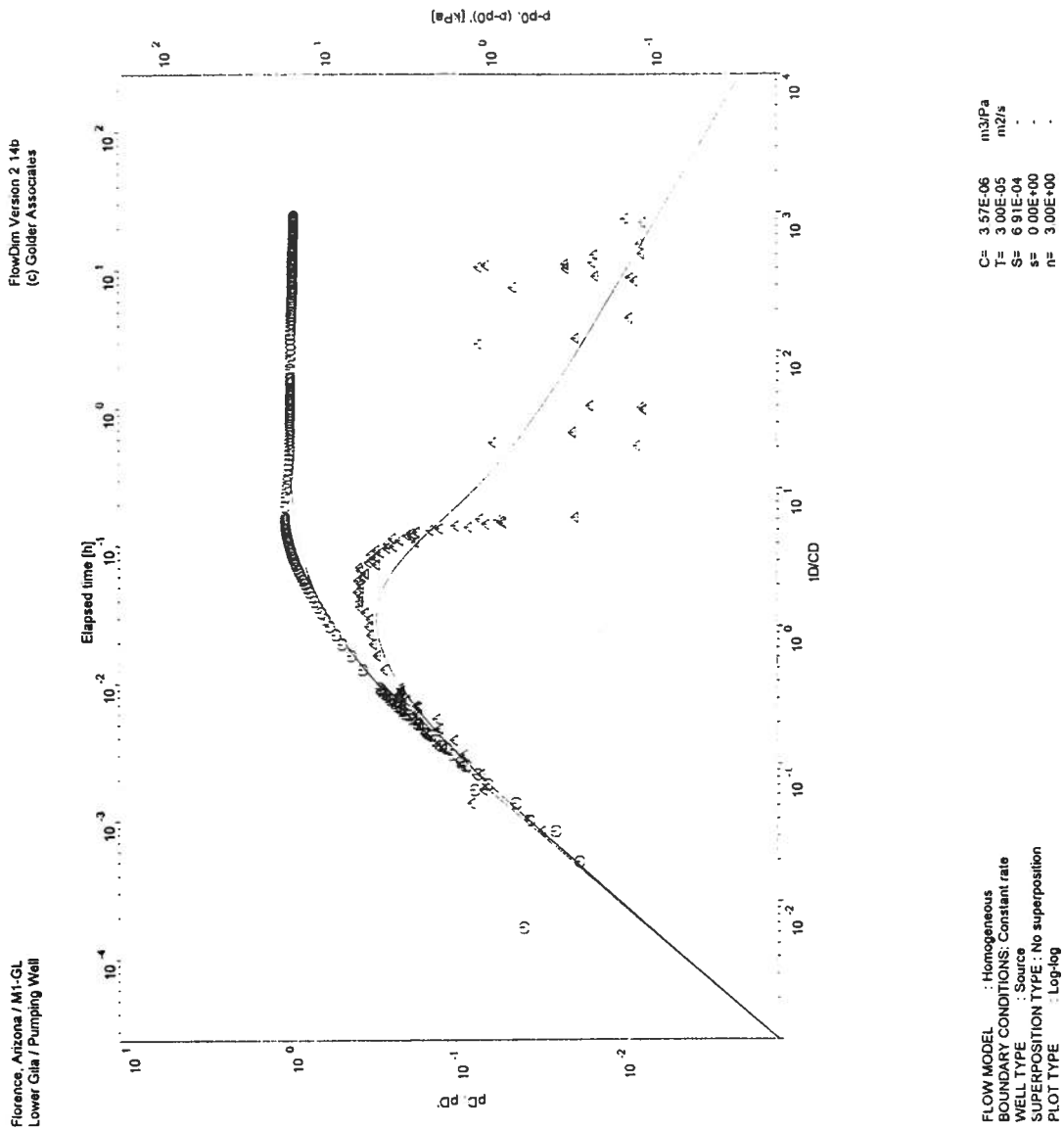
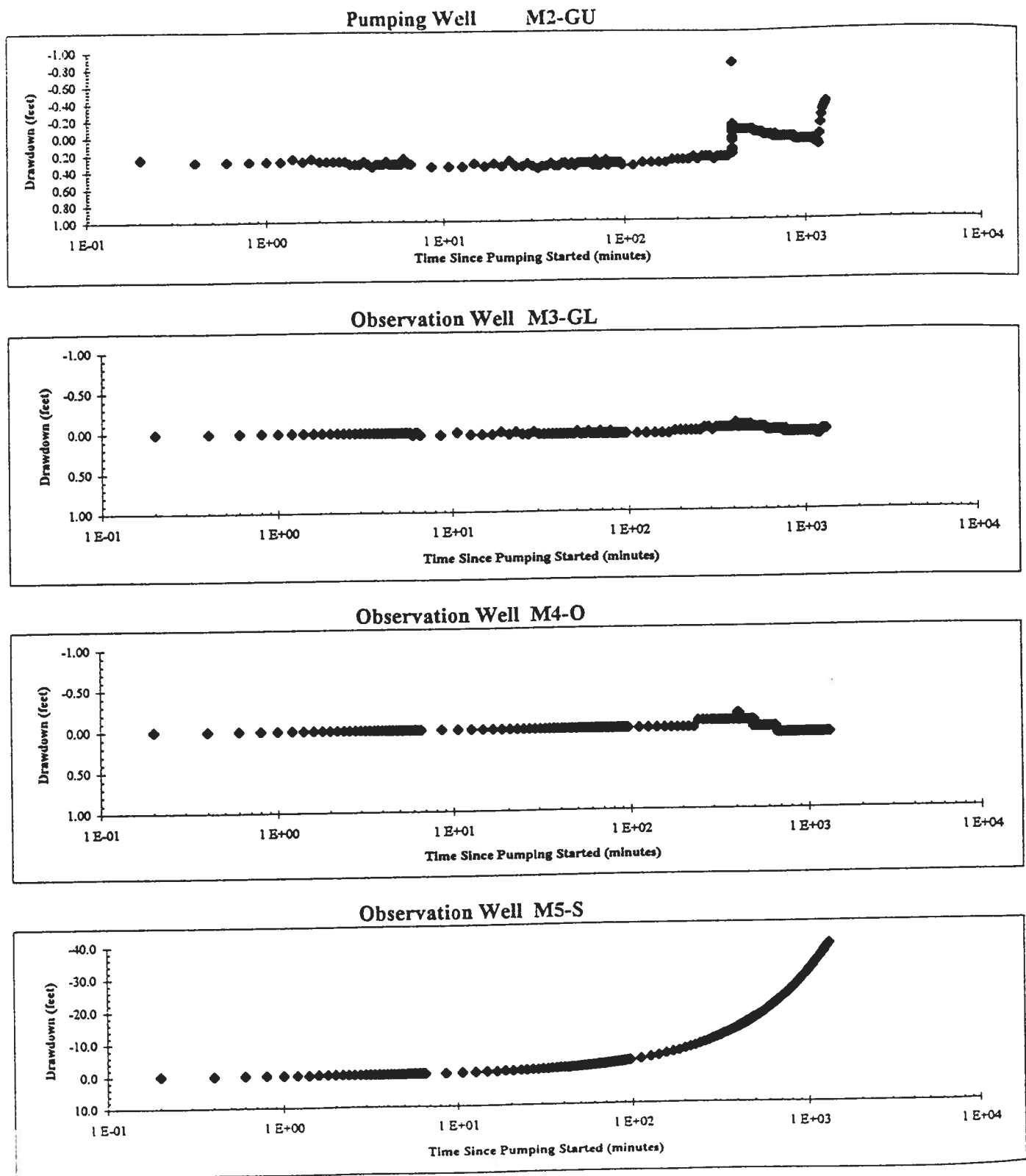
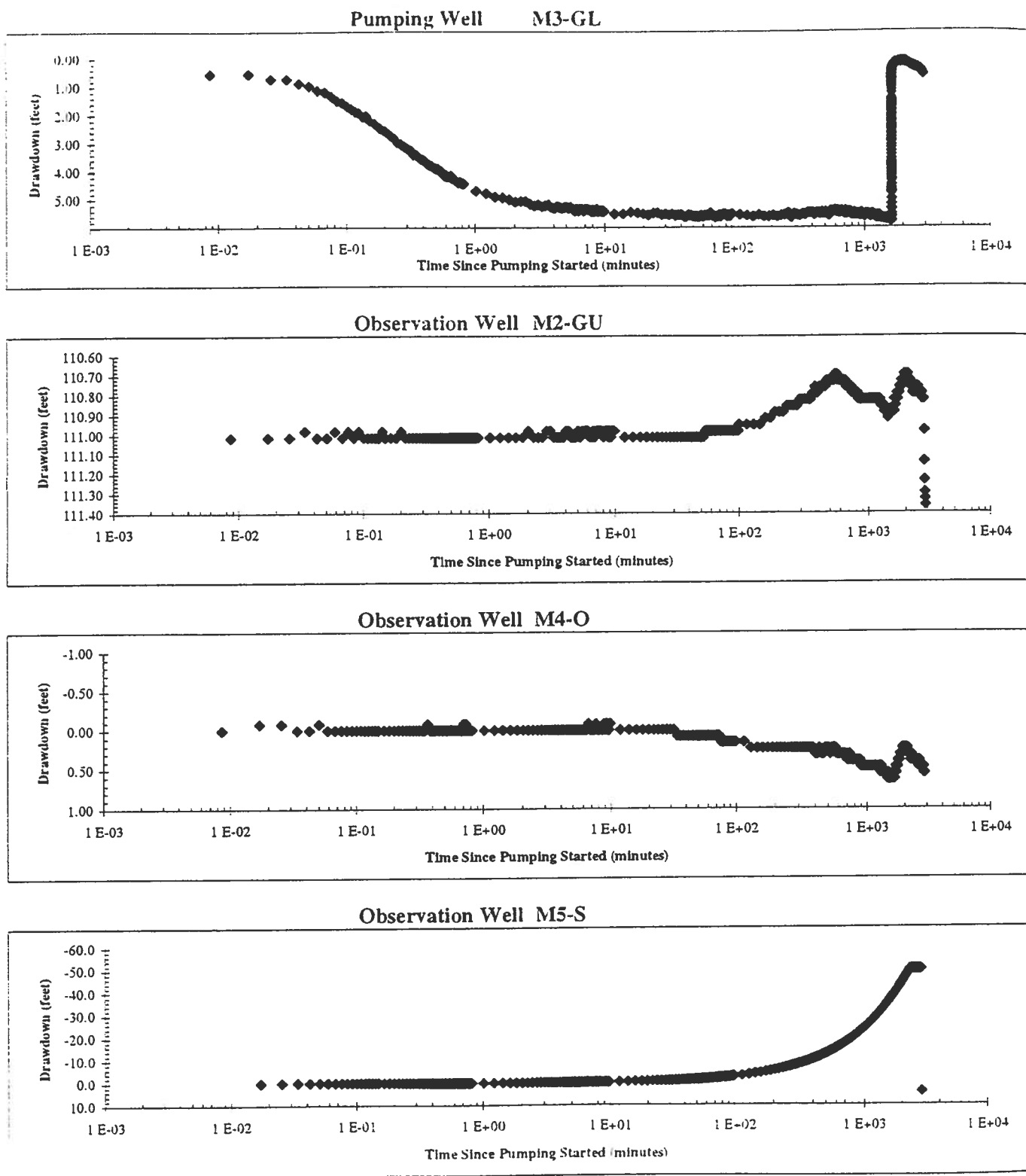
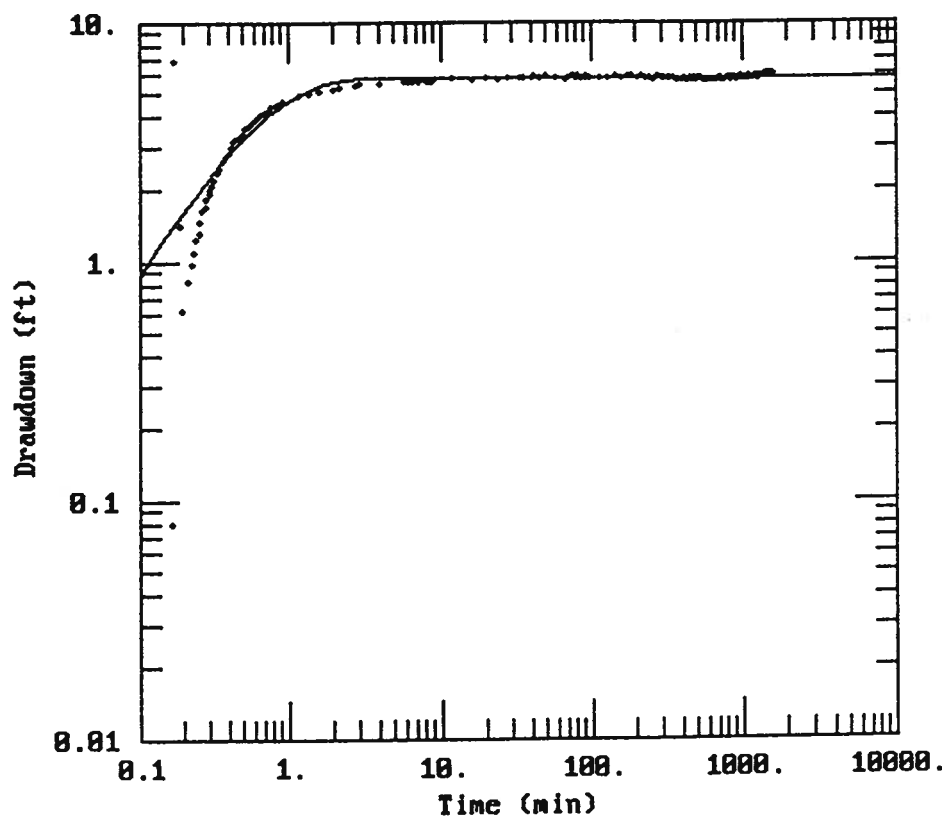


Figure 1D M1-GL (3D) FlowDim™ Analysis Log-Log Plot

**Figure 2A M2-GU Semi-Log Aquifer Test Plot**

**Figure 3A M3-GL Semi-Log Aquifer Test Plot**



DATA SET:
M3-GL.DAT
01/05/96

AQUIFER MODEL:
Leaky

SOLUTION METHOD:
Moench

TEST DATA:
Q = 10. gal/min
r = 0. ft
r_c = 0.2083 ft
r_w = 0.2083 ft
b = 400. ft

PARAMETER ESTIMATES:
T = 669.4 ft²/day
S = 8.351E-06
r/B = 1.023
β = 1.E-05
S_w = 12.
α = 8.886E-06

Figure 3B M3-GL Aqtesolv™ Analysis Log-Log Plot

Hydraulic Conductivity Calculation for a Cylindrical Source

Well Name:	M3-GL
Sink Radius:	6.35E-02 m
Sink Screened Interval:	12.19 m
Pseudo-Transmissivity:	2.80E-05 m ² /sec
Pseudo-Storage:	1.06E-04
Anisotropy Ratio:	1.00

Pseudo-Spherical Radius:

 $r_{sw} = 1.16 \text{ m}$ Hydraulic Conductivity: $2.42\text{E-}05 \text{ m/sec} = 6.85 \text{ ft/day}$ Specific Storage: $9.14\text{E-}05 \text{ 1/m} = 2.79\text{E-}05 \text{ 1/ft}$

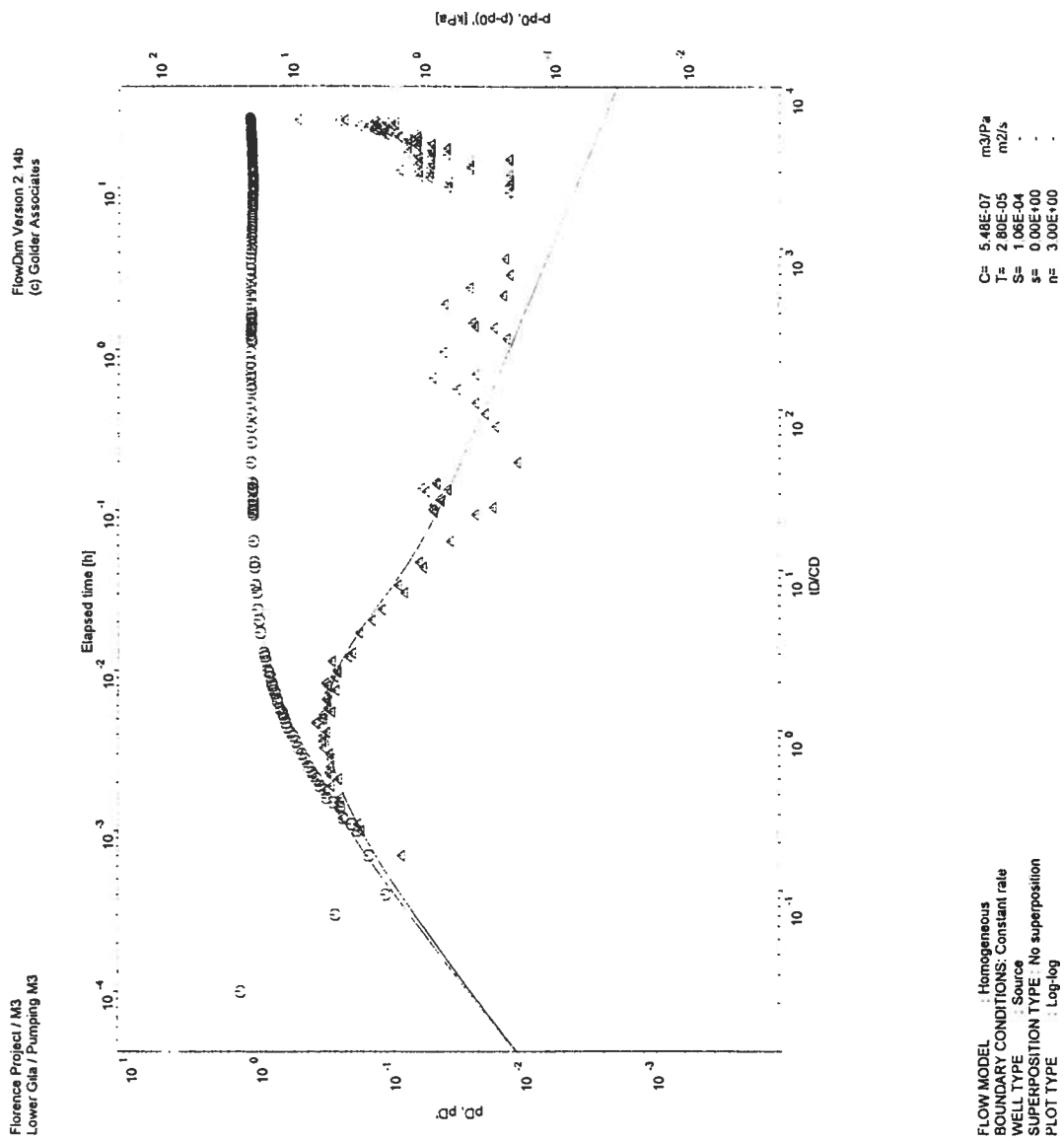
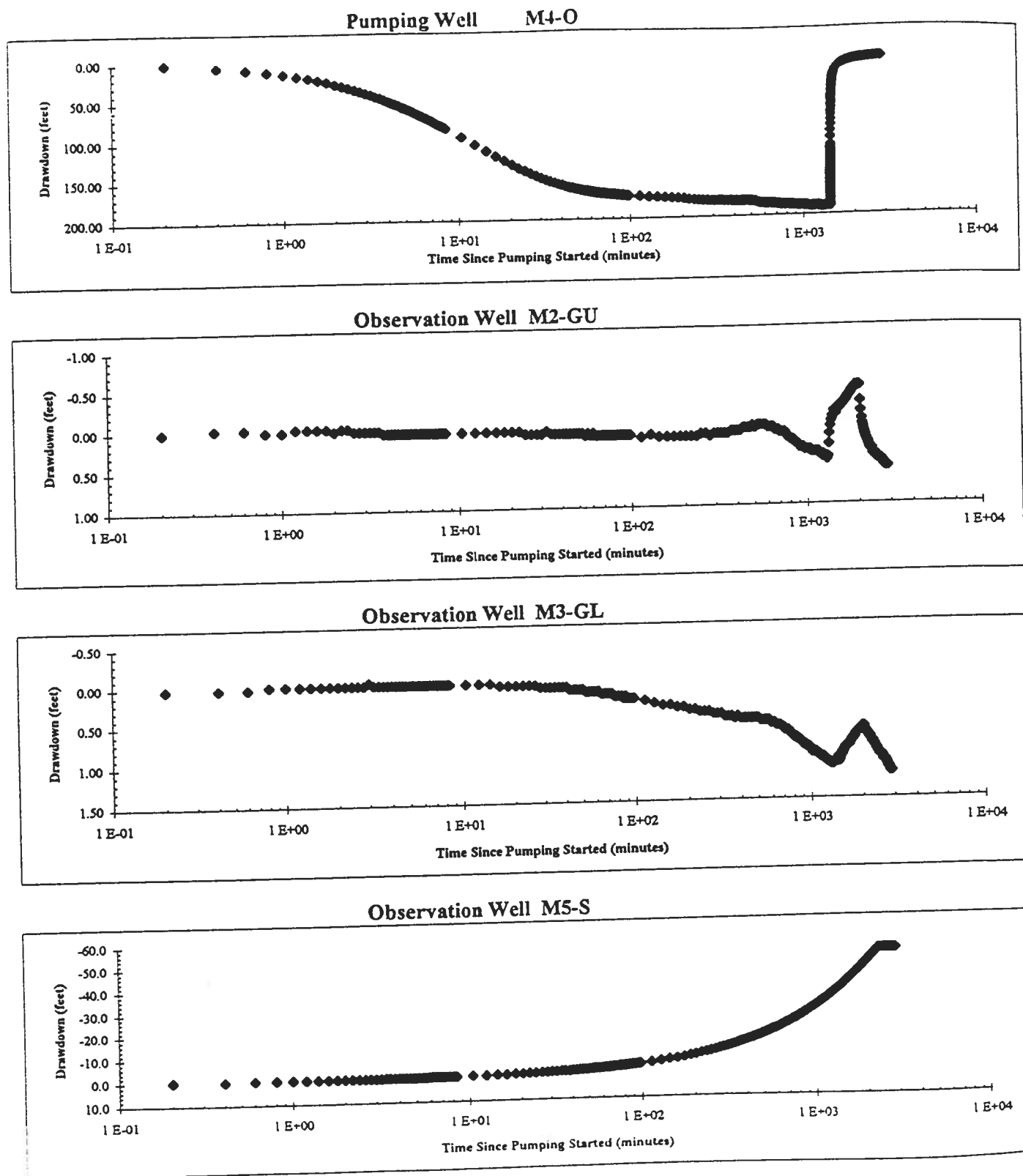
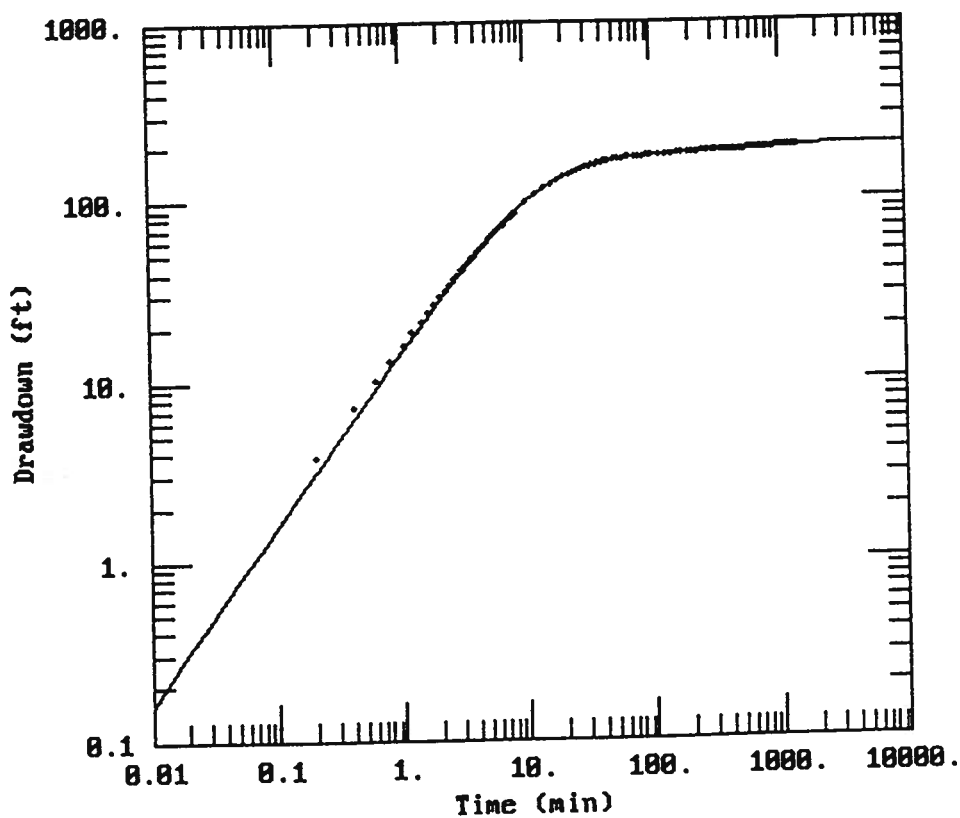


Figure 3D M3-GL(3D) FlowDim™ Analysis Log-Log Plot

**Figure 4A M4-O Semi-Log Aquifer Test Plot**



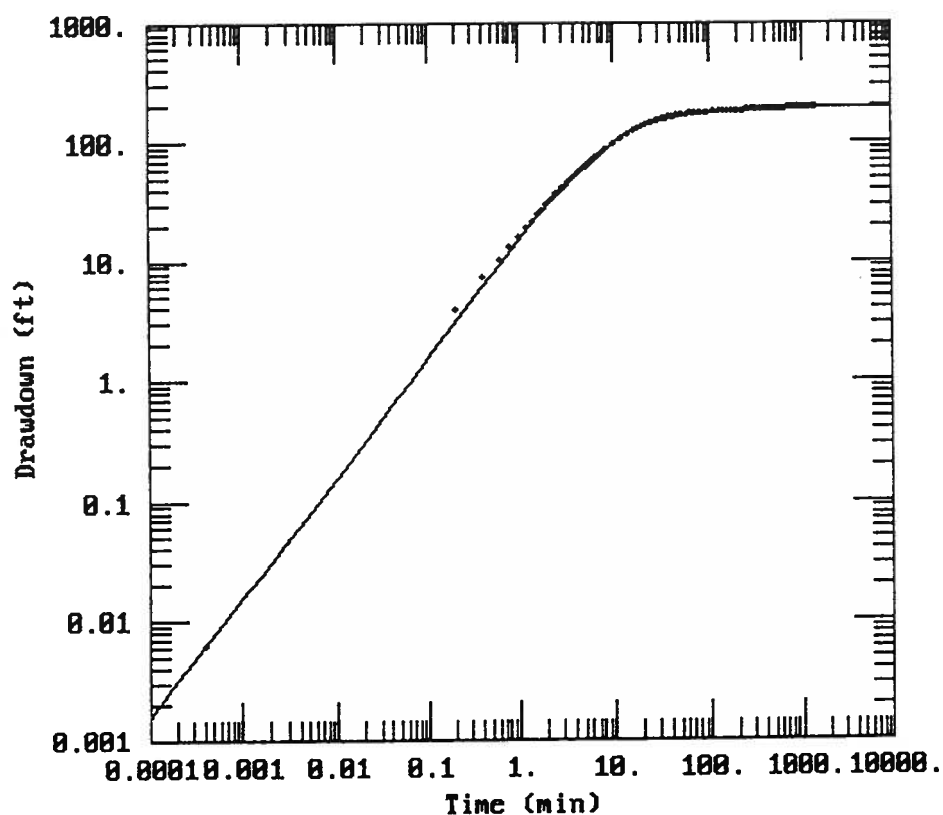
DATA SET:
M4-O.DAT
01/05/96

AQUIFER MODEL:
Leaky
SOLUTION METHOD:
Moench

TEST DATA:
Q = 15. gal/min
r = 0. ft
r_c = 0.2083 ft
r_w = 0.2083 ft
b = 800. ft

PARAMETER ESTIMATES:
T = 16.11 ft²/day
S = 0.03452
r/B = 0.03798
B = 0.06029
S_w = 3.594
α = 0.03698

Figure 4B1 M4-O Aqtesolv™ Analysis Log-Log Plot



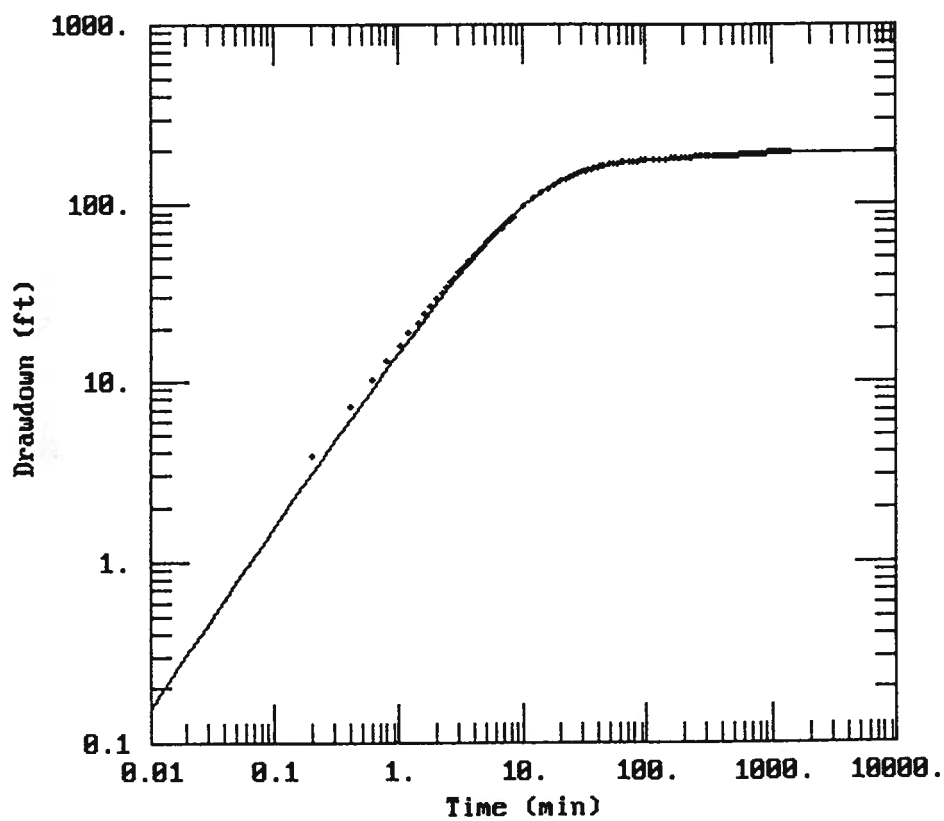
DATA SET:
M4-O.DAT
02/01/96

AQUIFER MODEL:
Leaky
SOLUTION METHOD:
Moench

TEST DATA:
Q = 15. gal/min
r = 0. ft
r_c = 0.2083 ft
r_w = 0.2083 ft
b = 800. ft

PARAMETER ESTIMATES:
T = 8.238 ft²/day
S = 0.004476
r/B = 0.4498
β = 10.
Sw = 2.308
α = 0.004723

Figure 4B2 M4-O Aqtesolv™ Analysis Log-Log Plot



DATA SET:
M4-O.DAT
02/01/96

AQUIFER MODEL:
Leaky
SOLUTION METHOD:
Moench

TEST DATA:
 $Q = 15.$ gal/min
 $r = 0.$ ft
 $r_c = 0.2083$ ft
 $r_w = 0.2083$ ft
 $b = 800.$ ft

PARAMETER ESTIMATES:
 $T = 10.67$ ft²/day
 $S = 0.09579$
 $r/B = 0.2873$
 $B = 1.285$
 $S_w = 3.046$
 $\alpha = 0.1$

Figure 4B3 M4-O Aqtesolv™ Analysis Log-Log Plot

Hydraulic Conductivity Calculation for a Cylindrical Source

Well Name:	M4-O
Sink Radius:	6.35E-02 m
Sink Screened Interval:	18.29 m
Pseudo-Transmissivity:	1.25E-06 m ² /sec
Pseudo-Storage:	3.40E-05
Anisotropy Ratio:	1.00

Pseudo-Spherical Radius:

$r_{sw} = 1.61 \text{ m}$

Hydraulic Conductivity: $7.74\text{E-}07 \text{ m/sec} = 0.22 \text{ ft/day}$

Specific Storage: $2.11\text{E-}05 \text{ 1/m} = 6.42\text{E-}06 \text{ 1/ft}$

Figure 4C M4-O (3D) FlowDim™ Analysis Summary

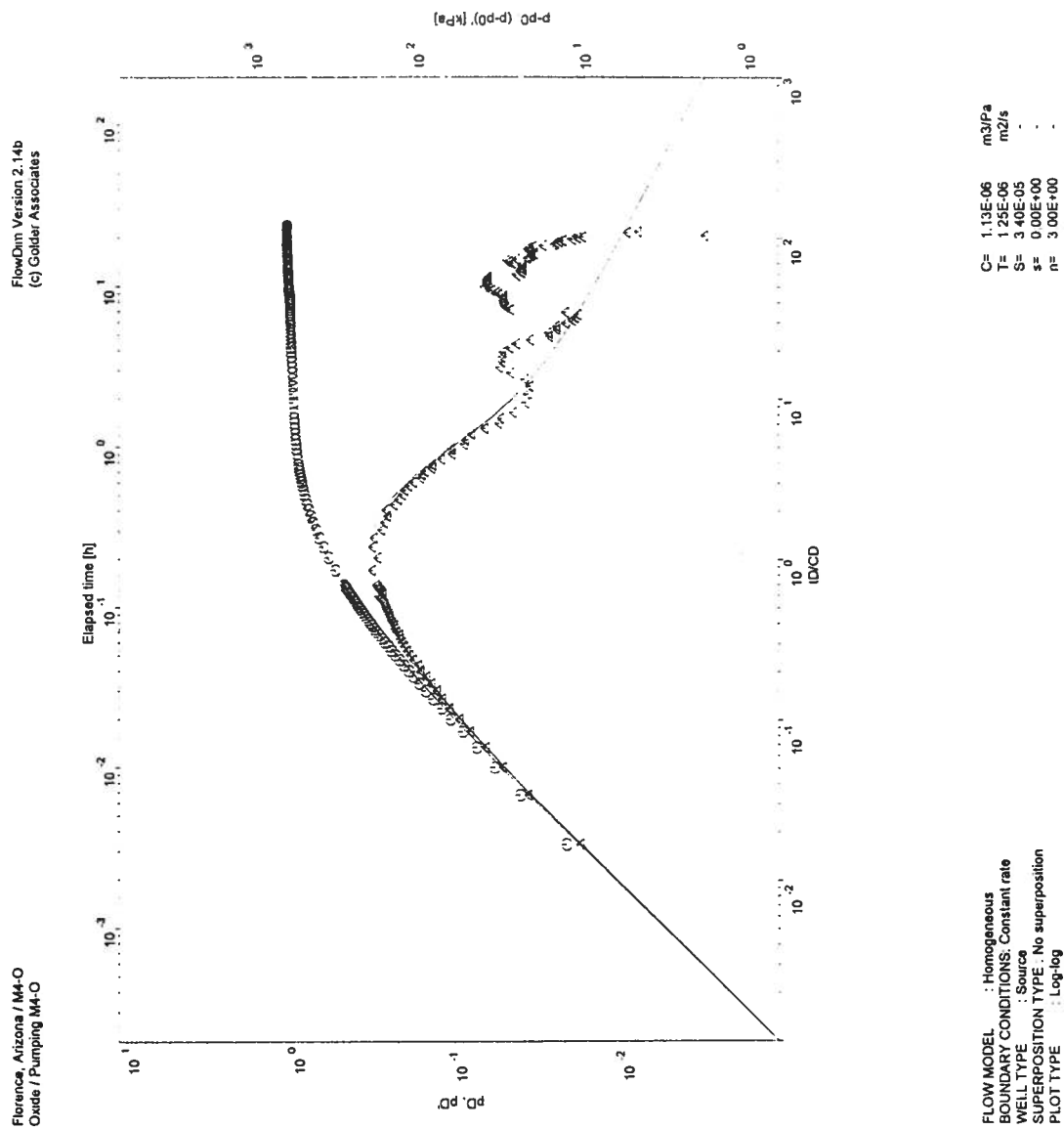


Figure 4D M4-O (3D) FlowDim™ Analysis Log-Log Plot

Hydraulic Conductivity Calculation for a Cylindrical Source

<u>PUMPING WELL</u>	M4-O	<u>OBSERVATION WELL</u>	M3_GL
Easting:	651635.2 ft	Easting	651636.8 ft
Northing:	743717.4 ft	Northing	743685.6 ft
Screen Top:	404.8 ft	Screen Top:	297.6 ft
Screen Bottom:	464.2 ft	Screen Bottom:	337.7 ft
Surface Elevation	1458.9 ft (amsl)	Surface Elevation	1458.8 ft
Radius:	7.62E-02 m	Screen Interval Mid-Point:	347.82 m
Screen Interval:	18.11 m	Distance to Sink:	14.6 m
Screen Interval Mid-Point:	312.24 m		

Pseudo-Transmissivity: 3.32E-05 m²/sec
 Pseudo-Storage: 3.19E-03
 Anisotropy Ratio: 1.00

Pseudo-Spherical Radius:

$$r_{sw} = 1.65 \text{ m}$$

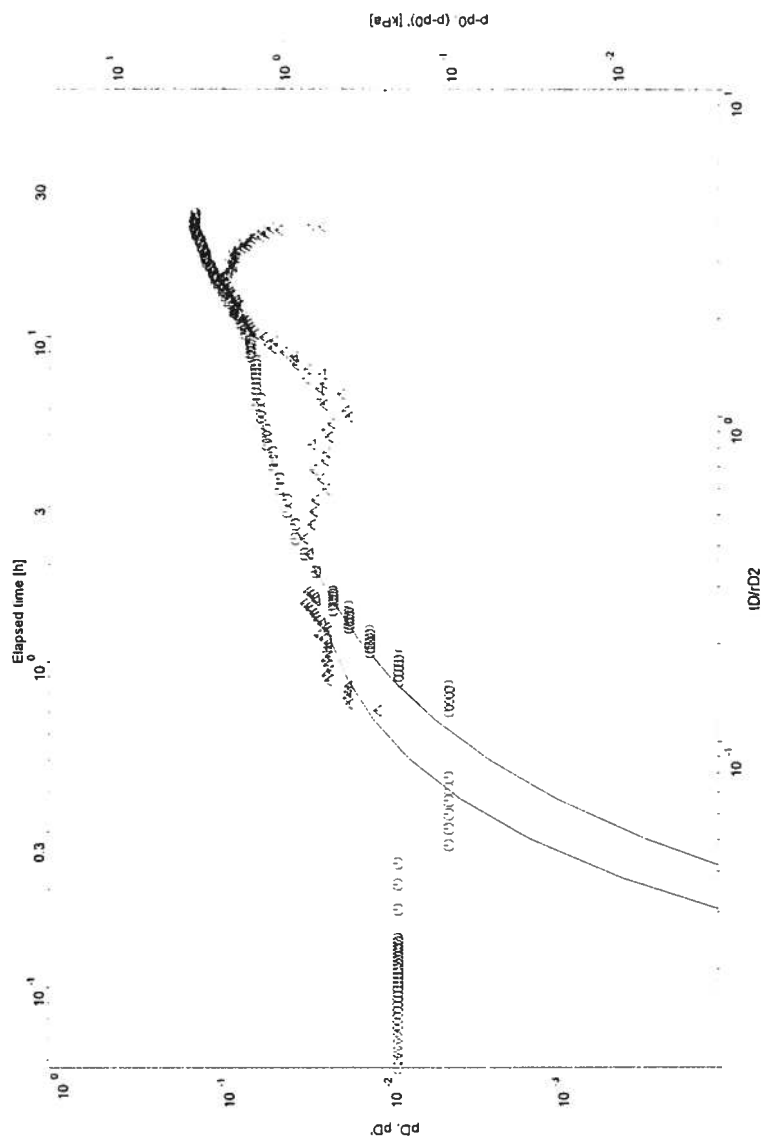
Hydraulic Conductivity: 2.01E-05 m/sec = 5.69 ft/day

Specific Storage: 2.49E-05 1/m = 7.60E-06 1/ft

Figure 4E M3-GL (3D) FlowDim™ Analysis Summary

FlowDim Version 2 14b
(c) Golder Associates

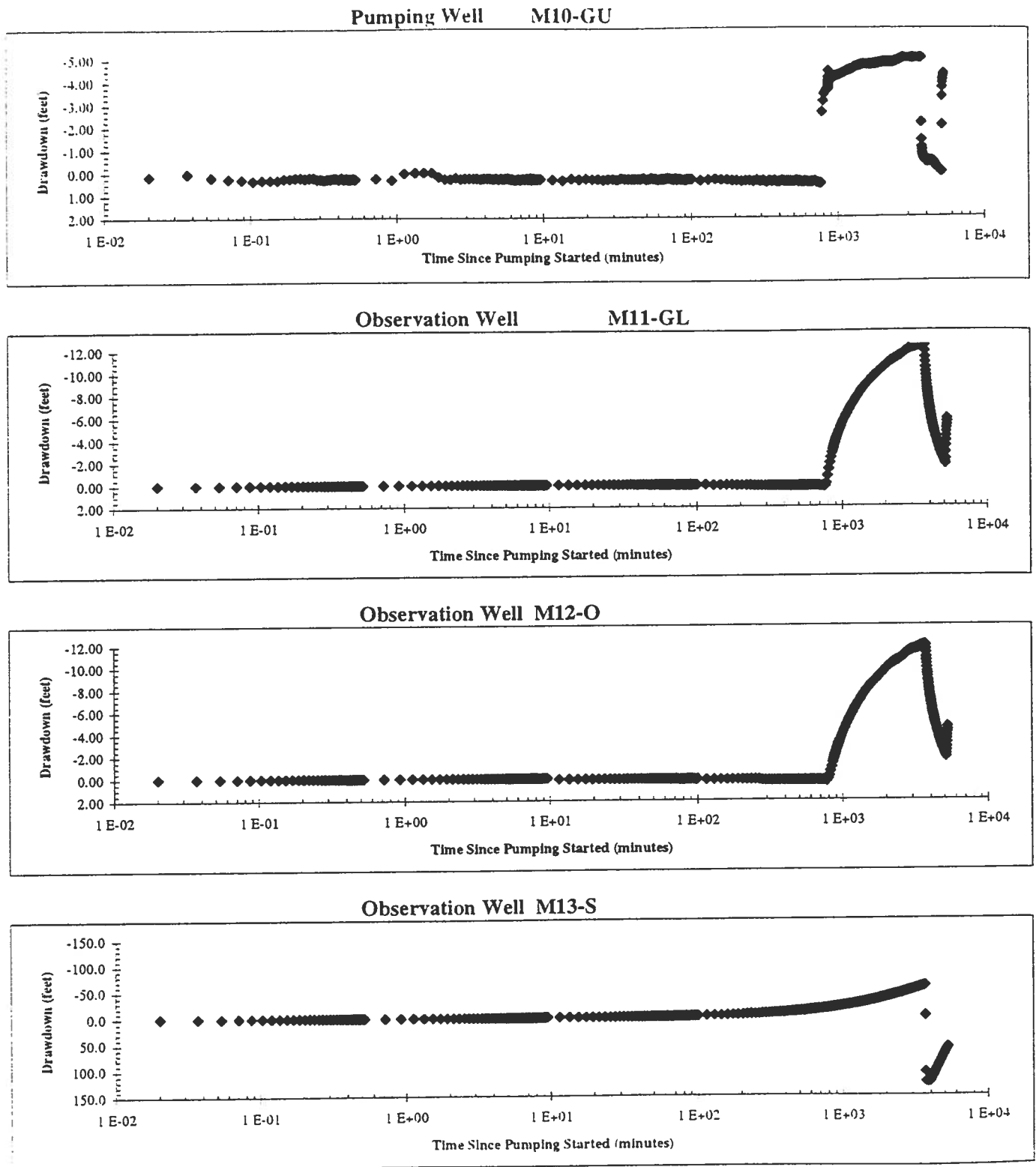
Florence Site / M3-GL
Lower Gila / Pumping M4-O

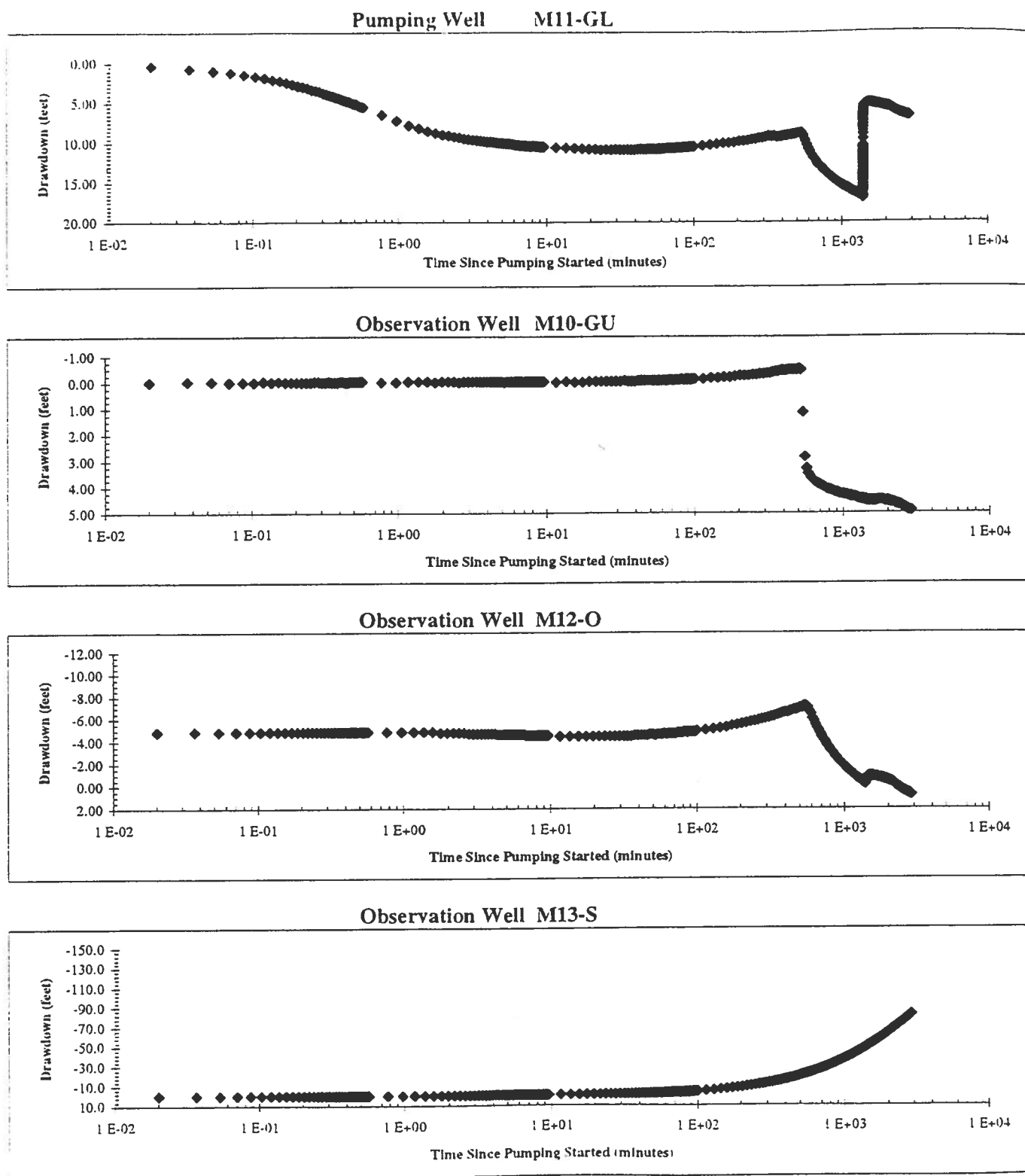


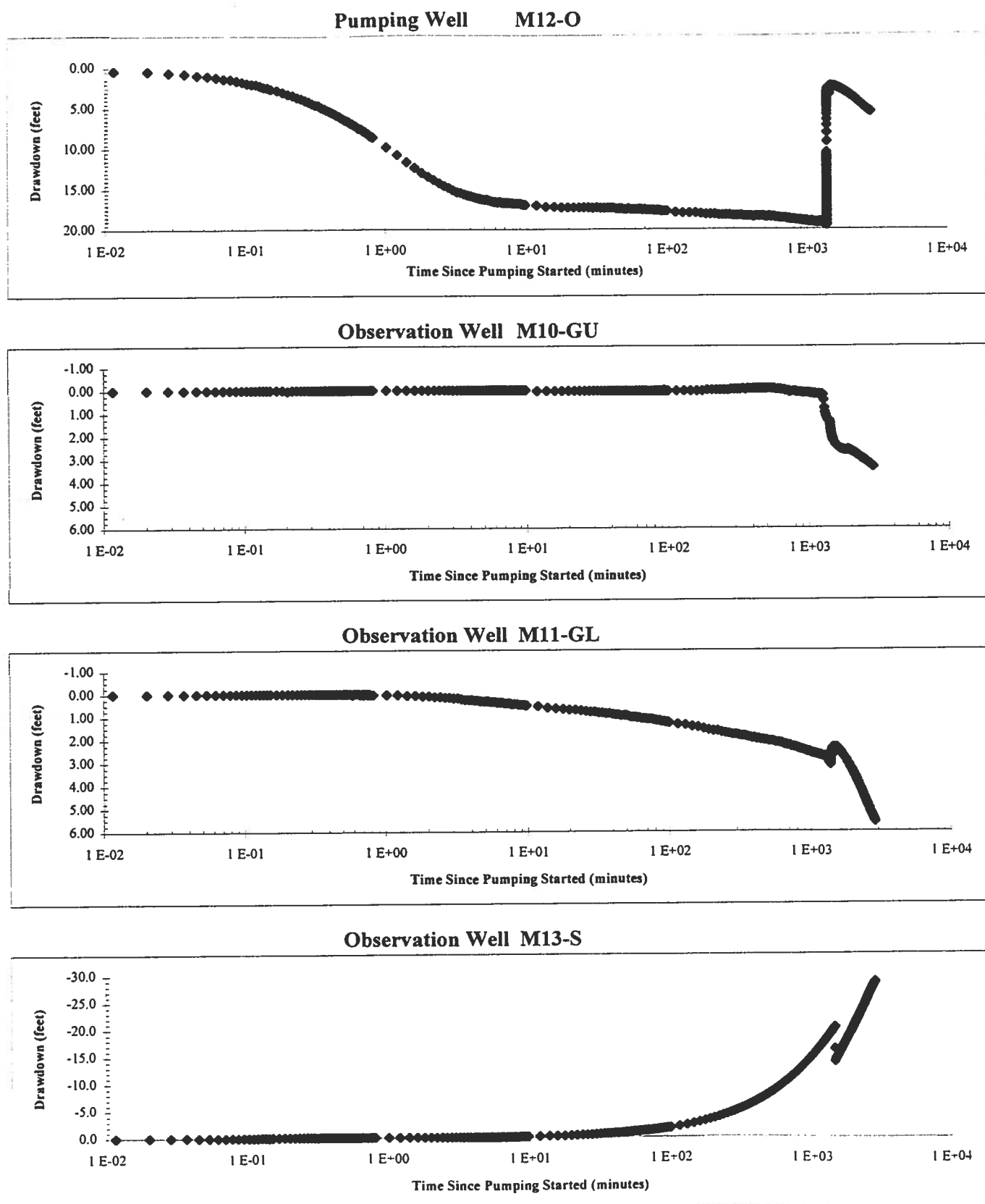
FLOW MODEL : Homogeneous
 BOUNDARY CONDITIONS: Constant rate
 WELL TYPE : Observation
 SUPERPOSITION TYPE: No superposition
 PLOT TYPE : Log-log

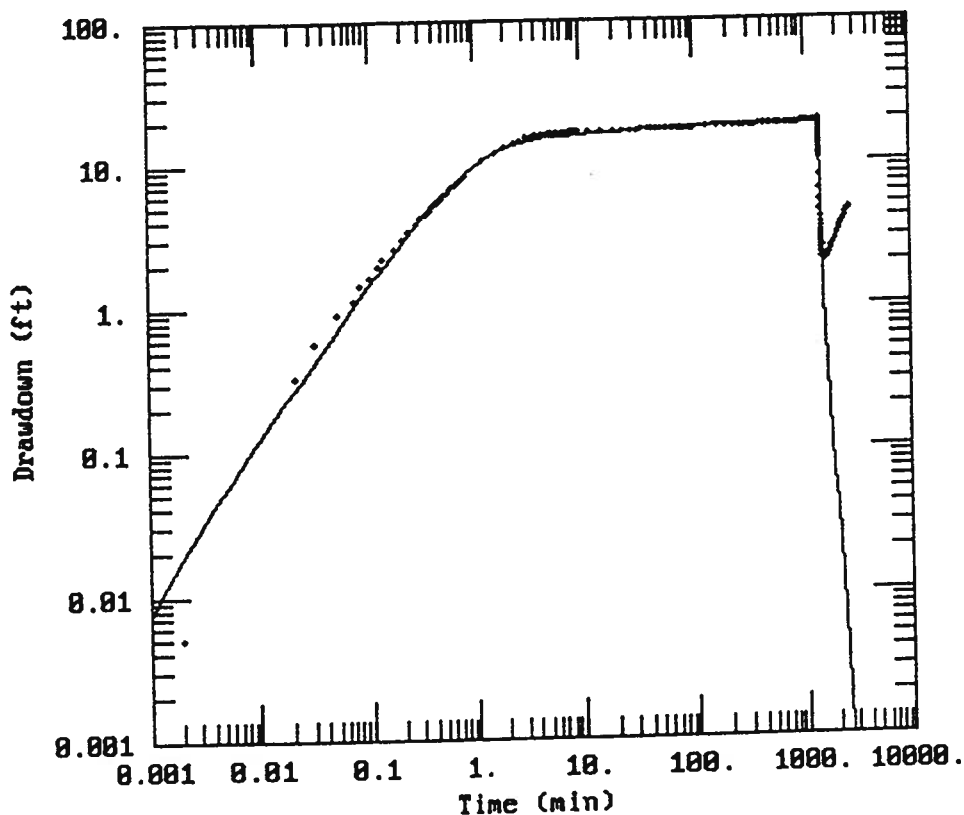
T= 3.32E-05 m2/s
 S= 3.19E-03
 rD= 8.65E+00
 n= 3.00E+00

Figure 4F M3-GL (3D) FlowDim™ Analysis Log-Log Plot

**Figure 5A M10-GU Semi-Log Aquifer Test Plot**

**Figure 6A M11-GL Semi-Log Aquifer Test Plot**

**Figure 7A M12-O Semi-Log Aquifer Test Plot**



DATA SET:
M12-O.OUT
81/16/96

AQUIFER MODEL:
Leaky
SOLUTION METHOD:
Moench

PROJECT DATA:
test date: July 31, 1995
test well: M12-0
obs. well: M12-0

TEST DATA:
 $Q = 15.$ gal/min
 $r = 0.208$ ft
 $r_c = 0.208$ ft
 $r_w = 0.208$ ft
 $b = 480.$ ft

PARAMETER ESTIMATES:
 $T = 149.9$ ft²/day
 $S = 0.0001622$
 $r/B = 0.00269$
 $\beta = 0.005152$
 $S_w = 9.484$
 $\alpha = 0.0006426$

Figure 7B M12-O Aqtesolv™ Analysis Log-Log Plot

Hydraulic Conductivity Calculation for a Cylindrical Source

Well Name:	M12-O
Sink Radius:	6.35E-02 m
Sink Screened Interval:	18.47 m
Pseudo-Transmissivity:	1.42E-05 m ² /sec
Pseudo-Storage:	3.36E-05
Anisotropy Ratio:	1.00

Pseudo-Spherical Radius:

 $r_{sw} = 1.63 \text{ m}$ Hydraulic Conductivity: $8.72\text{E-}06 \text{ m/sec} = 2.47 \text{ ft/day}$ Specific Storage: $2.06\text{E-}05 \text{ 1/m} = 6.29\text{E-}06 \text{ 1/ft}$ **Figure 7C M12-O FlowDim™ Analysis Summary**

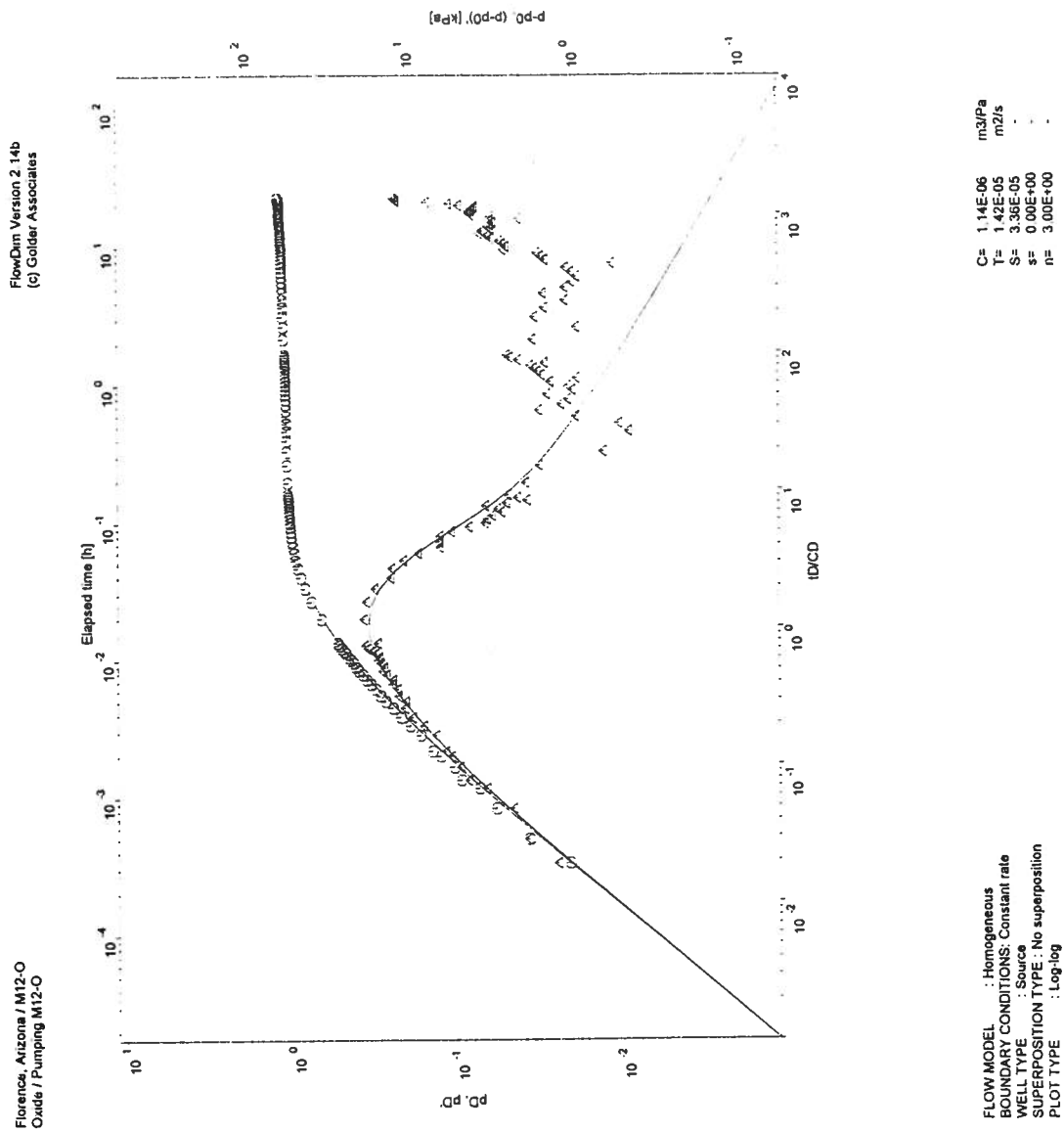
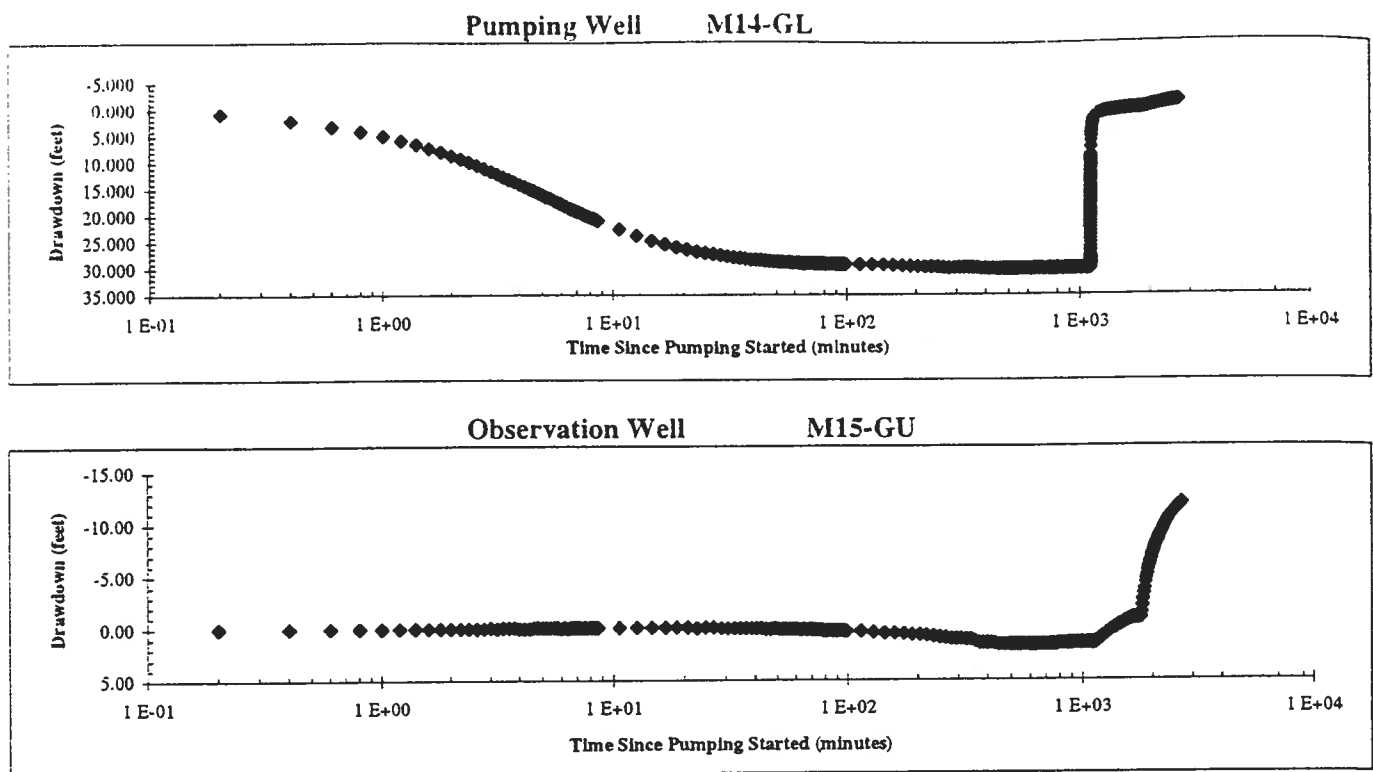


Figure 7D M12-O FlowDim™ Analysis Log-Log Plot

**Figure 8A M14-GL Semi-Log Aquifer Test Plot**

Hydraulic Conductivity Calculation for a Cylindrical Source

Well Name:	M14-GL
Sink Radius:	6.35E-02 m
Sink Screened Interval:	18.29 m
Pseudo-Transmissivity:	5.31E-06 m ² /sec
Pseudo-Storage:	6.65E-05
Anisotropy Ratio:	1.00

Pseudo-Spherical Radius:

$r_{sw} = 1.61 \text{ m}$

Hydraulic Conductivity: $3.29\text{E-}06 \text{ m/sec} = 0.93 \text{ ft/day}$

Specific Storage: $4.12\text{E-}05 \text{ 1/m} = 1.26\text{E-}05 \text{ 1/ft}$

Figure 8B M14-GL (3D) FlowDim™ Analysis Summary

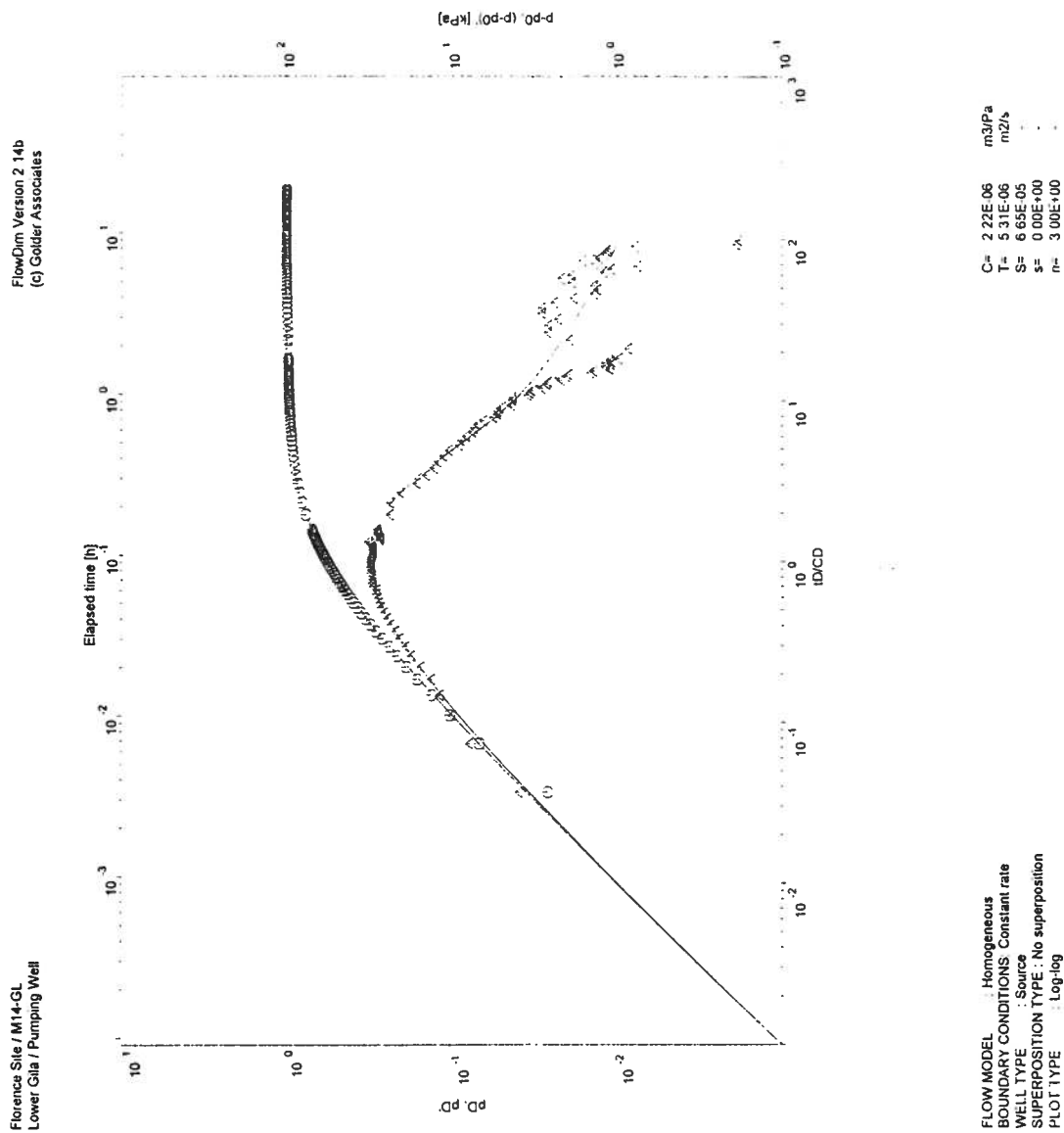
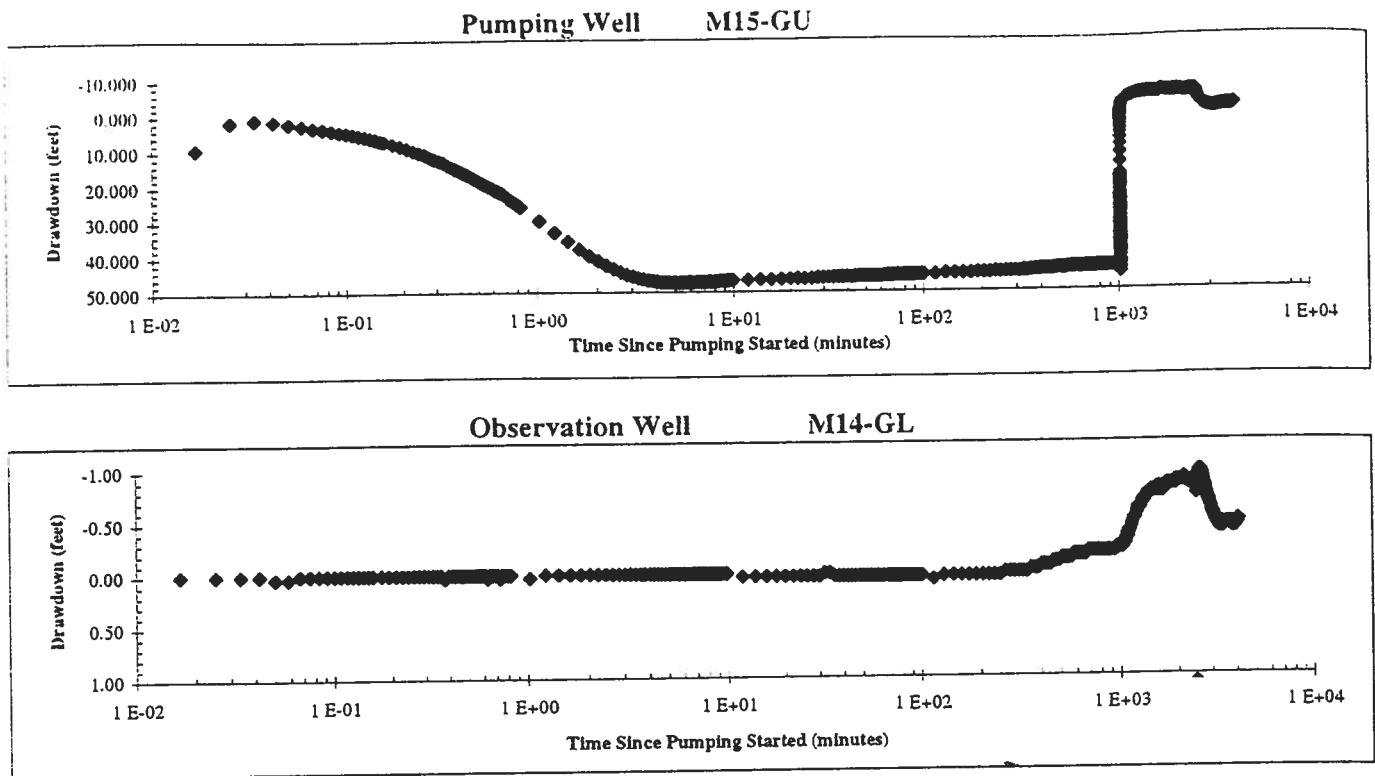
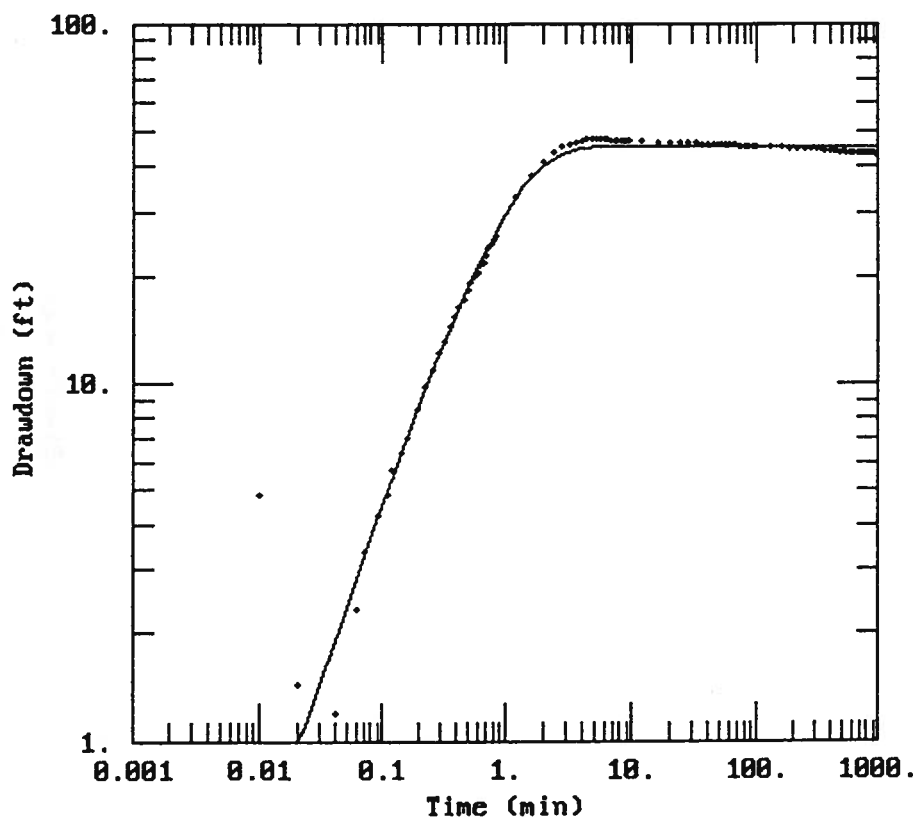


Figure 8C M14-GL (3D) FlowDim™ Analysis Log-Log Plot

**Figure 9A M15-GU Semi-Log Aquifer Test Plot**



DATA SET:
M15-GU.DAT
01/05/96

AQUIFER MODEL:
Leaky
SOLUTION METHOD:
Moench

TEST DATA:
 $Q = 10.$ gal/min
 $r = 0.$ ft
 $r_w = 0.208$ ft
 $b = 600.$ ft

PARAMETER ESTIMATES:
 $T = 26.46$ ft²/day
 $S = 0.000124$
 $r/B = 0.0049$
 $\beta = 0.0006586$
 $S_w = 1.307$
 $\alpha = 0.0006004$

Figure 9B M15-GU Aqtesolv™ Analysis Log-Log Plot

Hydraulic Conductivity Calculation for a Cylindrical Source

Well Name:	M15-GU
Sink Radius:	6.35E-02 m
Sink Screened Interval:	12.19 m
Pseudo-Transmissivity:	3.78E-06 m ² /sec
Pseudo-Storage:	1.69E-06
Anisotropy Ratio:	1.00

Pseudo-Spherical Radius:

 $r_{sw} = 1.16 \text{ m}$ Hydraulic Conductivity: $3.26\text{E-}06 \text{ m/sec} = 0.92 \text{ ft/day}$ Specific Storage: $1.46\text{E-}06 \text{ 1/m} = 4.44\text{E-}07 \text{ 1/ft}$ **Figure 9C M15-GU FlowDim™ Analysis Summary**

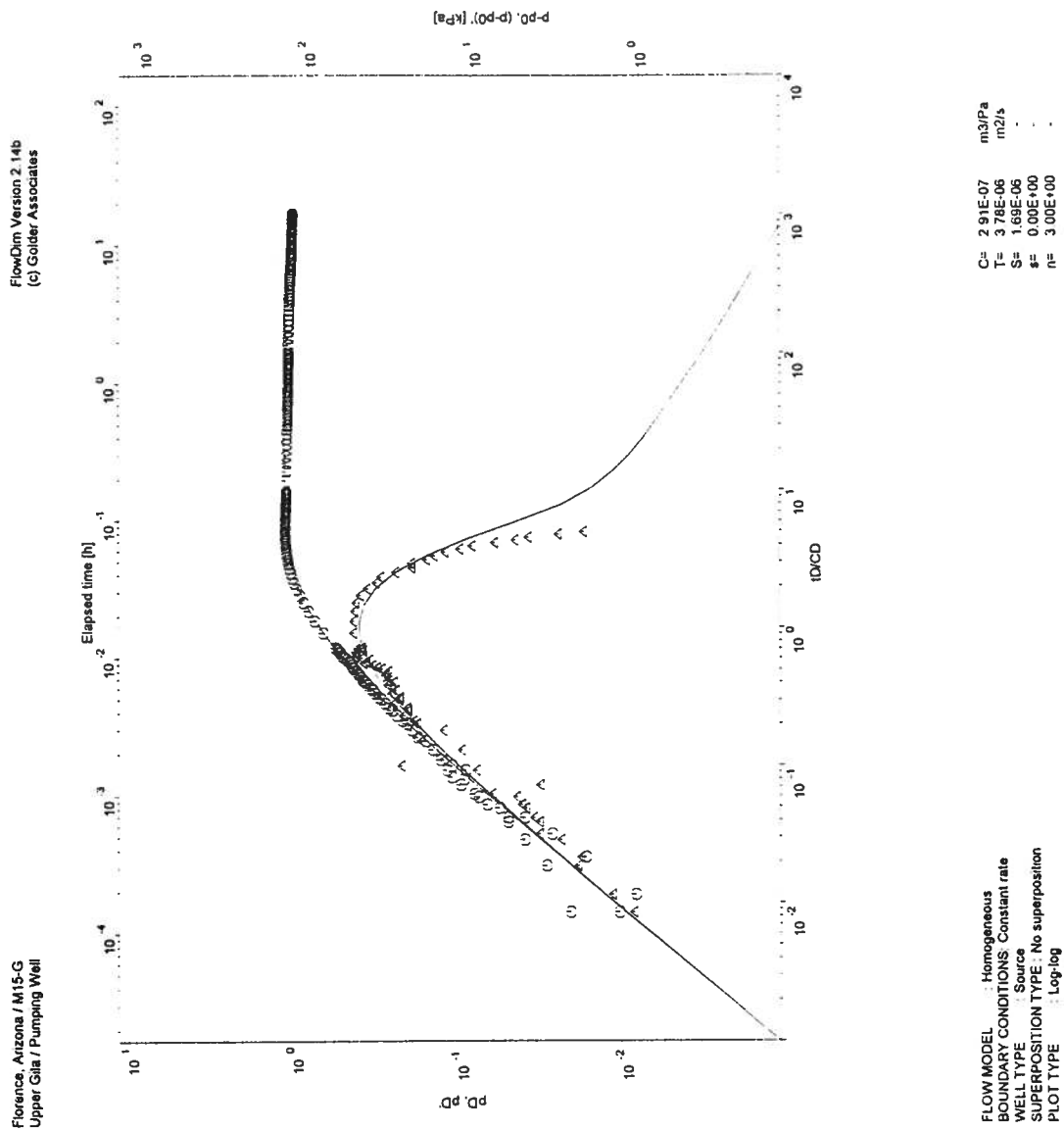


Figure 9D M15-GU FlowDim™ Analysis Log-Log Plot

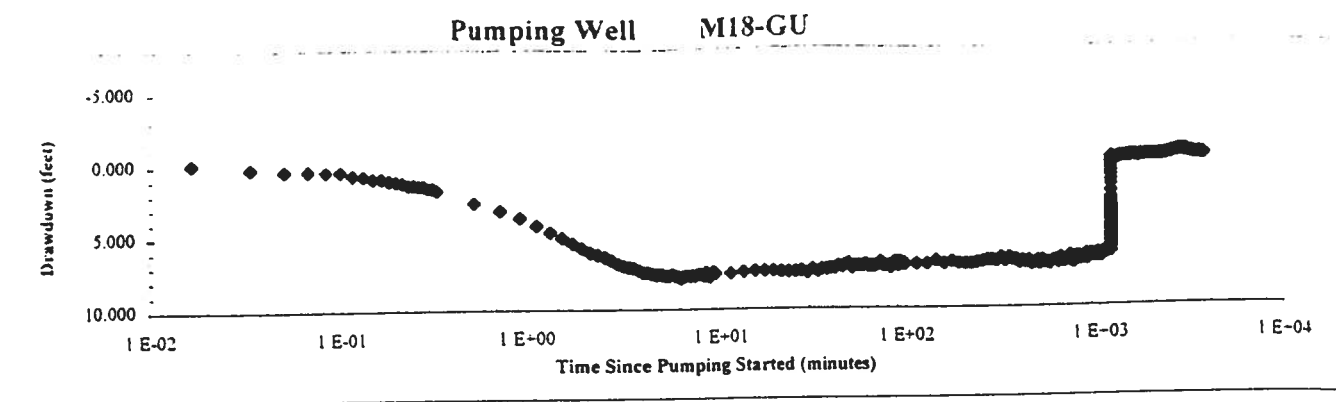
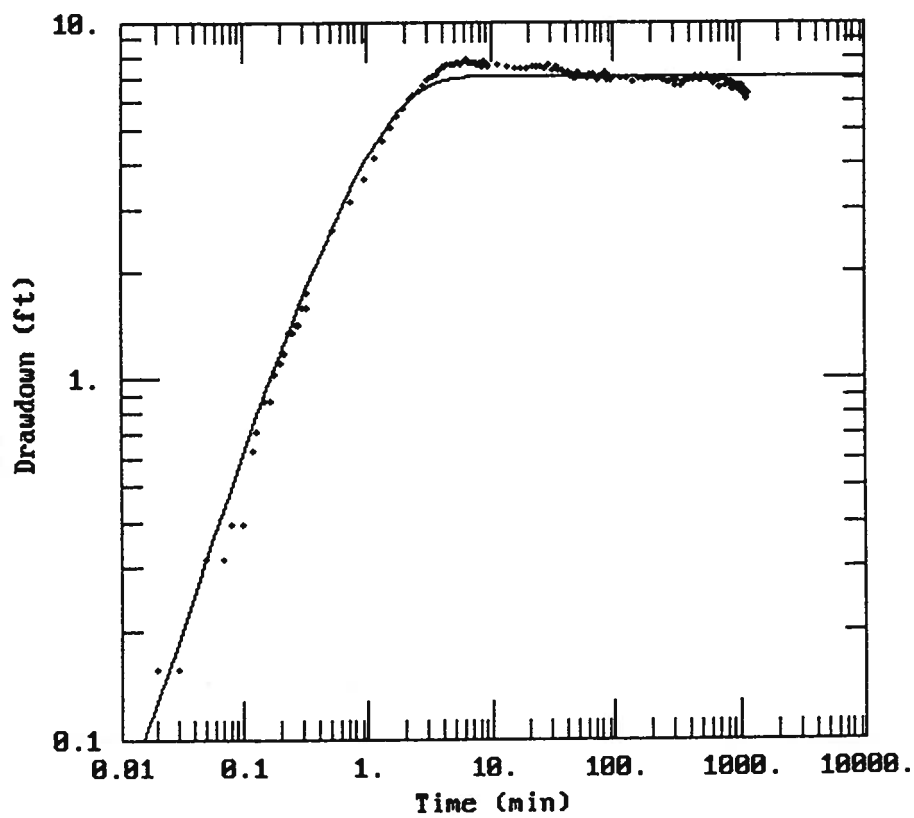


Figure 10A M18-GU Semi-Log Aquifer Test Plot



DATA SET:
M18-GU.DAT
01/05/96

AQUIFER MODEL:
Leaky
SOLUTION METHOD:
Moench

TEST DATA:
 $Q = 10.$ gal/min
 $r = 0.$ ft
 $r_c = 0.2083$ ft
 $r_w = 0.2083$ ft
 $b = 300.$ ft

PARAMETER ESTIMATES:
 $T = 160.5$ ft²/day
 $S = 0.002585$
 $r/B = 0.07248$
 $\beta = 1.175E-05$
 $S_w = 0.9311$
 $\alpha = 0.001706$

Figure 10B M18-GU Aqtesolv™ Analysis Log-Log Plot

Hydraulic Conductivity Calculation for a Cylindrical Source

Well Name:	M18-GU
Sink Radius:	6.35E-02 m
Sink Screened Interval:	12.19 m
Pseudo-Transmissivity:	2.13E-05 m ² /sec
Pseudo-Storage:	1.33E-05
Anisotropy Ratio:	1.00

Pseudo-Spherical Radius:

 $r_{sw} = 1.16 \text{ m}$ Hydraulic Conductivity: $1.84\text{E-}05 \text{ m/sec} = 5.21 \text{ ft/day}$ Specific Storage: $1.15\text{E-}05 \text{ 1/m} = 3.50\text{E-}06 \text{ 1/ft}$ **Figure 10C M18-GU (3D) FlowDim™ Analysis Summary**

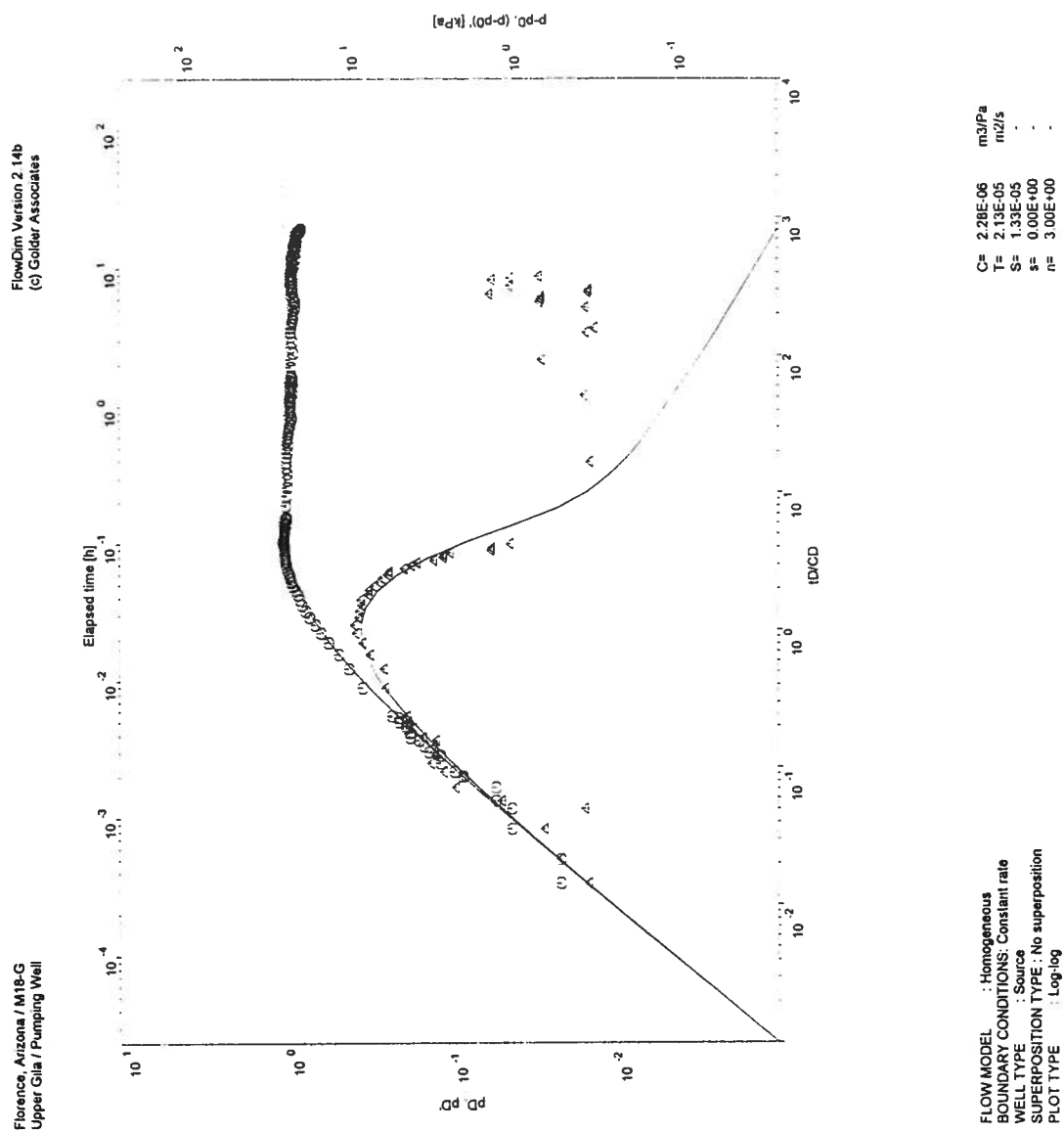


Figure 10D M18-GU (3D) FlowDim™ Analysis Log-Log Plot

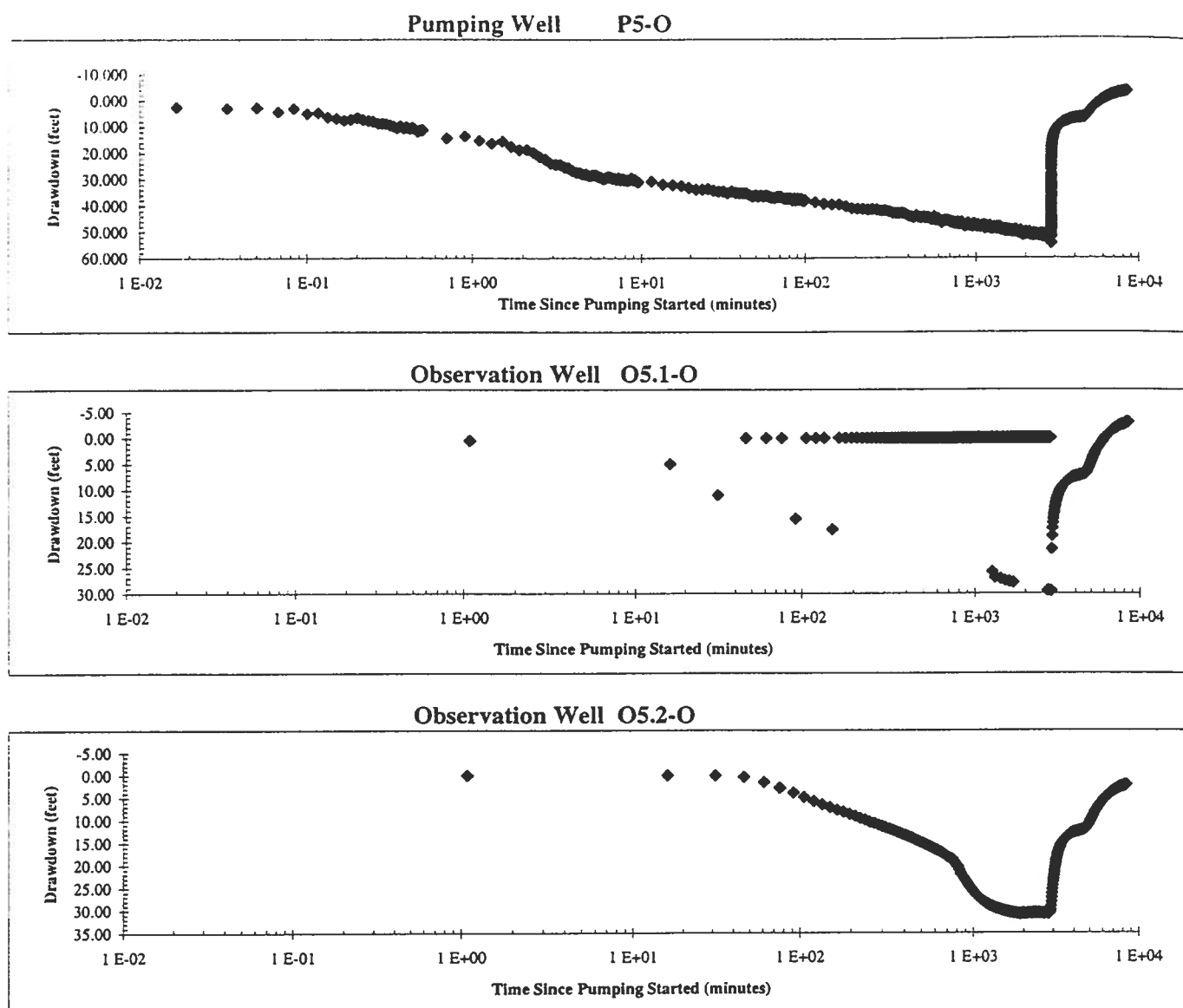


Figure 11A P5-O Semi-Log Aquifer Test Plot

FlowDim Analysis File :**P5OD.DAT**

	Parameter		Units
r_w	Well radius	0.076	m
μ	Groundwater viscosity	1.00E-03	Pa s
ρ	Groundwater density	1.00E+03	kg/m ³
c_t	Total compressibility	5.40E-10	1/Pa
ϕ	Porosity of formation	5.00	%
C	Wellbore storage	3.10E-06	m ³ /Pa
h	Length of aquifer tested	72.54	m

Skin Factor Calculation

Assuming formation storativity, the skin factor (s) can be calculated from the following equation.

$$s = \frac{\ln (C_D e^{2s} 2 \pi \phi c_t h r_w^2 / C)}{2}$$

Match Point Parameters From Analysis

$C_D e^{2s}$	1.0000E+02
Pm (1/KPa)	5.1000E-02
Tm (hr)	2.4500E+02

Results

T(m ² /sec)	K (feet/min)	K (ft/day)	K (m/s)	K (cm/s)	Skin
3.29E-04	8.93E-04	1.29	4.54E-06	4.54E-04	-3.04

Figure 11B P5-O FlowDim™ Analysis Summary
Golder Associates

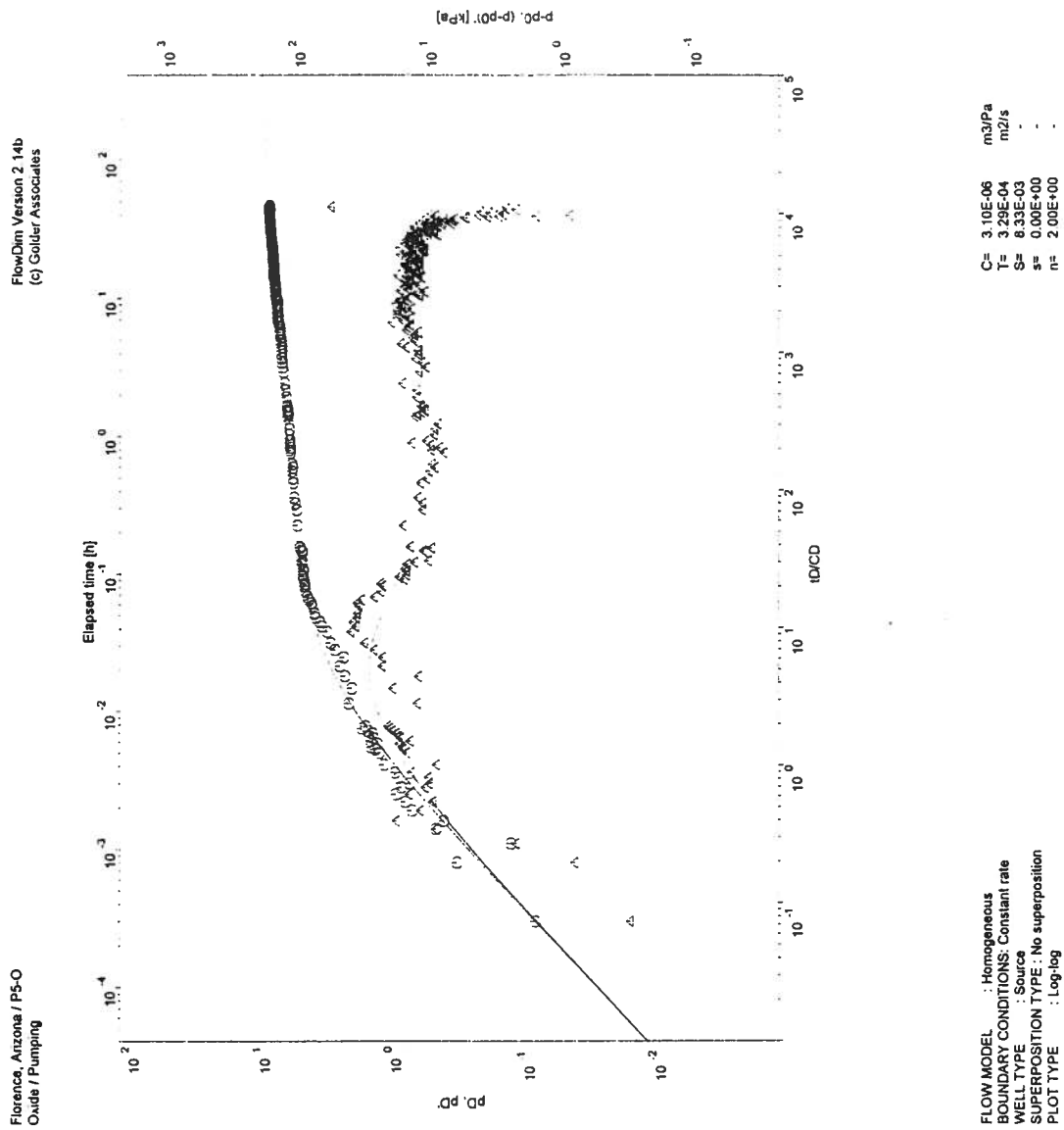


Figure 11C P5-O FlowDim™ Analysis Log-Log Plot

FlowDim Analysis File :

O52-OD.DAT

	Parameter		Units
r_w	Well radius	0.076	m
μ	Groundwater viscosity	1.00E-03	Pa s
ρ	Groundwater density	1.00E+03	kg/m ³
c_t	Total compressibility	5.40E-10	1/Pa
ϕ	Porosity of formation	5.00	%
C	Wellbore storage	n/a	m ³ /Pa
h	Length of aquifer tested	17.98	m

Skin Factor Calculation

Assuming formation storativity, the skin factor (s) can be calculated from the following equation.

$$s = \frac{\ln (C_D e^{2s} 2 \pi \phi c_t h r_w^2 / C)}{2}$$

Match Point Parameters From Analysis

$C_D e^{2s}$	n/a
P_m (1/KPa)	2.1600E-02
T_m (hr)	3.5400E-01

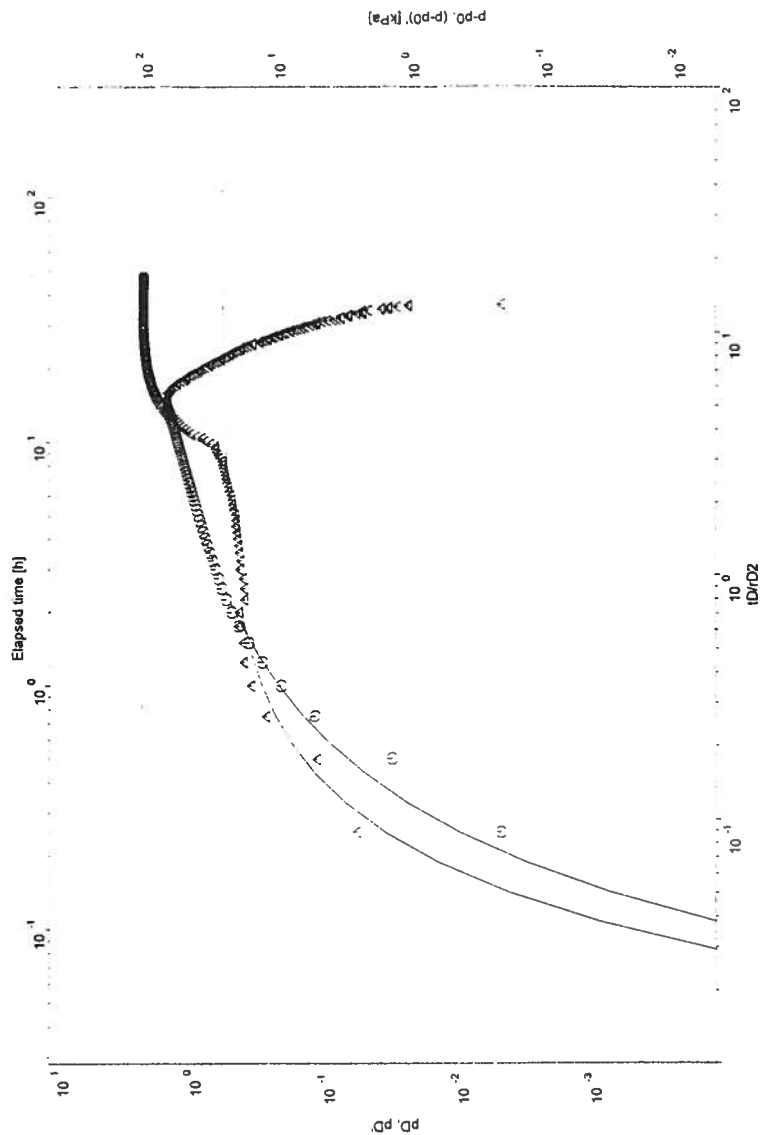
Results

T(m ² /sec)	K (feet/min)	K (ft/day)	K (m/s)	K (cm/s)	Skin
1.41E-04	1.54E-03	2.22	7.84E-06	7.84E-04	#####

Figure 11D O5.2-O FlowDim™ Analysis Summary
Golder Associates

FlowDim Version 2.14b
(c) Golder Associates

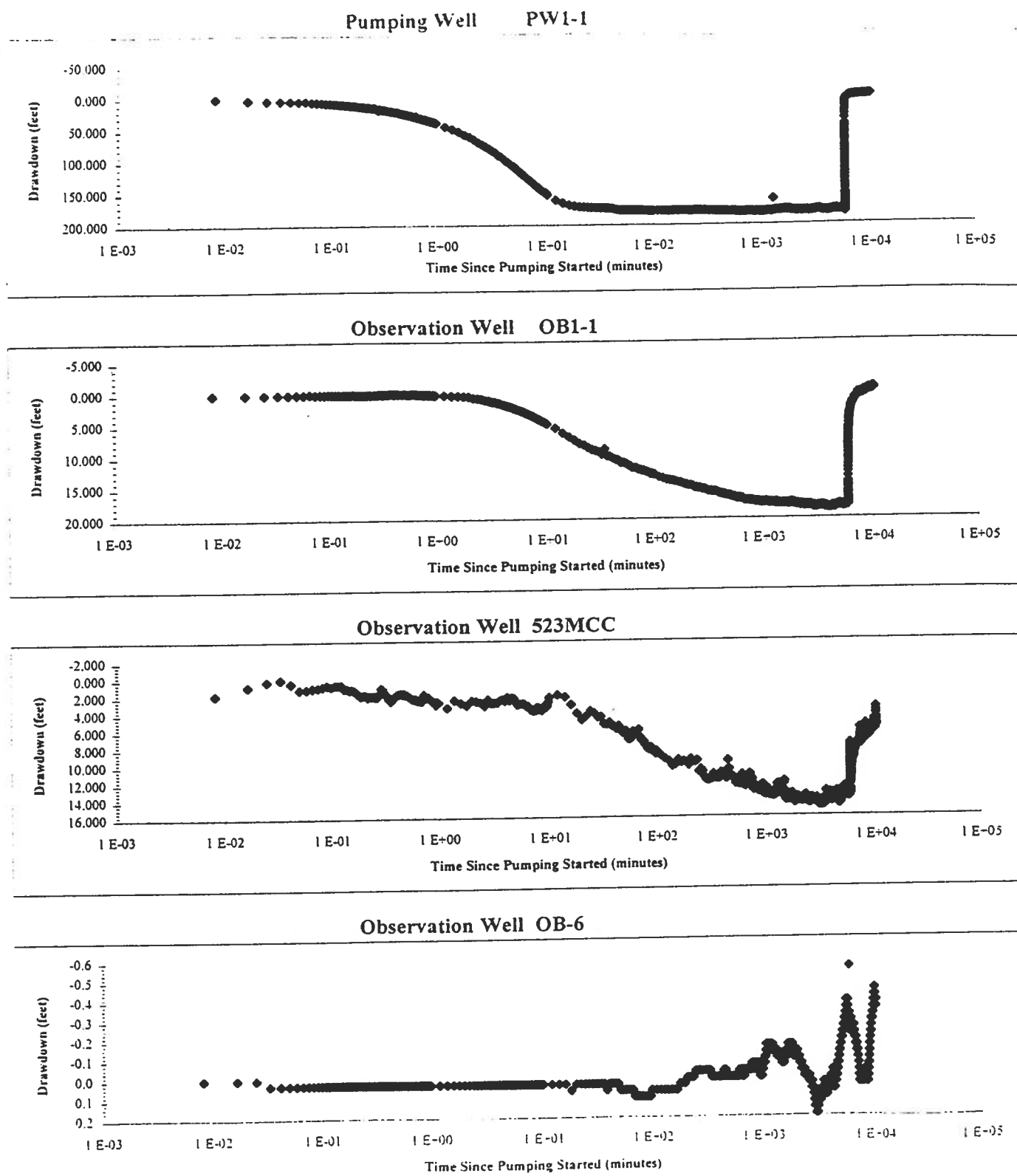
Florence Site / O5.2-O
Oxide / Pumping P5-O

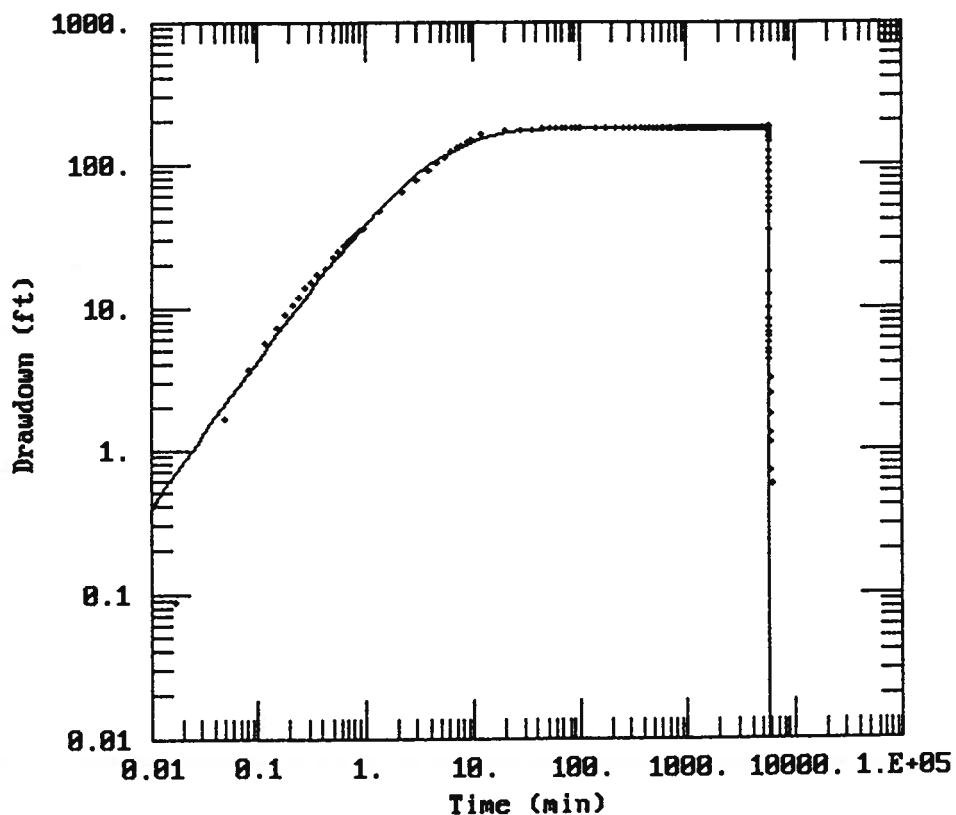


T= 1.41E-04 m2/s
S= 2.30E-02
rD= 1.04E+02
n= 2.00E+00

FLOW MODEL : Homogeneous
BOUNDARY CONDITIONS: Constant rate
WELL TYPE : Observation
SUPERPOSITION TYPE : No superposition
PLOT TYPE : Log-log

Figure 11E O5.2-O FlowDim™ Analysis Log-Log Plot

**Figure 12A PW1-1 Semi-Log Aquifer Test Plot**



DATA SET:
PW1-1.DAT
01/17/96

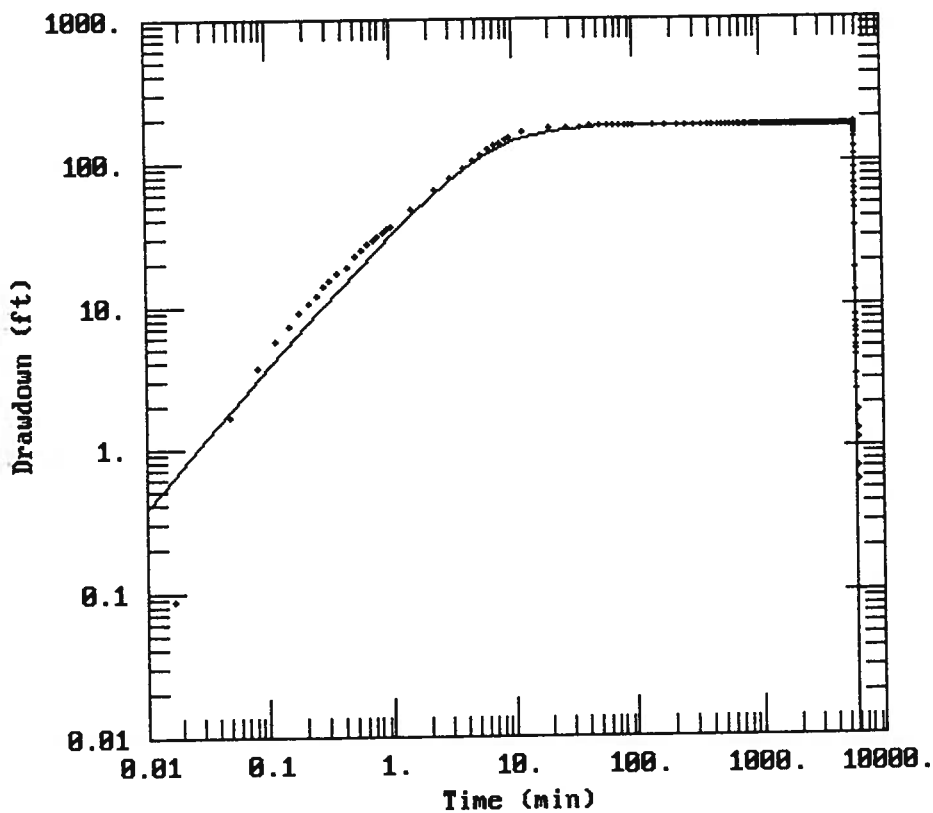
AQUIFER MODEL:
Leaky

SOLUTION METHOD:
Moench

TEST DATA:
Q = 33. gal/min
r = 0.25 ft
r_c = 0.25 ft
r_w = 0.25 ft
b = 760. ft

PARAMETER ESTIMATES:
T = 14.23 ft²/day
S = 0.001032
r/B = 0.1
B = 0.2
S_w = 0.25
α = 0.0025

Figure 12B PW1-1 Aqtesolv™ Analysis Log-Log Plot



DATA SET:
PW1-1.DAT
02/04/96

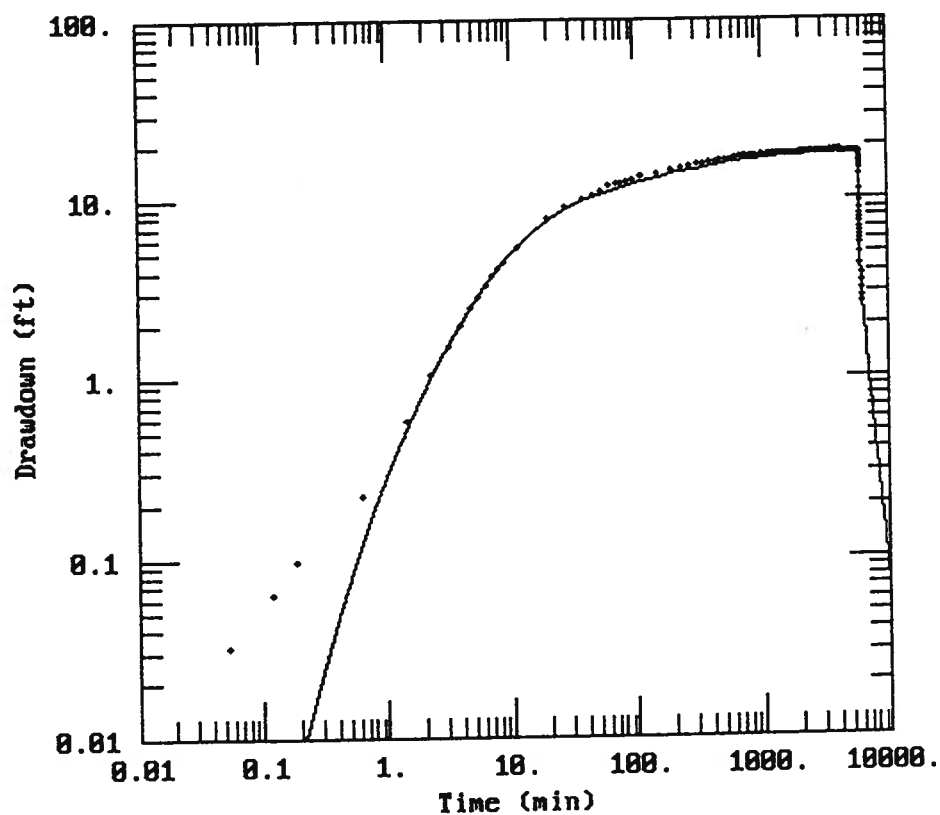
AQUIFER MODEL:
Leaky

SOLUTION METHOD:
Moench

TEST DATA:
Q = 33. gal/min
r = 0.25 ft
r_c = 0.25 ft
r_w = 0.25 ft
b = 760. ft

PARAMETER ESTIMATES:
T = 26.67 ft²/day
S = 0.0001111
r/B = 0.01031
B = 0.01272
S_w = 0.
α = 0.0001865

Figure 12C PW1-1 Aqtesolv™ Analysis Log-Log Plot



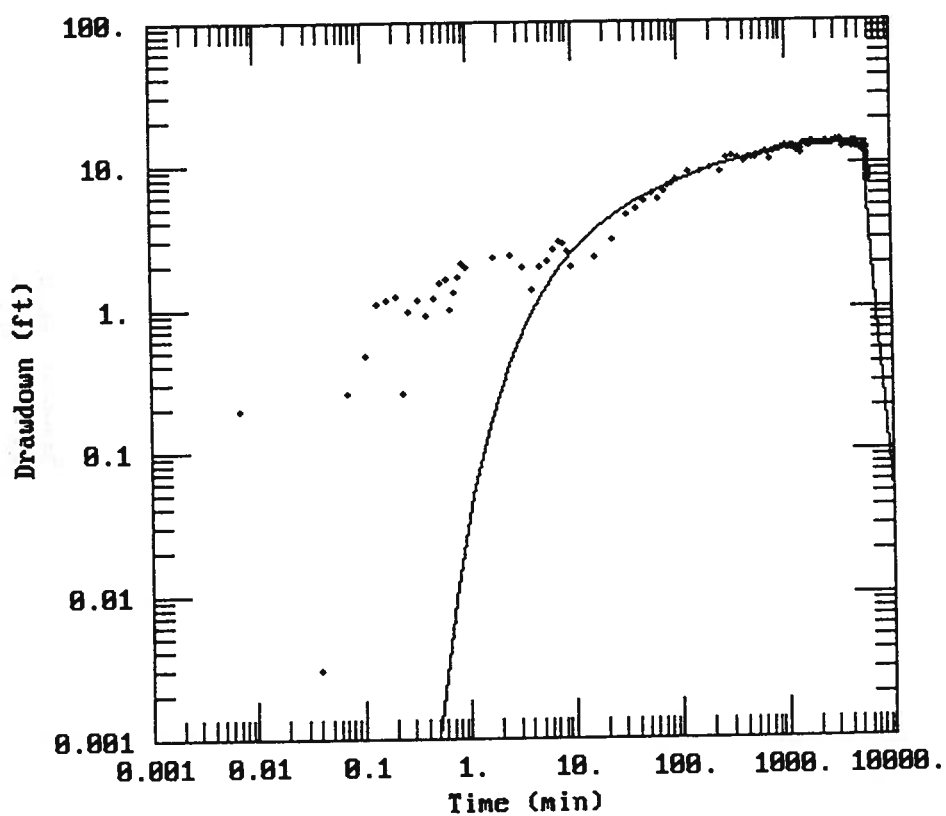
DATA SET:
OB1-1.DAT
01/17/96

AQUIFER MODEL:
Leaky
SOLUTION METHOD:
Moench

TEST DATA:
Q = 33. gal/min
r = 48.9 ft
r_c = 0.25 ft
r_w = 0.25 ft
b = 760. ft

PARAMETER ESTIMATES:
T = 213.8 ft²/day
S = 5.392E-05
r/B = 0.025
B = 0.005276
S_w = 0.03872
α = 1.328E-05

Figure 12D OB1-1 Aqtesolv™ Analysis Log-Log Plot



DATA SET:
523MCCA.DAT
01/30/96

AQUIFER MODEL:
Leaky
SOLUTION METHOD:
Moench

TEST DATA:
Q = 33. gal/min
r = 267.4 ft
r_c = 0.25 ft
r_w = 0.25 ft
b = 760. ft

PARAMETER ESTIMATES:
T = 128.8 ft²/day
S = 1.539E-05
r/B = 0.2
B = 0.1443
S_w = 0.
α = 0.01

Figure 12E 523MCC Aqtesolv™ Analysis Log-Log Plot

Hydraulic Conductivity Calculation for a Cylindrical Source

Well Name:	PW1-1
Sink Radius:	7.62E-02 m
Sink Screened Interval:	115.82 m
Pseudo-Transmissivity:	2.90E-06 m ² /sec
Pseudo-Storage:	3.15E-06
Anisotropy Ratio:	1.00

Pseudo-Spherical Radius:

 $r_{sw} = 7.90 \text{ m}$ Hydraulic Conductivity: $3.67\text{E-}07 \text{ m/sec} = 0.10 \text{ ft/day}$ Specific Storage: $3.99\text{E-}07 \text{ 1/m} = 1.21\text{E-}07 \text{ 1/ft}$ **Figure 12F PW1-1 (3D) FlowDim™ Analysis Summary**

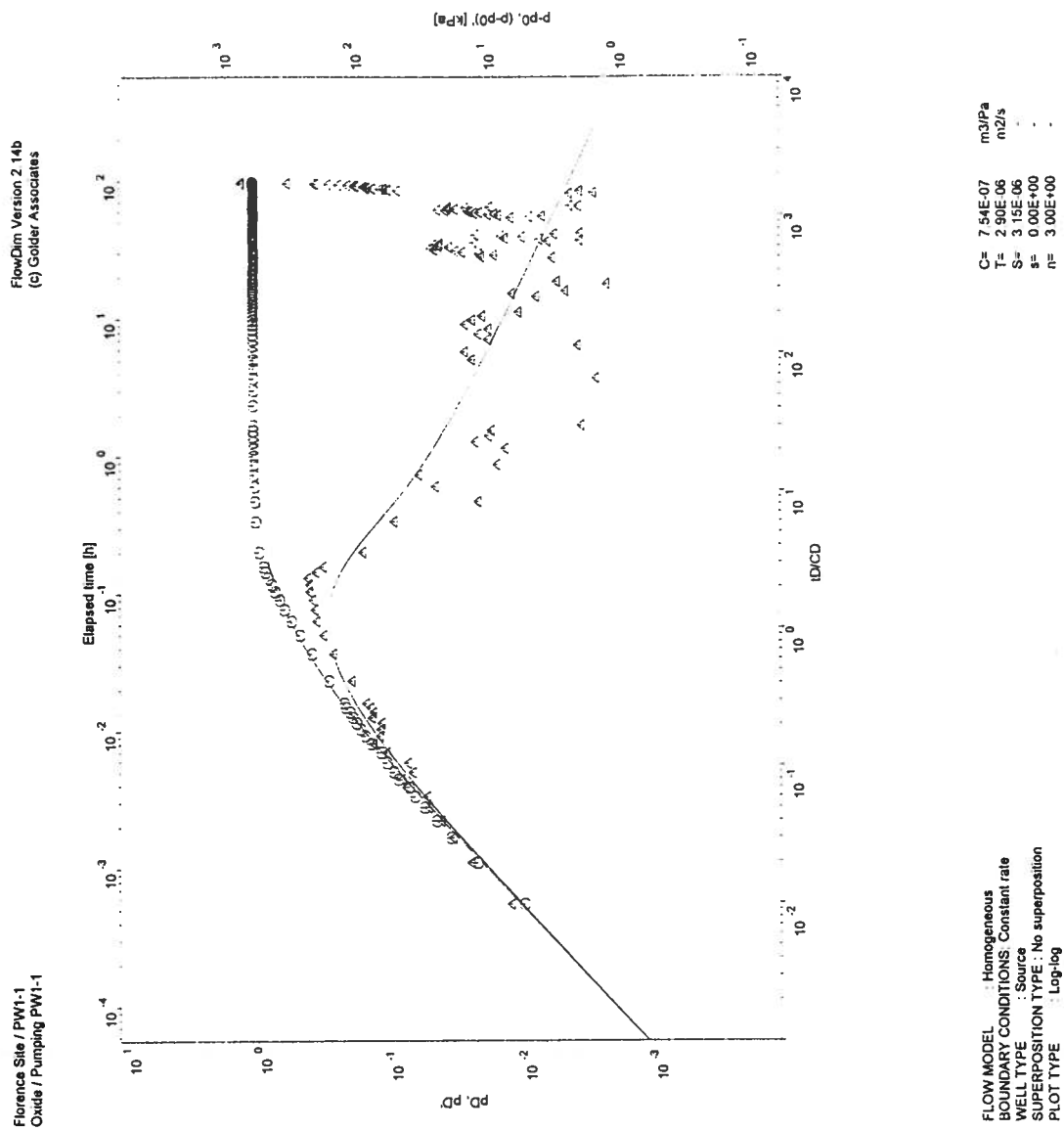


Figure 12G PW1-1 (3D) FlowDim™ Analysis Log-Log Plot

Hydraulic Conductivity Calculation for a Cylindrical Source

PUMPING WELL

	PW1-1	
Easting:	648742.2	ft
Northing:	746476.5	ft
Screen Top:	360.0	ft
Screen Bottom:	740.0	ft
Surface Elevation	1477	ft (amsl)
Radius:	7.62E-02	m
Screen Interval:	115.82	m
Screen Interval Mid-Point:	282.55	m

OBSERVATION WELL

	OB1-1	
Easting	648750.1	ft
Northing	746428.3	ft
Screen Top:	780.7	ft
Screen Bottom:	740.0	ft
Surface Elevation	1476.5	ft
Screen Interval Mid-Point:	218.29	m
Distance to Sink:	24.6	m

Pseudo-Transmissivity:	8.69E-06	m ² /sec
Pseudo-Storage:	2.41E-05	
Anisotropy Ratio:	1.00	

Pseudo-Spherical Radius:

$r_{sw} = 7.90 \text{ m}$

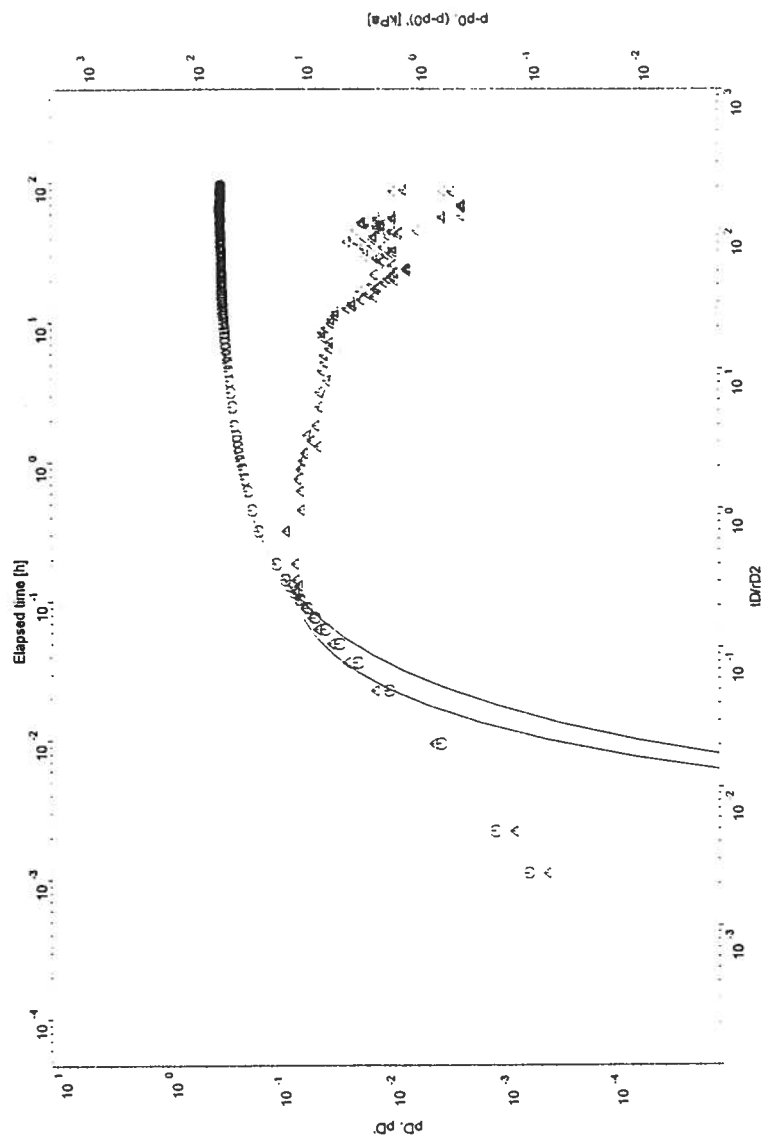
Hydraulic Conductivity: $1.10\text{E-}06 \text{ m/sec} = 0.31 \text{ ft/day}$

Specific Storage: $3.14\text{E-}07 \text{ 1/m} = 9.59\text{E-}08 \text{ 1/ft}$

Figure 12H OB1-1 (3D) FlowDim™ Analysis Summary

FlowDim Version 2.14b
(c) Golder Associates

Florence Site / OBI-1
Oxide / Pumping PWI-1



T= 8.69E-06 m2/s
S= 2.41E-05
rD= 3.11E+00
n= 3.00E+00

FLOW MODEL : Homogeneous
BOUNDARY CONDITIONS: Constant rate
WELL TYPE : Observation
SUPERPOSITION TYPE : No superposition
PLOT TYPE : Log-log

Figure 12I OBI-1 (3D) FlowDim™ Analysis Log-Log Plot

Hydraulic Conductivity Calculation for a Cylindrical Source

<u>PUMPING WELL</u>	PW1-1	<u>OBSERVATION WELL</u>	523CMM
Easting:	648742.2 ft	Easting	648476.0 ft
Northing:	746476.5 ft	Northing	746502.0 ft
Screen Top:	360.0 ft	Screen Top:	320.0 ft
Screen Bottom:	740.0 ft	Screen Bottom:	690.0 ft
Surface Elevation	1477 ft (amsl)	Surface Elevation	1476.5 ft
Radius:	<u>7.62E-02 m</u>	Screen Interval Mid-Point:	<u>296.11 m</u>
Screen Interval:	<u>115.82 m</u>	Distance to Sink:	<u>81.6 m</u>
Screen Interval Mid-Point:	<u>282.55 m</u>		

Pseudo-Transmissivity: 3.61E-06 m²/sec
 Pseudo-Storage: 2.66E-04
 Anisotropy Ratio: 1.00

Pseudo-Spherical Radius:

$$r_{sw} = 7.90 \text{ m}$$

Hydraulic Conductivity: 4.57E-07 m/sec = 0.13 ft/day

Specific Storage: 3.16E-07 1/m = 9.62E-08 1/ft

Figure 12J 523MCC (3D) FlowDim™ Analysis Summary

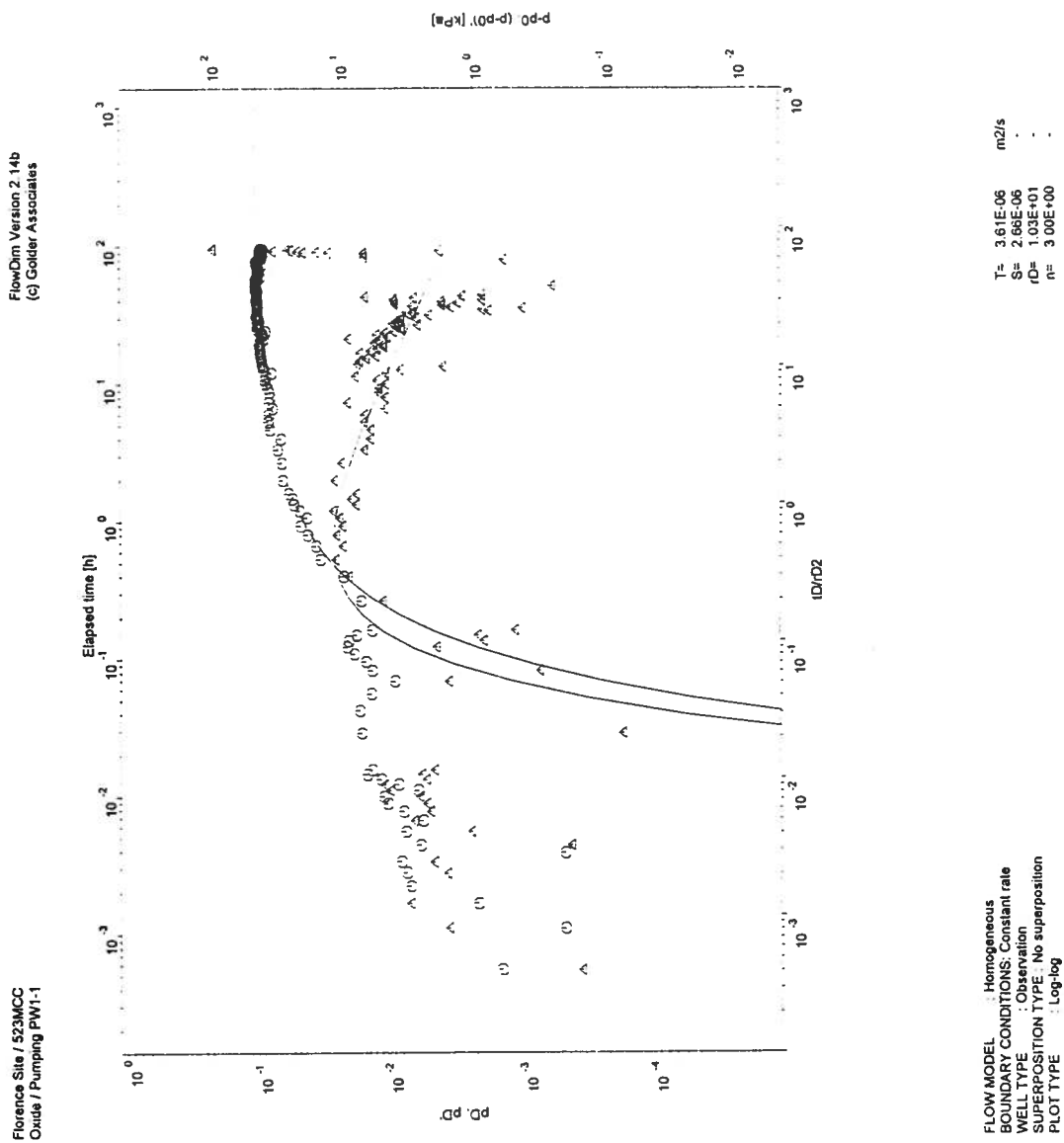
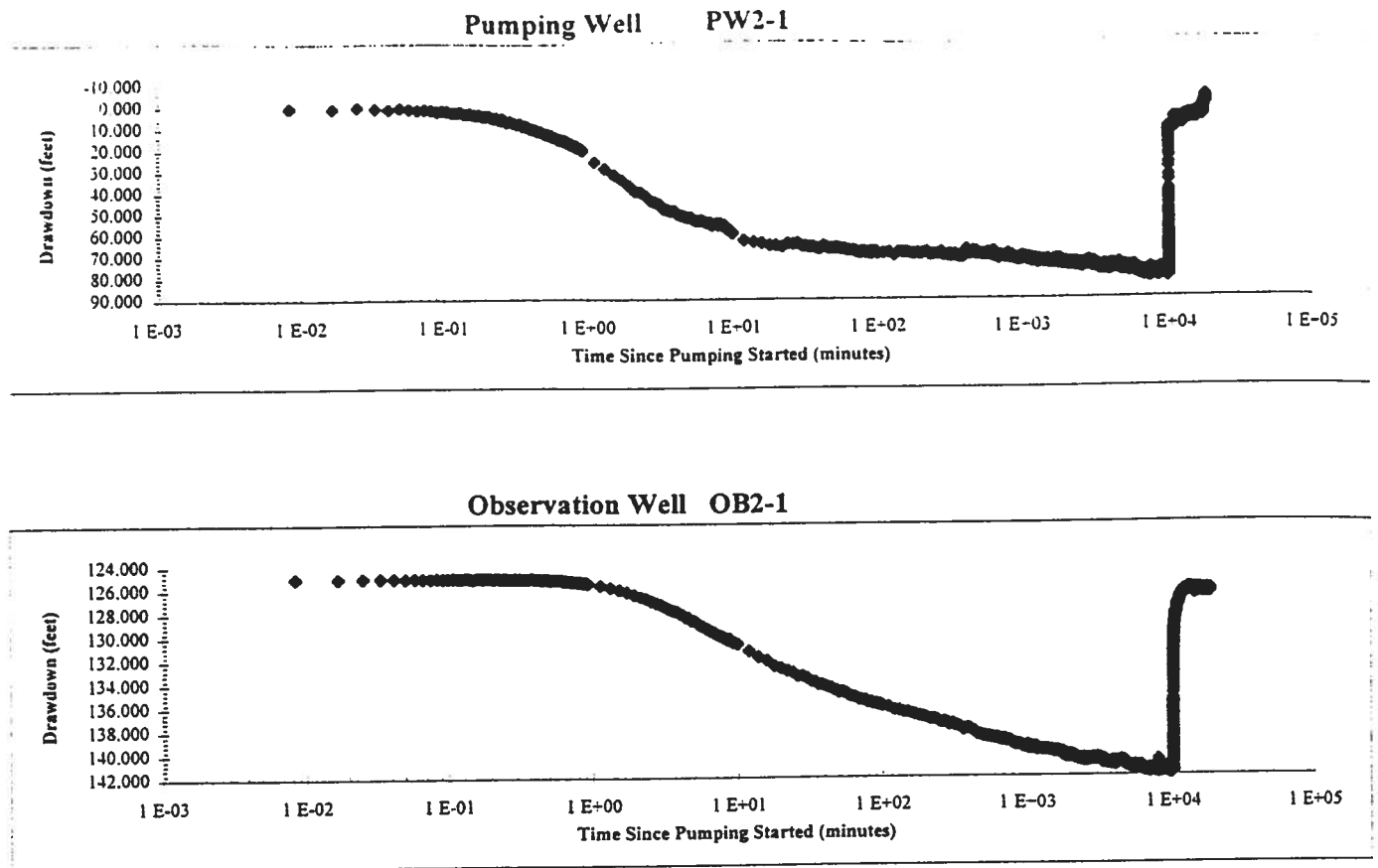
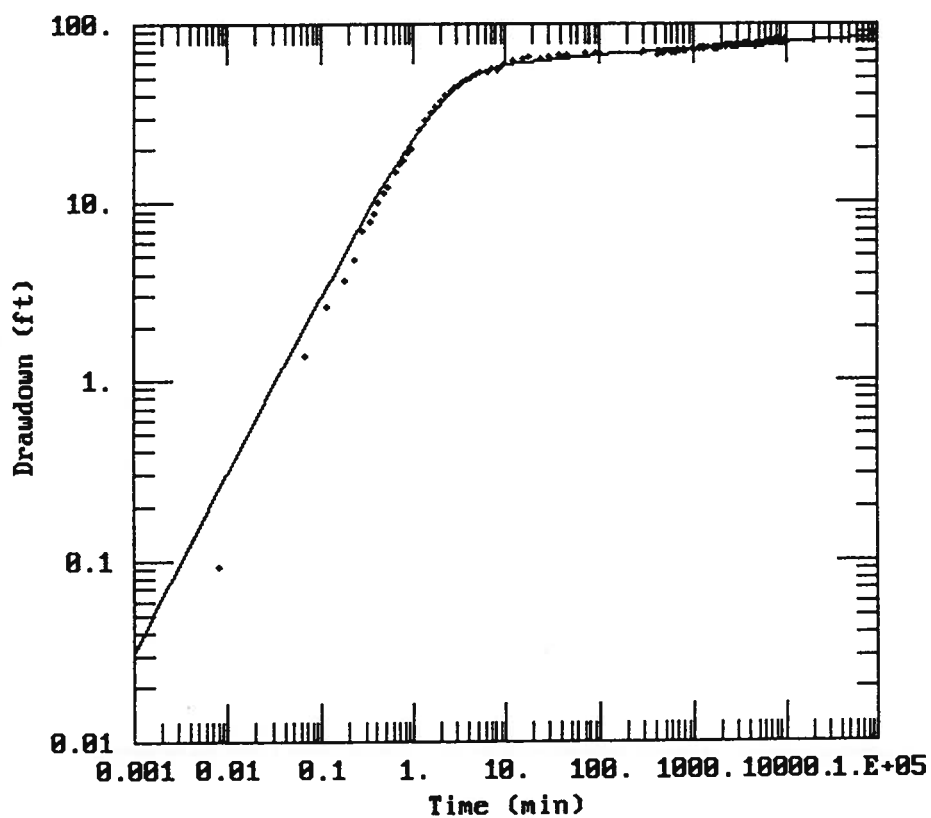


Figure 12K 523MCC (3D) FlowDim™ Analysis Log-Log Plot





DATA SET:
PW2-1.DAT
02/05/96

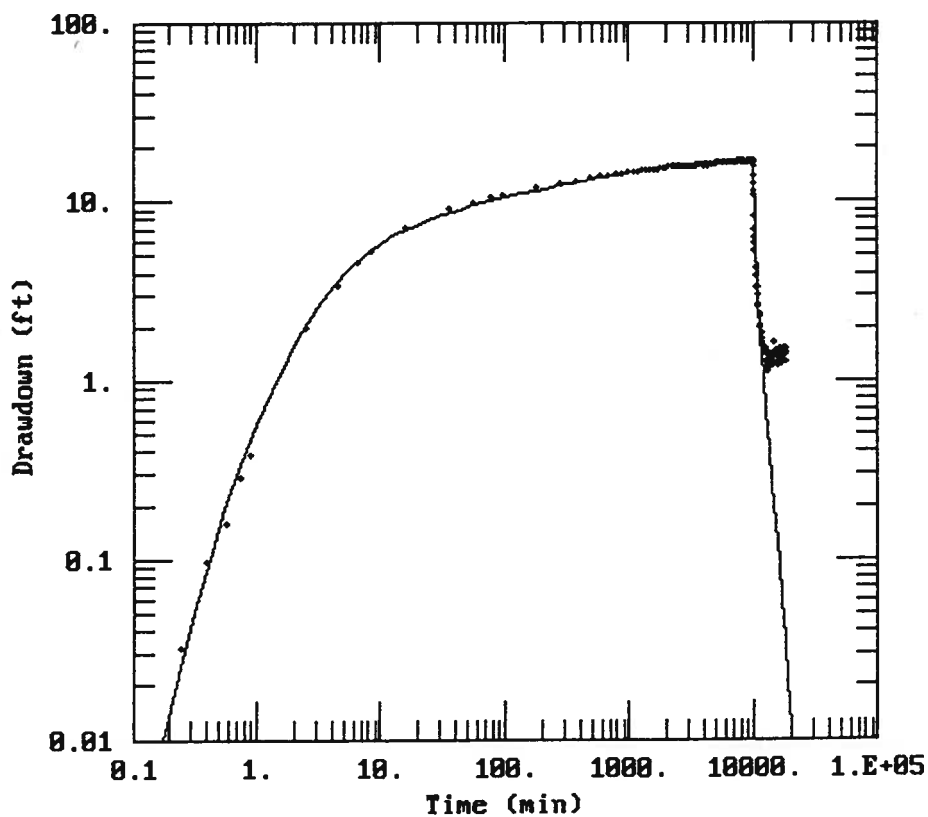
AQUIFER MODEL:
Leaky

SOLUTION METHOD:
Moench

TEST DATA:
Q = 50. gal/min
r = 0. ft
r_c = 0.25 ft
r_w = 0.25 ft
b = 1000. ft

PARAMETER ESTIMATES:
T = 149.5 ft²/day
S = 0.0002183
r/B = 0.0002181
B = 0.01627
S_w = 1.5
α = 0.0001955

Figure 13B PW2-1 Aqtesolv™ Analysis Log-Log Plot



DATA SET:
OB2-1.DAT
02/05/96

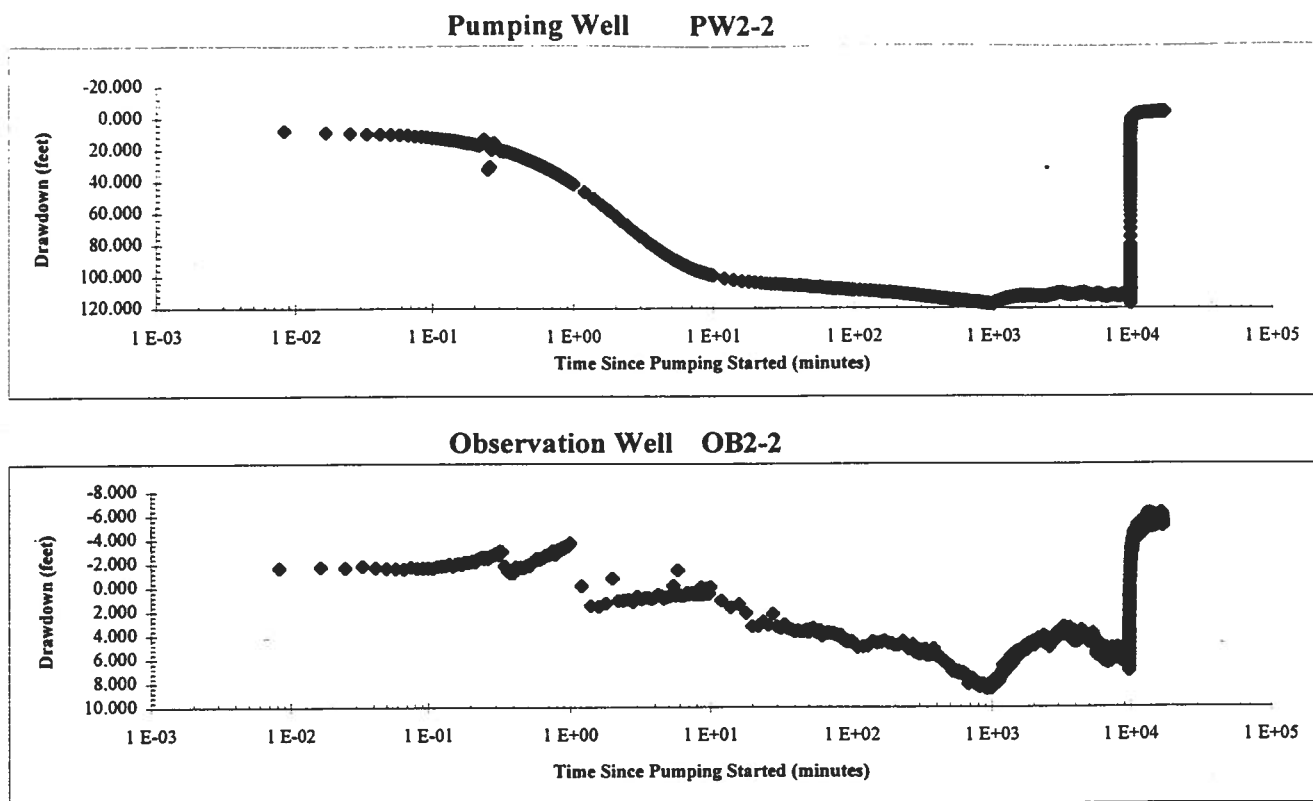
AQUIFER MODEL:
Leaky

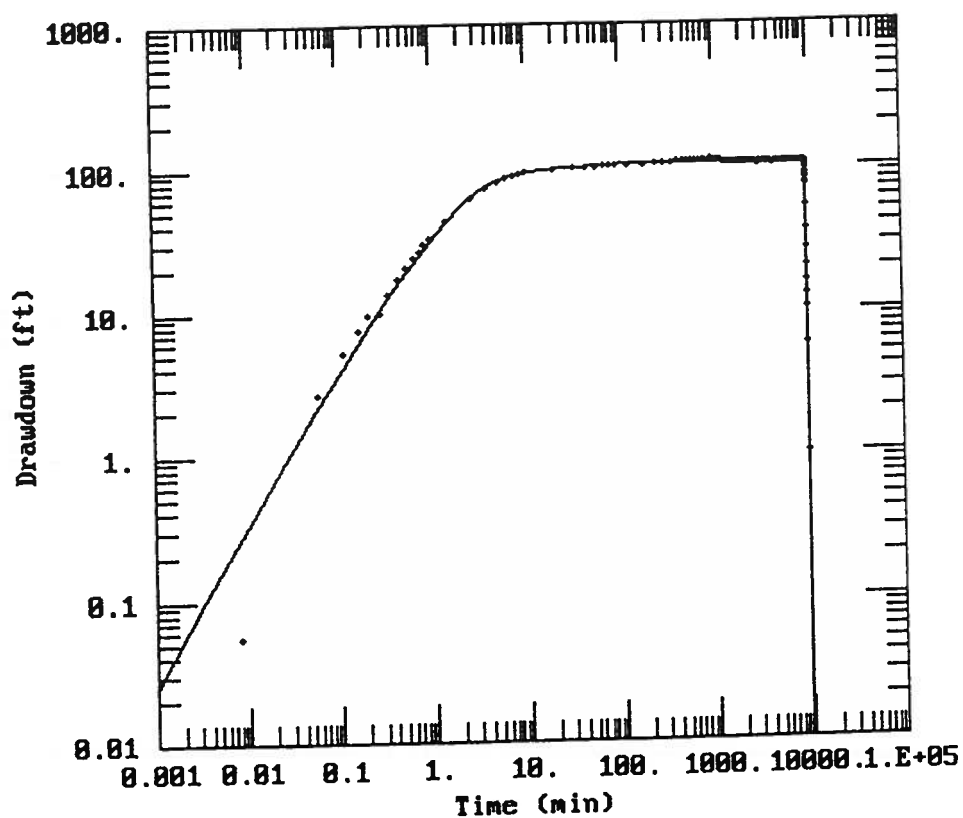
SOLUTION METHOD:
Moench

TEST DATA:
Q = 50. gal/min
r = 96.9 ft
r_c = 0.25 ft
r_w = 0.25 ft
b = 640. ft

PARAMETER ESTIMATES:
T = 229.2 ft²/day
S = 1.664E-05
r/B = 0.09565
β = 0.1771
S_w = 0.
α = 1.E-05

Figure 13C OB2-1 Aqtesolv™ Analysis Log-Log Plot





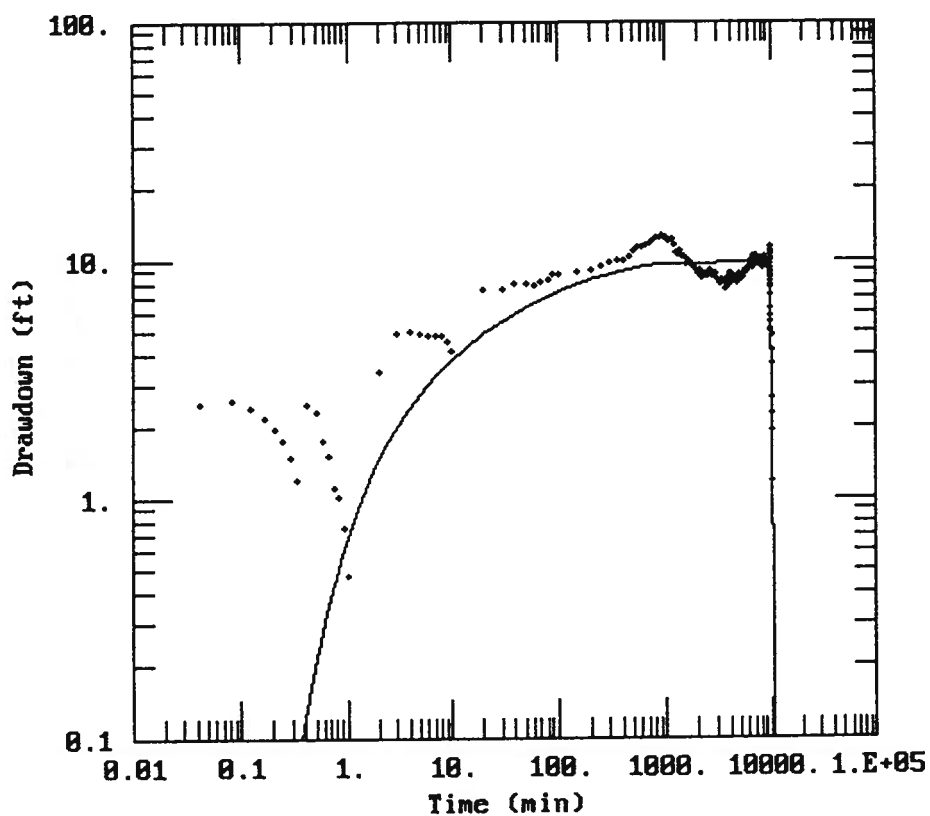
DATA SET:
PW2-2.DAT
01/17/96

AQUIFER MODEL:
Leaky
SOLUTION METHOD:
Moench

TEST DATA:
 $Q = 45. \text{ gal/min}$
 $r = 0.25 \text{ ft}$
 $r_c = 0.25 \text{ ft}$
 $r_w = 0.25 \text{ ft}$
 $b = 800. \text{ ft}$

PARAMETER ESTIMATES:
 $T = 88.11 \text{ ft}^2/\text{day}$
 $S = 3.361\text{E-}05$
 $r/B = 0.001403$
 $\beta = 0.001082$
 $S_w = 2.77$
 $\alpha = 7.334\text{E-}05$

Figure 14B PW2-2 Aqtesolv™ Analysis Log-Log Plot



DATA SET:
OB2-2.DAT
02/05/96

AQUIFER MODEL:
Leaky
SOLUTION METHOD:
Moench

TEST DATA:
Q = 45. gal/min
r = 49.2 ft
r_c = 0.25 ft
r_w = 0.25 ft
b = 800. ft

PARAMETER ESTIMATES:
T = 328.6 ft²/day
S = 0.0002649
r/B = 0.114
B = 0.05221
S_w = 0.
α = 0.1

Figure 14C OB2-2 Aqtesolv™ Analysis Log-Log Plot

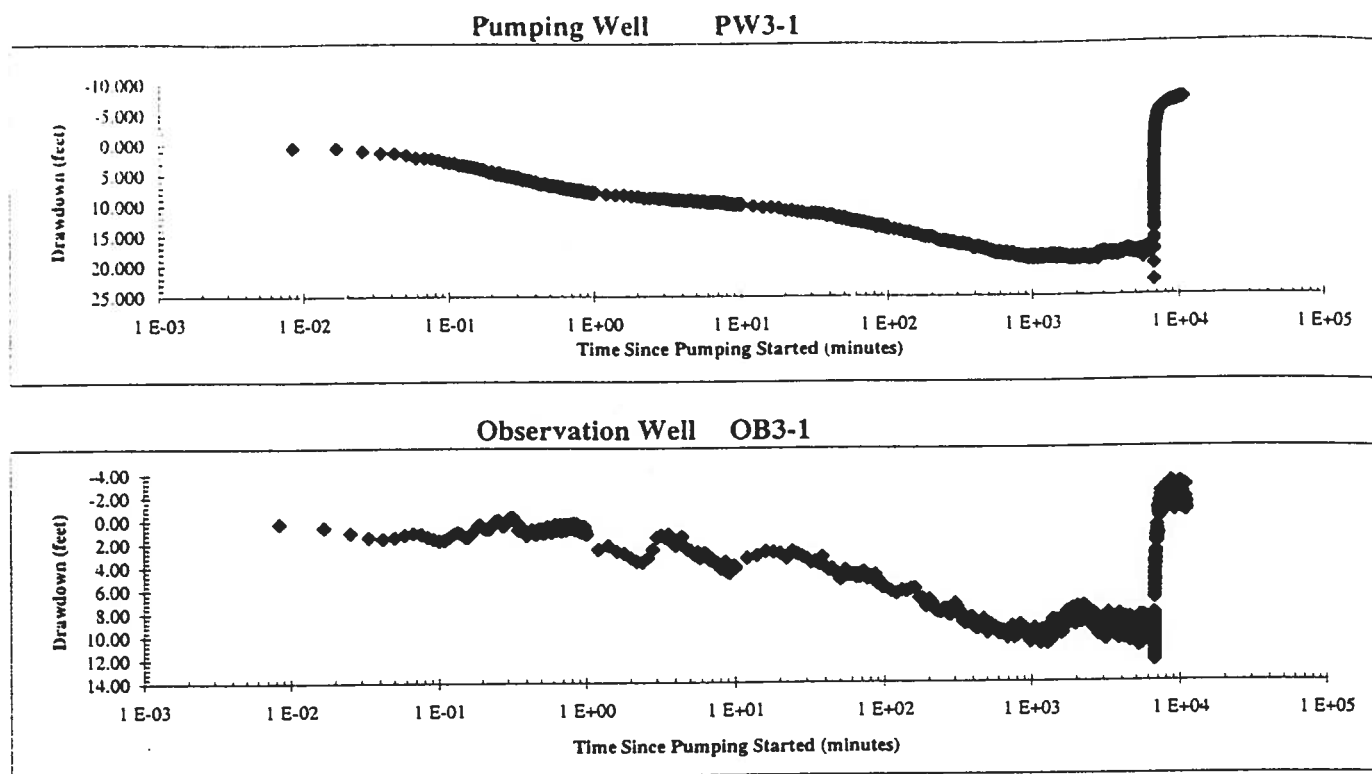
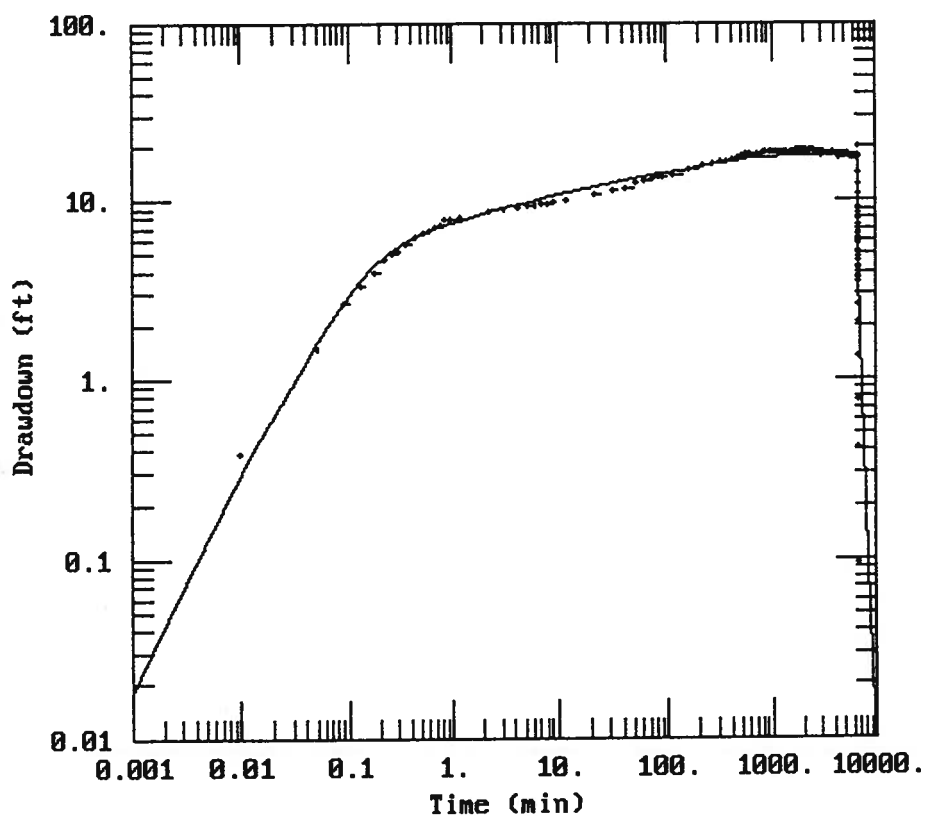


Figure 15A PW3-1 Semi-Log Aquifer Test Plot



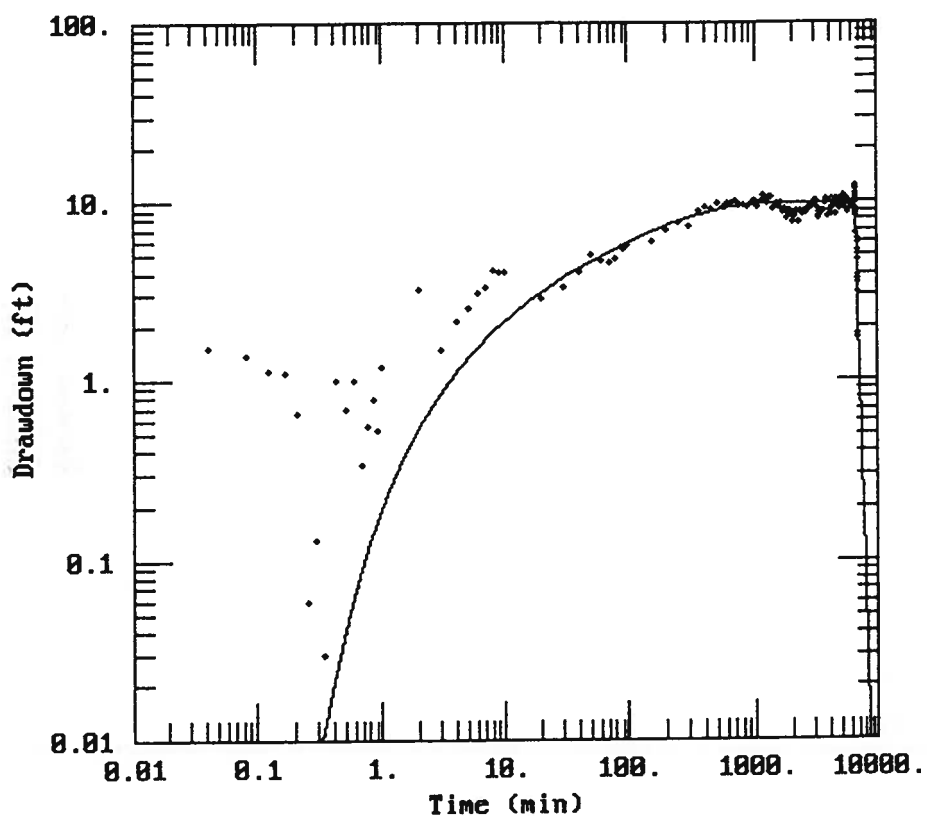
DATA SET:
PW3-1B.DAT
01/31/96

AQUIFER MODEL:
Leaky
SOLUTION METHOD:
Moench

TEST DATA:
Q = 58. gal/min
r = 0.25 ft
r_c = 0.25 ft
r_w = 0.25 ft
b = 800. ft

PARAMETER ESTIMATES:
T = 254.4 ft²/day
S = 0.001223
r/B = 0.09
p = 4.
Sw = 7.
α = 0.017

Figure 15B PW3-1 Aqtesolv™ Analysis Log-Log Plot



DATA SET:
OB3-1.DAT
02/05/96

AQUIFER MODEL:
Leaky

SOLUTION METHOD:
Moench

TEST DATA:
Q = 50. gal/min
r = 49.6 ft
r_c = 0.25 ft
r_w = 0.25 ft
b = 800. ft

PARAMETER ESTIMATES:
T = 146.5 ft²/day
S = 0.0001585
r/B = 0.4915
β = 0.9907
S_w = 0.
α = 0.017

Figure 15C OB3-1 Aqtesolv™ Analysis Log-Log Plot

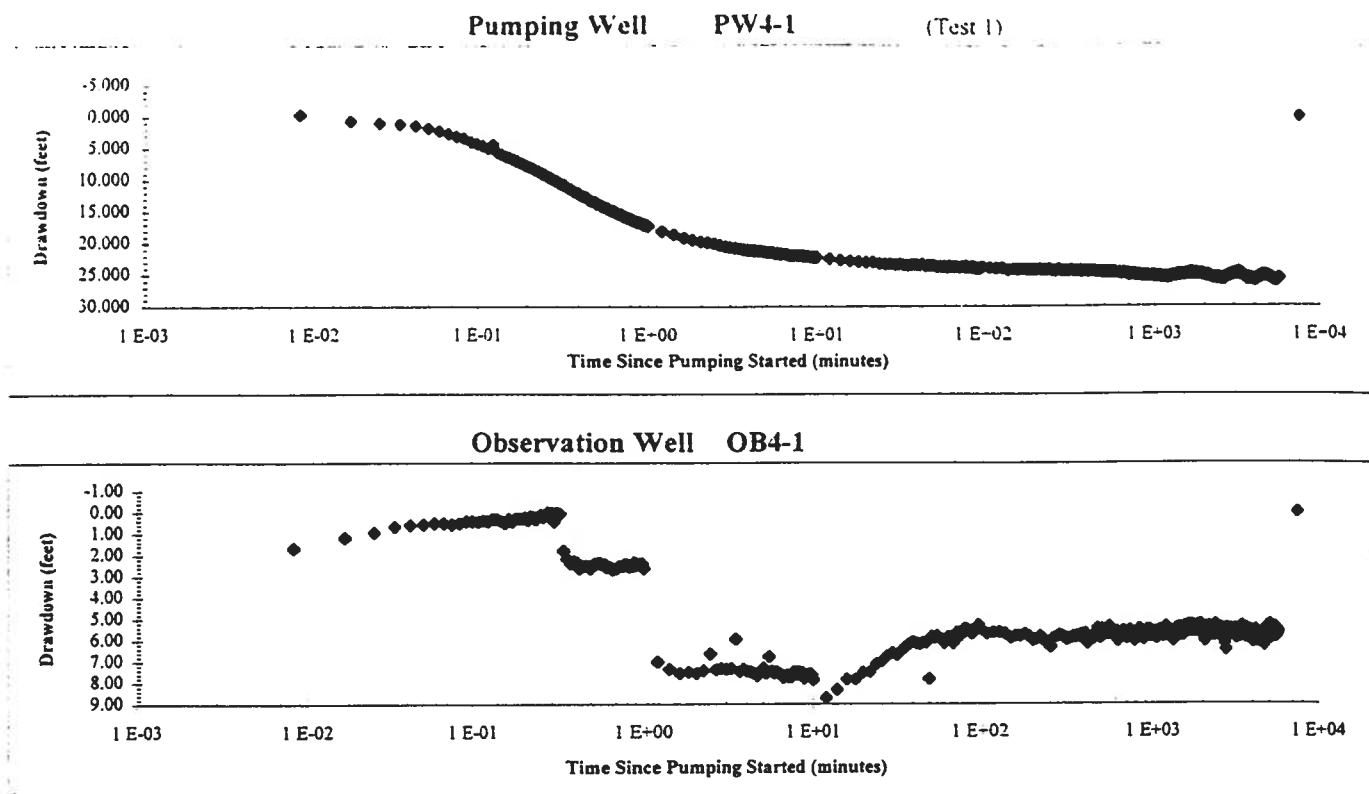
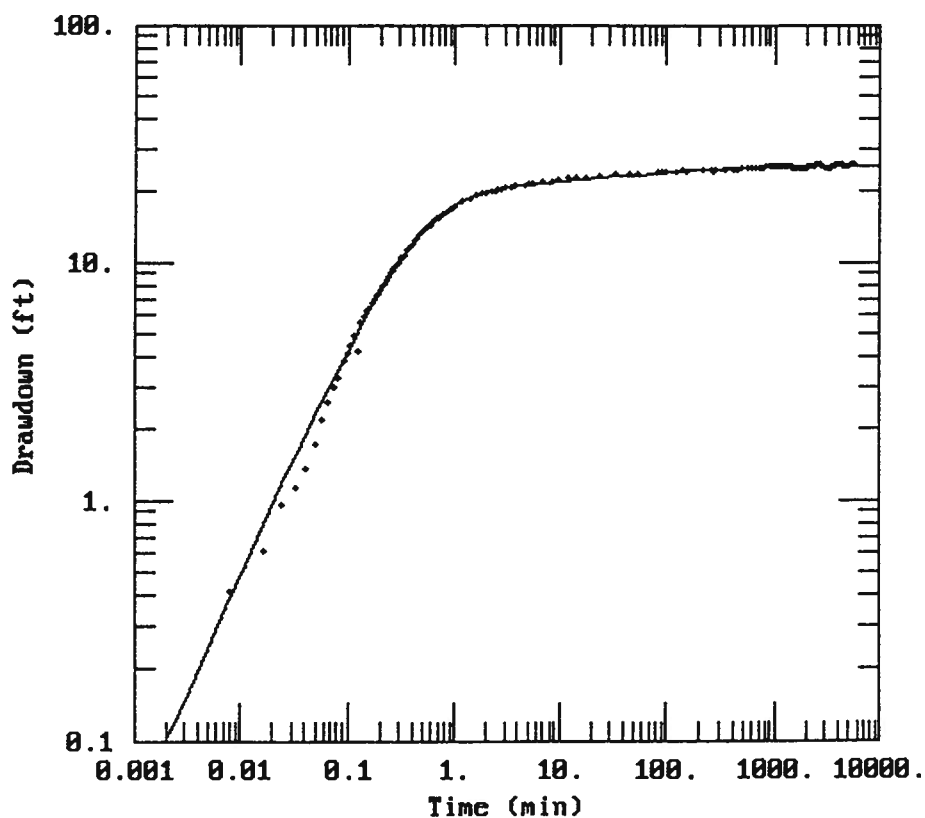


Figure 16A PW4-1 (Test 1) Semi-Log Aquifer Test Plot



DATA SET:
PW4-1.DAT
01/05/96

AQUIFER MODEL:
Leaky

SOLUTION METHOD:
Moench

TEST DATA:
 $Q = 71. \text{ gal/min}$
 $r = 0. \text{ ft}$
 $r_c = 0.25 \text{ ft}$
 $r_w = 0.25 \text{ ft}$
 $b = 800. \text{ ft}$

PARAMETER ESTIMATES:
 $T = 1251.7 \text{ ft}^2/\text{day}$
 $S = 0.02937$
 $r/B = 0.001467$
 $B = 1.E-05$
 $S_w = 7.99$
 $\alpha = 0.02949$

Figure 16B PW4-1 (Test 1) Aqtesolv™ Analysis Log-Log Plot

Hydraulic Conductivity Calculation for a Cylindrical Source

Well Name:	PW4-1
Sink Radius:	7.62E-02 m
Sink Screened Interval:	103.63 m
Pseudo-Transmissivity:	4.63E-05 m ² /sec
Pseudo-Storage:	7.29E-06
Anisotropy Ratio:	1.00

Pseudo-Spherical Radius:

 $r_{sw} = 7.18 \text{ m}$ Hydraulic Conductivity: $6.45\text{E-}06 \text{ m/sec} = 1.83 \text{ ft/day}$ Specific Storage: $1.02\text{E-}06 \text{ 1/m} = 3.09\text{E-}07 \text{ 1/ft}$ **Figure 16C PW4-1 (Test 1) (3D) FlowDim™ Analysis Summary**

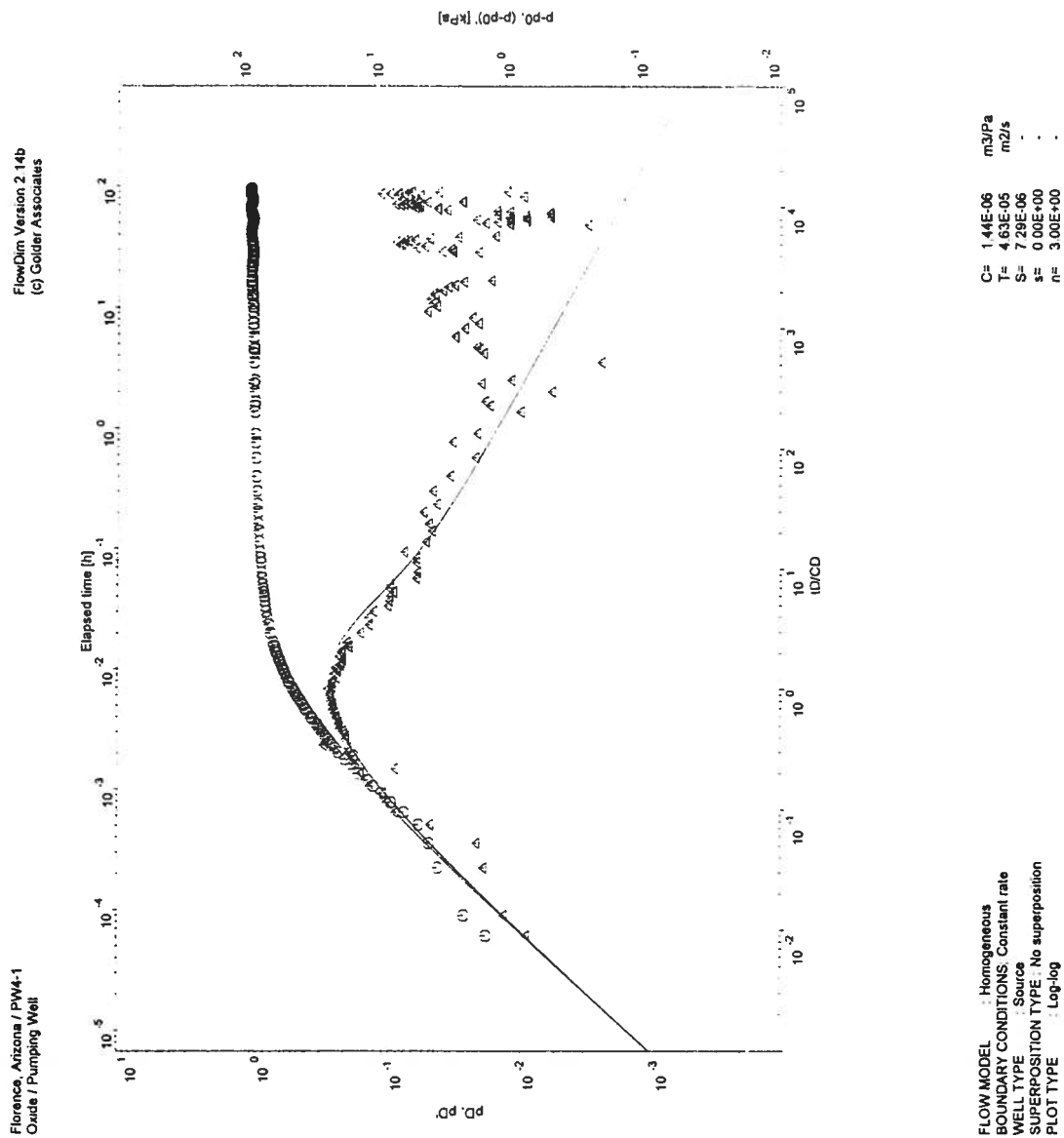


Figure 16D PW4-1 (Test 1) (3D) FlowDim™ Analysis Log-Log Plot

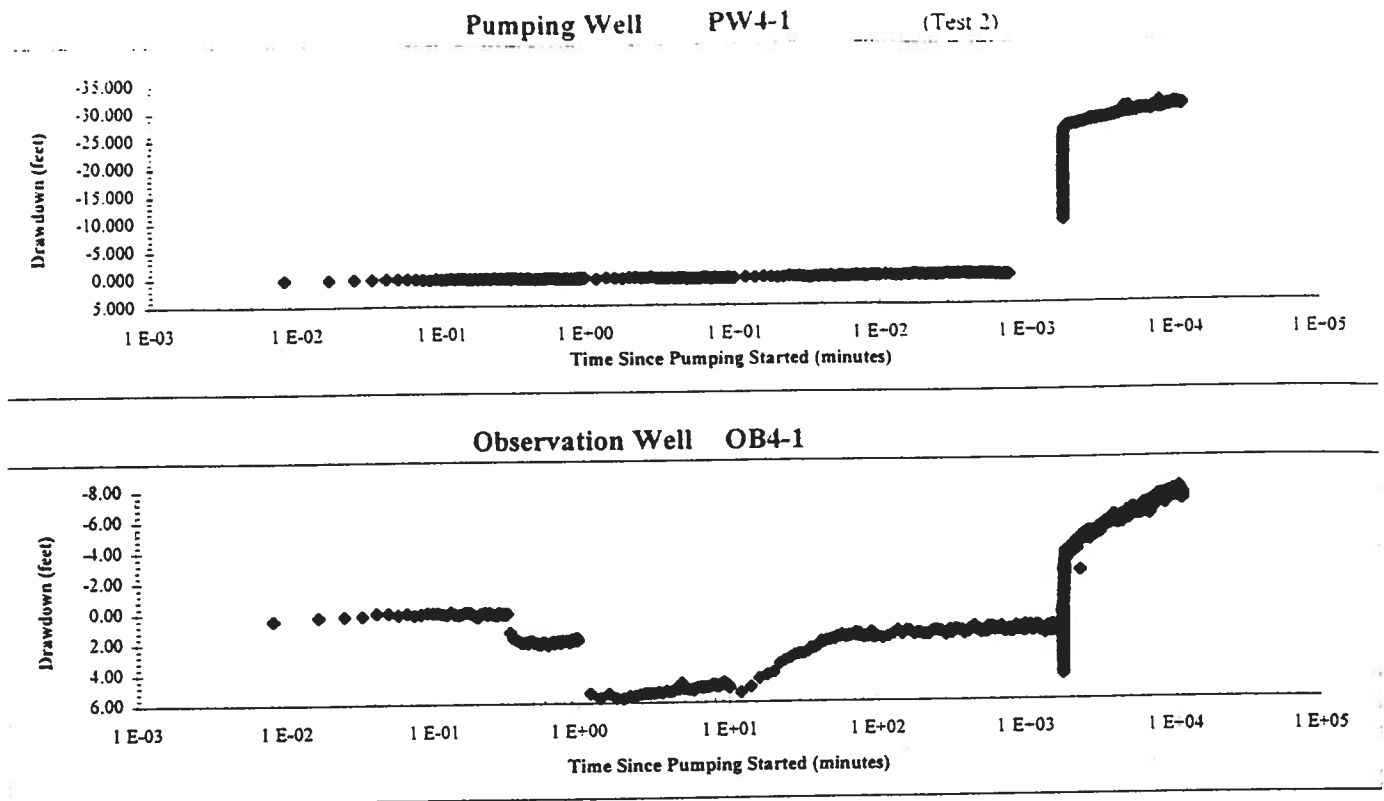
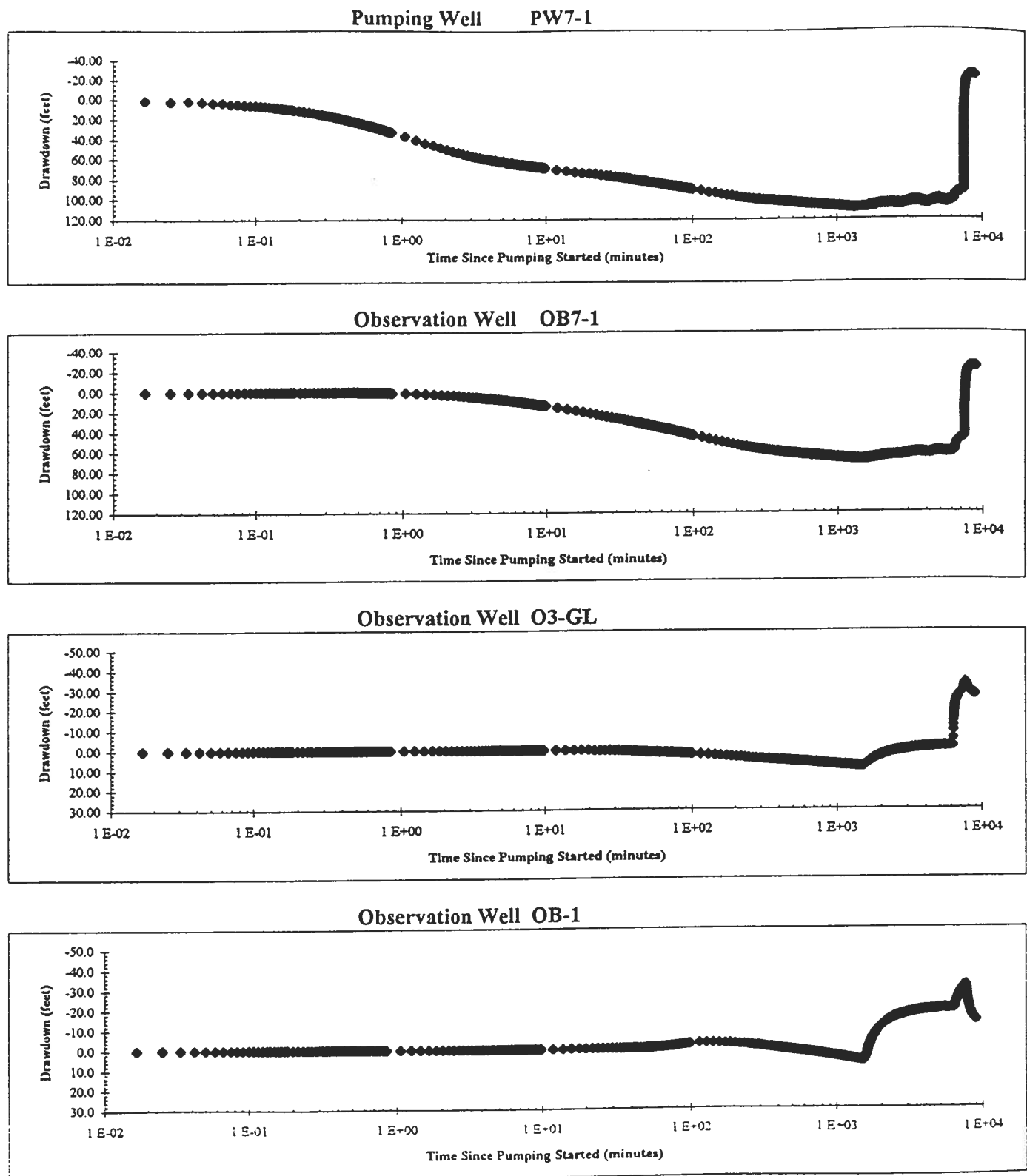


Figure 17A PW4-1 (Test 2) Semi-Log Aquifer Test Plot

**Figure 18A PW7-1 Semi-Log Aquifer Test Plot**

FlowDim Analysis File :

PW7-1dda.fdl

	Parameter		Units
r_w	Well radius	0.076	m
μ	Groundwater viscosity	1.000E-03	Pa s
ρ	Groundwater density	1.000E+03	kg/m ³
c_t	Total compressibility	5.400E-10	1/Pa
ϕ	Porosity of formation	5.00	%
C	Wellbore storage	6.871E-07	m ³ /Pa
h	Length of aquifer tested	103.63	m

Skin Factor Calculation

Assuming formation storativity, the skin factor (s) can be calculated from the following equation.

$$s = \frac{\ln (C_D e^{2s} 2 \pi \phi c_t h r_w^2 / C)}{2}$$

Match Point Parameters From Analysis

$C_D e^{2s}$	1.0000E+02
P_{DM}	2.1298E-02
T_{DM}	2.8162E+02

Results

T(m ² /sec)	K (feet/min)	K (feet/day)	K (m/s)	K (cm/s)	Skin
8.40E-05	1.59E-04	0.23	8.10E-07	8.10E-05	-2.10

Figure 18B PW7-1 FlowDim™ Analysis Summary

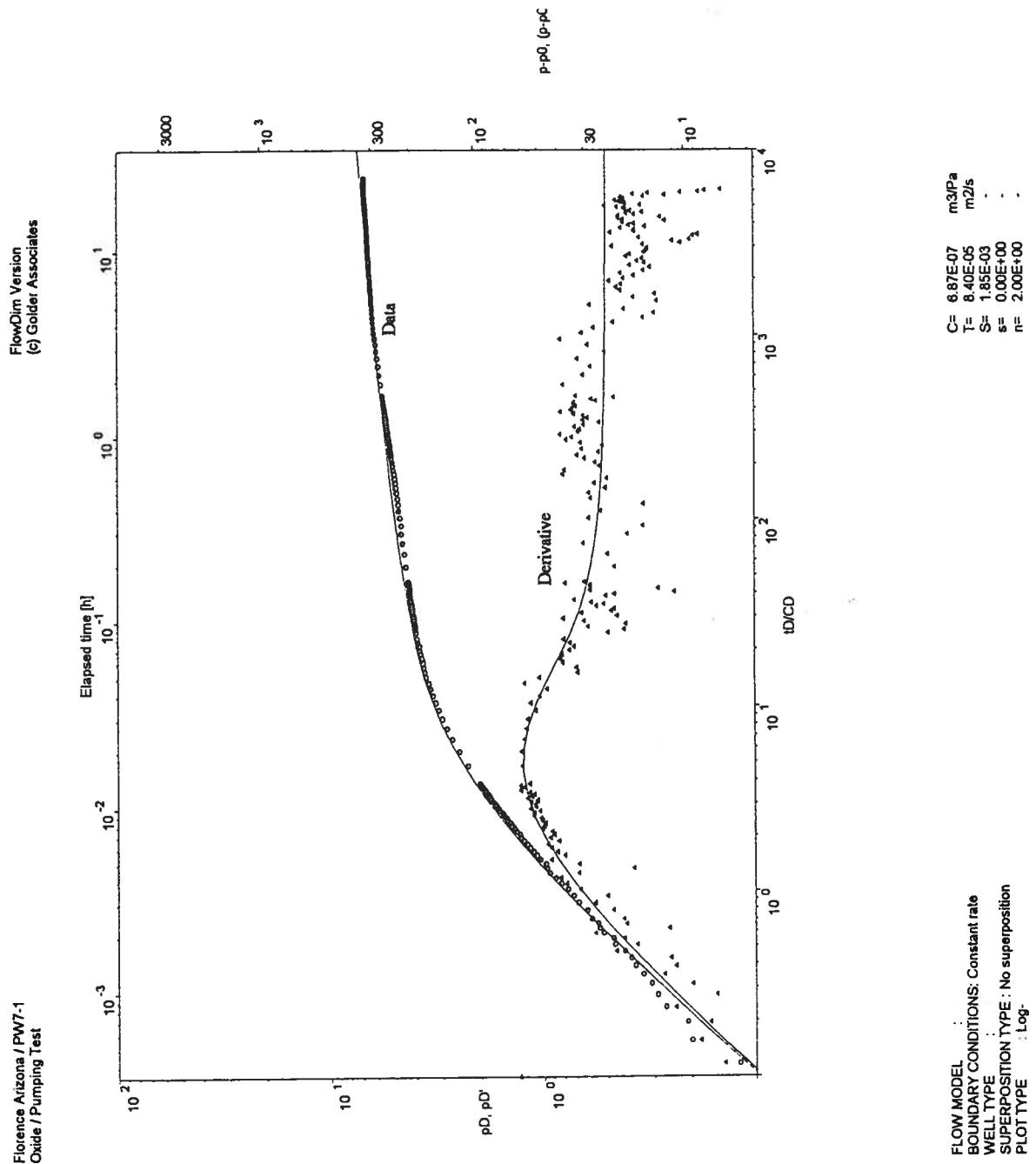


Figure 18C PW7-1 FlowDim™ Analysis Log-Log Plot

FlowDim Analysis File :

ob7-1dda.fd1

	Parameter		Units
r_w	Well radius	0.076	m
μ	Groundwater viscosity	1.000E-03	Pa s
ρ	Groundwater density	1.000E+03	kg/m ³
c_t	Total compressibility	5.400E-10	1/Pa
ϕ	Porosity of formation	5.00	%
C	Wellbore storage	N/A	m ³ /Pa
h	Length of aquifer tested	103.63	m

Skin Factor Calculation

Assuming formation storativity, the skin factor (s) can be calculated from the following equation.

$$s = \frac{\ln (C_D e^{2s} 2 \pi \phi c_t h r_w^2 / C)}{2}$$

Match Point Parameters From Analysis

$C_D e^{2s}$	N/A
P_{DM}	1.2560E-02
T_{DM}	5.7458E+00

Results

T(m ² /sec)	K (feet/min)	K(feet/dat)	K (m/s)	K (cm/s)	Skin
4.95E-05	9.40E-05	0.14	4.78E-07	4.78E-05	#####

Figure 18D OB7-1 FlowDim™ Analysis Summary

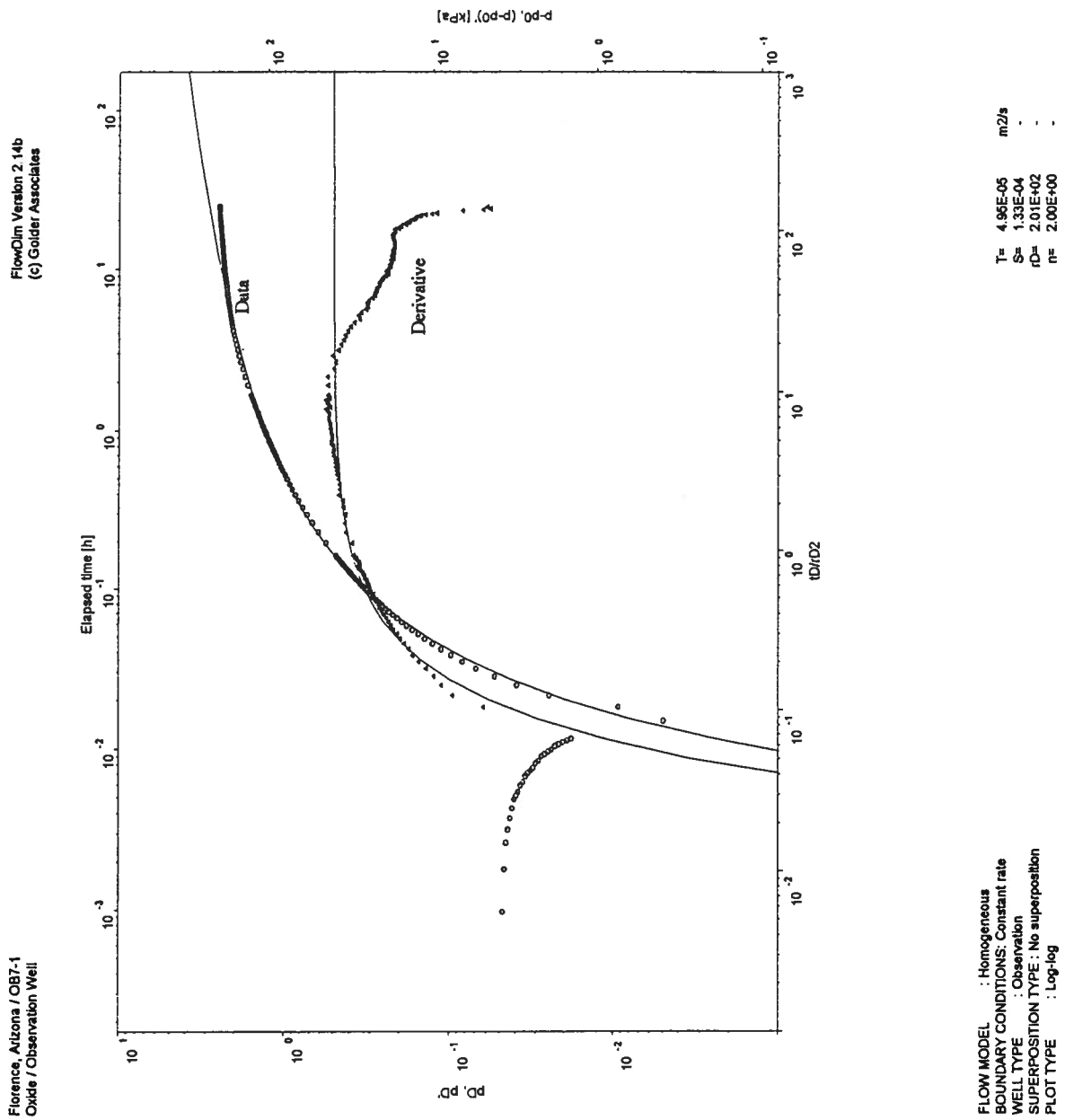
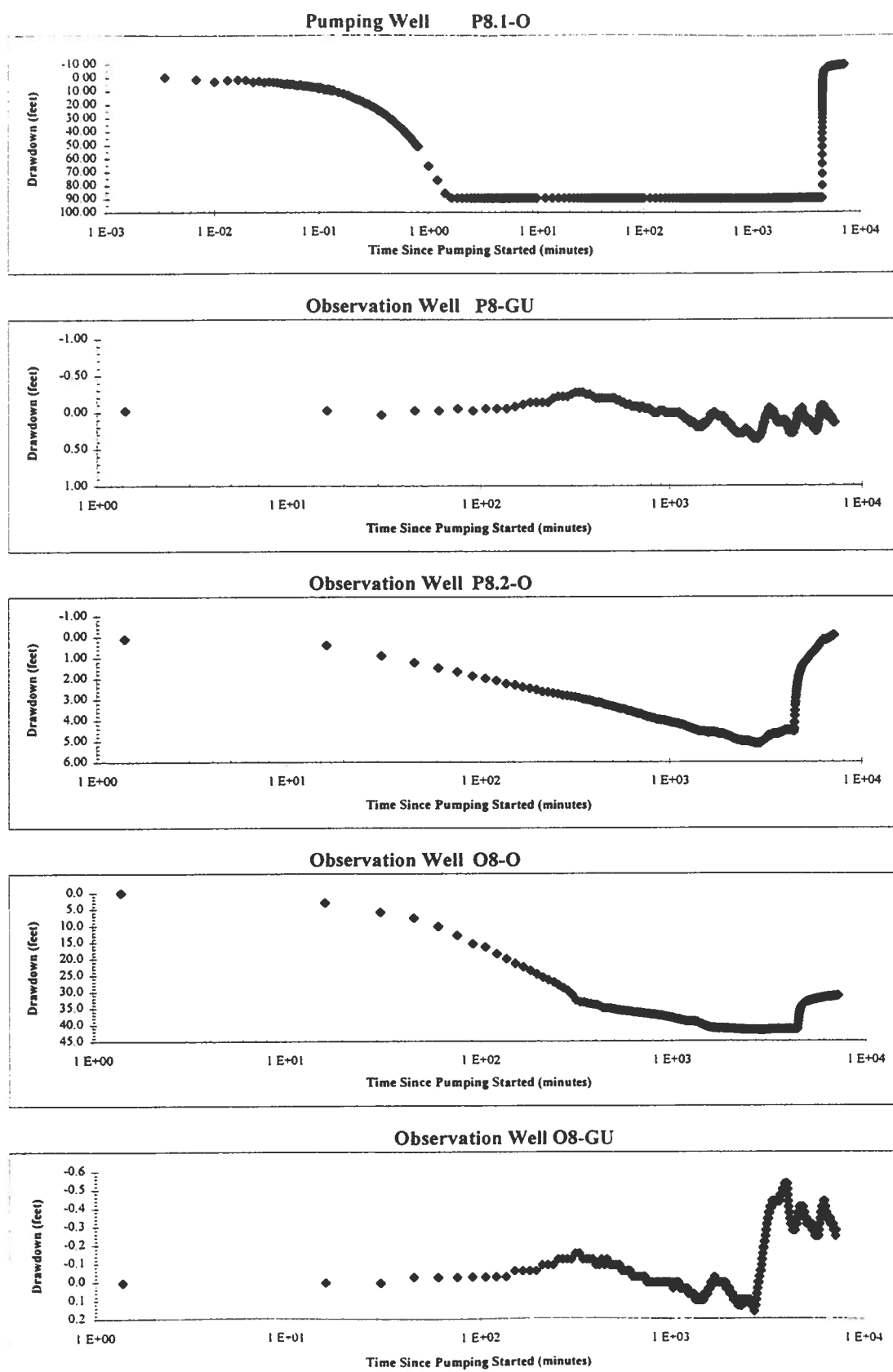


Figure 18E OB7-1 FlowDim™ Analysis Log-Log Plot

**Figure 19A P8.1-O Semi-Log Aquifer Test Plot**

Hydraulic Conductivity Calculation for a Cylindrical Source

Well Name:	P8.1-O
Sink Radius:	7.62E-02 m
Sink Screened Interval:	55.02 m
Pseudo-Transmissivity:	5.69E-06 m ² /sec
Pseudo-Storage:	1.48E-04
Anisotropy Ratio:	1.00

Pseudo-Spherical Radius:

 $r_{sw} = 4.18 \text{ m}$ Hydraulic Conductivity: $1.36\text{E-}06 \text{ m/sec} = 0.39 \text{ ft/day}$ Specific Storage: $3.54\text{E-}05 \text{ 1/m} = 1.08\text{E-}05 \text{ 1/ft}$ **Figure 19B P8.1-O (3D) FlowDim™ Analysis Summary**

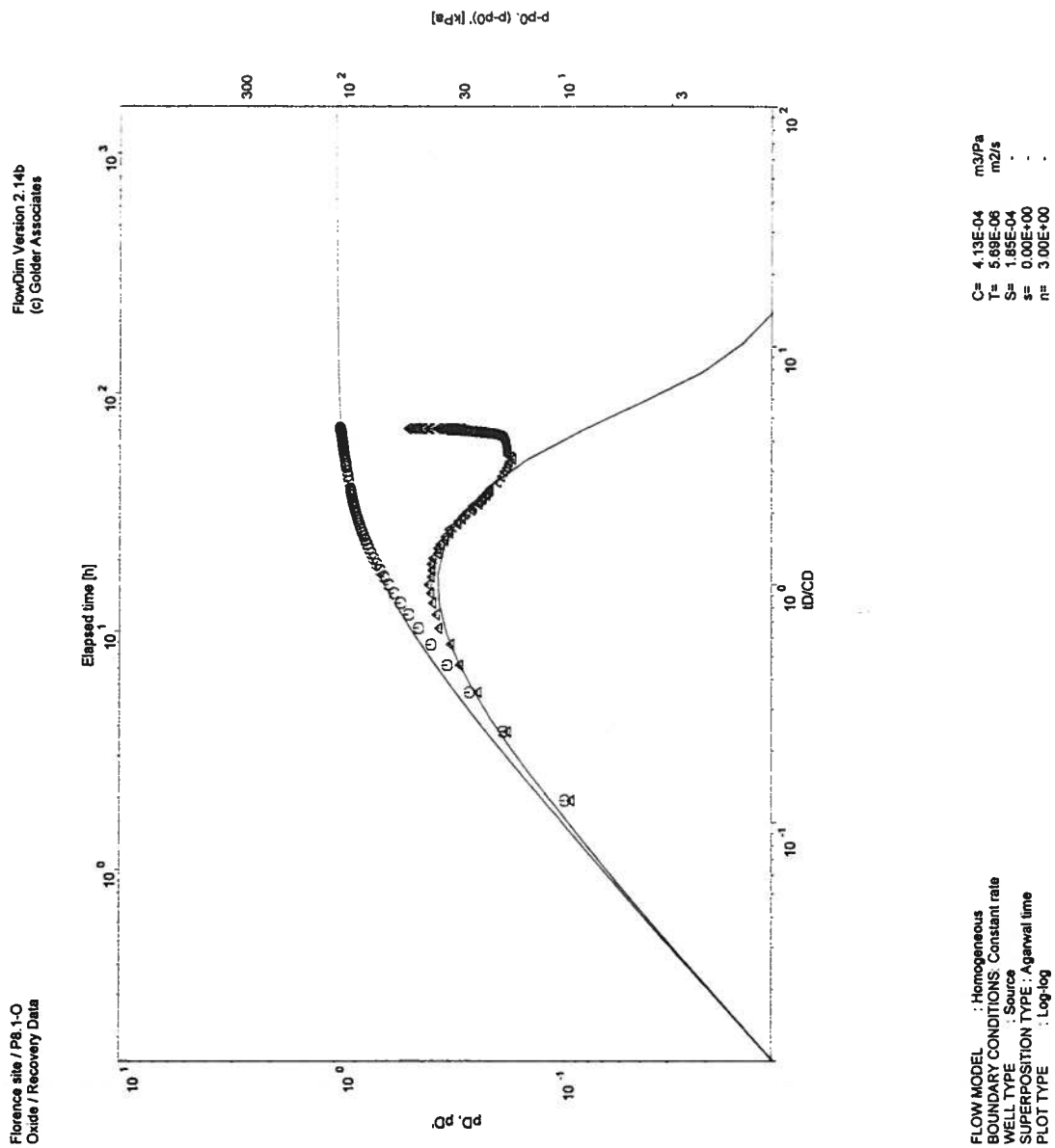
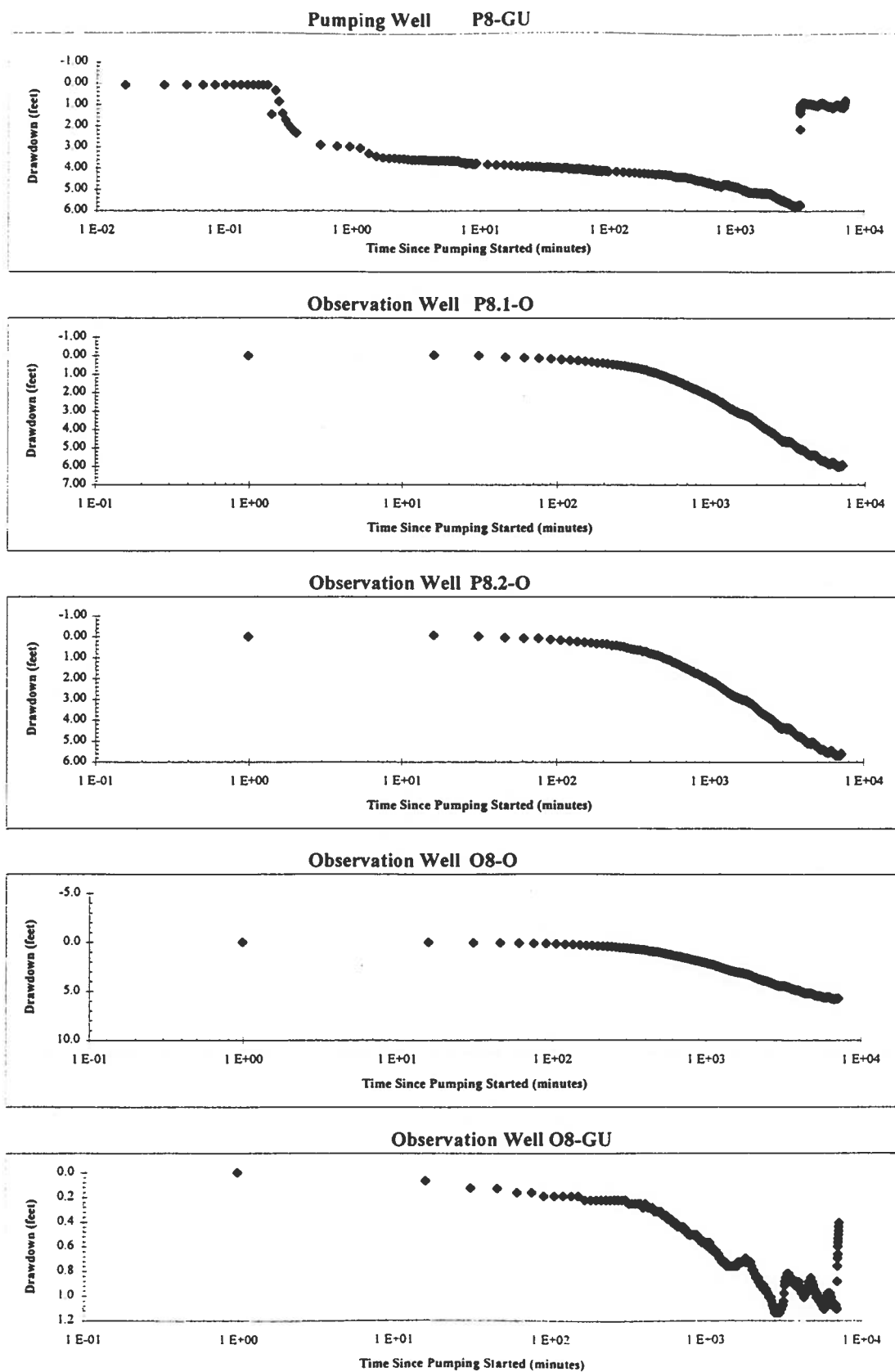


Figure 19C P8.1-O (3D) FlowDim™ Analysis Log-Log Plot

**Figure 20A P8-GU Semi-Log Aquifer Test Plot**

FlowDim Analysis File :

p8-gud.dat

	Parameter		Units
r_w	Well radius	0.076	m
μ	Groundwater viscosity	1.00E-03	Pa s
ρ	Groundwater density	1.00E+03	kg/m ³
c_t	Total compressibility	5.40E-10	1/Pa
ϕ	Porosity of formation	10.00	%
C	Wellbore storage	1.19E-05	m ³ /Pa
h	Length of aquifer tested	36.58	m

Skin Factor Calculation

Assuming formation storativity, the skin factor (s) can be calculated from the following equation.

$$s = \frac{\ln (C_D e^{2s} 2 \pi \phi c_t h r_w^2 / C)}{2}$$

Match Point Parameters From Analysis

$C_D e^{2s}$	1.0000E+06
P_{DM}	9.0703E-01
T_{DM}	1.5374E+03

Results

T(m ² /sec)	K (feet/min)	K (ft/day)	K (m/s)	K (cm/s)	Skin
7.91E-03	4.26E-02	61.31	2.16E-04	2.16E-02	0.90

Figure 20B P8-GU FlowDim™ Analysis Summary

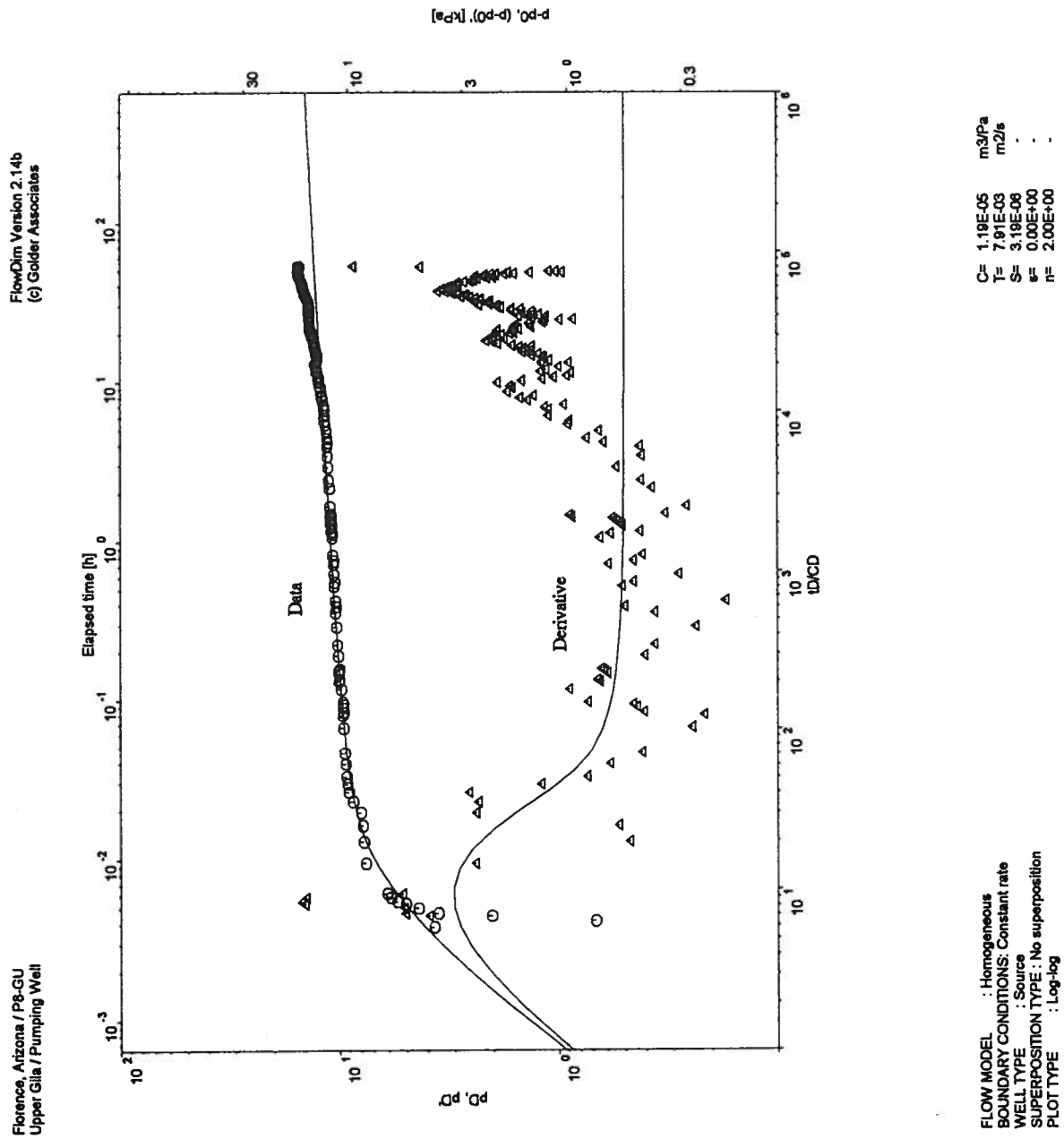
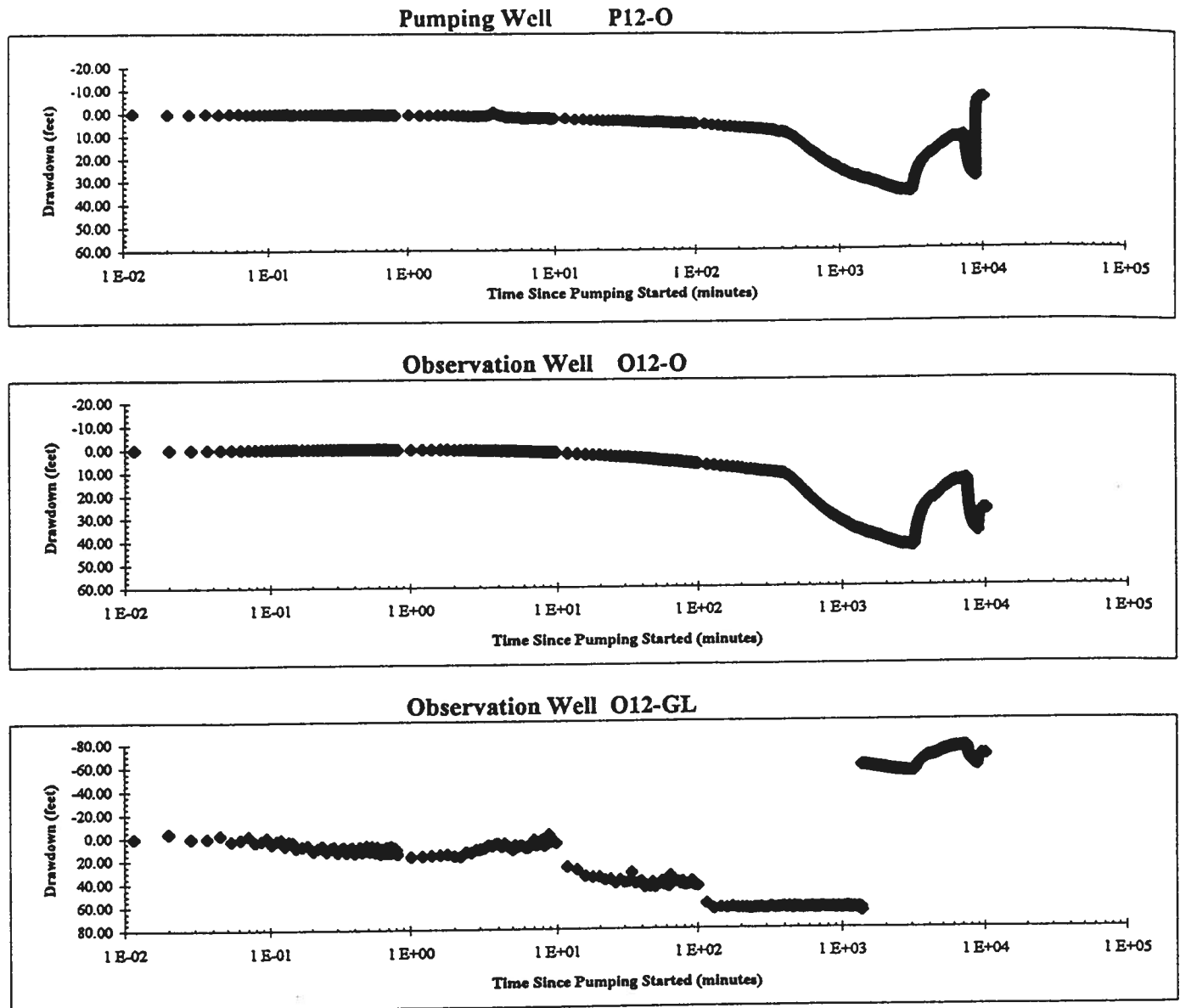


Figure 20C P8-GU FlowDim™ Analysis Log-Log Plot

**Figure 21A P12-O Semi-Log Aquifer Test Plot**

P12-O.ANL, Data Plots

Golder Associates

FlowDim Analysis File :

P12-oddc.fd1

	Parameter		Units
r_w	Well radius	0.076	m
μ	Groundwater viscosity	1.000E-03	Pa s
ρ	Groundwater density	1.000E+03	kg/m ³
c_t	Total compressibility	5.400E-10	1/Pa
ϕ	Porosity of formation	10.00	%
C	Wellbore storage	4.640E-06	m ³ /Pa
h	Length of aquifer tested	152.40	m

Skin Factor Calculation

Assuming formation storativity, the skin factor (s) can be calculated from the following equation.

$$s = \frac{\ln (C_D e^{2s} 2 \pi \phi c_t h r_w^2 / C)}{2}$$

Match Point Parameters From Analysis

$C_D e^{2s}$	3.0000E+00
P_{DM}	3.1823E-02
T_{DM}	1.0126E+02

Results

T(m ² /sec)	K (feet/min)	K (feet/day)	K (m/s)	K (cm/s)	Skin
2.04E-04	2.63E-04	0.38	1.34E-06	1.34E-04	-4.27

Figure 21B P12-O FlowDim™ Analysis Summary

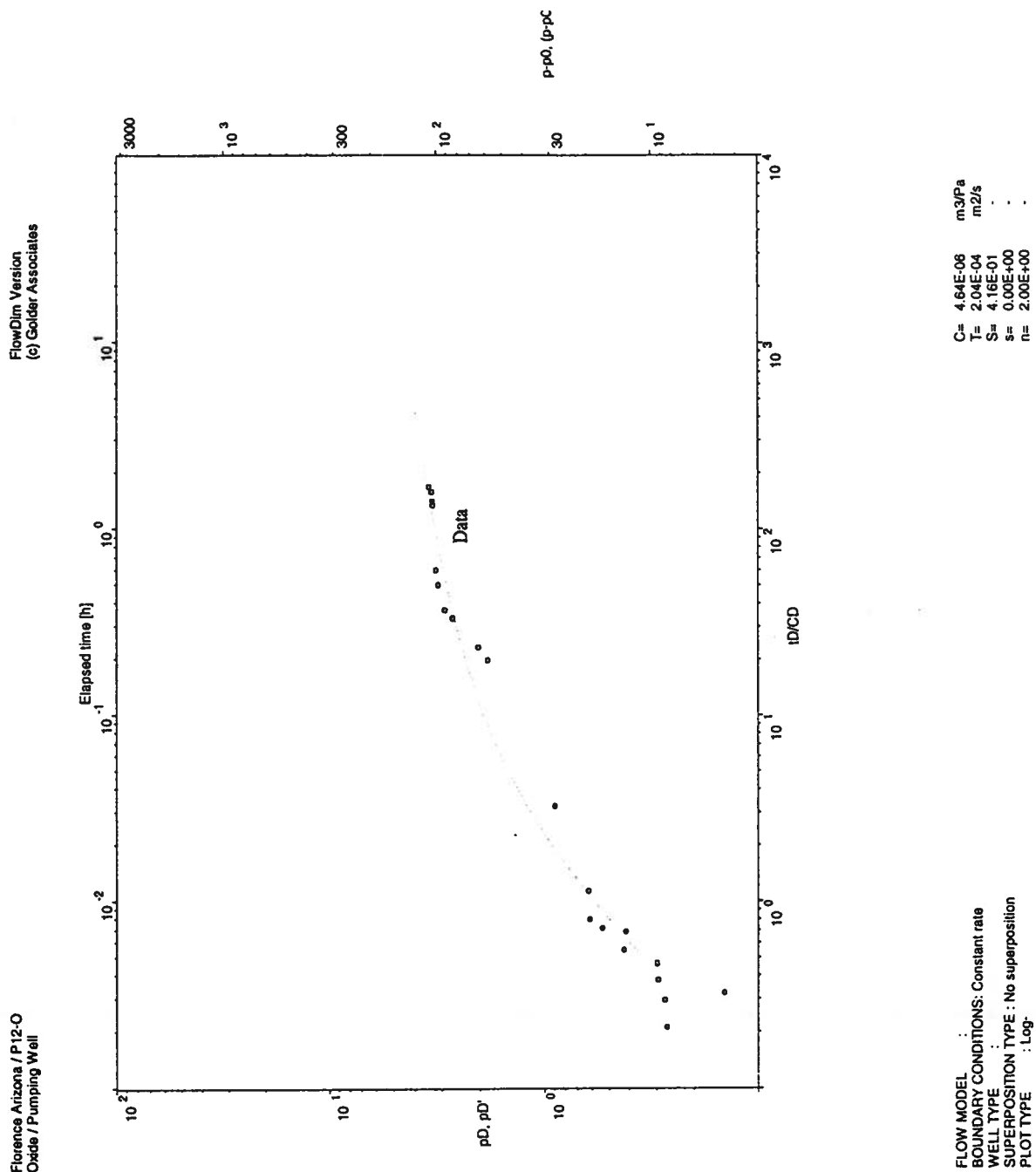


Figure 21C P12-O FlowDim™ Analysis Log-Log Plot

FlowDim Analysis File :**O12-O.DAT**

	Parameter		Units
r_w	Well radius	0.051	m
μ	Groundwater viscosity	1.000E-03	Pa s
ρ	Groundwater density	1.000E+03	kg/m ³
c_t	Total compressibility	5.400E-10	1/Pa
ϕ	Porosity of formation	10.00	%
C	Wellbore storage	N/A	m ³ /Pa
h	Length of aquifer tested	152.40	m

Skin Factor Calculation

Assuming formation storativity, the skin factor (s) can be calculated from the following equation.

$$s = \frac{\ln (C_D e^{2s} 2 \pi \phi c_t h r_w^2 / C)}{2}$$

Match Point Parameters From Analysis

$C_D e^{2s}$	N/A
Pm (1/KPa)	5.0164E-02
Tm (hr)	1.0792E+00

Results

T(m ² /sec)	K (feet/min)	K(feet/dat)	K (m/s)	K (cm/s)	Skin
4.05E-04	5.23E-04	0.75	2.66E-06	2.66E-04	#####

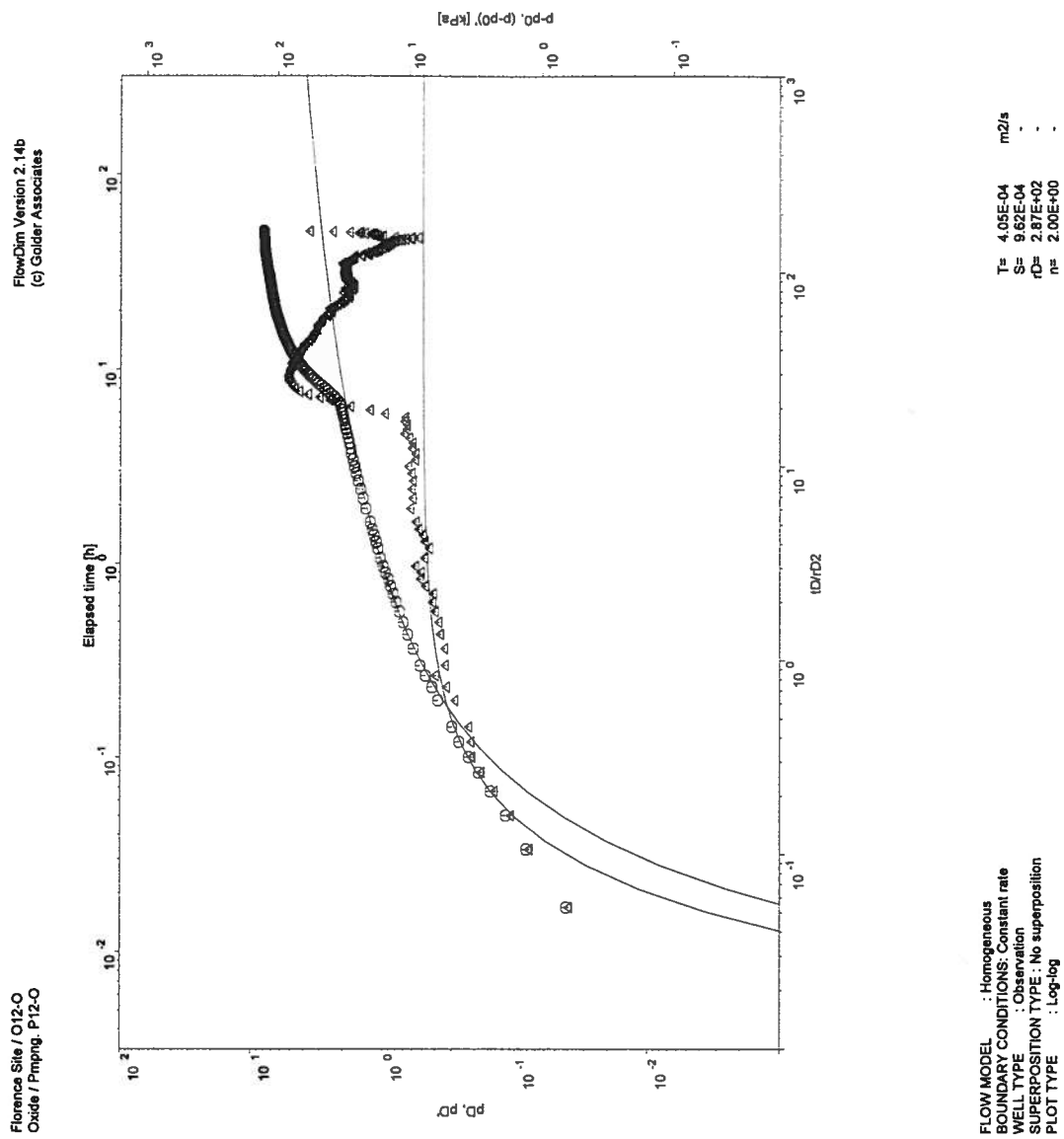
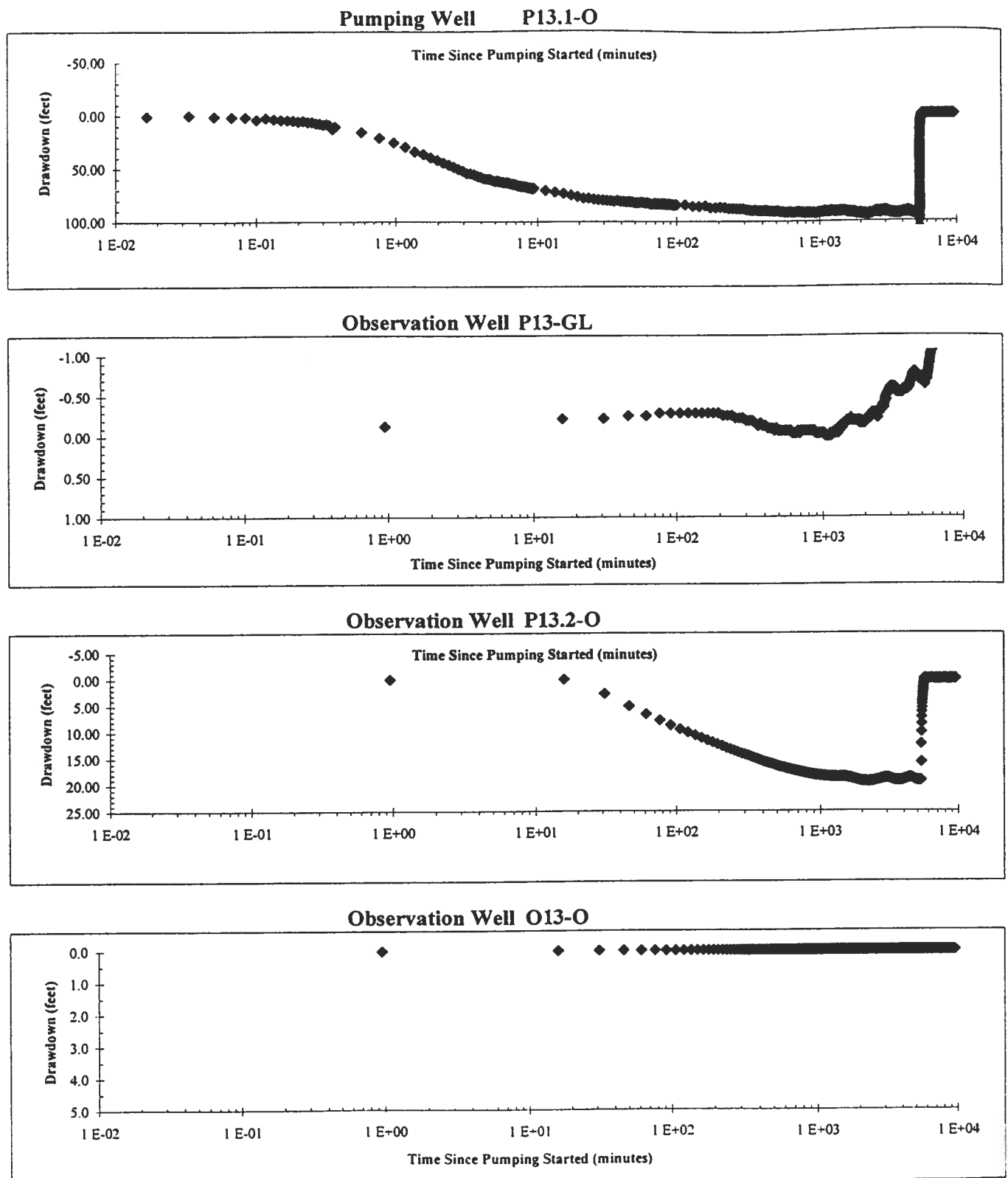


Figure 21E O12-O FlowDim™ Analysis Log-Log Plot

**Figure 22A P13.1-O Semi-Log Aquifer Test Plot**

Hydraulic Conductivity Calculation for a Cylindrical Source

Well Name:	P13.1-O
Sink Radius:	7.62E-02 m
Sink Screened Interval:	206.35 m
Pseudo-Transmissivity:	8.01E-06 m ² /sec
Pseudo-Storage:	5.29E-06
Anisotropy Ratio:	1.00

Pseudo-Spherical Radius:

 $r_{sw} = 13.05 \text{ m}$ Hydraulic Conductivity: $6.14\text{E-}07 \text{ m/sec} = 0.17 \text{ ft/day}$ Specific Storage: $4.05\text{E-}07 \text{ 1/m} = 1.24\text{E-}07 \text{ 1/ft}$ **Figure 22B P13.1-O (3D) FlowDim™ Analysis Summary**

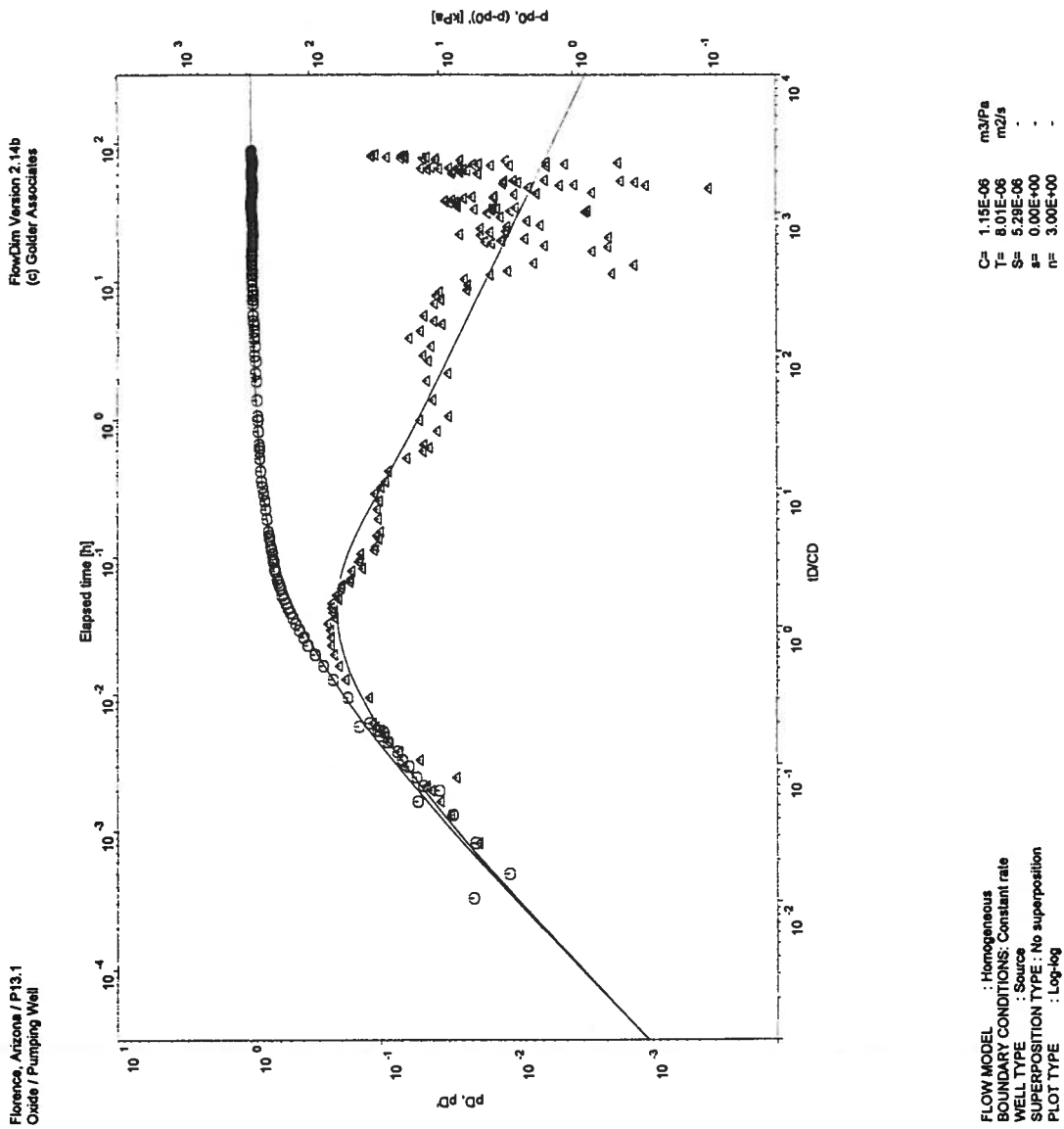


Figure 22C P13.1-O (3D) FlowDim™ Analysis Log-Log Plot

Hydraulic Conductivity Calculation for a Cylindrical Source

PUMPING WELL

Easting:	647551.2	ft
Northing:	746799.4	ft
Screen Top:	771.7	ft
Screen Bottom:	1448.9	ft
Surface Elevation	1478.5	ft (amsl)
Radius:	7.62E-02	m
Screen Interval:	206.40	m
Screen Interval Mid-Point:	112.23	m

OBSERVATION WELL

Easting	647653.8	ft
Northing	746807.6	ft
Screen Top:	780.7	ft
Screen Bottom:	1379.4	ft
Surface Elevation	1479.2	ft
Screen Interval Mid-Point:	121.67	m
Distance to Sink:	31.5	m

Pseudo-Transmissivity:	1.36E-05	m ² /sec
Pseudo-Storage:	1.38E-04	
Anisotropy Ratio:	1.00	

Pseudo-Spherical Radius:

$r_{sw} = 13.06 \text{ m}$

Hydraulic Conductivity: $1.04\text{E-}06 \text{ m/sec} = 0.30 \text{ ft/day}$

Specific Storage: $1.82\text{E-}06 \text{ 1/m} = 5.53\text{E-}07 \text{ 1/ft}$

Figure 22D P13.2-O (3D) FlowDim™ Analysis Summary

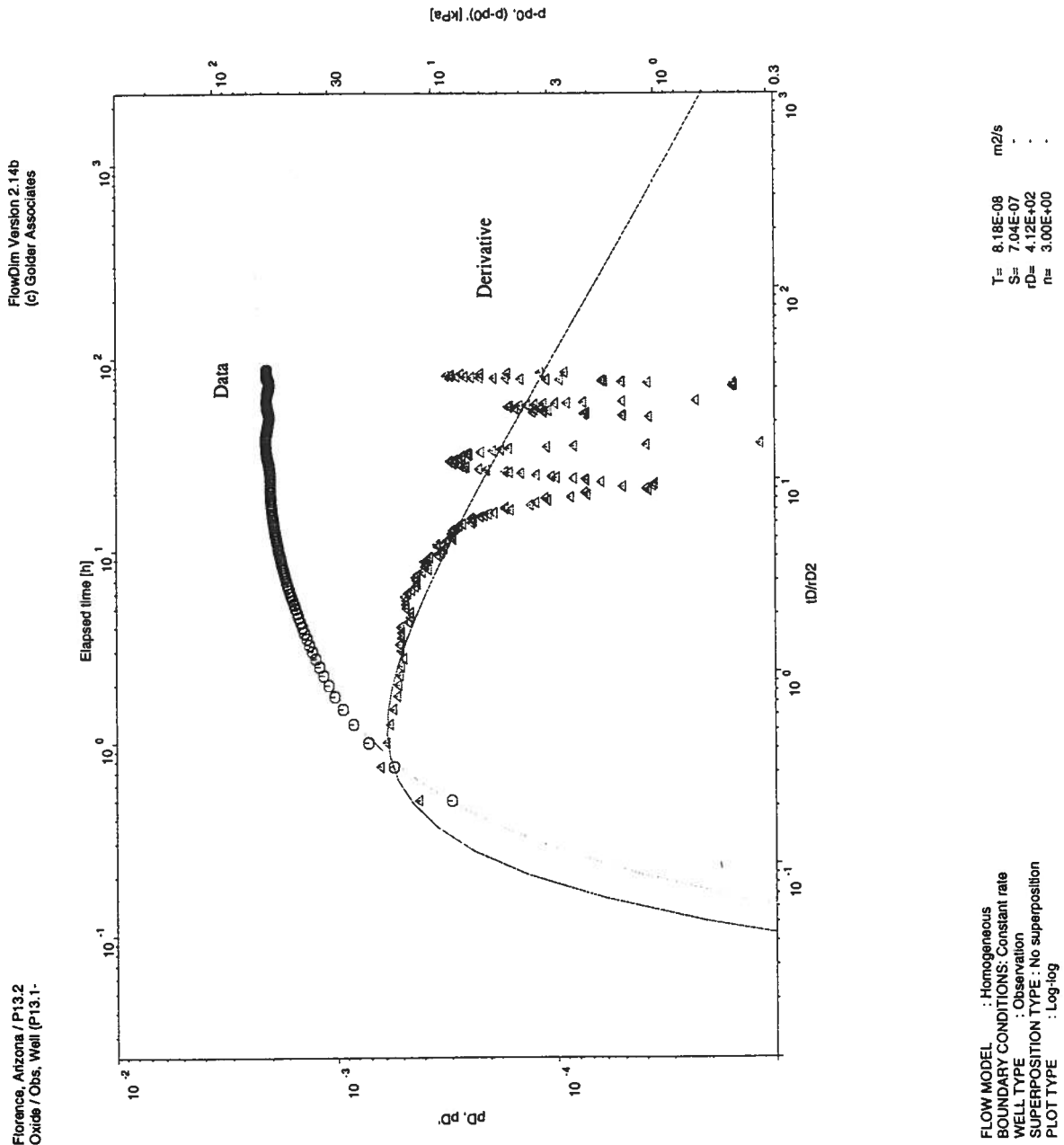


Figure 22E P13.2-O (3D) FlowDim™ Analysis Log-Log Plot

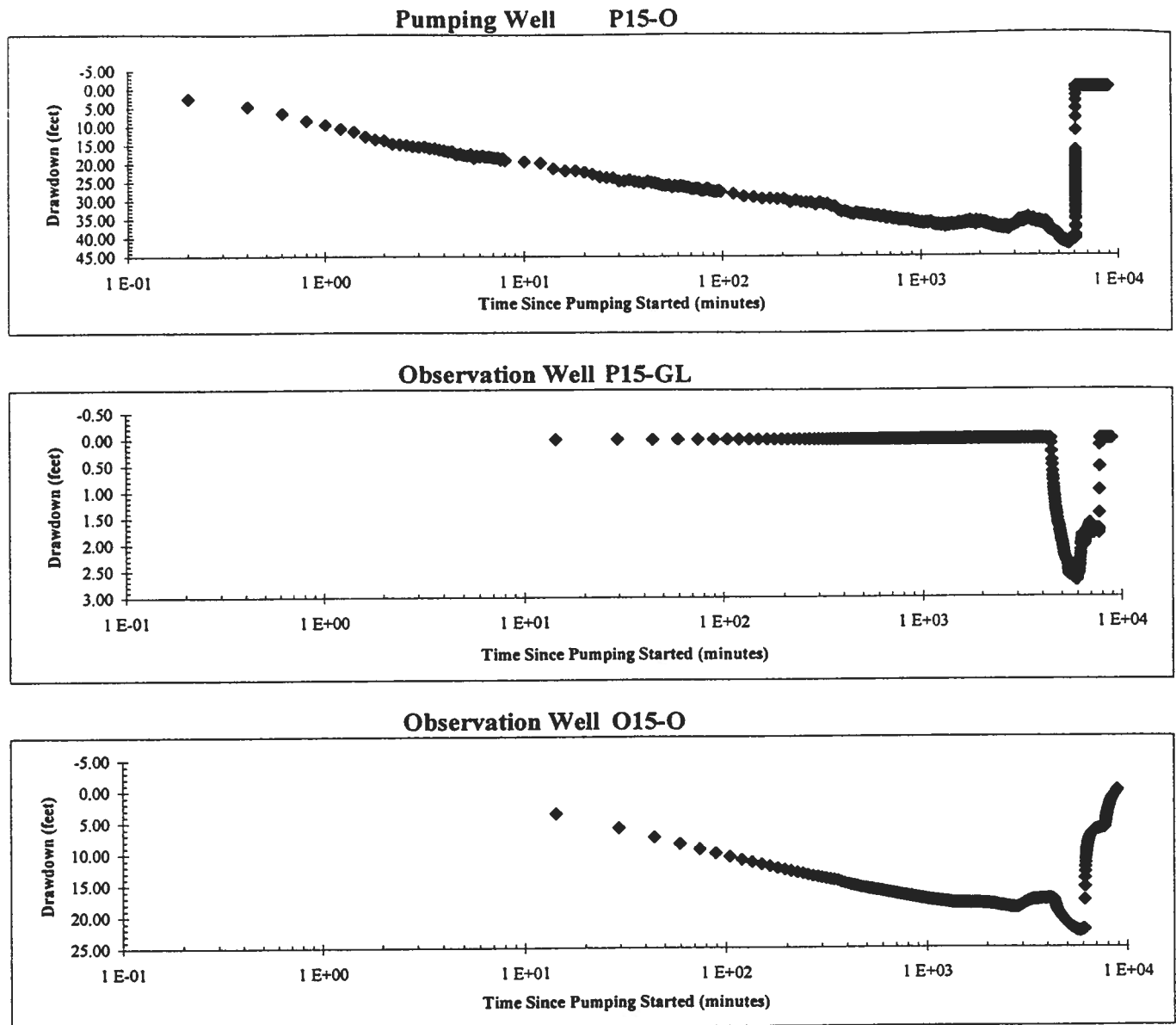


Figure 23A P15-O Semi-Log Aquifer Test Plot

FlowDim Analysis File :

P150d.dat

	Parameter		Units
r_w	Well radius	0.076	m
μ	Groundwater viscosity	1.00E-03	Pa s
ρ	Groundwater density	1.00E+03	kg/m ³
c_t	Total compressibility	5.40E-10	1/Pa
ϕ	Porosity of formation	0.05	%
C	Wellbore storage	4.94E-06	m ³ /Pa
h	Length of aquifer tested	219.46	m

Skin Factor Calculation

Assuming formation storativity, the skin factor (s) can be calculated from the following equation.

$$s = \frac{\ln (C_D e^{2s} 2 \pi \phi c_t h r_w^2 / C)}{2}$$

Match Point Parameters From Analysis

$C_D e^{2s}$	1.0000E+02
P_{DM}	6.6100E-02
T_{DM}	1.7940E+02

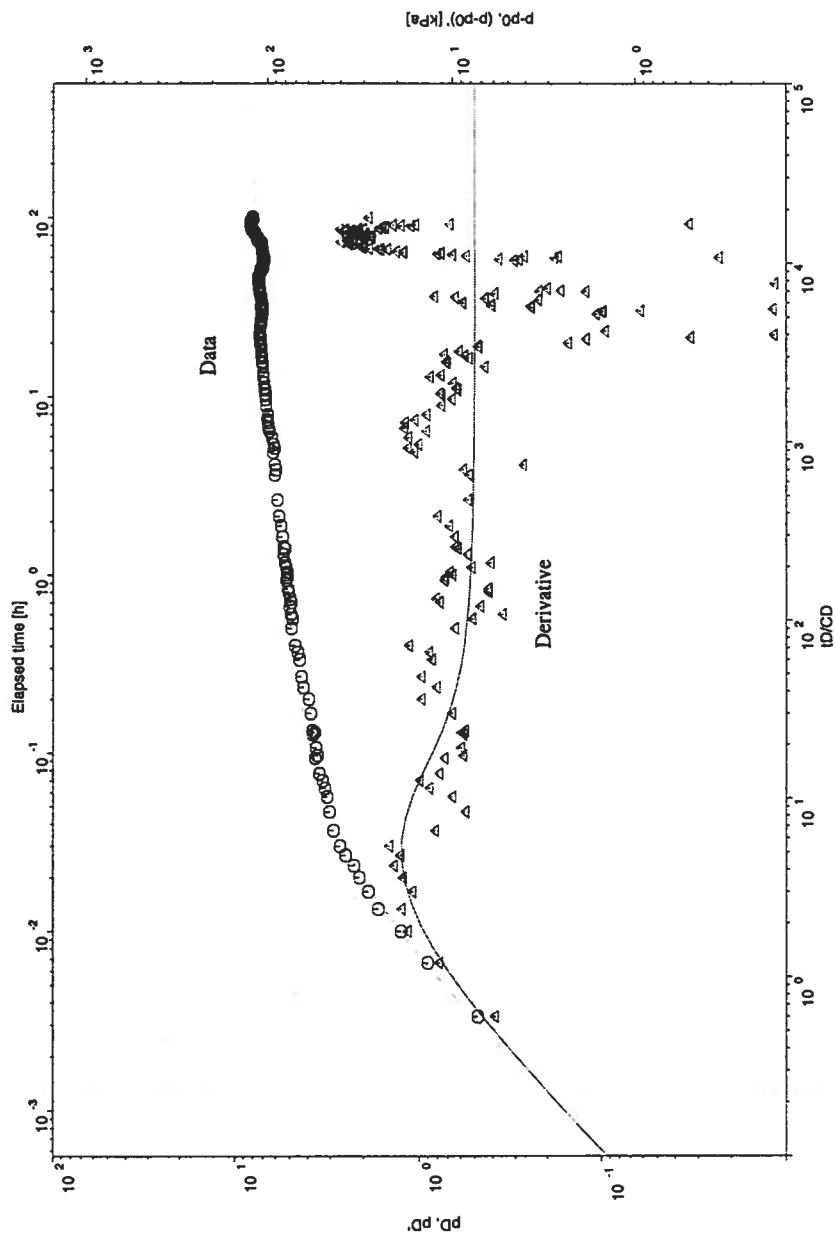
Results

T(m ² /sec)	K (feet/min)	K (ft/day)	K (m/s)	K (cm/s)	Skin
3.84E-04	3.44E-04	0.50	1.75E-06	1.75E-04	-5.02

Figure 23B P15-O FlowDim™ Analysis Summary

Florence, Arizona / P15-O
Oxide / Pumping Well

FlowDim Version 2.14b
(c) Golder Associates



C= 4.94E-08 m³/Pa
T= 3.84E-04 m²/s
S= 1.33E-02
s= 0.00E+00
n= 2.00E+00

FLOW MODEL : Homogeneous
BOUNDARY CONDITIONS: Constant rate
WELL TYPE : Source
SUPERPOSITION TYPE : No superposition
PLOT TYPE : Log-log

Figure 23C P15-O FlowDim™ Analysis Log-Log Plot

Hydraulic Conductivity Calculation for a Cylindrical Source

PUMPING WELL

	P15-O	
Easting:	647596.4	ft
Northing:	745428.6	ft
Screen Top:	580	ft
Screen Bottom:	1300.5	ft
Surface Elevation	1468	ft (amsl)
Radius:	7.62E-02	m
Screen Interval:	219.61	m
Screen Interval Mid-Point:	160.86	m

OBSERVATION WELL

	O15-O	
Easting	647508.4	ft
Northing	745376.9	ft
Screen Top:	632.2	ft
Screen Bottom:	1295.6	ft
Surface Elevation	1467.5	ft
Screen Interval Mid-Point:	153.50	m
Distance to Sink:	31.2	m

Pseudo-Transmissivity: 2.56E-05 m²/sec
 Pseudo-Storage: 2.24E-04
 Anisotropy Ratio: 1.00

Pseudo-Spherical Radius:

$$r_{sw} = 13.78 \text{ m}$$

Hydraulic Conductivity: 1.86E-06 m/sec = 0.53 ft/day

Specific Storage: 3.18E-06 1/m = 9.68E-07 1/ft

Figure 23D O15-O (3D) FlowDim™ Analysis Summary

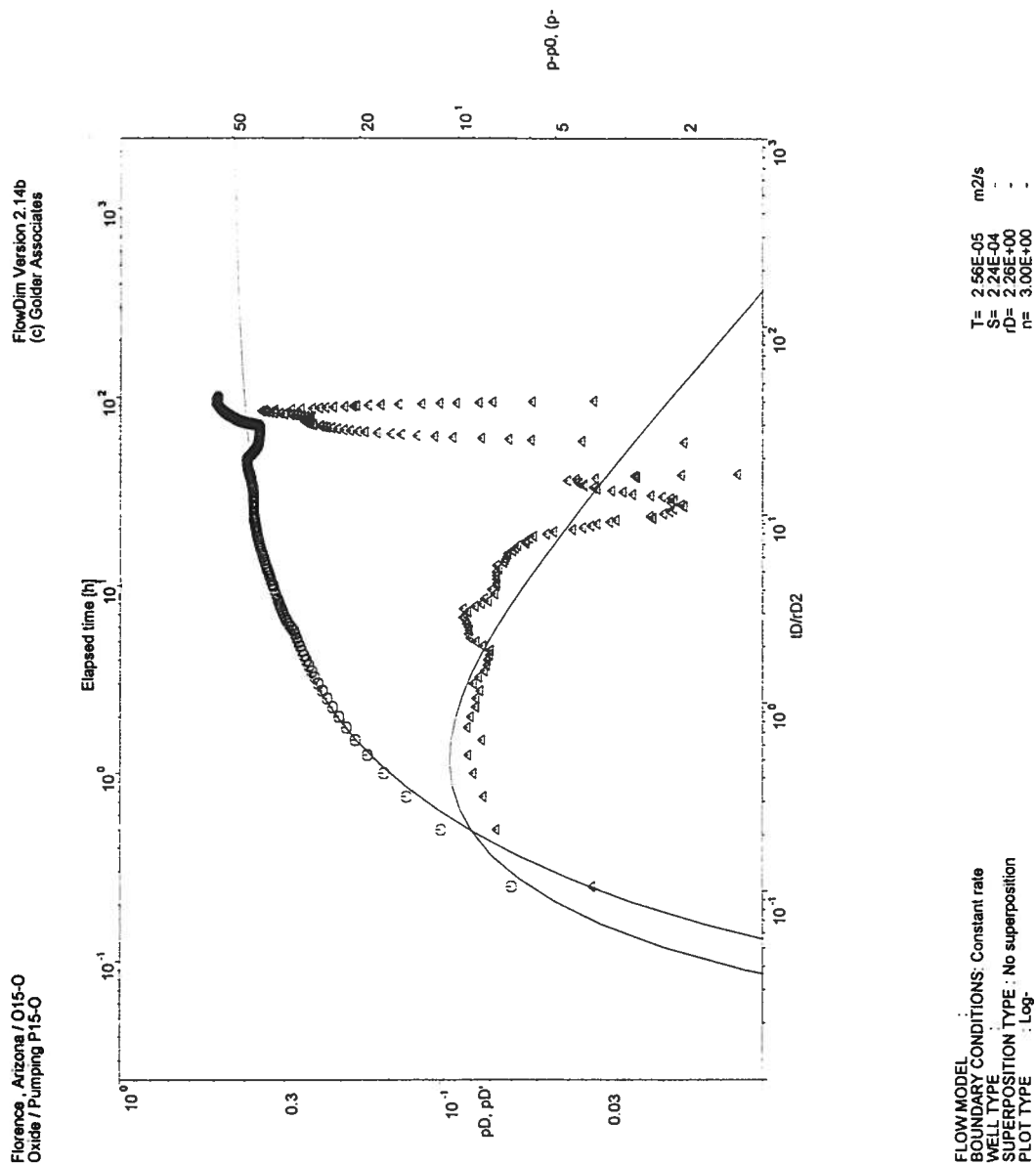


Figure 23E O15-O (3D) FlowDim™ Analysis Log-Log Plot

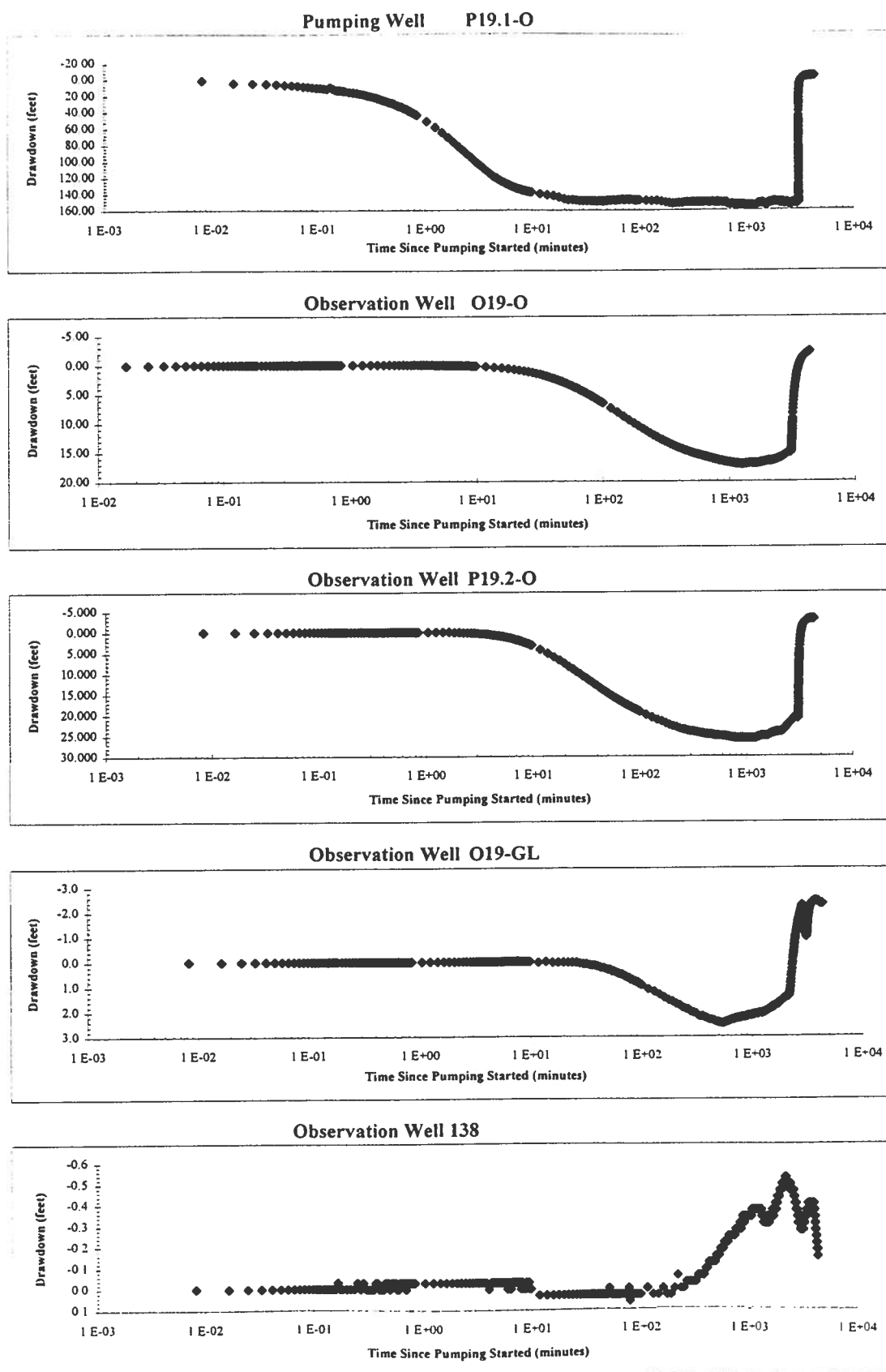


Figure 24A P19.1-O Semi-Log Aquifer Test Plot

Hydraulic Conductivity Calculation for a Cylindrical Source

Well Name:	P19.1-O
Sink Radius:	7.62E-02 m
Sink Screened Interval:	60.35 m
Pseudo-Transmissivity:	2.36E-06 m ² /sec
Pseudo-Storage:	1.60E-06
Anisotropy Ratio:	1.00

Pseudo-Spherical Radius:

 $r_{sw} = 4.52 \text{ m}$ Hydraulic Conductivity: $5.22\text{E-}07 \text{ m/sec} = 0.15 \text{ ft/day}$ Specific Storage: $3.54\text{E-}07 \text{ 1/m} = 1.08\text{E-}07 \text{ 1/ft}$ **Figure 24B P19.1-O (3D) FlowDim™ Analysis Summary**

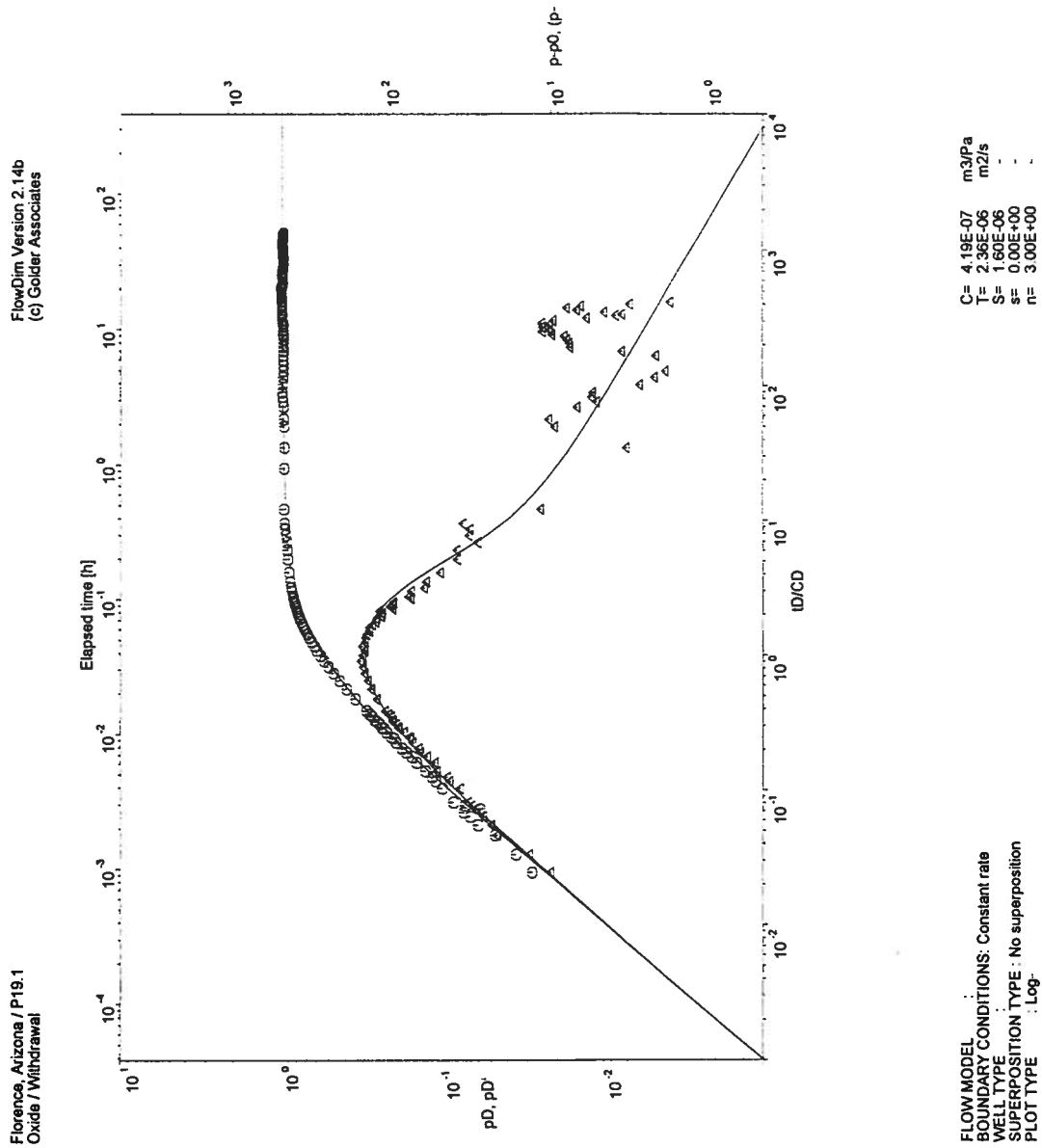


Figure 24C P19.1-O (3D) FlowDim™ Analysis Log-Log Plot

Hydraulic Conductivity Calculation for a Cylindrical Source

PUMPING WELL

Easting:	P19.1-O	648427.9	ft
Northing:		747345.8	ft
Screen Top:		402.25	ft
Screen Bottom:		600.45	ft
Surface Elevation		1483	ft (amsl)
Radius:		7.62E-02	m
Screen Interval:		60.41	m
Screen Interval Mid-Point:		299.21	m

OBSERVATION WELL

Easting	O19-O	648359.5	ft
Northing		747350.4	ft
Screen Top:		409.8	ft
Screen Bottom:		607.6	ft
Surface Elevation		1482.7	ft
Screen Interval Mid-Point:		296.88	m
Distance to Sink:		20.9	m

Pseudo-Transmissivity:	3.06E-06	m ² /sec
Pseudo-Storage:	1.19E-04	
Anisotropy Ratio:	1.00	

Pseudo-Spherical Radius:

$r_{sw} = 4.52 \text{ m}$

Hydraulic Conductivity: $6.76\text{E-}07 \text{ m/sec} = 0.19 \text{ ft/day}$

Specific Storage: $1.23\text{E-}06 \text{ 1/m} = 3.75\text{E-}07 \text{ 1/ft}$

Figure 24D O19-O (3D) FlowDim™ Analysis Summary

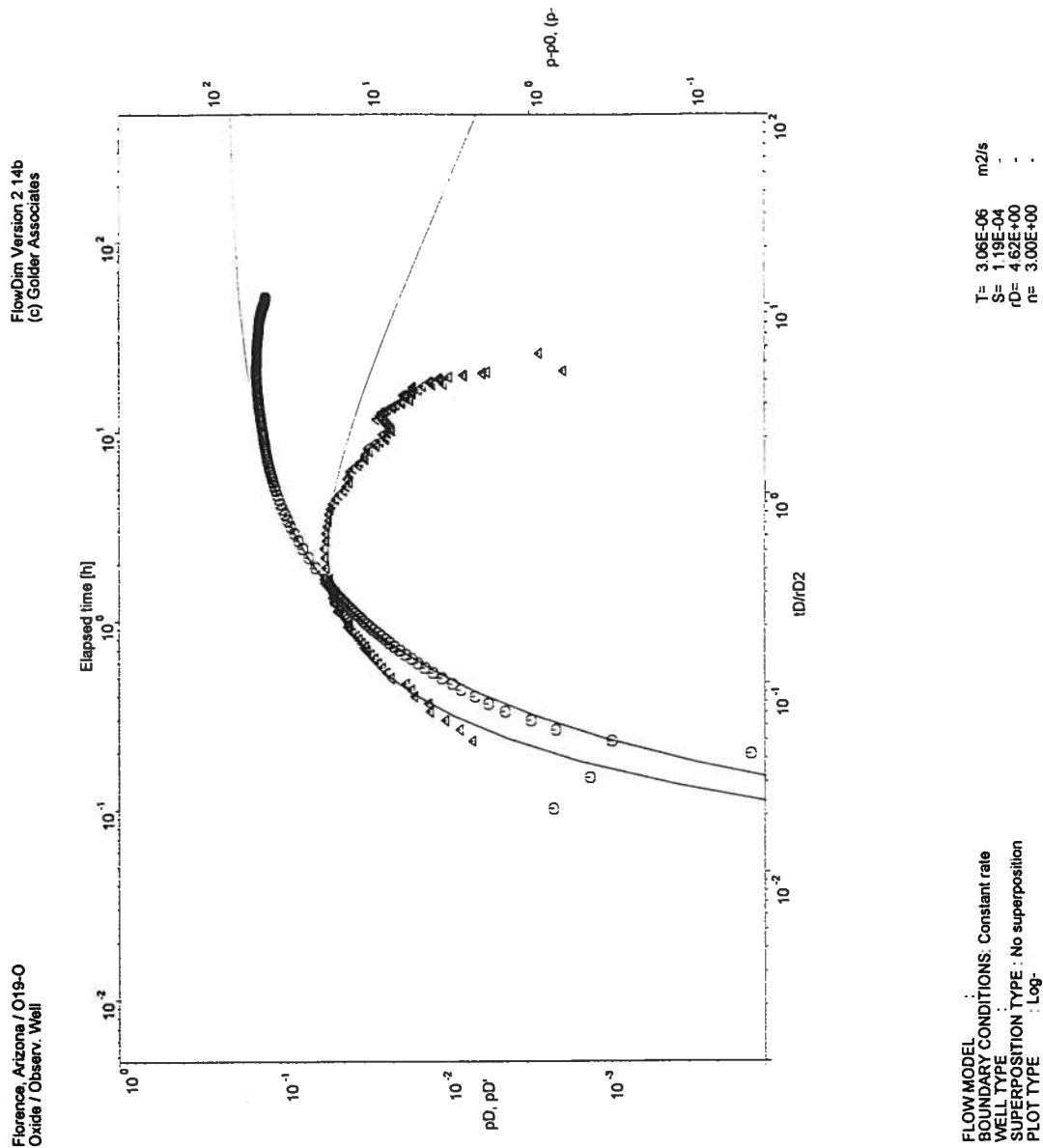


Figure 24E O19-O (3D) FlowDim™ Analysis Log-Log Plot

Hydraulic Conductivity Calculation for a Cylindrical Source

PUMPING WELL

Easting:	648427.9	ft
Northing:	747345.8	ft
Screen Top:	402.25	ft
Screen Bottom:	600.45	ft
Surface Elevation	1483	ft (amsl)
Radius:	7.62E-02	m
Screen Interval:	60.41	m
Screen Interval Mid-Point:	299.21	m

OBSERVATION WELL

Easting	648397.1	ft
Northing	747413.6	ft
Screen Top:	404.5	ft
Screen Bottom:	602.0	ft
Surface Elevation	1482.6	ft
Screen Interval Mid-Point:	298.51	m
Distance to Sink:	22.7	m

Pseudo-Transmissivity:	2.23E-06	m ² /sec
Pseudo-Storage:	1.65E-05	
Anisotropy Ratio:	1.00	

Pseudo-Spherical Radius:

$r_{sw} = 4.52 \text{ m}$

Hydraulic Conductivity: $4.93\text{E-}07 \text{ m/sec} = 0.14 \text{ ft/day}$

Specific Storage: $1.45\text{E-}07 \text{ 1/m} = 4.41\text{E-}08 \text{ 1/ft}$

Figure 24F P19.2-O (3D) FlowDim™ Analysis Summary

Golder Associates

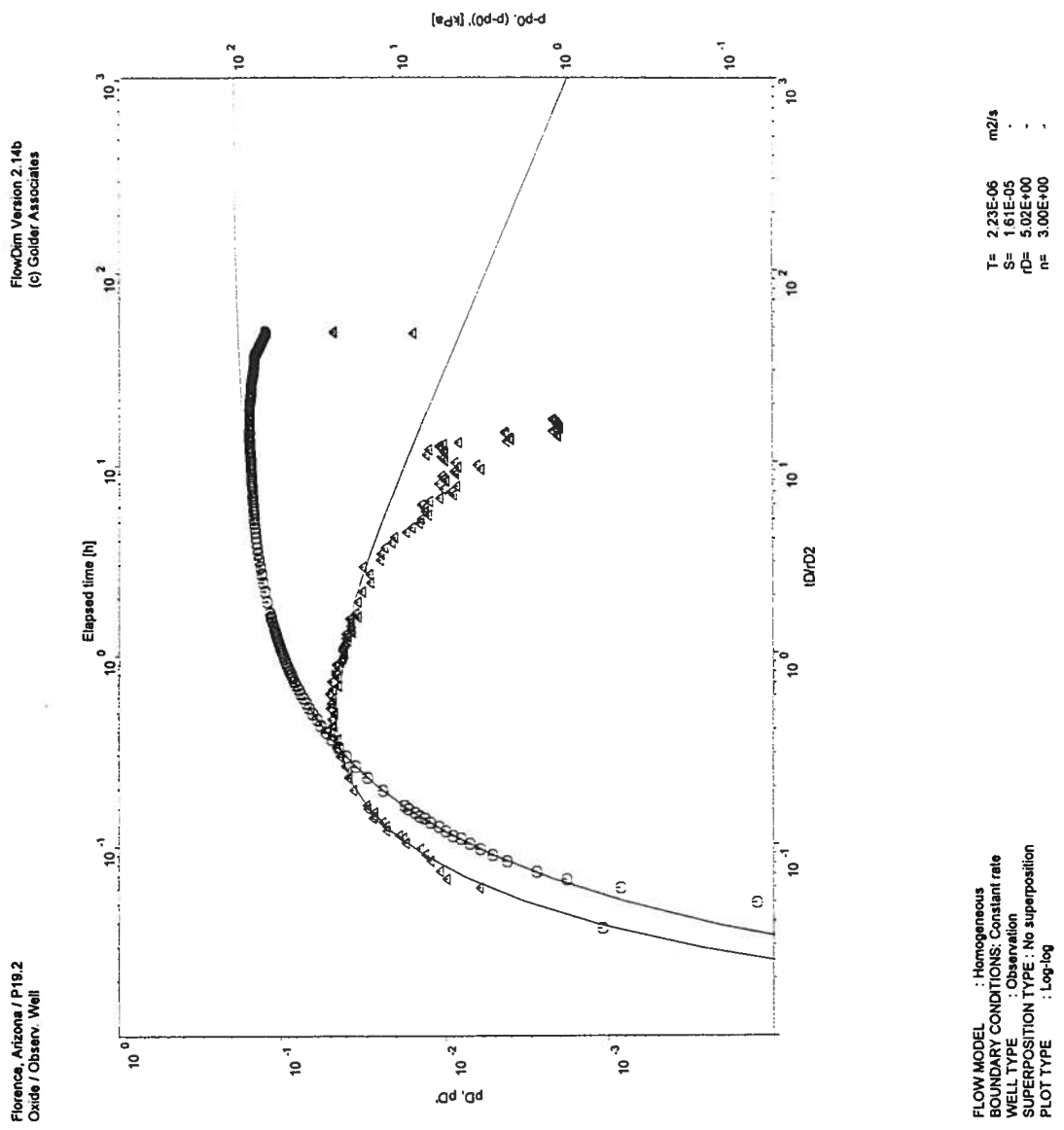


Figure 24G P19.2-O (3D) FlowDim™ Analysis Log-Log Plot

Hydraulic Conductivity Calculation for a Cylindrical Source

PUMPING WELL

Easting:	648427.9	ft
Northing:	747345.8	ft
Screen Top:	402.25	ft
Screen Bottom:	600.45	ft
Surface Elevation	1483	ft (amsl)
Radius:	7.62E-02	m
Screen Interval:	60.41	m
Screen Interval Mid-Point:	299.21	m

OBSERVATION WELL

Easting	648233.6	ft
Northing	747359.3	ft
Screen Top:	375.0	ft
Screen Bottom:	435.1	ft
Surface Elevation	1481.7	ft
Screen Interval Mid-Point:	328.16	m
Distance to Sink:	60.0	m

Pseudo-Transmissivity:	6.72E-06	m ² /sec
Pseudo-Storage:	3.51E-05	
Anisotropy Ratio:	1.00	

Pseudo-Spherical Radius:

$r_{sw} = 4.52 \text{ m}$

Hydraulic Conductivity: $1.49\text{E-}06 \text{ m/sec} = 0.42 \text{ ft/day}$

Specific Storage: $4.41\text{E-}08 \text{ 1/m} = 1.34\text{E-}08 \text{ 1/ft}$

Figure 24H O19-GL (3D) FlowDim™ Analysis Summary

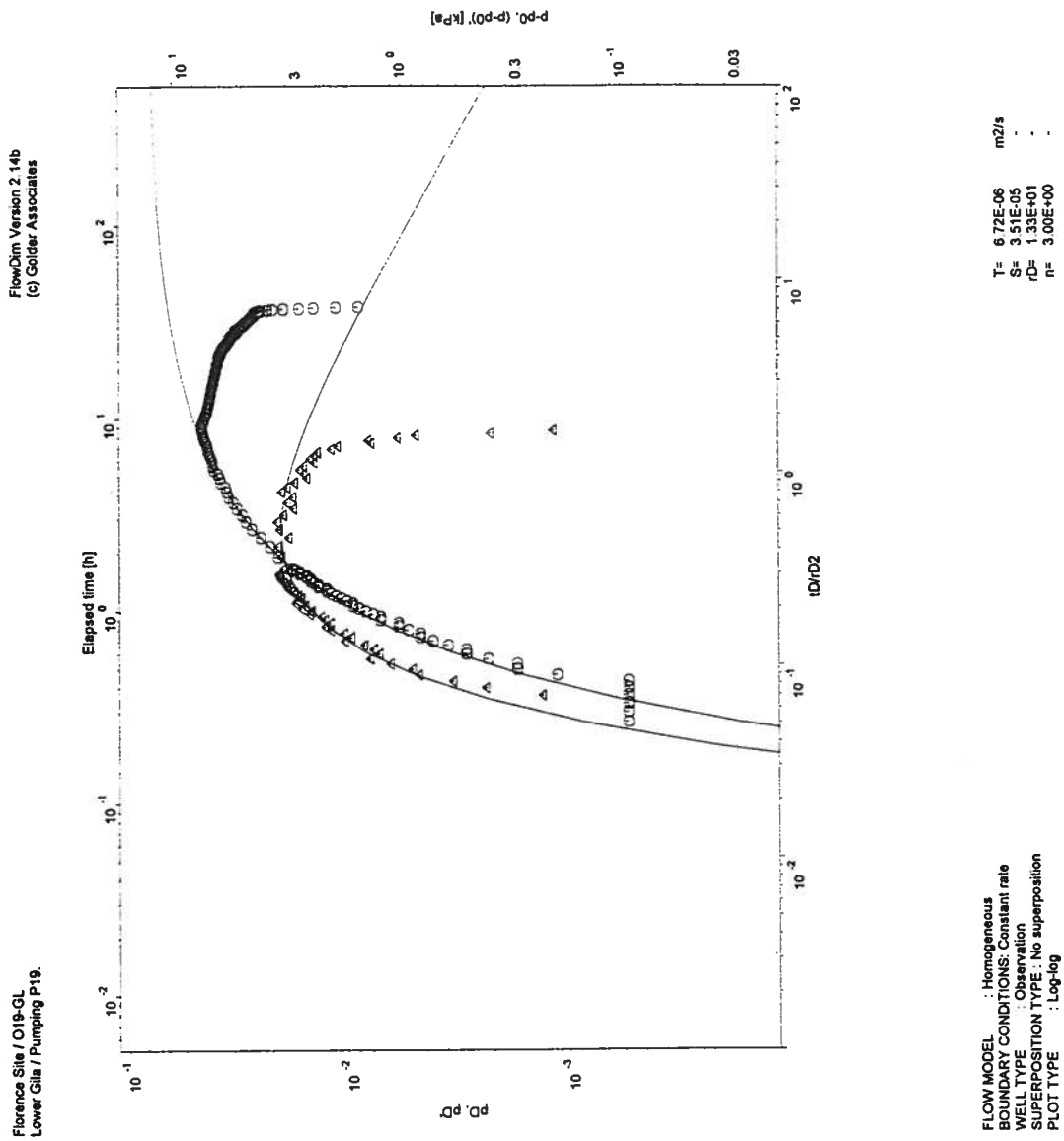


Figure 24I O19-GL (3D) FlowDim™ Analysis Log-Log Plot

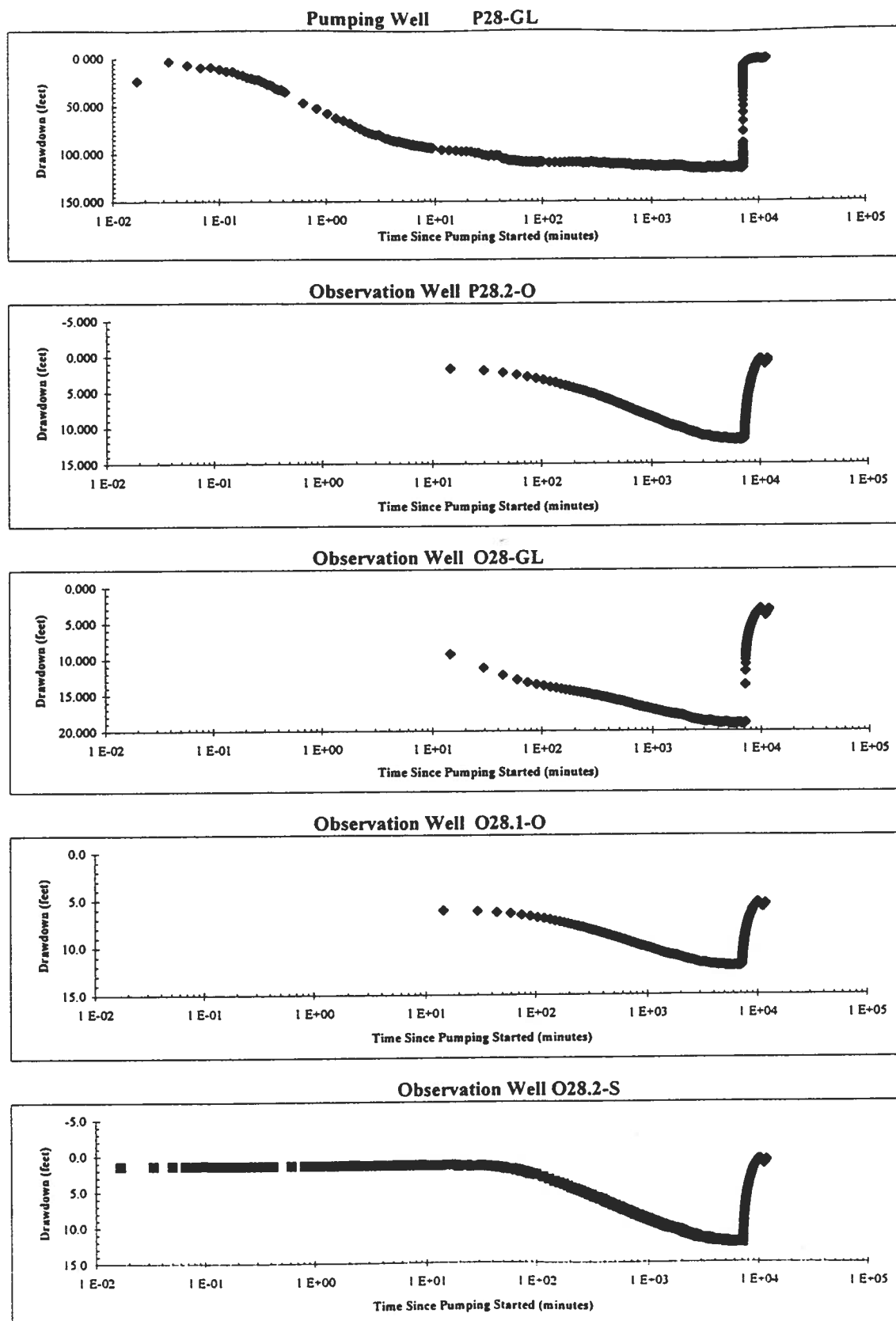


Figure 25A P28-GL Semi-Log Aquifer Test Plot

Hydraulic Conductivity Calculation for a Cylindrical Source

Well Name:	P28-GL
Sink Radius:	6.35E-02 m
Sink Screened Interval:	9.14 m
Pseudo-Transmissivity:	1.11E-05 m ² /sec
Pseudo-Storage:	5.88E-04
Anisotropy Ratio:	1.00

Pseudo-Spherical Radius:

 $r_{sw} = 0.92 \text{ m}$ Hydraulic Conductivity: $1.21\text{E-}05 \text{ m/sec} = 3.42 \text{ ft/day}$ Specific Storage: $6.37\text{E-}04 \text{ 1/m} = 1.94\text{E-}04 \text{ 1/ft}$ **Figure 25B P28-GL (3D) FlowDim™ Analysis Summary**

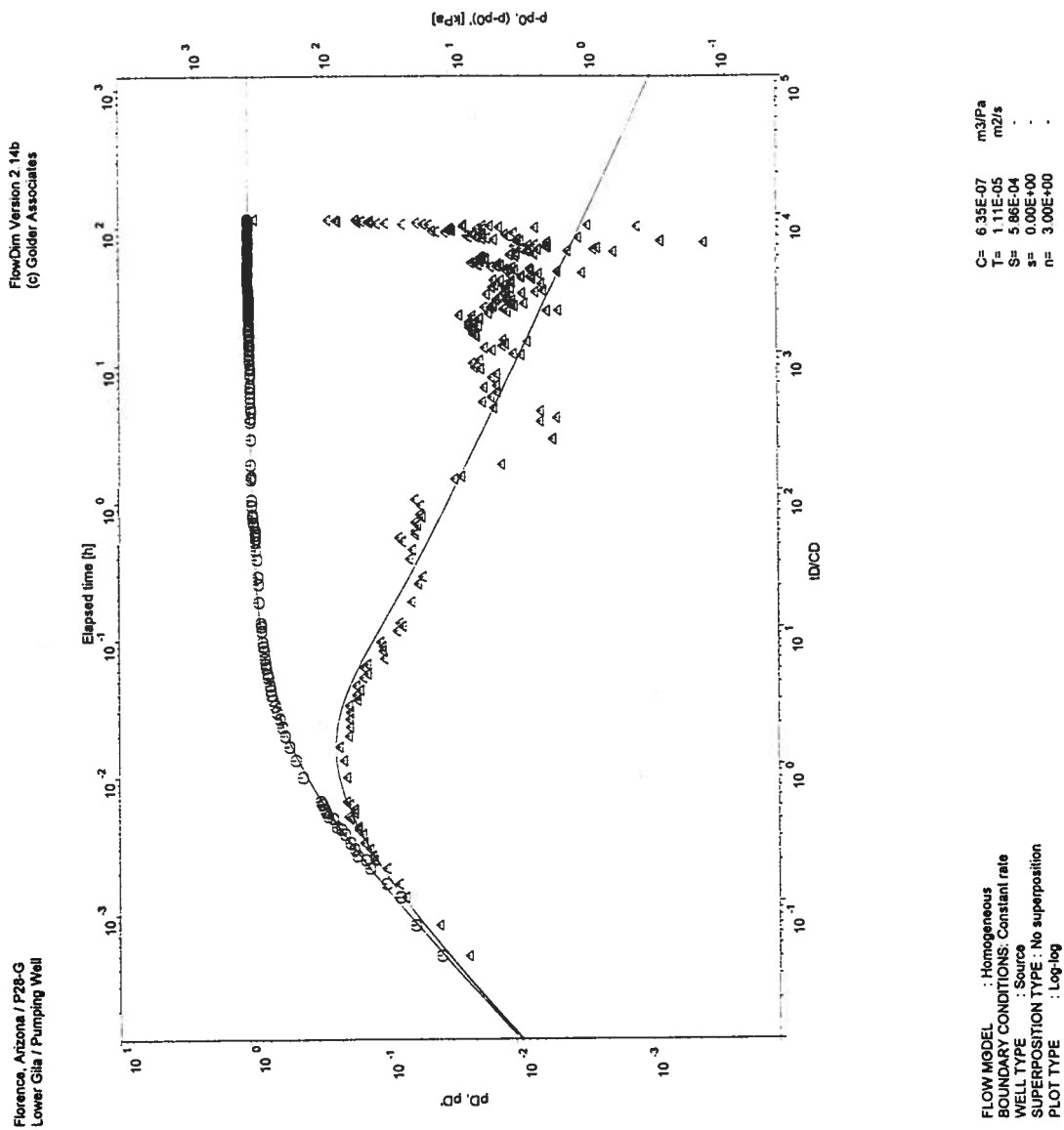


Figure 25C P28-GL (3D) FlowDim™ Analysis Log-Log Plot

Hydraulic Conductivity Calculation for a Cylindrical Source

PUMPING WELL

	P28-GL	
Easting:	651085.7	ft
Northing:	745535.8	ft
Screen Top:	279.0	ft
Screen Bottom:	309.0	ft
Surface Elevation	1464	ft (amsl)
Radius:	6.35E-02	m
Screen Interval:	9.14	m
Screen Interval Mid-Point:	356.62	m

OBSERVATION WELL

	O28-GL	
Easting	650966.7	ft
Northing	745592.7	ft
Screen Top:	267.7	ft
Screen Bottom:	306.8	ft
Surface Elevation	1464.8	ft
Screen Interval Mid-Point:	358.92	m
Distance to Sink:	40.2	m

Pseudo-Transmissivity: 2.70E-06 m²/sec
 Pseudo-Storage: 2.18E-05
 Anisotropy Ratio: 1.00

Pseudo-Spherical Radius:

$$r_{sw} = 0.92 \text{ m}$$

Hydraulic Conductivity: 2.93E-06 m/sec = 0.83 ft/day

Specific Storage: 1.24E-08 1/m = 3.78E-09 1/ft

Figure 25D O28-GL (3D) FlowDim™ Analysis Summary



Hydraulic Conductivity Calculation for a Cylindrical Source

PUMPING WELL

Easting:	651085.7	ft
Northing:	745535.8	ft
Screen Top:	279.0	ft
Screen Bottom:	309.0	ft
Surface Elevation	1464	ft (amsl)
Radius:	6.35E-02	m
Screen Interval:	9.14	m
Screen Interval Mid-Point:	356.62	m

OBSERVATION WELL

Easting	651118.2	ft
Northing	745516.2	ft
Screen Top:	398.3	ft
Screen Bottom:	497.0	ft
Surface Elevation	1465.4	ft
Screen Interval Mid-Point:	310.21	m
Distance to Sink:	18.3	m

Pseudo-Transmissivity:	4.93E-06	m ² /sec
Pseudo-Storage:	6.15E-04	
Anisotropy Ratio:	1.00	

Pseudo-Spherical Radius:

$r_{sw} = 0.92 \text{ m}$

Hydraulic Conductivity: $5.36\text{E-}06 \text{ m/sec} = 1.52 \text{ ft/day}$

Specific Storage: $1.69\text{E-}06 \text{ 1/m} = 5.17\text{E-}07 \text{ 1/ft}$

Figure 25F P28.2-O (3D) FlowDim™ Analysis Summary

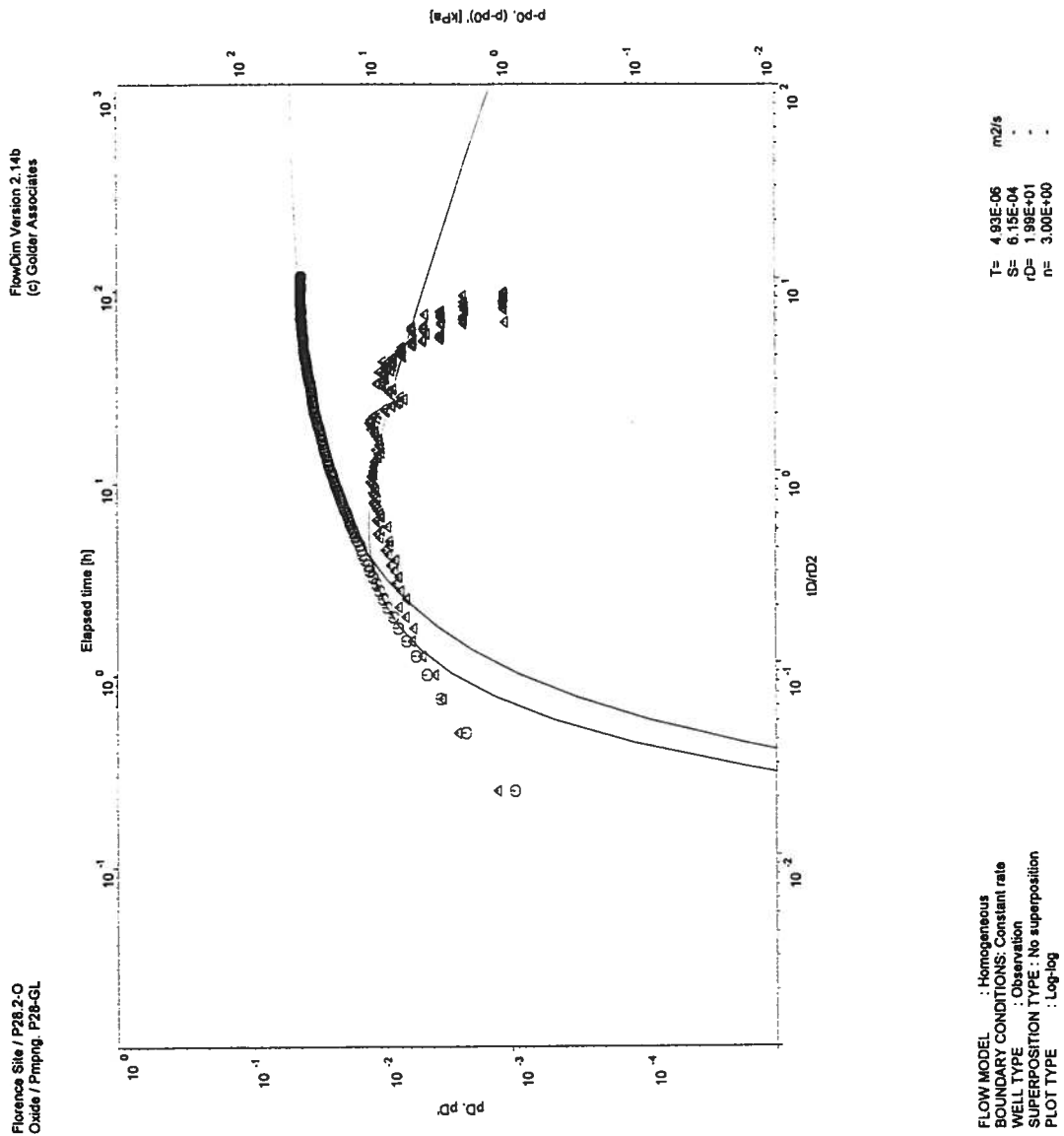


Figure 25G P28.2-O (3D) FlowDim™ Analysis Log-Log Plot

Hydraulic Conductivity Calculation for a Cylindrical Source

PUMPING WELL

Easting:	651085.7	ft
Northing:	745535.8	ft
Screen Top:	279.0	ft
Screen Bottom:	309.0	ft
Surface Elevation	1464	ft (amsl)
Radius:	6.35E-02	m
Screen Interval:	9.14	m
Screen Interval Mid-Point:	356.62	m

OBSERVATION WELL

Easting	651027.9	ft
Northing	745652.0	ft
Screen Top:	394.7	ft
Screen Bottom:	493.7	ft
Surface Elevation	1464.6	ft
Screen Interval Mid-Point:	311.02	m
Distance to Sink:	42.0	m

Pseudo-Transmissivity:	3.94E-06	m ² /sec
Pseudo-Storage:	7.78E-05	
Anisotropy Ratio:	1.00	

Pseudo-Spherical Radius:

$r_{sw} = 0.92 \text{ m}$

Hydraulic Conductivity: $4.28\text{E-}06 \text{ m/sec} = 1.21 \text{ ft/day}$

Specific Storage: $4.07\text{E-}08 \text{ 1/m} = 1.24\text{E-}08 \text{ 1/ft}$

Figure 25H O28.1-O (3D) FlowDim™ Analysis Summary

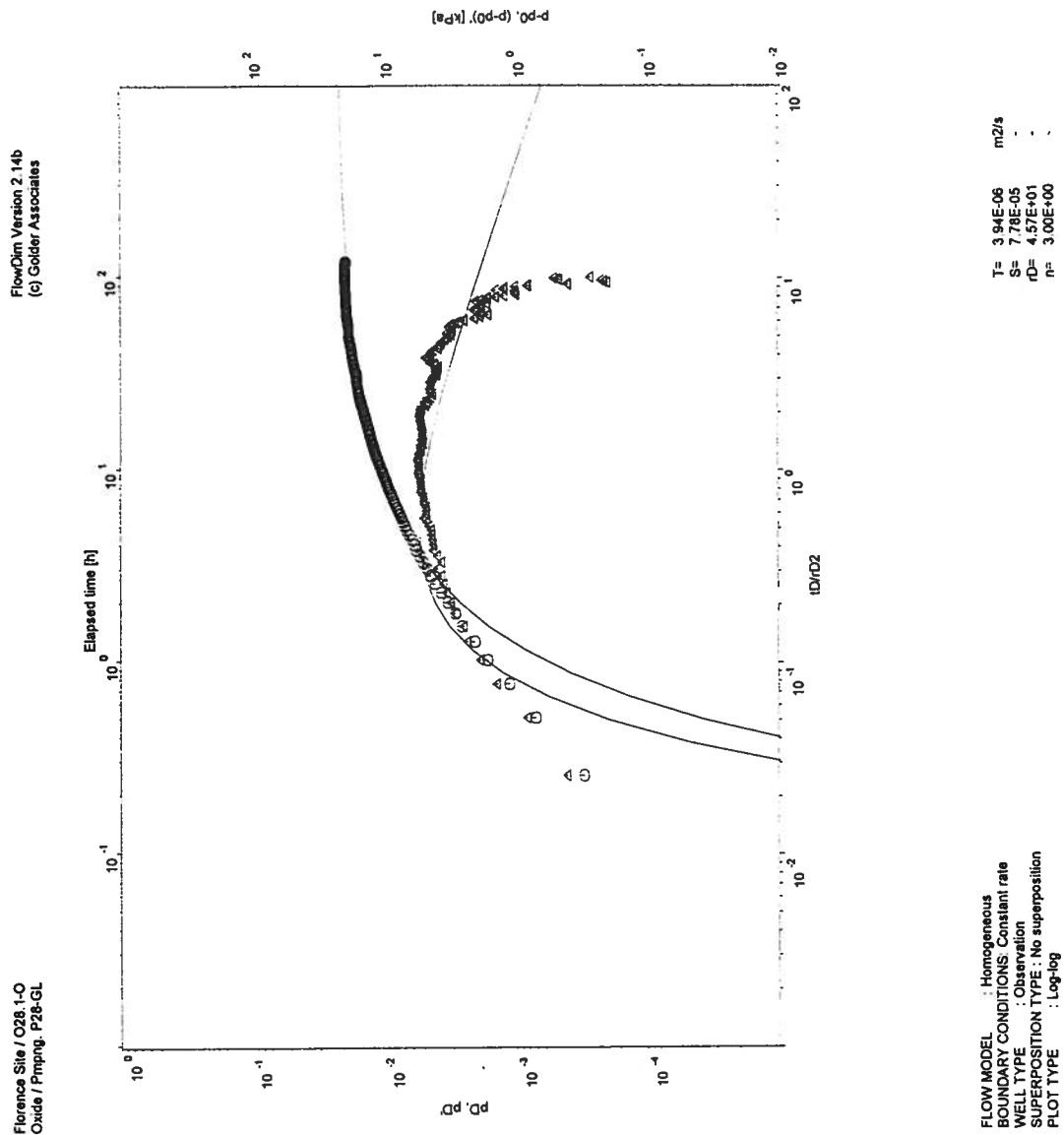


Figure 25I O28.1-O (3D) FlowDim™ Analysis Log-Log Plot

Hydraulic Conductivity Calculation for a Cylindrical Source

PUMPING WELL

Easting:	651085.7	ft
Northing:	745535.8	ft
Screen Top:	279.0	ft
Screen Bottom:	309.0	ft
Surface Elevation	1464	ft (amsl)
Radius:	6.35E-02	m
Screen Interval:	9.14	m
Screen Interval Mid-Point:	356.62	m

OBSERVATION WELL

Easting	651124.0	ft
Northing	745621.1	ft
Screen Top:	454.4	ft
Screen Bottom:	493.3	ft
Surface Elevation	1464.8	ft
Screen Interval Mid-Point:	302.04	m
Distance to Sink:	33.0	m

Pseudo-Transmissivity:	2.69E-06	m ² /sec
Pseudo-Storage:	7.80E-05	
Anisotropy Ratio:	1.00	

Pseudo-Spherical Radius:

$r_{sw} = 0.92 \text{ m}$

Hydraulic Conductivity: $2.92\text{E-}06 \text{ m/sec} = 0.83 \text{ ft/day}$

Specific Storage: $6.59\text{E-}08 \text{ 1/m} = 2.01\text{E-}08 \text{ 1/ft}$

Figure 25J O28.2-S (3D) FlowDim™ Analysis Summary

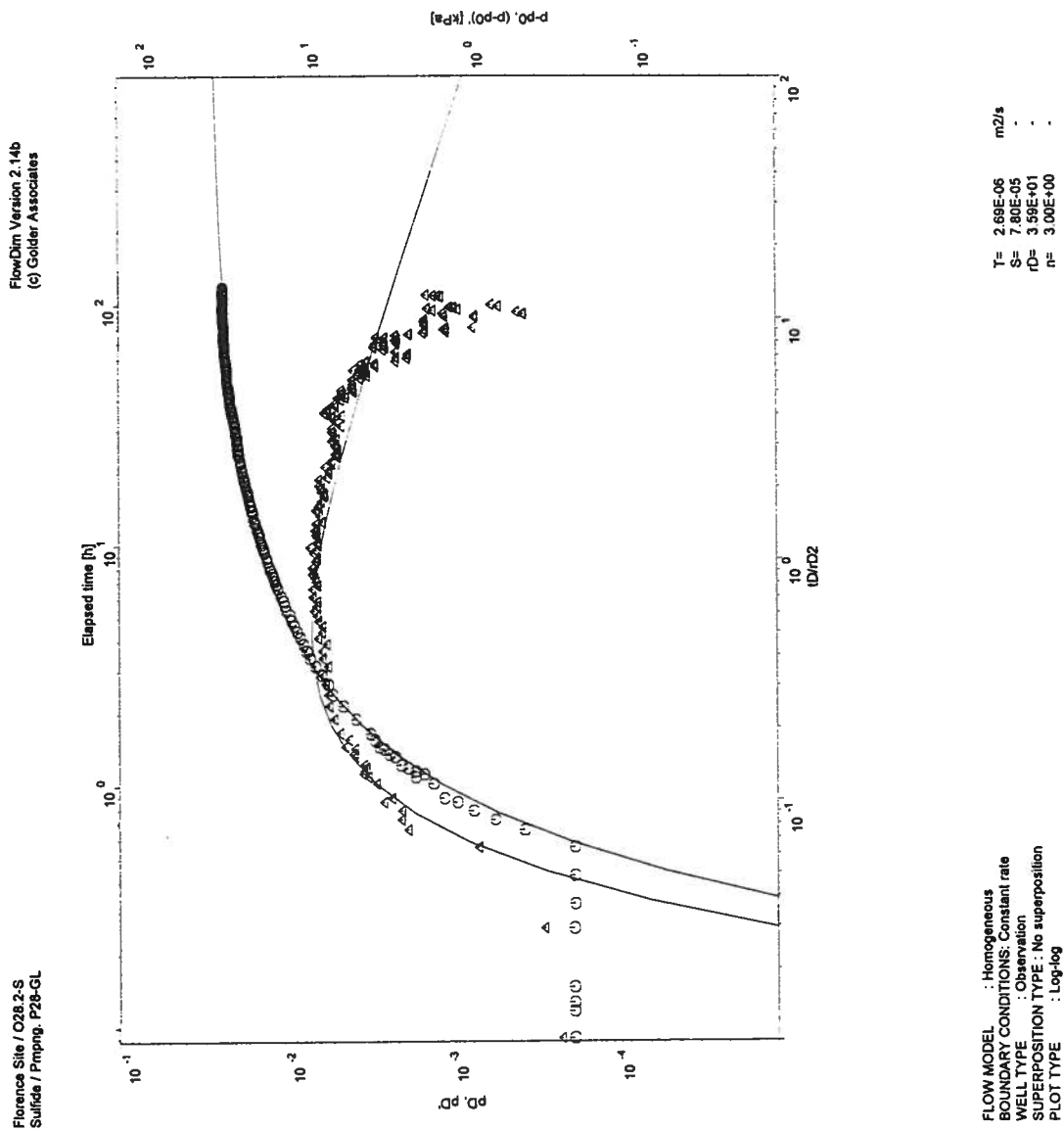


Figure 25K O28.2-S (3D) FlowDim™ Analysis Log-Log Plot

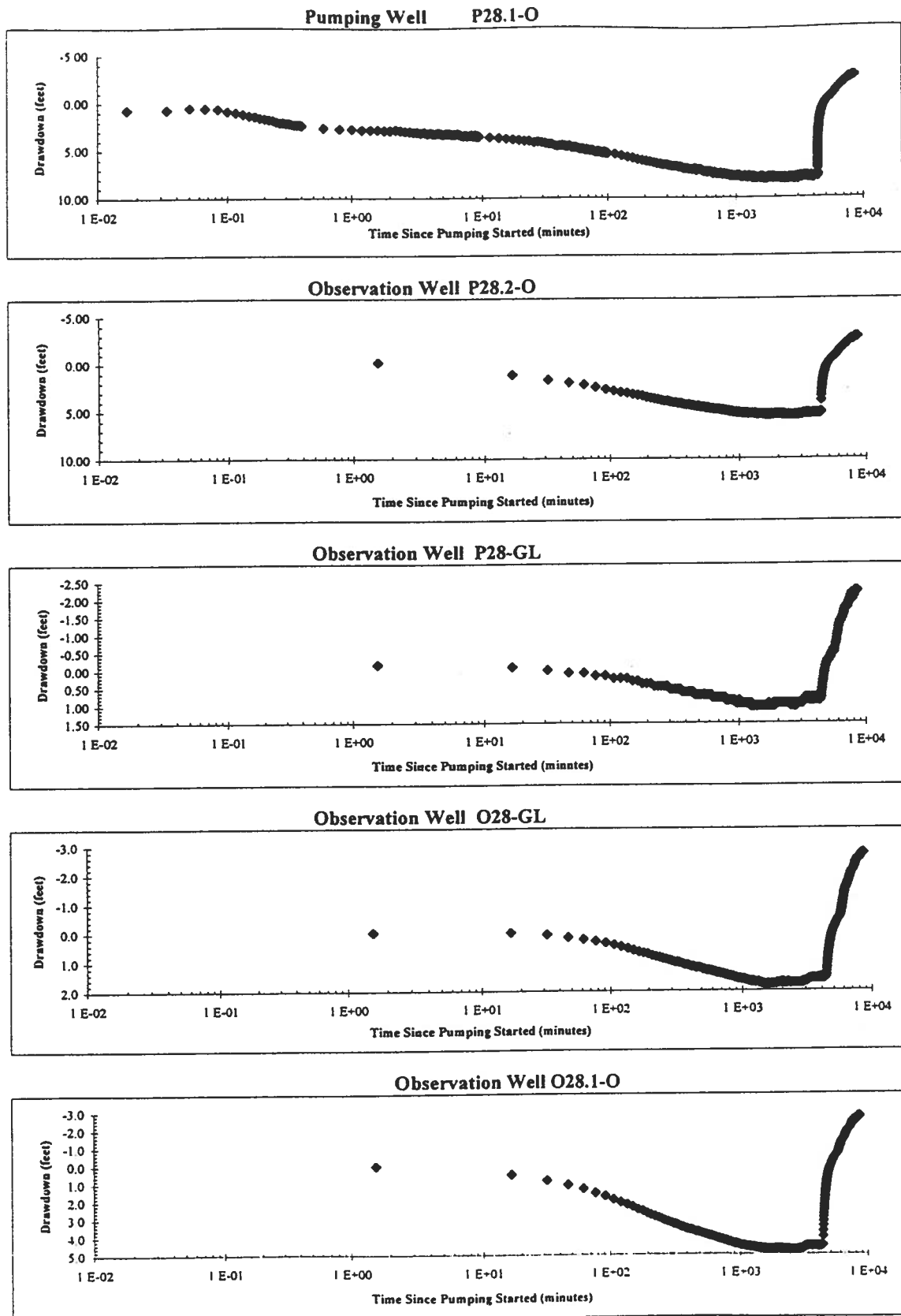


Figure 26A P28.1-O Semi-Log Aquifer Test Plot

FlowDim Analysis File : p281-oad.dat

	Parameter		Units
r_w	Well radius	0.067	m
μ	Groundwater viscosity	1.00E-03	Pa s
ρ	Groundwater density	1.00E+03	kg/m ³
c_t	Total compressibility	5.40E-10	1/Pa
ϕ	Porosity of formation	5.00	%
C	Wellbore storage	1.50E-04	m ³ /Pa
h	Length of aquifer tested	30.48	m

Skin Factor Calculation

Assuming formation storativity, the skin factor (s) can be calculated from the following equation.

$$s = \frac{\ln (C_D e^{2s} 2 \pi \phi c_t h r_w^2 / C)}{2}$$

Match Point Parameters From Analysis

$C_D e^{2s}$	1.0000E+01
P_{DM}	2.8879E-01
T_{DM}	1.2647E+01

Results

T(m ² /sec)	K (feet/min)	K (ft/day)	K (m/s)	K (cm/s)	Skin
8.25E-04	5.33E-03	7.68	2.71E-05	2.71E-03	-6.69

Figure 26B P28.1-O FlowDim™ Analysis Summary

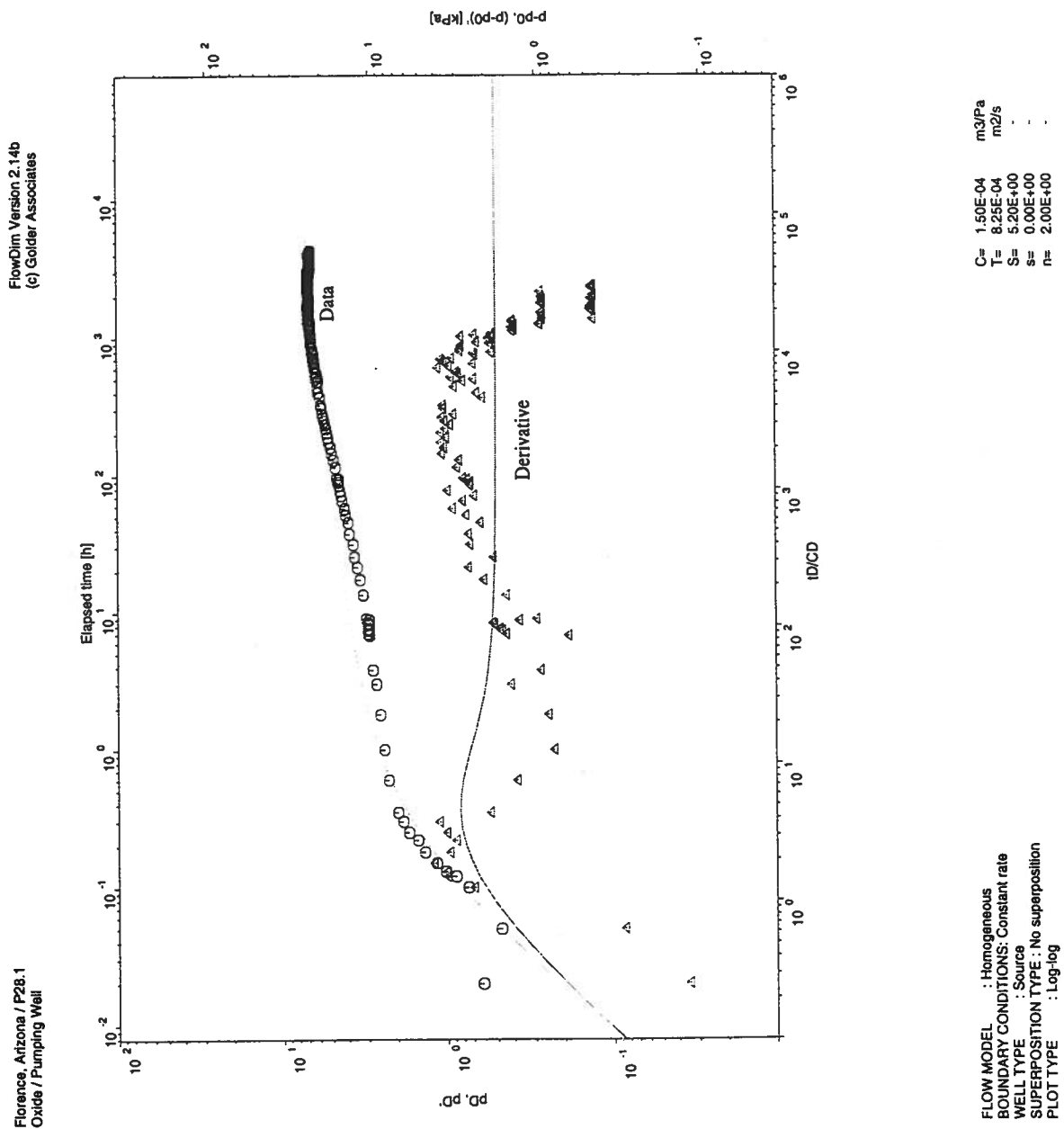


Figure 26C P28.1-O FlowDim™ Analysis Log-Log Plot

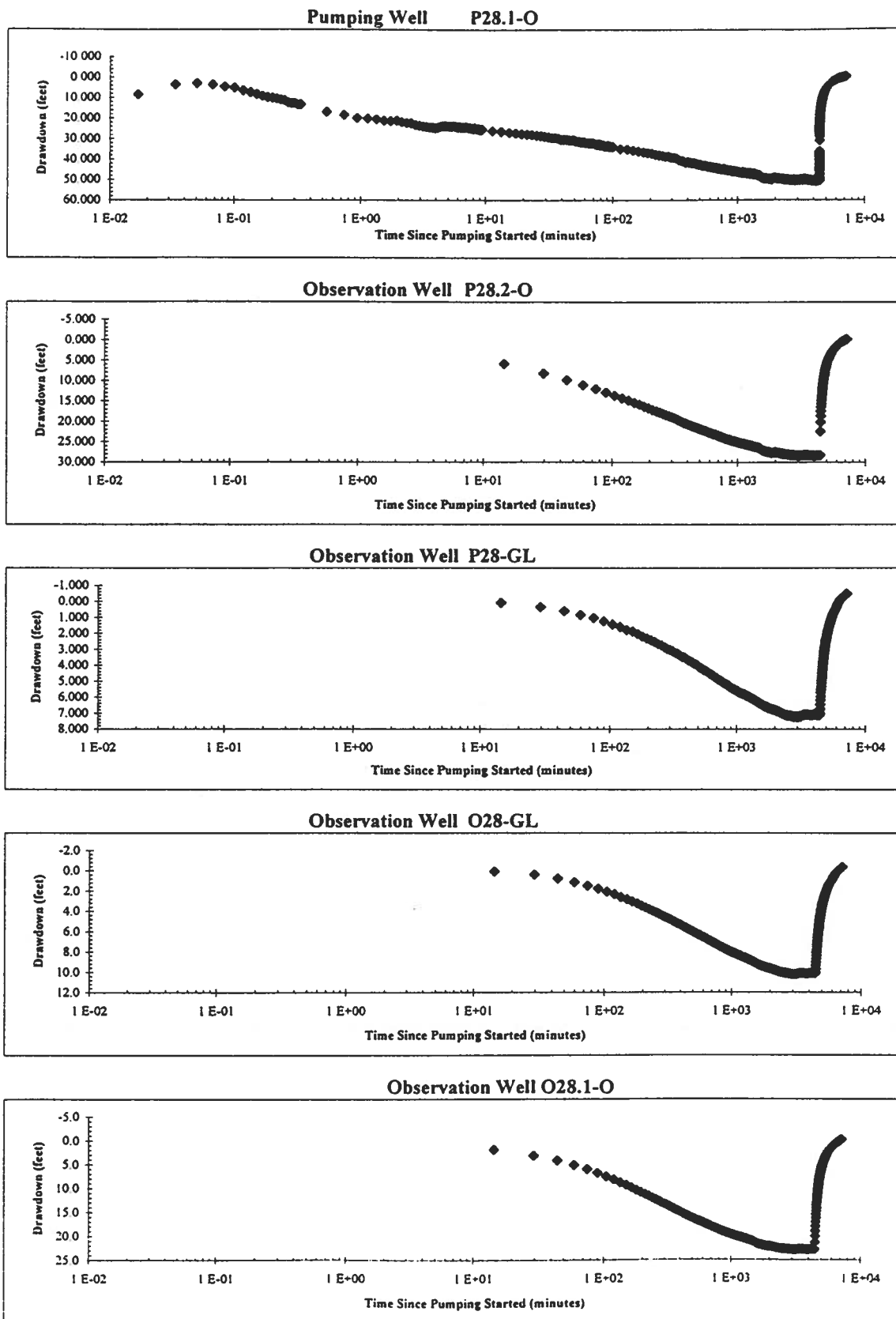


Figure 27A P28.1-O (Test 2) Semi-Log Aquifer Test Plot

FlowDim Analysis File :

p281-obd.dat

	Parameter		Units
r_w	Well radius	0.076	m
μ	Groundwater viscosity	1.00E-03	Pa s
ρ	Groundwater density	1.00E+03	kg/m ³
c_t	Total compressibility	5.40E-10	1/Pa
ϕ	Porosity of formation	5.00	%
C	Wellbore storage	1.28E-06	m ³ /Pa
h	Length of aquifer tested	30.48	m

Skin Factor Calculation

Assuming formation storativity, the skin factor (s) can be calculated from the following equation.

$$s = \frac{\ln (C_D e^{2s} 2 \pi \phi c_t h r_w^2 / C)}{2}$$

Match Point Parameters From Analysis

$C_D e^{2s}$	1.0000E+01
P_{DM}	4.6017E-02
T_{DM}	6.9315E+02

Results

T(m ² /sec)	K (feet/min)	K (ft/day)	K (m/s)	K (cm/s)	Skin
3.86E-04	2.49E-03	3.59	1.26E-05	1.26E-03	-4.18

Figure 27B P28.1-O (Test 2) FlowDim™ Analysis Summary

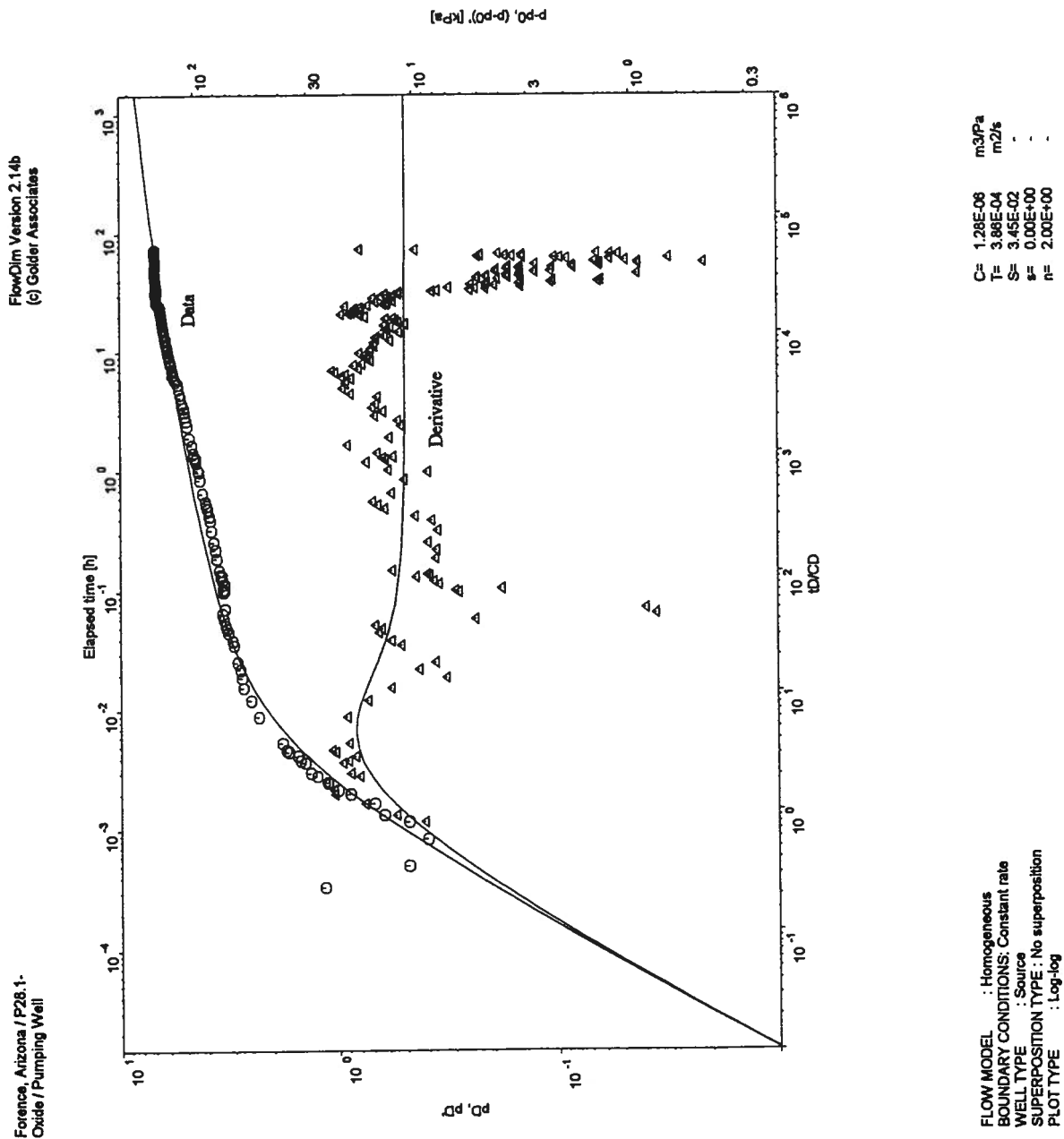


Figure 27C P28.1-O (Test 2) FlowDim™ Analysis Log-Log Plot

FlowDim Analysis File : p282-obd.dat

	Parameter		Units
r_w	Well radius	0.051	m
μ	Groundwater viscosity	1.00E-03	Pa s
ρ	Groundwater density	1.00E+03	kg/m ³
c_t	Total compressibility	5.40E-10	1/Pa
ϕ	Porosity of formation	5.00	%
C	Wellbore storage	NA	m ³ /Pa
h	Length of aquifer tested	30.18	m

Skin Factor Calculation

Assuming formation storativity, the skin factor (s) can be calculated from the following equation.

$$s = \frac{\ln (C_D e^{2s} 2 \pi \phi c_t h r_w^2 / C)}{2}$$

Match Point Parameters From Analysis

$C_D e^{2s}$	2.0000E+00
P_{DM}	3.3963E-02
T_{DM}	3.9303E+00

Results

T(m ² /sec)	K (feet/min)	K (ft/day)	K (m/s)	K (cm/s)	Skin
2.84E-04	1.86E-03	2.67	9.43E-06	9.43E-04	#####

Figure 27D P28.2-O (Test 2) FlowDim™ Analysis Summary

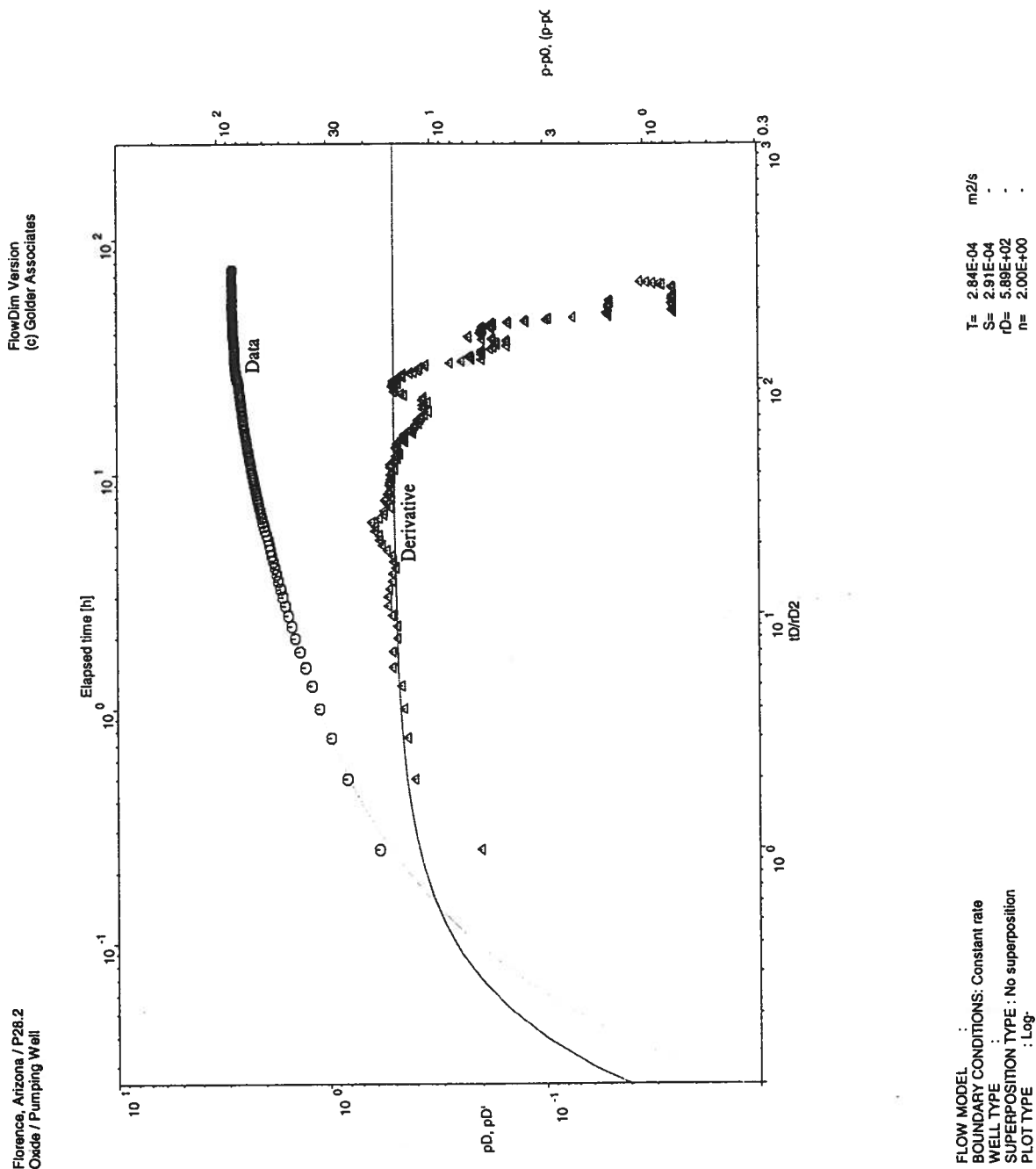


Figure 27E P28.2-O (Test 2) FlowDim™ Analysis Log-Log Plot

Hydraulic Conductivity Calculation for a Cylindrical Source

PUMPING WELL

	P28.1-O	
Easting:	650998.3	ft
Northing:	745558.5	ft
Screen Top:	300.0	ft
Screen Bottom:	400.0	ft
Surface Elevation	1464.9	ft (amsl)
Radius:	7.62E-02	m
Screen Interval:	30.48	m
Screen Interval Mid-Point:	339.82	m

OBSERVATION WELL

	O28.1-O	
Easting	651027.9	ft
Northing	745652.0	ft
Screen Top:	394.7	ft
Screen Bottom:	493.7	ft
Surface Elevation	1464.6	ft
Screen Interval Mid-Point:	311.02	m
Distance to Sink:	31.2	m

Pseudo-Transmissivity: 4.59E-06 m²/sec
 Pseudo-Storage: 8.46E-05
 Anisotropy Ratio: 1.00

Pseudo-Spherical Radius:

$r_{sw} = 2.54 \text{ m}$

Hydraulic Conductivity: 1.80E-06 m/sec = 0.51 ft/day

Specific Storage: 2.22E-07 1/m = 6.76E-08 1/ft

Figure 27F O28.1-O (3D) (Test 2) FlowDim™ Analysis Summary

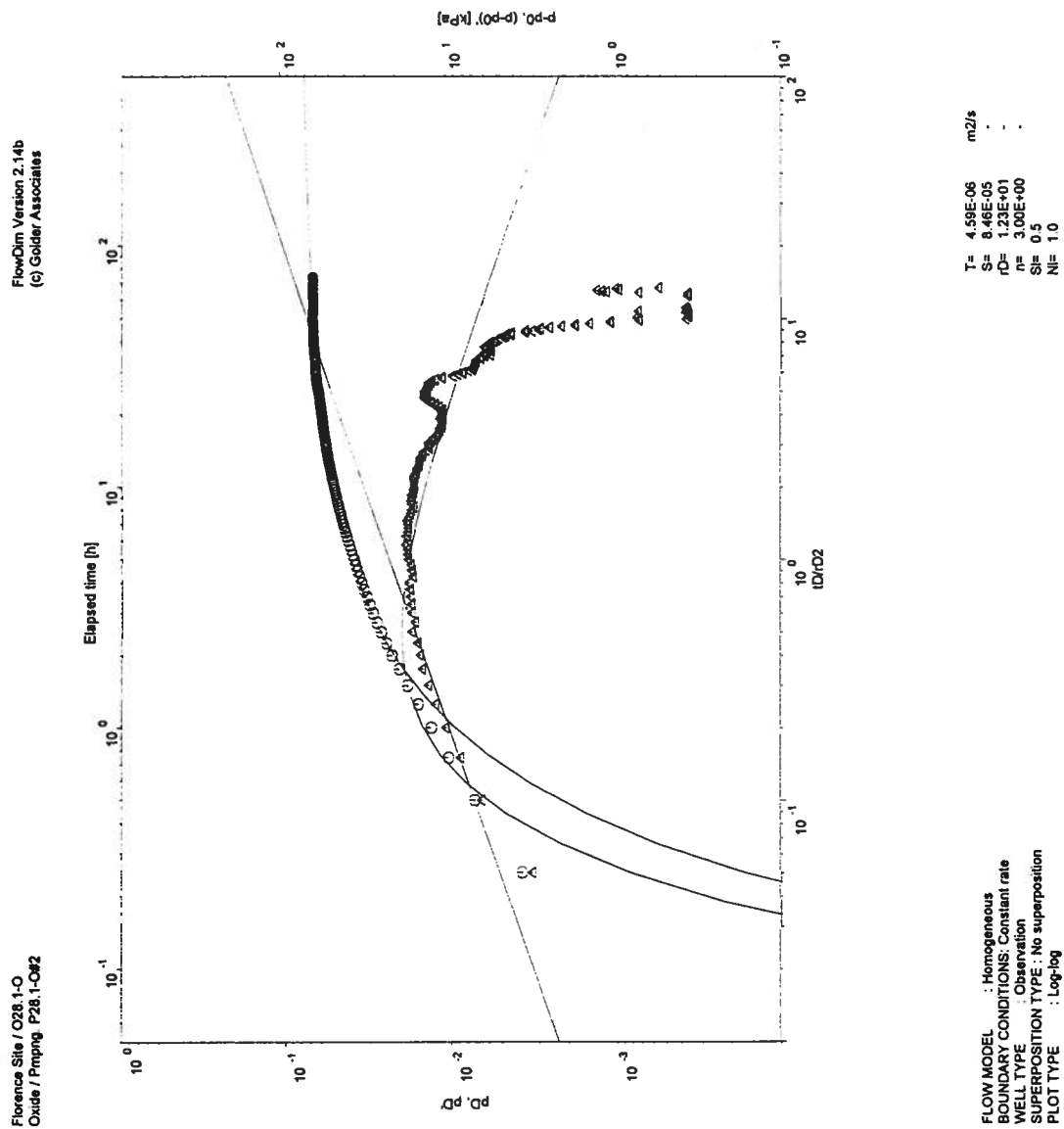


Figure 27G O28.1-O (3D) (Test 2) FlowDim™ Analysis Log-Log Plot

Hydraulic Conductivity Calculation for a Cylindrical Source

PUMPING WELL

Easting:	P28.1-O	650998.3	ft
Northing:		745558.5	ft
Screen Top:		300.0	ft
Screen Bottom:		400.0	ft
Surface Elevation		1464.9	ft (amsl)
Radius:		7.62E-02	m
Screen Interval:		30.48	m
Screen Interval Mid-Point:		339.82	m

OBSERVATION WELL

Easting	P28-GL	651085.7	ft
Northing		745535.8	ft
Screen Top:		279.0	ft
Screen Bottom:		309.0	ft
Surface Elevation		1464	ft
Screen Interval Mid-Point:		356.62	m
Distance to Sink:		28.0	m

Pseudo-Transmissivity:	1.36E-05	m ² /sec
Pseudo-Storage:	6.49E-04	
Anisotropy Ratio:	1.00	

Pseudo-Spherical Radius:

$$r_{sw} = 2.54 \text{ m}$$

Hydraulic Conductivity:	5.35E-06 m/sec	=	1.52 ft/day
-------------------------	----------------	---	-------------

Specific Storage:	2.10E-06 1/m	=	6.41E-07 1/ft
-------------------	--------------	---	---------------

Figure 27H P28-GL (3D) (Test 2) FlowDim™ Analysis Summary

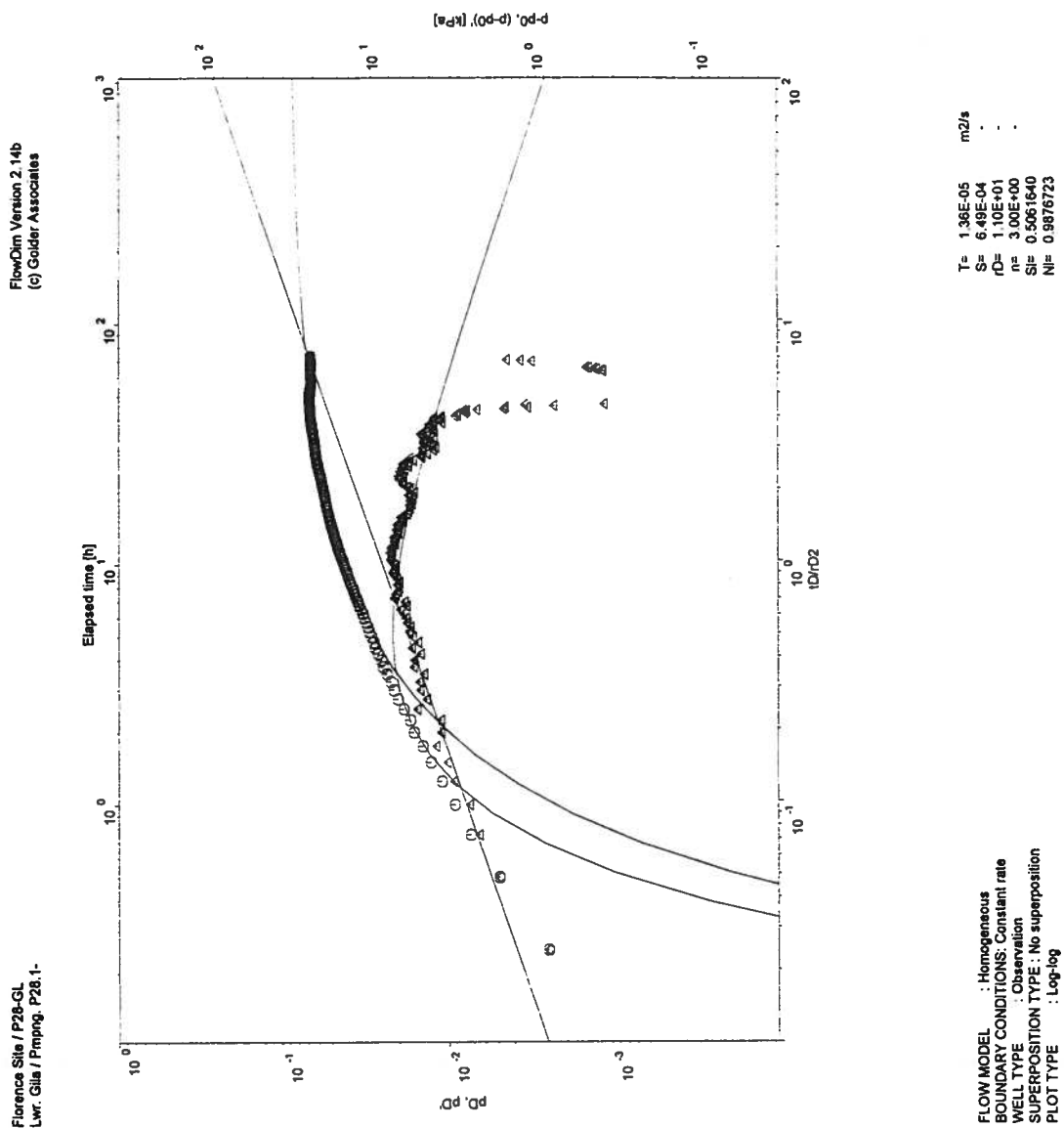


Figure 27I P28-GL (3D) (Test 2) FlowDim™ Analysis Log-Log Plot

Hydraulic Conductivity Calculation for a Cylindrical Source

PUMPING WELL

Easting:	650998.3	ft
Northing:	745558.5	ft
Screen Top:	300.0	ft
Screen Bottom:	400.0	ft
Surface Elevation	1464.9	ft (amsl)
Radius:	7.62E-02	m
Screen Interval:	30.48	m
Screen Interval Mid-Point:	339.82	m

OBSERVATION WELL

Easting	650966.7	ft
Northing	745592.7	ft
Screen Top:	267.7	ft
Screen Bottom:	306.8	ft
Surface Elevation	1464.8	ft
Screen Interval Mid-Point:	358.92	m
Distance to Sink:	15.3	m

Pseudo-Transmissivity:	1.76E-05	m ² /sec
Pseudo-Storage:	2.53E-03	
Anisotropy Ratio:	1.00	

Pseudo-Spherical Radius:

$r_{sw} = 2.54 \text{ m}$

Hydraulic Conductivity: $6.92\text{E-}06 \text{ m/sec} = 1.96 \text{ ft/day}$

Specific Storage: $2.74\text{E-}05 \text{ 1/m} = 8.35\text{E-}06 \text{ 1/ft}$

Figure 27J O28-GL (3D) (Test 2) FlowDim™ Analysis Summary

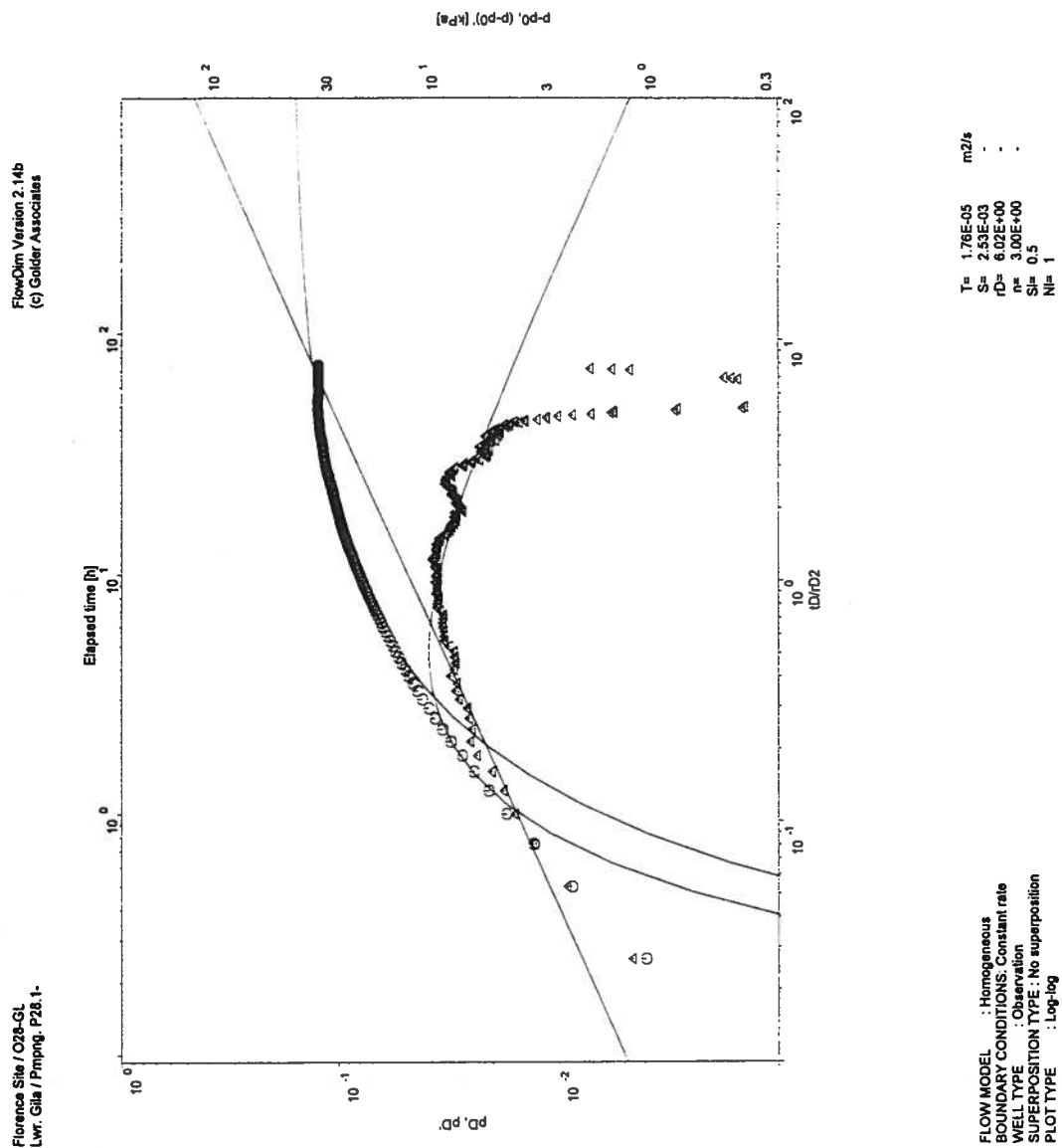


Figure 27K O28-GL (3D) (Test 2) FlowDim™ Analysis Log-Log Plot

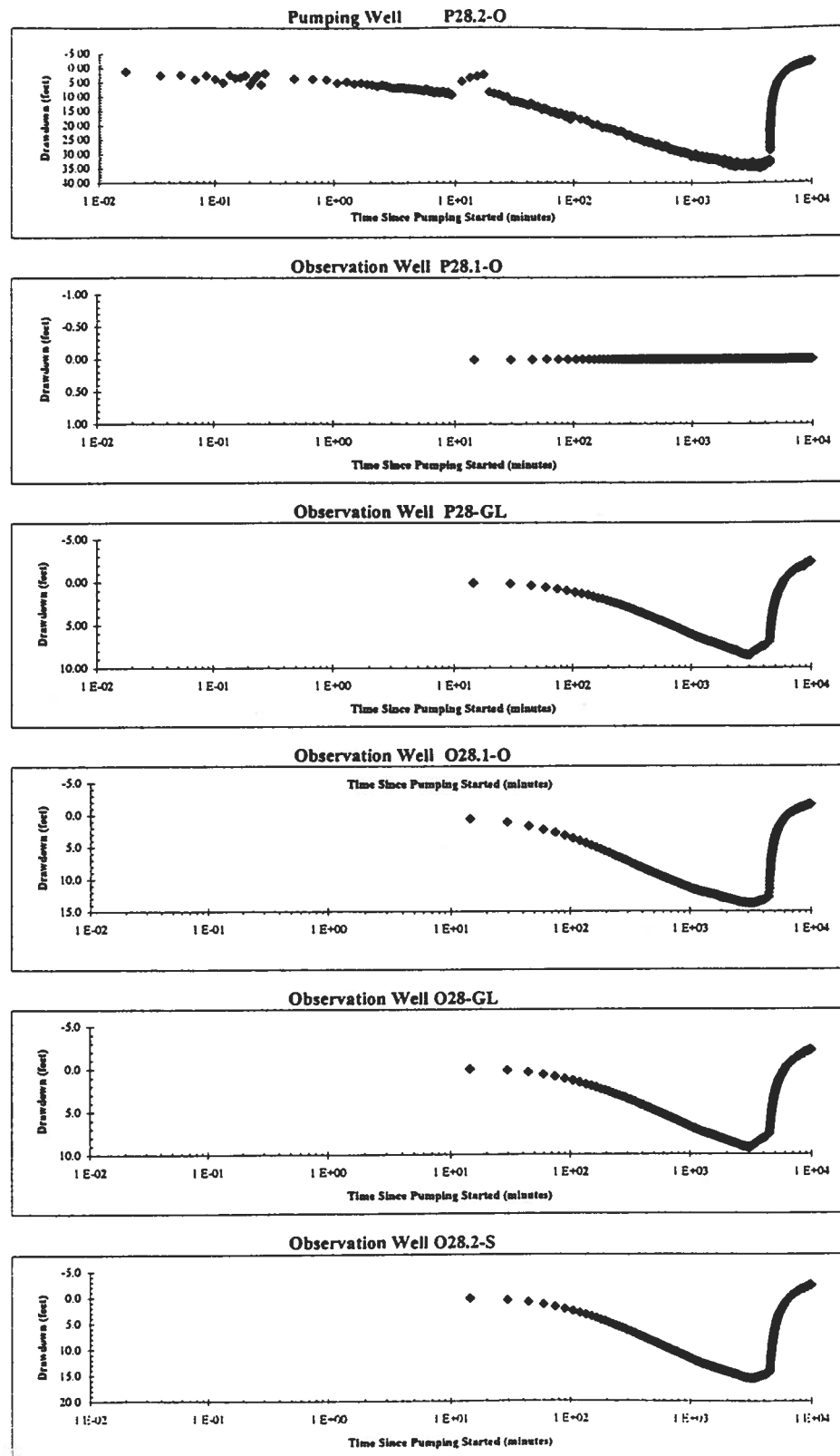


Figure 28A P28.2-O Semi-Log Aquifer Test Plot

FlowDim Analysis File :**p282-od.dat**

	Parameter		Units
r_w	Well radius	0.076	m
μ	Groundwater viscosity	1.00E-03	Pa s
ρ	Groundwater density	1.00E+03	kg/m ³
c_t	Total compressibility	5.40E-10	1/Pa
ϕ	Porosity of formation	5.00	%
C	Wellbore storage	1.41E-04	m ³ /Pa
h	Length of aquifer tested	30.18	m

Skin Factor Calculation

Assuming formation storativity, the skin factor (s) can be calculated from the following equation.

$$s = \frac{\ln (C_D e^{2s} 2 \pi \phi c_t h r_w^2 / C)}{2}$$

Match Point Parameters From Analysis

$C_D e^{2s}$	1.0000E+01
Pm (1/KPa)	4.4105E-02
Tm (hr)	5.4115E+00

Results

T(m ² /sec)	K (feet/min)	K (ft/day)	K (m/s)	K (cm/s)	Skin
3.30E-04	2.15E-03	3.10	1.09E-05	1.09E-03	-6.53

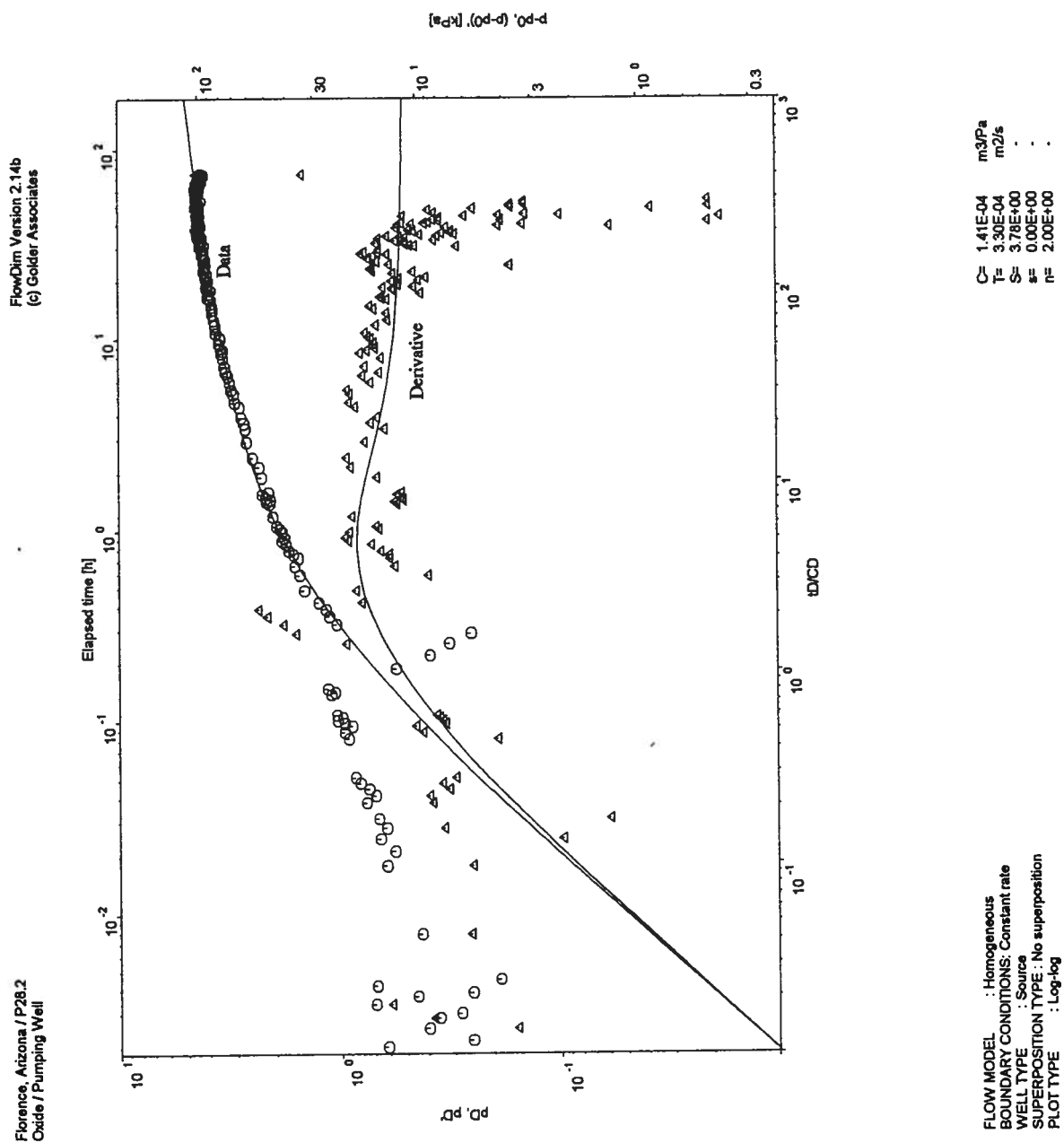


Figure 28C P28.2-O FlowDim™ Analysis Log-Log Plot

Hydraulic Conductivity Calculation for a Cylindrical Source

PUMPING WELL

Easting:	651118.2	ft
Northing:	745516.2	ft
Screen Top:	398.3	ft
Screen Bottom:	497.0	ft
Surface Elevation	1465.4	ft (amsl)
Radius:	7.62E-02	m
Screen Interval:	30.08	m
Screen Interval Mid-Point:	310.21	m

OBSERVATION WELL

Easting	651027.9	ft
Northing	745652.0	ft
Screen Top:	394.7	ft
Screen Bottom:	493.7	ft
Surface Elevation	1464.6	ft
Screen Interval Mid-Point:	311.02	m
Distance to Sink:	49.7	m

Pseudo-Transmissivity:	3.80E-06	m ² /sec
Pseudo-Storage:	3.56E-05	
Anisotropy Ratio:	1.00	

Pseudo-Spherical Radius:

$r_{sw} = 2.52 \text{ m}$

Hydraulic Conductivity: $1.51\text{E-}06 \text{ m/sec} = 0.43 \text{ ft/day}$

Specific Storage: $3.62\text{E-}08 \text{ 1/m} = 1.10\text{E-}08 \text{ 1/ft}$

Figure 28D O28.1-O (3D) FlowDim™ Analysis Summary

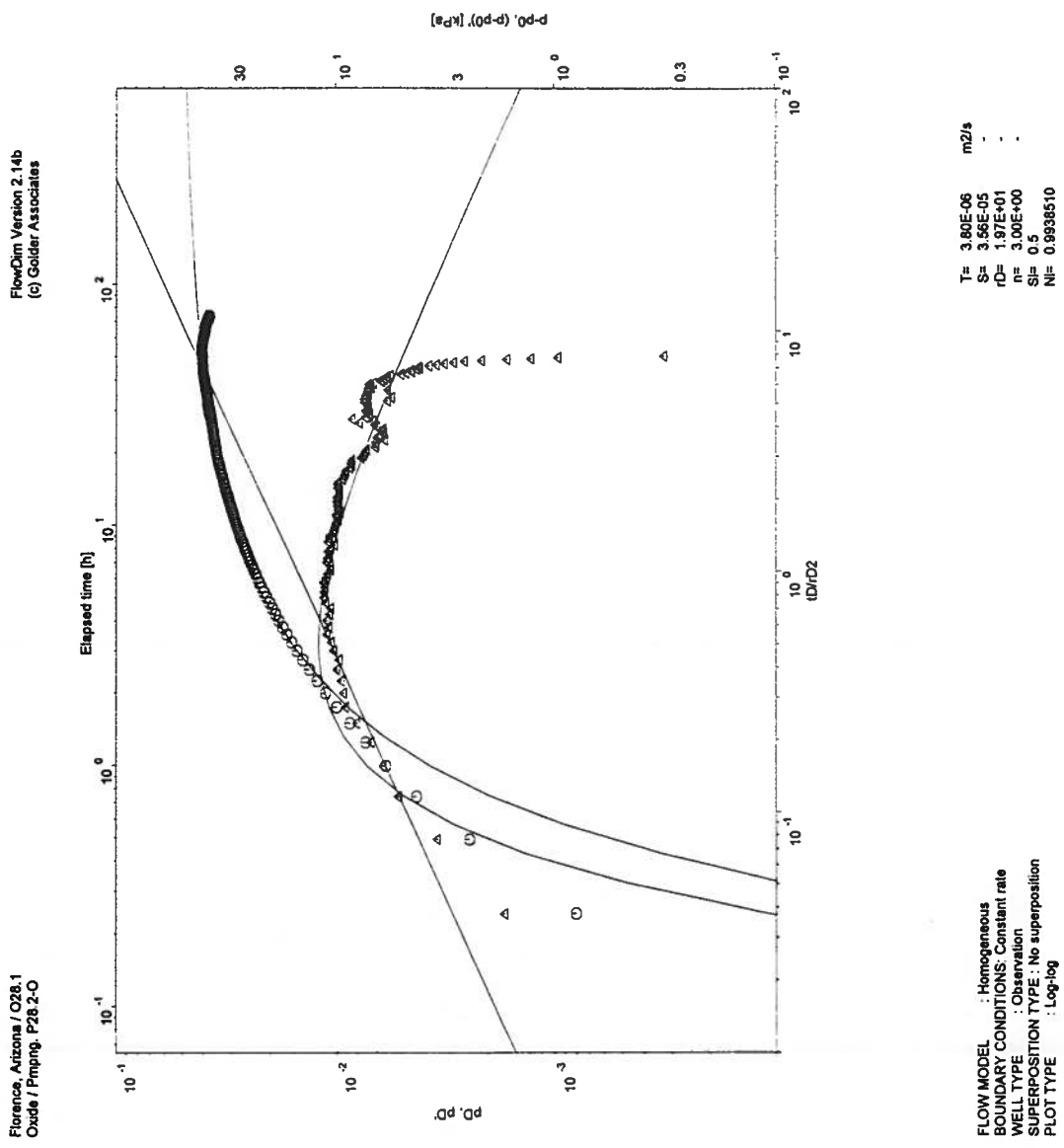


Figure 28E O28.1-O (3D) FlowDim™ Analysis Log-Log Plot

Hydraulic Conductivity Calculation for a Cylindrical Source

PUMPING WELL

Easting:	651118.2	ft
Northing:	745516.2	ft
Screen Top:	398.3	ft
Screen Bottom:	497.0	ft
Surface Elevation	1465.4	ft (amsl)
Radius:	7.62E-02	m
Screen Interval:	30.08	m
Screen Interval Mid-Point:	310.21	m

OBSERVATION WELL

Easting	651085.7	ft
Northing	745535.8	ft
Screen Top:	279.0	ft
Screen Bottom:	309.0	ft
Surface Elevation	1464	ft
Screen Interval Mid-Point:	356.62	m
Distance to Sink:	18.3	m

Pseudo-Transmissivity:	1.57E-05	m ² /sec
Pseudo-Storage:	2.09E-03	
Anisotropy Ratio:	1.00	

Pseudo-Spherical Radius:

$r_{sw} = 2.52 \text{ m}$

Hydraulic Conductivity: $6.24\text{E-}06 \text{ m/sec} = 1.77 \text{ ft/day}$

Specific Storage: $1.58\text{E-}05 \text{ 1/m} = 4.80\text{E-}06 \text{ 1/ft}$

Figure 28F P28-GL (3D) FlowDim™ Analysis Summary

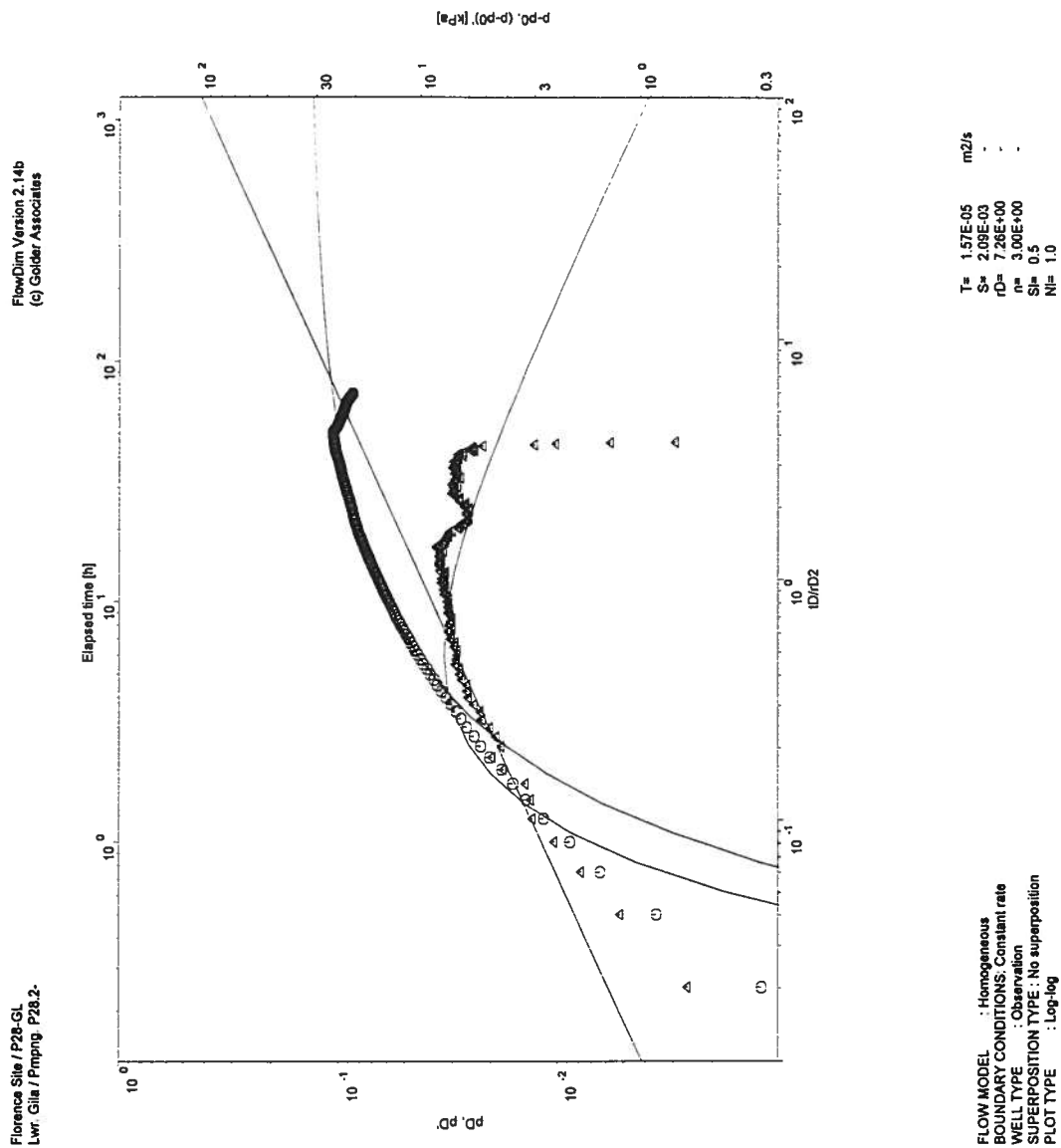


Figure 28G P28-GL (3D) FlowDim™ Analysis Log-Log Plot

Hydraulic Conductivity Calculation for a Cylindrical Source

PUMPING WELL

Easting:	651118.2	ft
Northing:	745516.2	ft
Screen Top:	398.3	ft
Screen Bottom:	497.0	ft
Surface Elevation	1465.4	ft (amsl)
Radius:	7.62E-02	m
Screen Interval:	30.08	m
Screen Interval Mid-Point:	310.21	m

OBSERVATION WELL

Easting	650966.7	ft
Northing	745592.7	ft
Screen Top:	267.7	ft
Screen Bottom:	306.8	ft
Surface Elevation	1464.8	ft
Screen Interval Mid-Point:	358.92	m
Distance to Sink:	53.8	m

Pseudo-Transmissivity:	4.88E-06	m ² /sec
Pseudo-Storage:	6.25E-05	
Anisotropy Ratio:	1.00	

Pseudo-Spherical Radius:

$r_{sw} = 2.52 \text{ m}$

Hydraulic Conductivity: $1.94\text{E-}06 \text{ m/sec} = 0.55 \text{ ft/day}$

Specific Storage: $5.43\text{E-}08 \text{ 1/m} = 1.65\text{E-}08 \text{ 1/ft}$

Figure 28H O28-GL (3D) FlowDim™ Analysis Summary

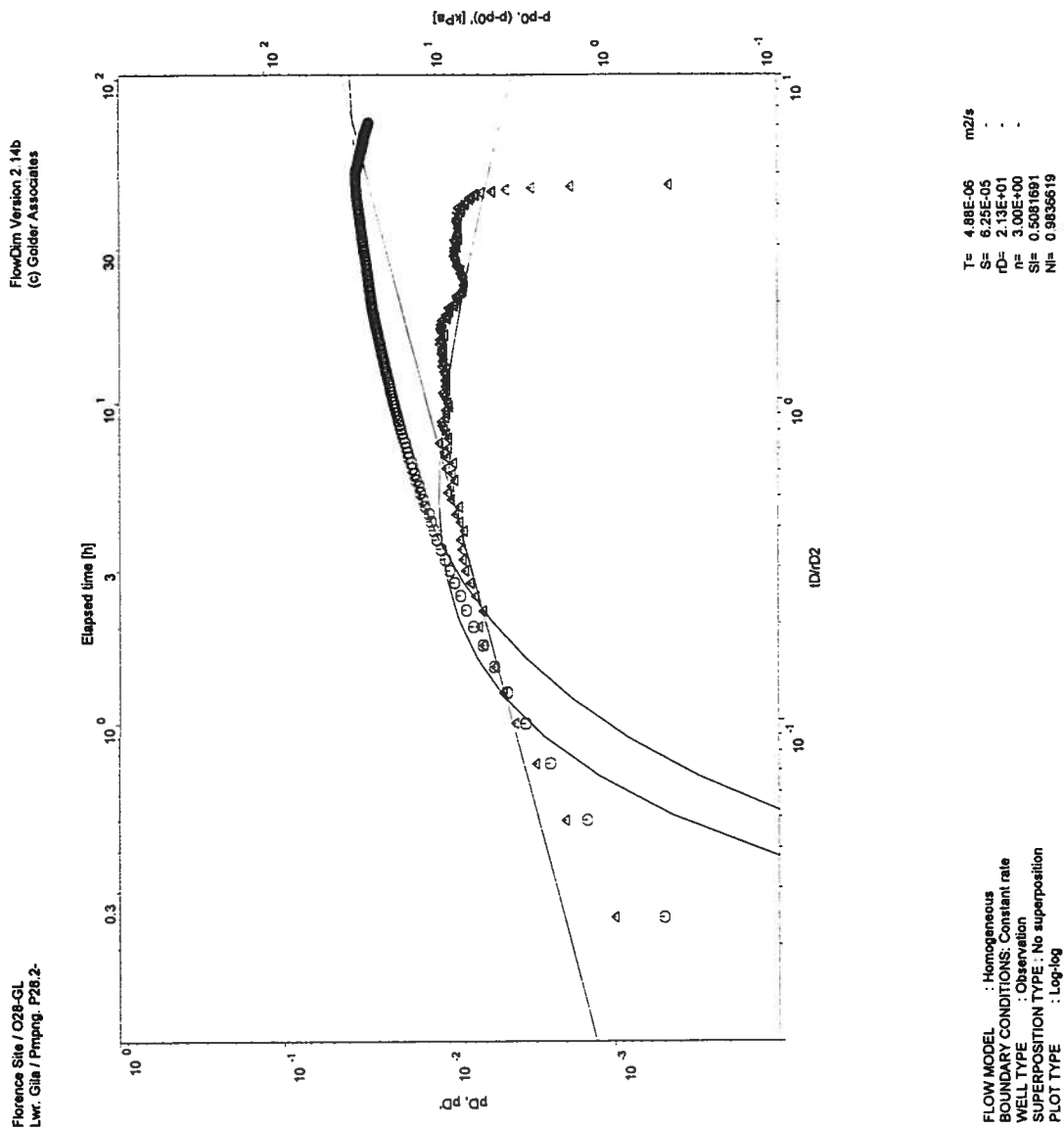


Figure 28I O28-GL (3D) FlowDim™ Analysis Log-Log Plot

Hydraulic Conductivity Calculation for a Cylindrical Source

PUMPING WELL

Easting:	651118.2	ft
Northing:	745516.2	ft
Screen Top:	398.3	ft
Screen Bottom:	497.0	ft
Surface Elevation	1465.4	ft (amsl)
Radius:	7.62E-02	m
Screen Interval:	30.08	m
Screen Interval Mid-Point:	310.21	m

OBSERVATION WELL

Easting	651124.0	ft
Northing	745621.1	ft
Screen Top:	454.4	ft
Screen Bottom:	493.3	ft
Surface Elevation	1464.8	ft
Screen Interval Mid-Point:	302.04	m
Distance to Sink:	32.1	m

Pseudo-Transmissivity:	3.13E-06	m ² /sec
Pseudo-Storage:	4.63E-05	
Anisotropy Ratio:	1.00	

Pseudo-Spherical Radius:

$r_{sw} = 2.52 \text{ m}$

Hydraulic Conductivity: $1.24\text{E-}06 \text{ m/sec} = 0.35 \text{ ft/day}$

Specific Storage: $1.13\text{E-}07 \text{ 1/m} = 3.44\text{E-}08 \text{ 1/ft}$

Figure 28J O28.2-S (3D) FlowDim™ Analysis Summary

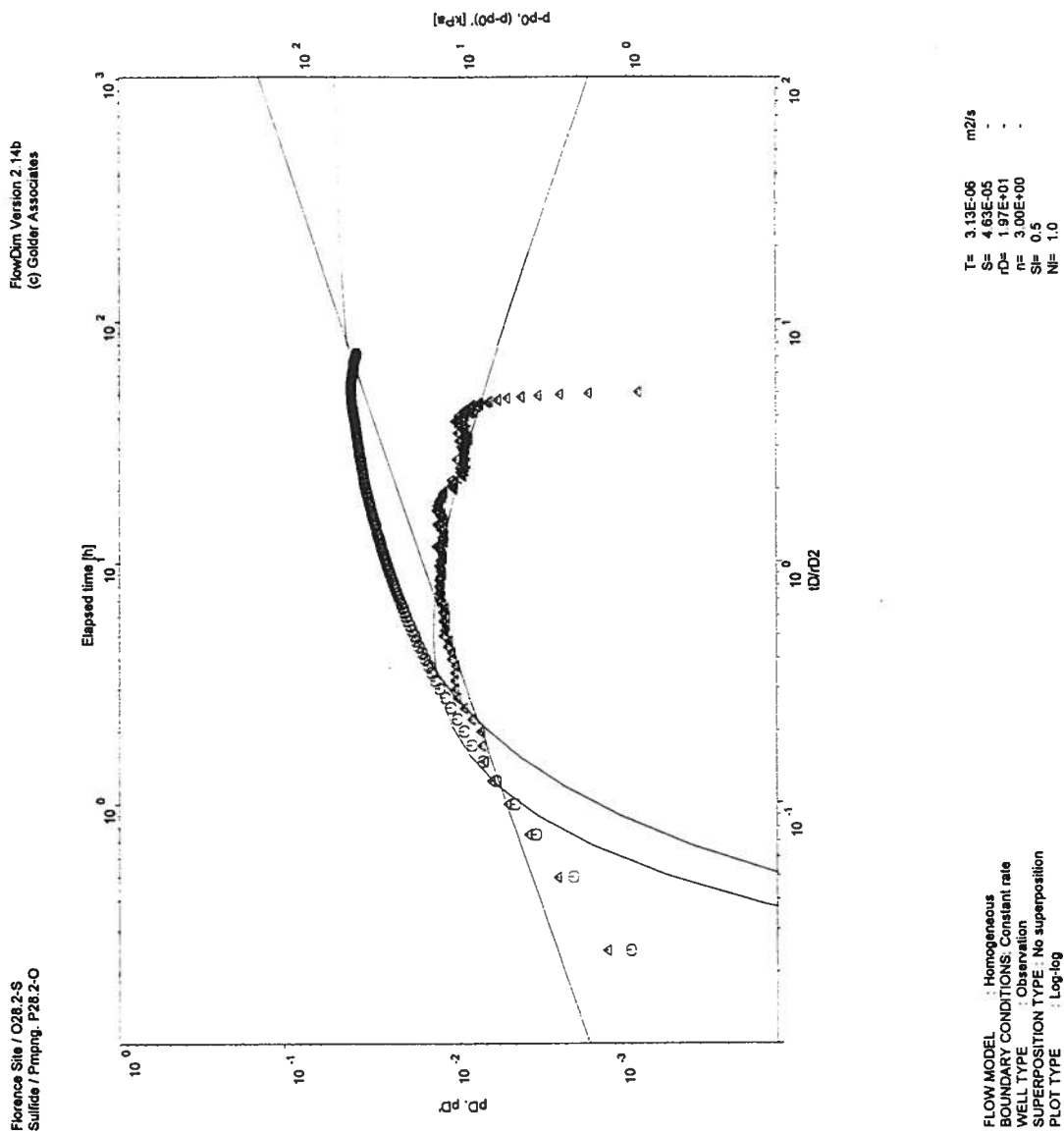


Figure 28K O28.2-S (3D) FlowDim™ Analysis Log-Log Plot

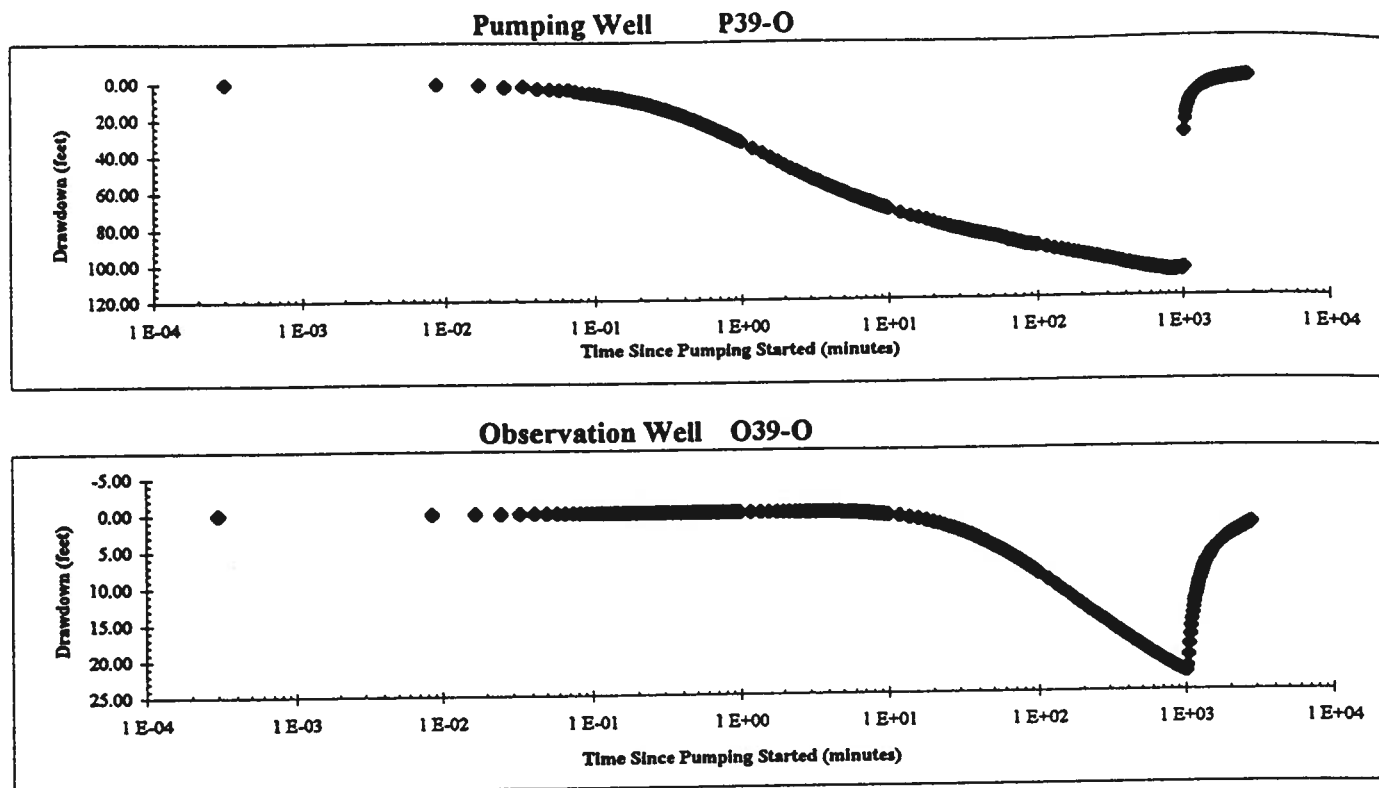


Figure 29A P39-O Semi-Log Aquifer Test Plot

P39-O.ANL, Data Plots

Golder Associates

FlowDim Analysis File : mf39pwpd.dat

	Parameter		Units
r_w	Well radius	0.130	m
μ	Groundwater viscosity	1.00E-03	Pa s
ρ	Groundwater density	1.00E+03	kg/m ³
c_t	Total compressibility	5.40E-10	1/Pa
ϕ	Porosity of formation	5.00	%
C	Wellbore storage	1.04E-06	m ³ /Pa
h	Length of aquifer tested	108.20	m

Skin Factor Calculation

Assuming formation storativity, the skin factor (s) can be calculated from the following equation.

$$s = \frac{\ln (C_D e^{2s} 2 \pi \phi c_t h r_w^2 / C)}{2}$$

Match Point Parameters From Analysis

$C_D e^{2s}$	1.0000E+02
P_{DM}	2.0728E-02
T_{DM}	2.4897E+02

Results

T(m ² /sec)	K (feet/min)	K (ft/day)	K (m/s)	K (cm/s)	Skin
1.12E-04	2.04E-04	0.29	1.04E-06	1.04E-04	-1.76

Figure 29B P39-O FlowDim™ Analysis Summary

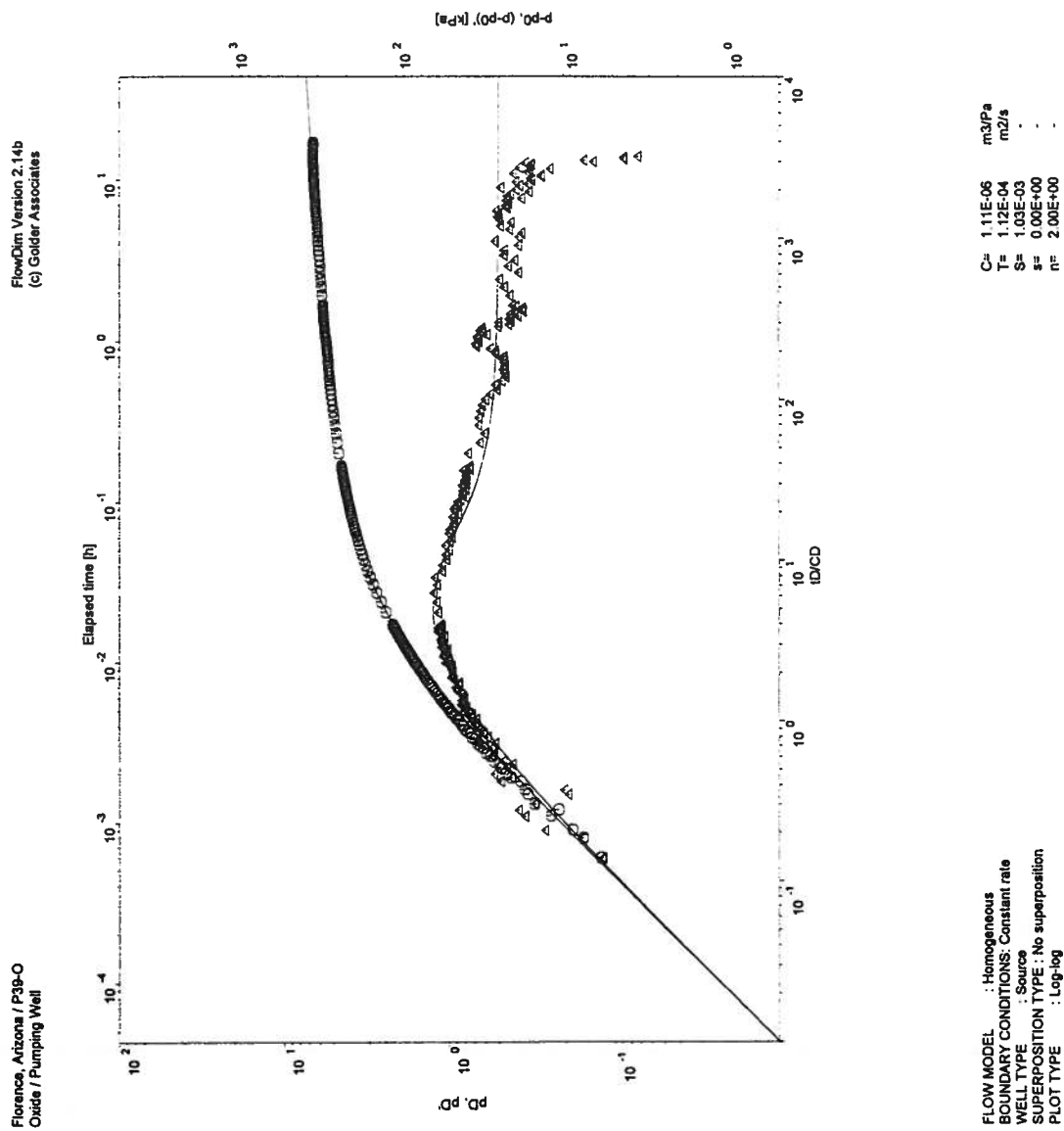


Figure 29C P39-O FlowDim™ Analysis Log-Log Plot

FlowDim Analysis File :

mf39owpd.dat

	Parameter		Units
r_w	Well radius	0.127	m
μ	Groundwater viscosity	1.00E-03	Pa s
ρ	Groundwater density	1.00E+03	kg/m ³
c_t	Total compressibility	5.40E-10	1/Pa
ϕ	Porosity of formation	50.00	%
C	Wellbore storage	NA	m ³ /Pa
h	Length of aquifer tested	126.80	m

Skin Factor Calculation

Assuming formation storativity, the skin factor (s) can be calculated from the following equation.

$$s = \frac{\ln (C_D e^{2s} 2 \pi \phi c_t h r_w^2 / C)}{2}$$

Match Point Parameters From Analysis

$C_D e^{2s}$	2.0000E+00
P_{DM}	2.6738E-02
T_{DM}	9.3173E-01

Results

T(m ² /sec)	K (feet/min)	K (ft/day)	K (m/s)	K (cm/s)	Skin
1.44E-04	2.24E-04	0.32	1.14E-06	1.14E-04	#####

Figure 29D O39-O FlowDim™ Analysis Summary

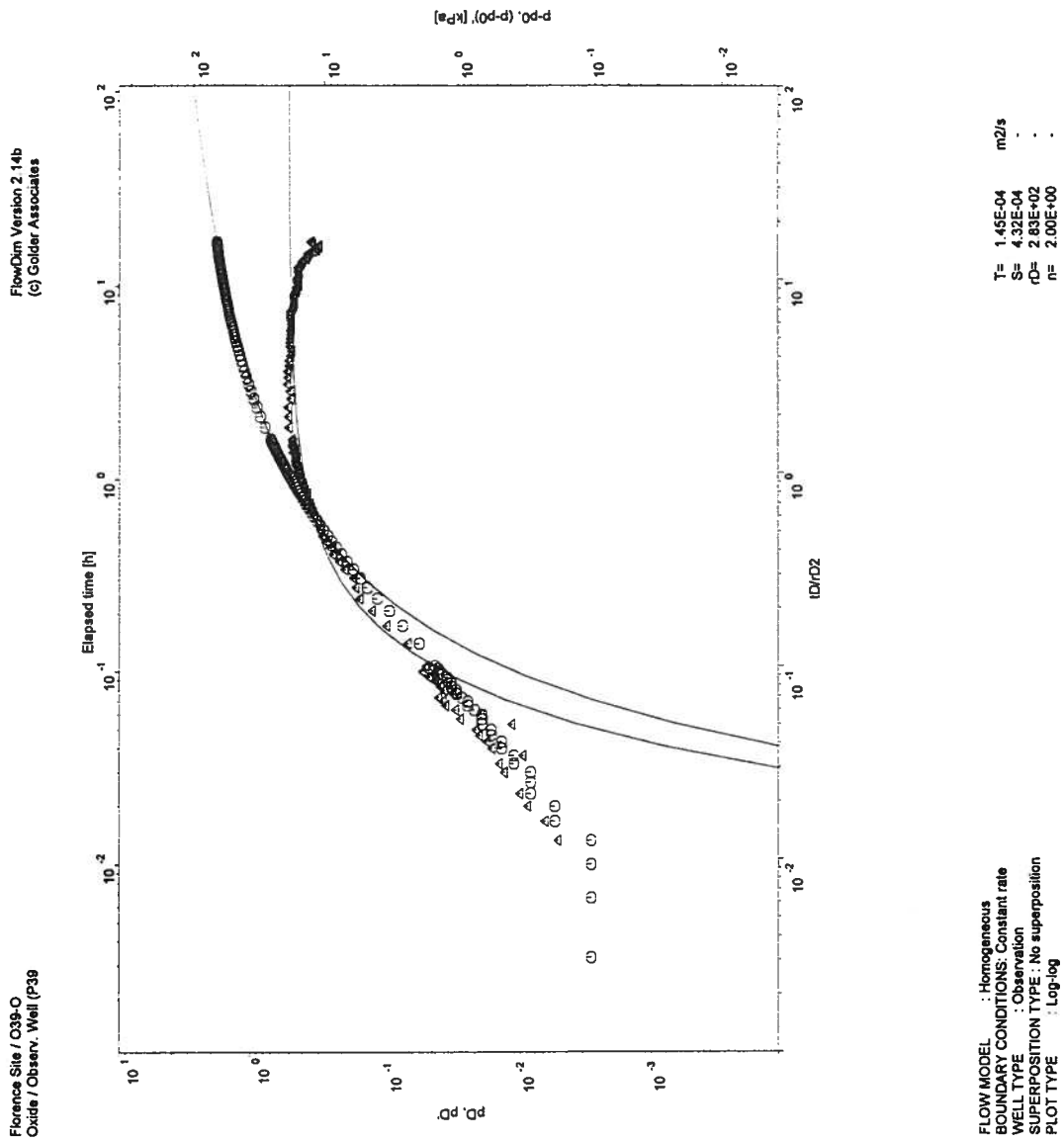
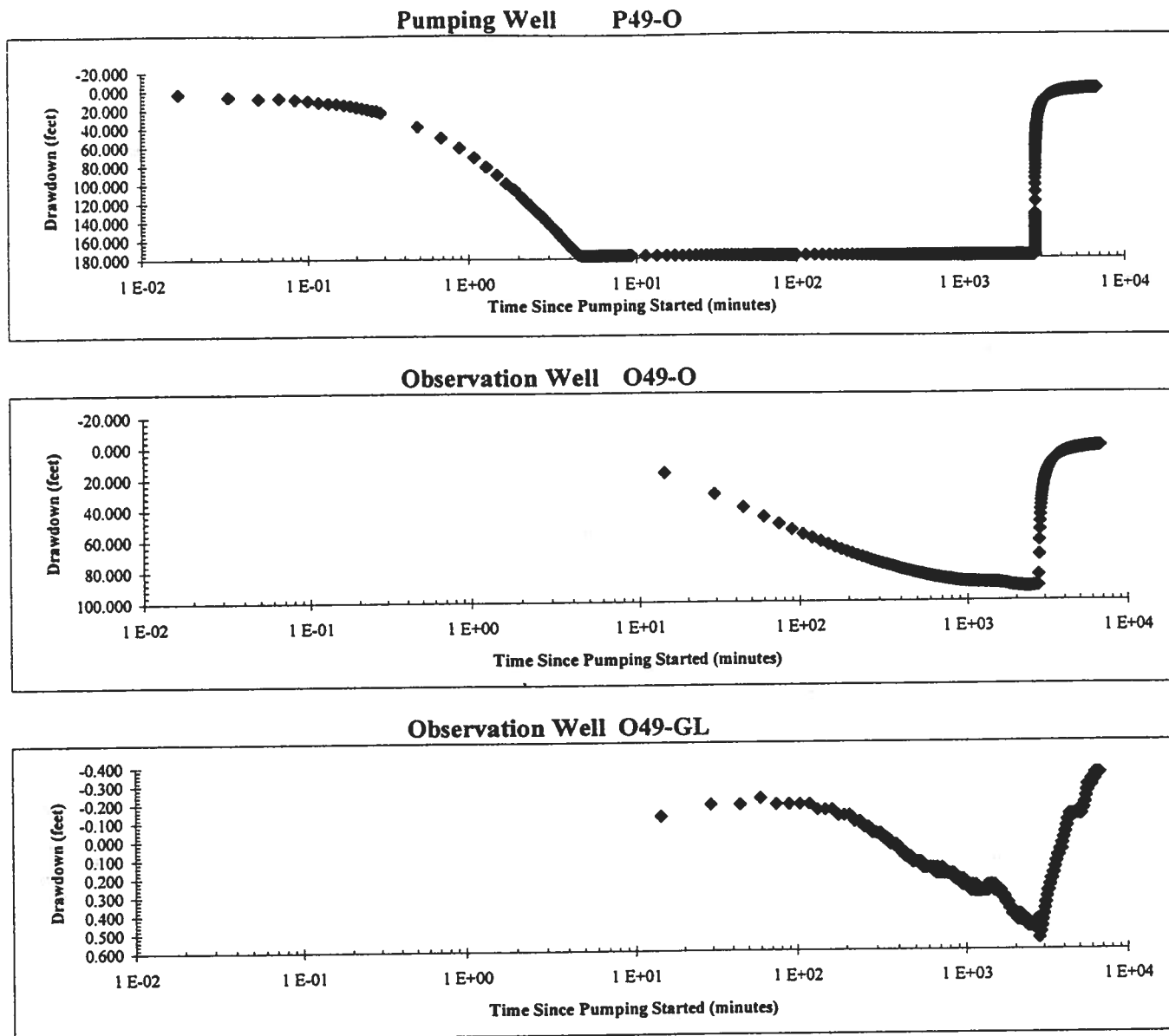


Figure 29E O39-O FlowDim™ Analysis Log-Log Plot

**Figure 30A P49-O Semi-Log Aquifer Test Plot**

Hydraulic Conductivity Calculation for a Cylindrical Source

Well Name:	P49-O
Sink Radius:	7.62E-02 m
Sink Screened Interval:	126.19 m
Pseudo-Transmissivity:	3.43E-06 m ² /sec
Pseudo-Storage:	6.40E-05
Anisotropy Ratio:	1.00

Pseudo-Spherical Radius:

$r_{sw} = 8.51 \text{ m}$

Hydraulic Conductivity: $4.05\text{E-}07 \text{ m/sec} = 0.11 \text{ ft/day}$

Specific Storage: $7.52\text{E-}06 \text{ 1/m} = 2.29\text{E-}06 \text{ 1/ft}$

Figure 30B P49-O (3D) FlowDim™ Analysis Summary

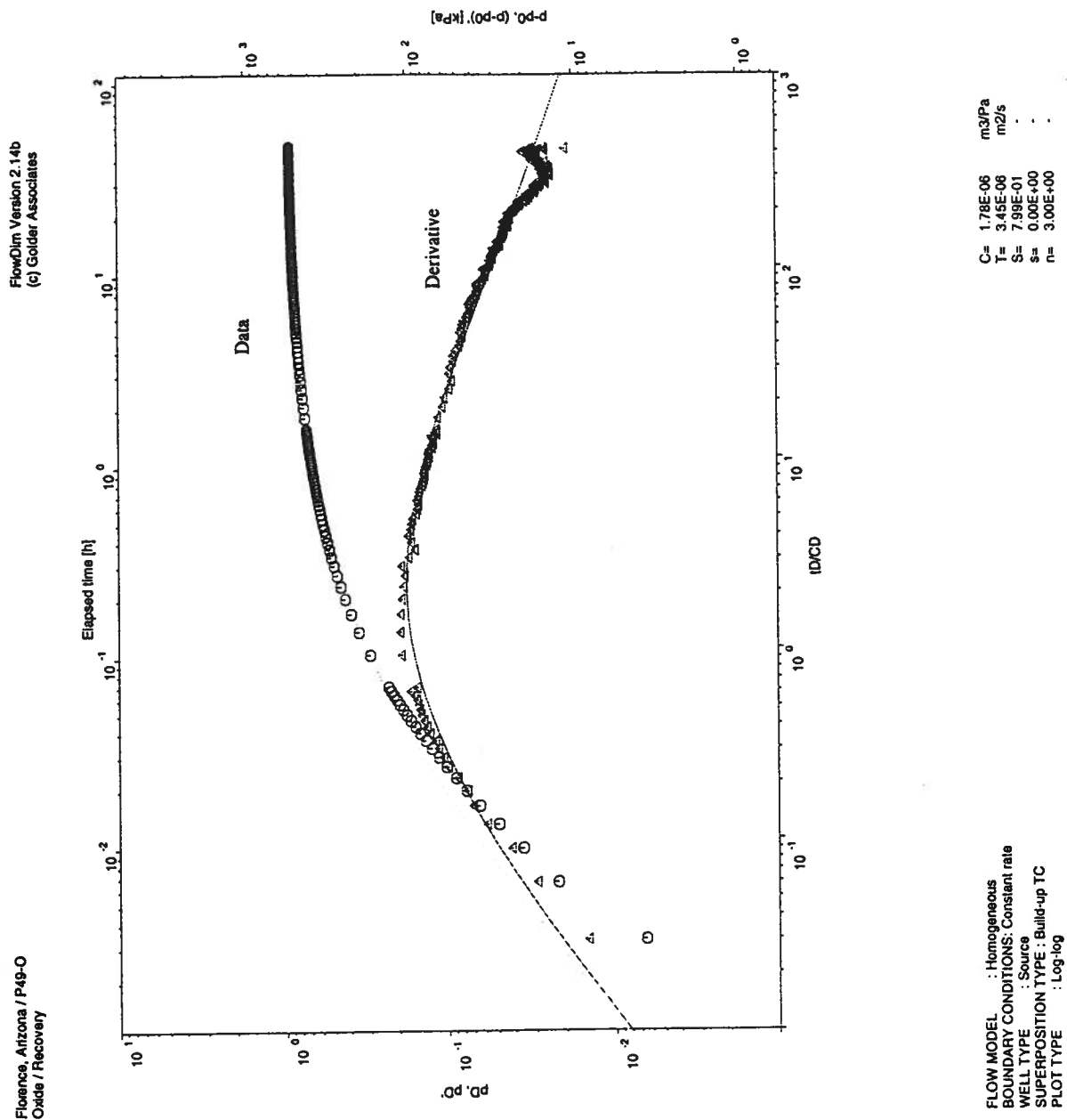


Figure 30C P49-O (3D) FlowDim™ Analysis Log-Log Plot

Hydraulic Conductivity Calculation for a Cylindrical Source

PUMPING WELL

Easting:	647611.9	ft
Northing:	744202.7	ft
Screen Top:	808.1	ft
Screen Bottom:	1222.3	ft
Surface Elevation	1461.8	ft (amsl)
Radius:	7.62E-02	m
Screen Interval:	126.25	m
Screen Interval Mid-Point:	136.12	m

OBSERVATION WELL

Easting	647517.2	ft
Northing	744195.3	ft
Screen Top:	832.8	ft
Screen Bottom:	1228.4	ft
Surface Elevation	1461.8	ft
Screen Interval Mid-Point:	131.43	m
Distance to Sink:	29.0	m

Pseudo-Transmissivity:	2.27E-06	m ² /sec
Pseudo-Storage:	1.74E-05	
Anisotropy Ratio:	1.00	

Pseudo-Spherical Radius:

$r_{sw} = 8.52 \text{ m}$

Hydraulic Conductivity: $2.67\text{E-}07 \text{ m/sec} = 0.08 \text{ ft/day}$

Specific Storage: $1.76\text{E-}07 \text{ 1/m} = 5.38\text{E-}08 \text{ 1/ft}$

Figure 30D O49-O (3D) FlowDim™ Analysis Summary

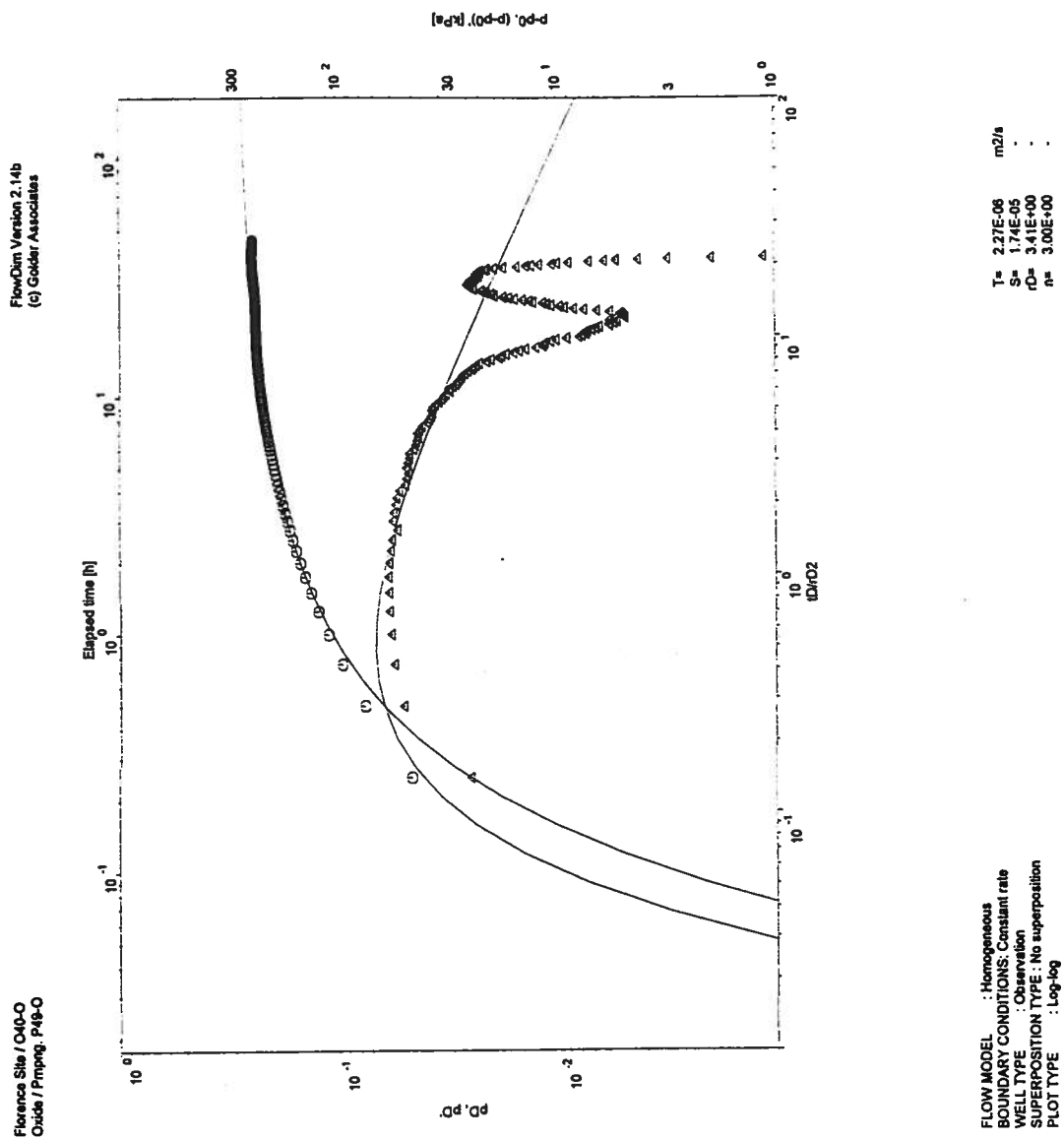


Figure 30E O49-O (3D) FlowDim™ Analysis Log-Log Plot

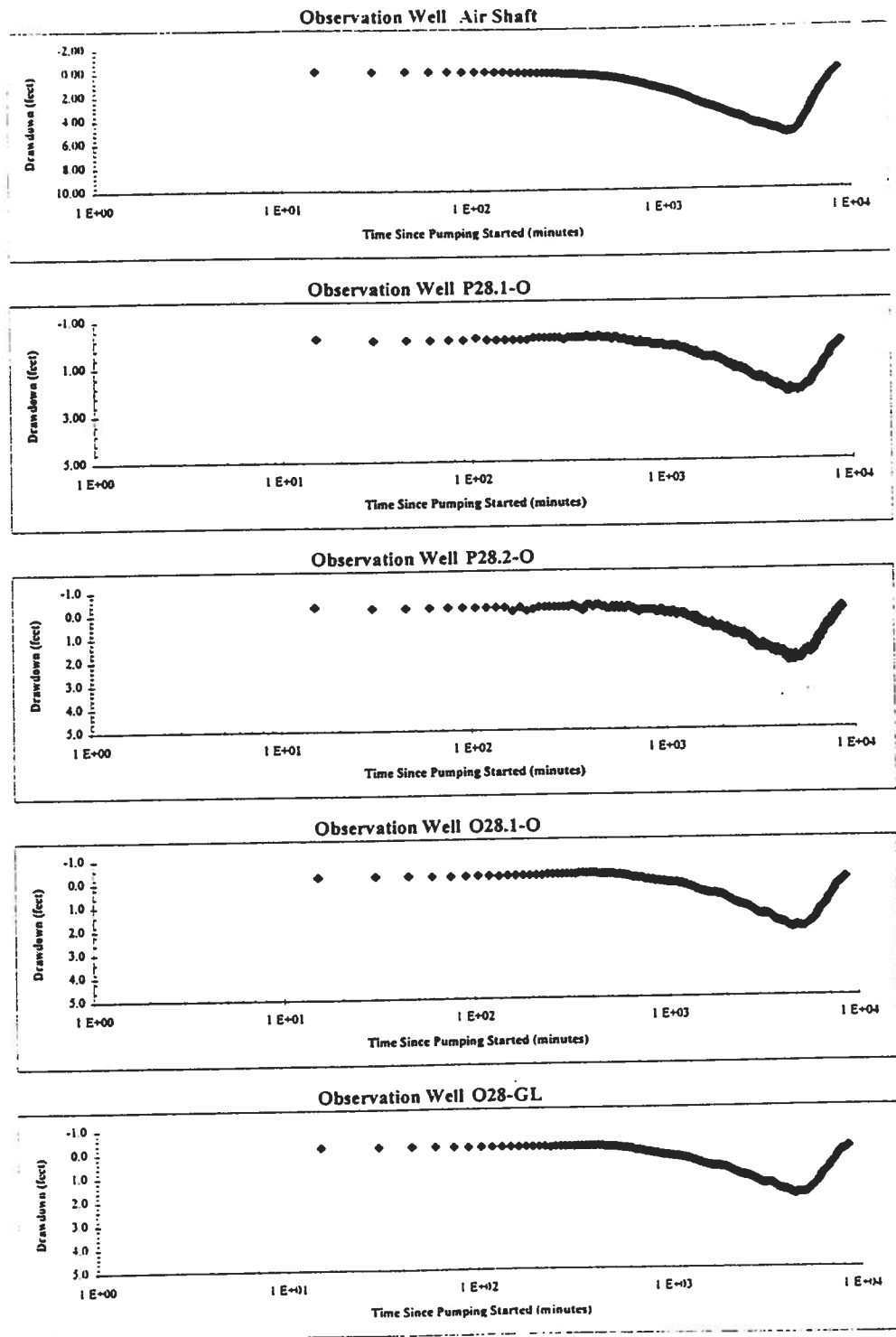


Figure 31A WW3 Observation Wells Semi-Log Aquifer Test Plot, page 1

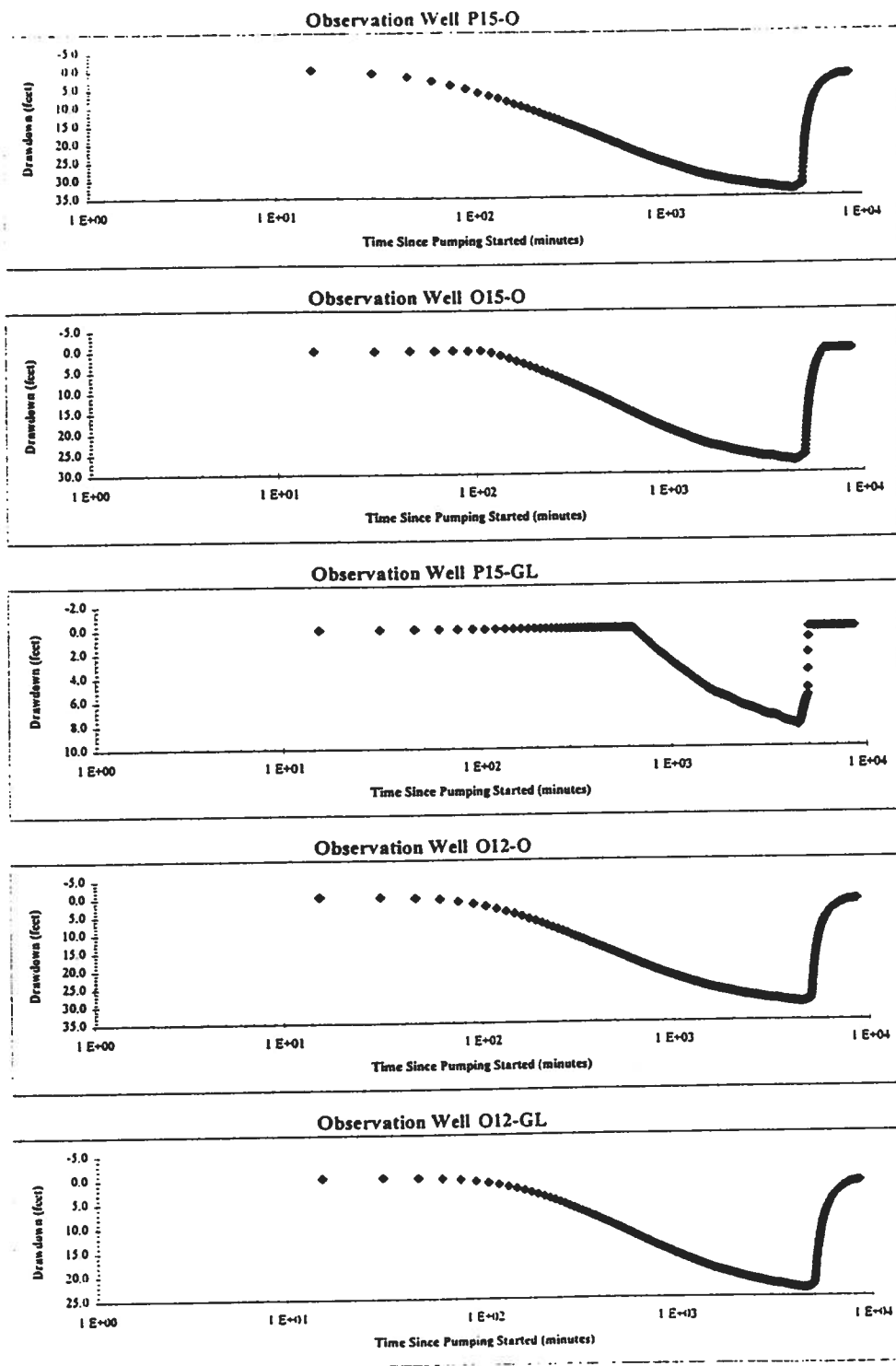


Figure 31B WW3 Observation Wells Semi-Log Aquifer Test Plot, page 2

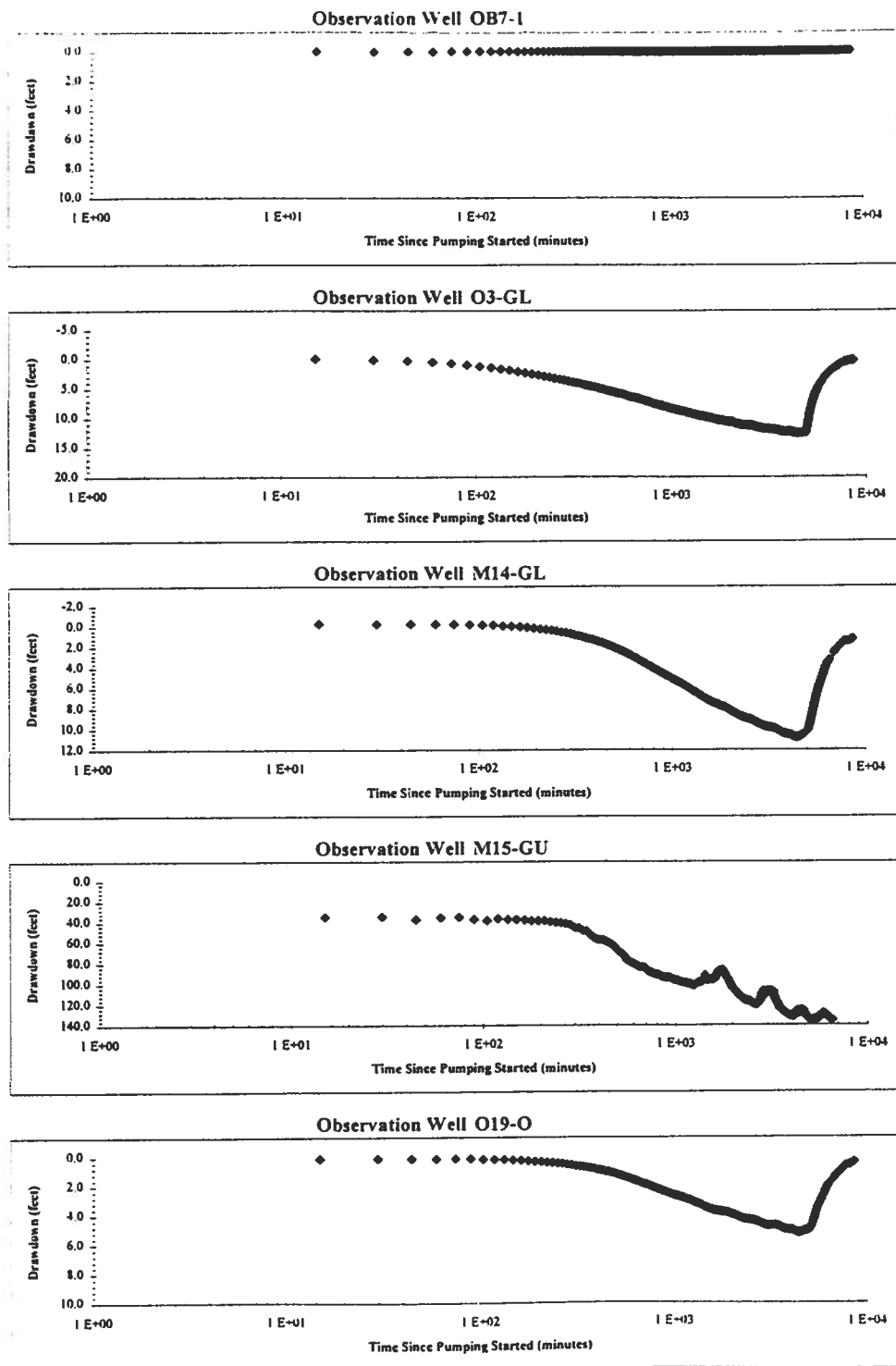


Figure 31C WW3 Observation Wells Semi-Log Aquifer Test Plot, page 3

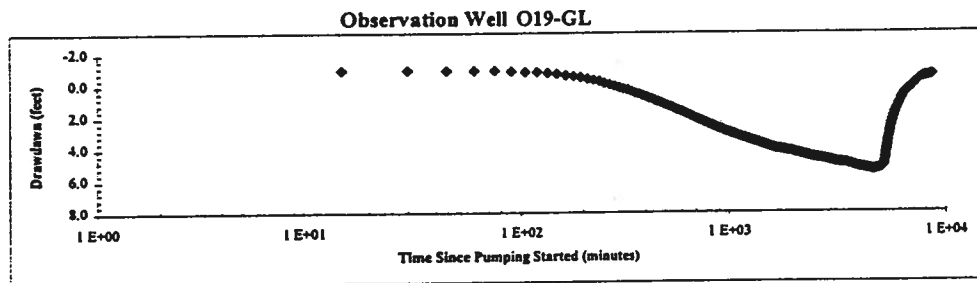


Figure 31D WW3 Observation Wells Semi-Log Aquifer Test Plot, page 4

FlowDim Analysis File : W3-P281O.DAT

	Parameter		Units
r_w	Well radius	N/A	m
μ	Groundwater viscosity	1.000E-03	Pa s
ρ	Groundwater density	1.000E+03	kg/m ³
c_t	Total compressibility	5.400E-10	1/Pa
ϕ	Porosity of formation	5.00	%
C	Wellbore storage	N/A	m ³ /Pa
h	Length of aquifer tested	211.23	m

Skin Factor Calculation

Assuming formation storativity, the skin factor (s) can be calculated from the following equation.

$$s = \frac{\ln (C_D e^{2s} 2 \pi \phi c_t h r_w^2 / C)}{2}$$

Match Point Parameters From Analysis

		Units
$C_D e^{2s}$	N/A	-
P_M (1/KPa)	N/A	-
T_M (hr)	N/A	-

Results

T(m ² /sec)	K (feet/min)	K(feet/day)	K (m/s)	K (cm/s)	Skin
2.23E-02	2.08E-02	29.93	1.06E-04	1.06E-02	#####

Figure 31E P28.1-O FlowDim™ Analysis Summary

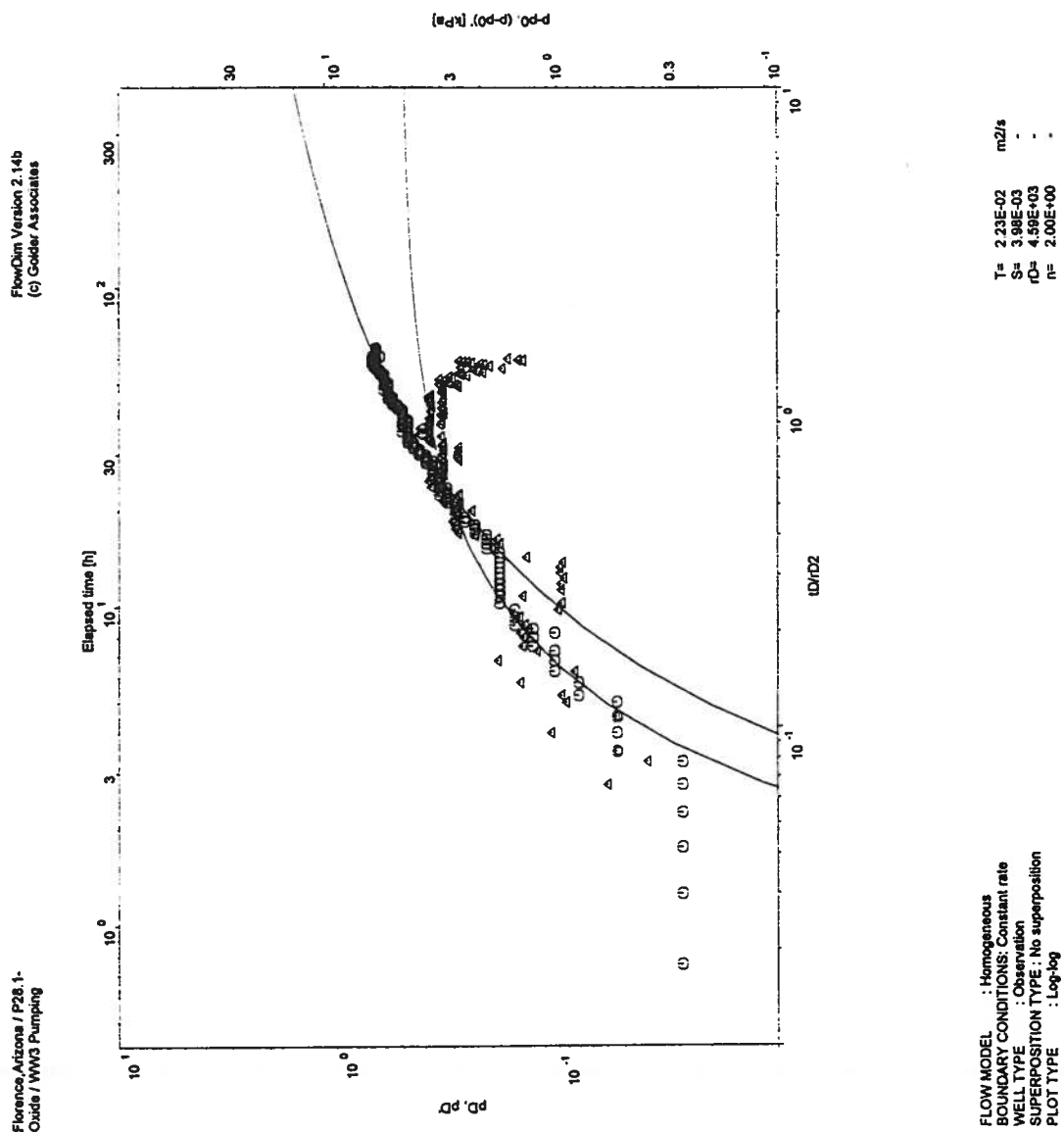


Figure 31F P28.1-O FlowDim™ Analysis Log-Log Plot

FlowDim Analysis File : W3-P282O.DAT

	Parameter		Units
r_w	Well radius	N/A	m
μ	Groundwater viscosity	1.000E-03	Pa s
ρ	Groundwater density	1.000E+03	kg/m ³
c_t	Total compressibility	5.400E-10	1/Pa
ϕ	Porosity of formation	5.00	%
C	Wellbore storage	N/A	m ³ /Pa
h	Length of aquifer tested	211.23	m

Skin Factor Calculation

Assuming formation storativity, the skin factor (s) can be calculated from the following equation.

$$s = \frac{\ln (C_D e^{2s} 2 \pi \phi c_t h r_w^2 / C)}{2}$$

Match Point Parameters From Analysis

		Units
$C_D e^{2s}$	N/A	-
P_M (1/KPa)	N/A	-
T_M (hr)	N/A	-

Results

T(m ² /sec)	K (feet/min)	K(feet/day)	K (m/s)	K (cm/s)	Skin
3.02E-02	2.81E-02	40.53	1.43E-04	1.43E-02	#####

Figure 31G P28.2-O FlowDim™ Analysis Summary

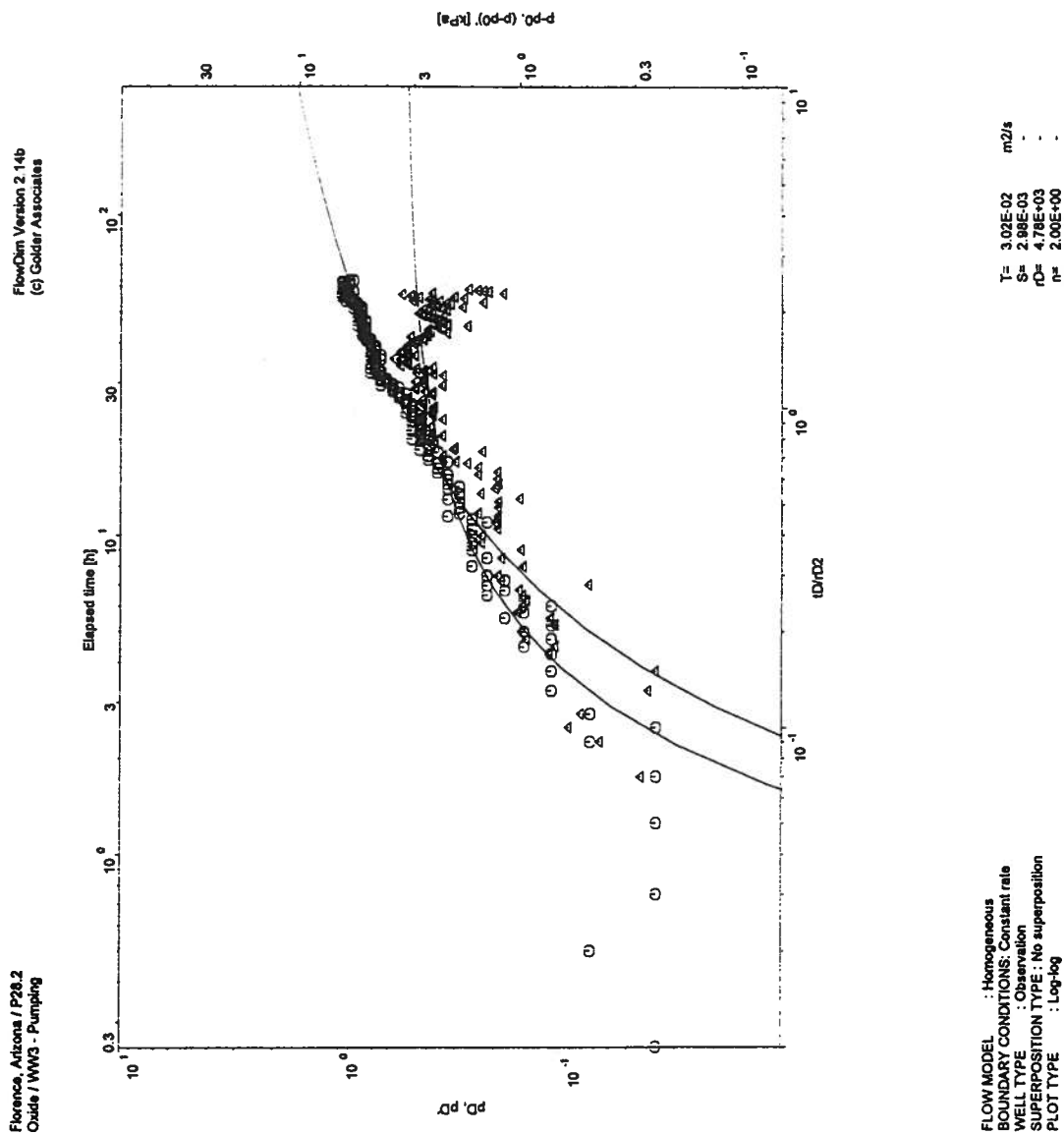


Figure 31H P28.2-O FlowDim™ Analysis Log-Log Plot

FlowDim Analysis File : W3-O281O.DAT

	Parameter		Units
r_w	Well radius	N/A	m
μ	Groundwater viscosity	1.000E-03	Pa s
ρ	Groundwater density	1.000E+03	kg/m ³
c_t	Total compressibility	5.400E-10	1/Pa
ϕ	Porosity of formation	5.00	%
C	Wellbore storage	N/A	m ³ /Pa
h	Length of aquifer tested	211.23	m

Skin Factor Calculation

Assuming formation storativity, the skin factor (s) can be calculated from the following equation.

$$s = \frac{\ln (C_D e^{2s} 2 \pi \phi c_t h r_w^2 / C)}{2}$$

Match Point Parameters From Analysis

		Units
$C_D e^{2s}$	N/A	-
P_M (1/KPa)	N/A	-
T_M (hr)	N/A	-

Results

T(m ² /sec)	K (feet/min)	K(feet/day)	K (m/s)	K (cm/s)	Skin
2.63E-02	2.45E-02	35.30	1.25E-04	1.25E-02	#####

Figure 31I O28.1-O FlowDim™ Analysis Summary

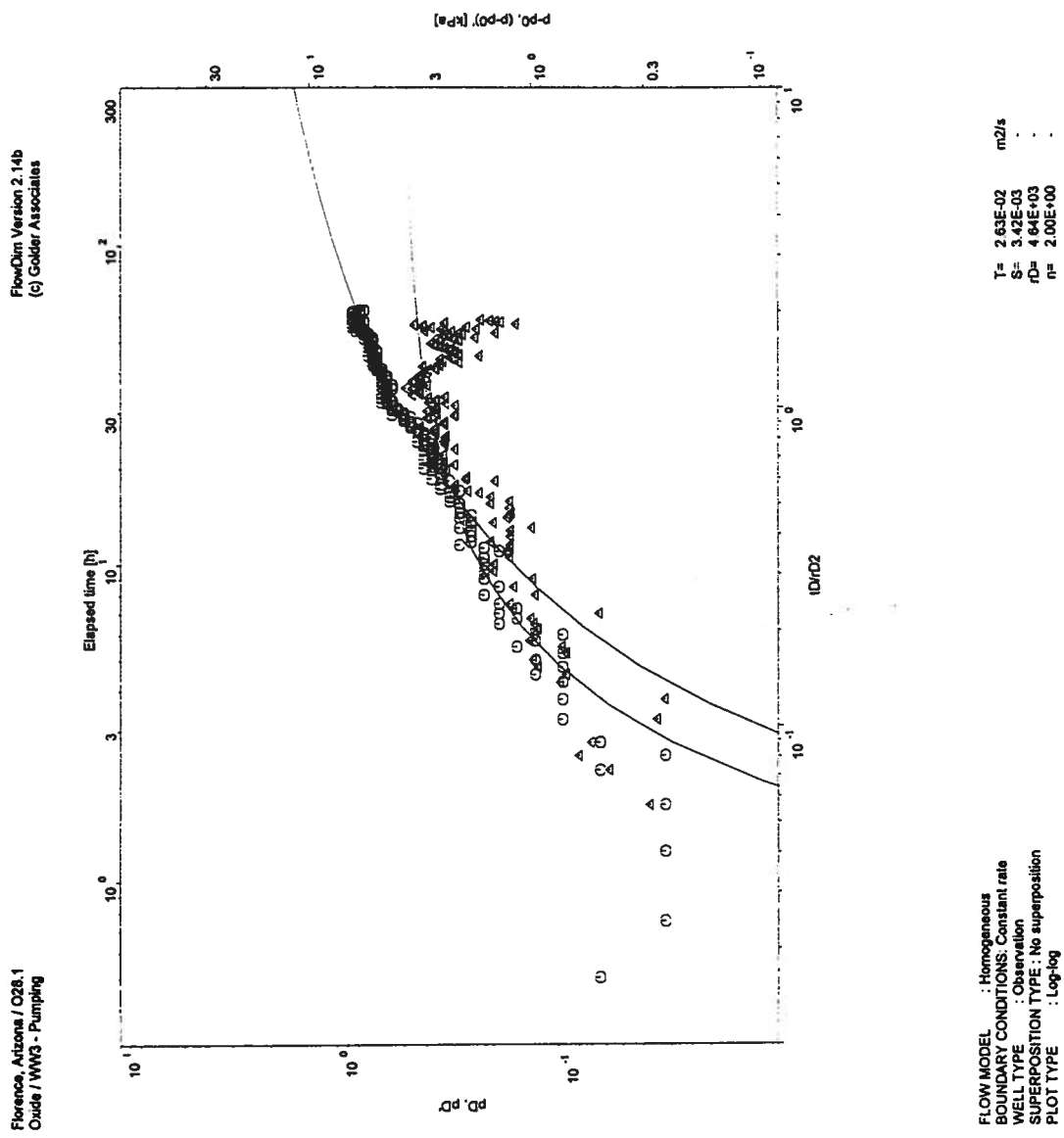


Figure 31J O28.1-O FlowDim™ Analysis Log-Log Plot

FlowDim Analysis File : W3-O281GL.DAT

	Parameter		Units
r_w	Well radius	N/A	m
μ	Groundwater viscosity	1.000E-03	Pa s
ρ	Groundwater density	1.000E+03	kg/m ³
c_t	Total compressibility	5.400E-10	1/Pa
ϕ	Porosity of formation	5.00	%
C	Wellbore storage	N/A	m ³ /Pa
h	Length of aquifer tested	211.23	m

Skin Factor Calculation

Assuming formation storativity, the skin factor (s) can be calculated from the following equation.

$$s = \frac{\ln (C_D e^{2s} 2 \pi \phi c_t h r_w^2 / C)}{2}$$

Match Point Parameters From Analysis

		Units
$C_D e^{2s}$	N/A	-
P_M (1/KPa)	N/A	-
T_M (hr)	N/A	-

Results

T(m ² /sec)	K (feet/min)	K(feet/day)	K (m/s)	K (cm/s)	Skin
2.89E-02	2.69E-02	38.78	1.37E-04	1.37E-02	#####

Figure 31K O28-GL FlowDim™ Analysis Summary

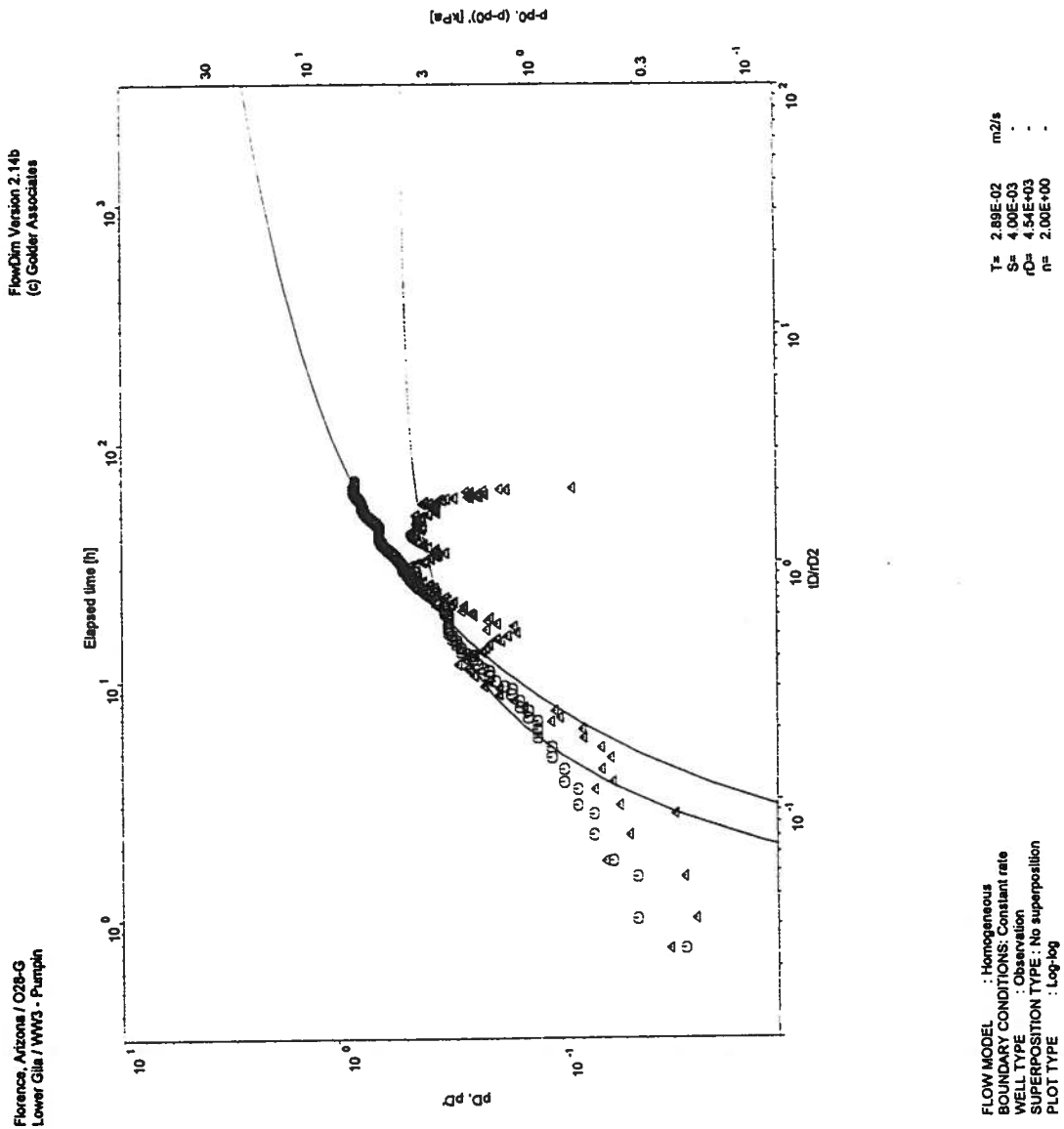


Figure 31L O28-GL FlowDim™ Analysis Log-Log Plot

Hydraulic Conductivity Calculation for a Cylindrical Source

Well Name:	P15-O
Sink Radius:	0.2 m
Sink Screened Interval:	211.23 m
Pseudo-Transmissivity:	$7.65\text{E-}05$ m ² /sec
Pseudo-Storage:	$6.04\text{E-}05$
Distance to Sink:	173.2 m
Anisotropy Ratio:	1.00

Pseudo-Spherical Radius:

$r_{sw} = 15.17$ m

Hydraulic Conductivity: $5.04\text{E-}06$ m/sec = 1.43 ft/day

Specific Storage: $3.05\text{E-}08$ 1/m = $9.31\text{E-}09$ 1/ft

Figure 31M P15-O (3D) FlowDim™ Analysis Summary

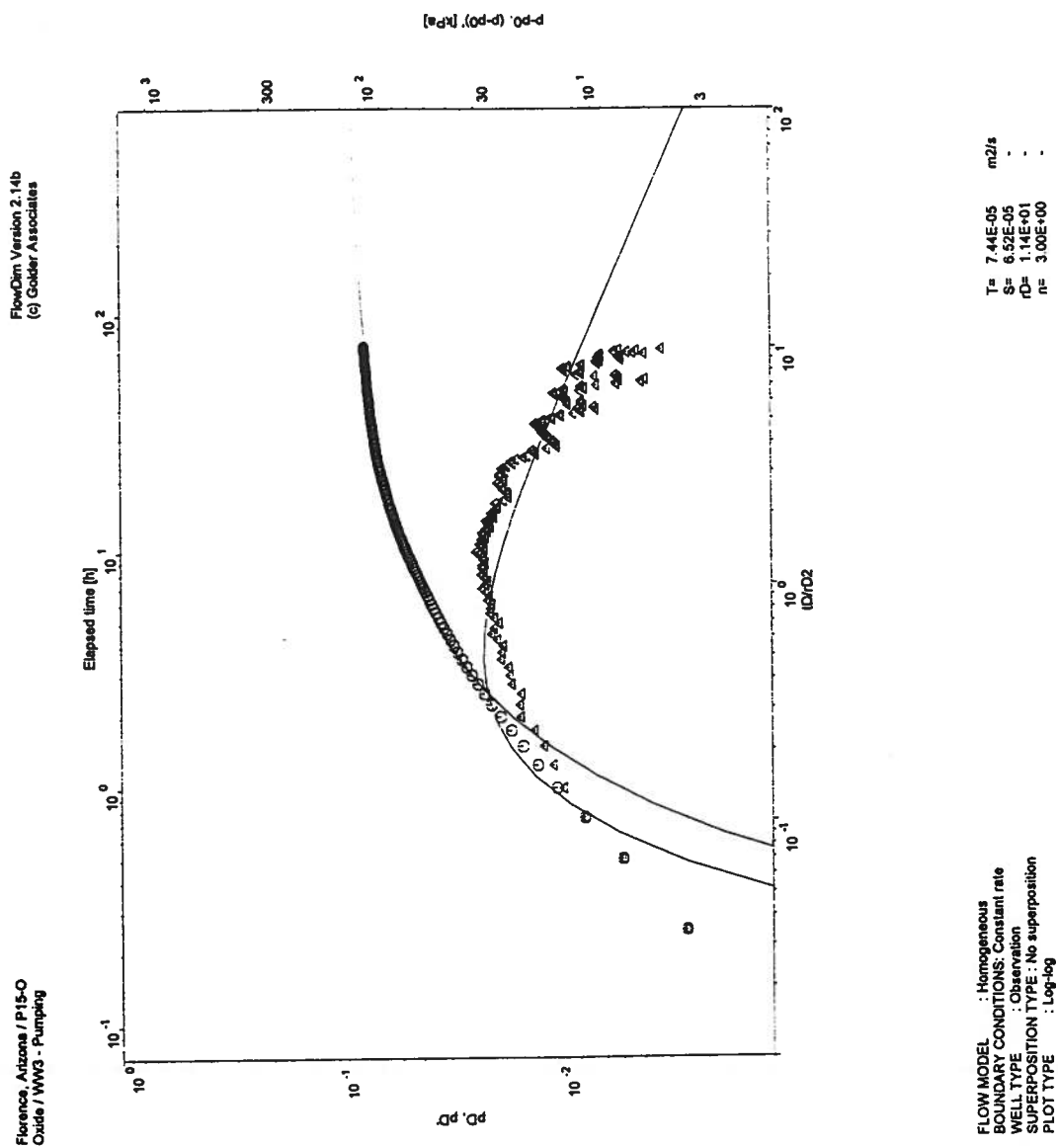


Figure 31N P15-O (3D) FlowDim™ Analysis Log-Log Plot

Hydraulic Conductivity Calculation for a Cylindrical Source

Well Name:	O15-O
Sink Radius:	0.2 m
Sink Screened Interval:	211.23 m
Pseudo-Transmissivity:	$7.08\text{E-}05$ m ² /sec
Pseudo-Storage:	$6.60\text{E-}05$
Distance to Sink:	202.9 m
Anisotropy Ratio:	1.00

Pseudo-Spherical Radius:

$r_{sw} = 15.17$ m

Hydraulic Conductivity: $4.67\text{E-}06$ m/sec = 1.32 ft/day

Specific Storage: $2.43\text{E-}08$ 1/m = $7.41\text{E-}09$ 1/ft

Figure 31O O15-O (3D) FlowDim™ Analysis Summary

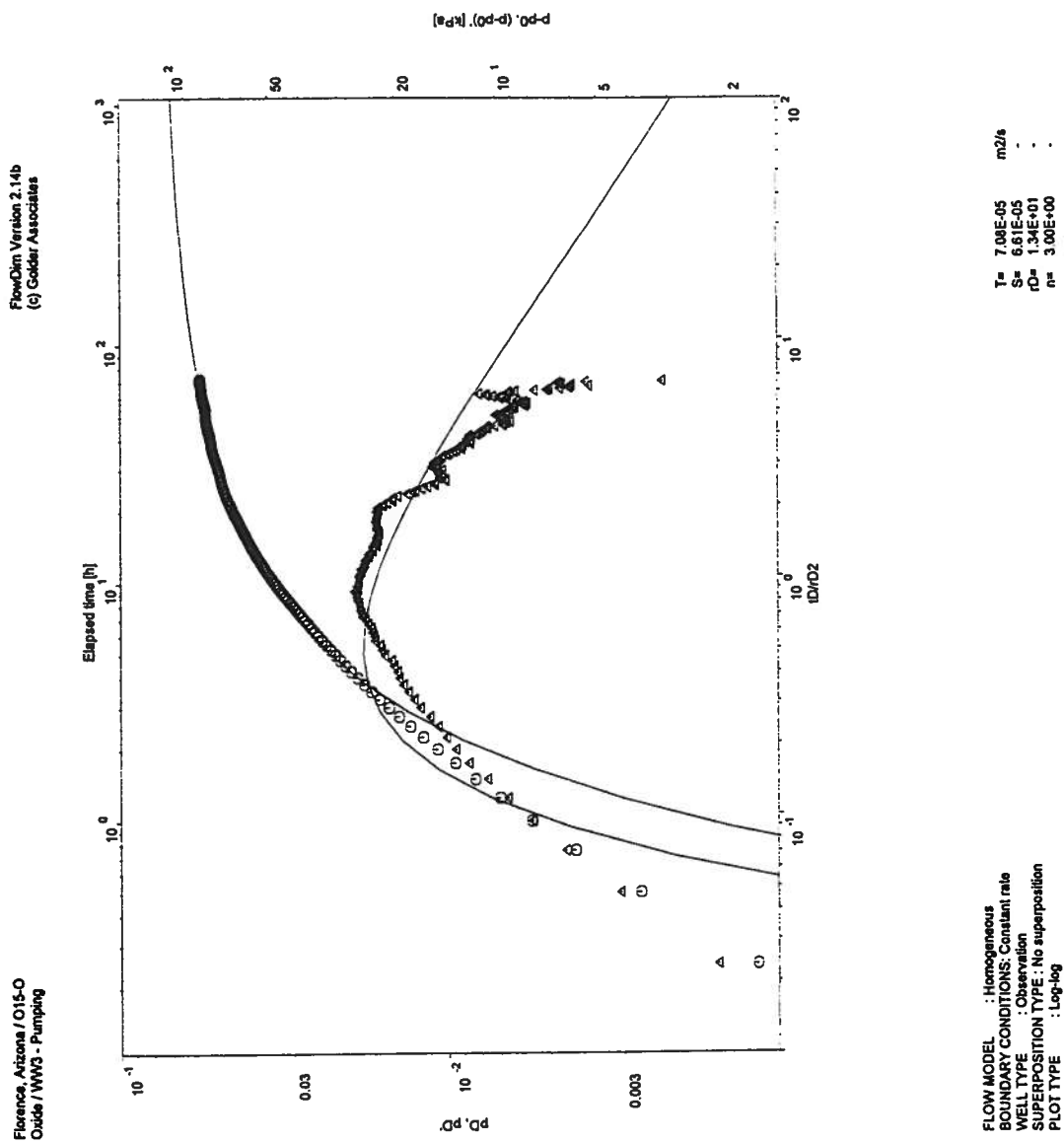


Figure 31P O15-O (3D) FlowDim™ Analysis Log-Log Plot

FlowDim Analysis File : W3-P15GL.DAT

	Parameter		Units
r_w	Well radius	N/A	m
μ	Groundwater viscosity	1.000E-03	Pa s
ρ	Groundwater density	1.000E+03	kg/m ³
c_t	Total compressibility	5.400E-10	1/Pa
ϕ	Porosity of formation	5.00	%
C	Wellbore storage	N/A	m ³ /Pa
h	Length of aquifer tested	211.23	m

Skin Factor Calculation

Assuming formation storativity, the skin factor (s) can be calculated from the following equation.

$$s = \frac{\ln (C_D e^{2s} 2 \pi \phi c_t h r_w^2 / C)}{2}$$

Match Point Parameters From Analysis

		Units
$C_D e^{2s}$	N/A	-
P_M (1/KPa)	N/A	-
T_M (hr)	N/A	-

Results

T(m ² /sec)	K (feet/min)	K(feet/day)	K (m/s)	K (cm/s)	Skin
1.28E-02	1.19E-02	17.18	6.06E-05	6.06E-03	#####

Figure 31Q P15-GL FlowDim™ Analysis Summary

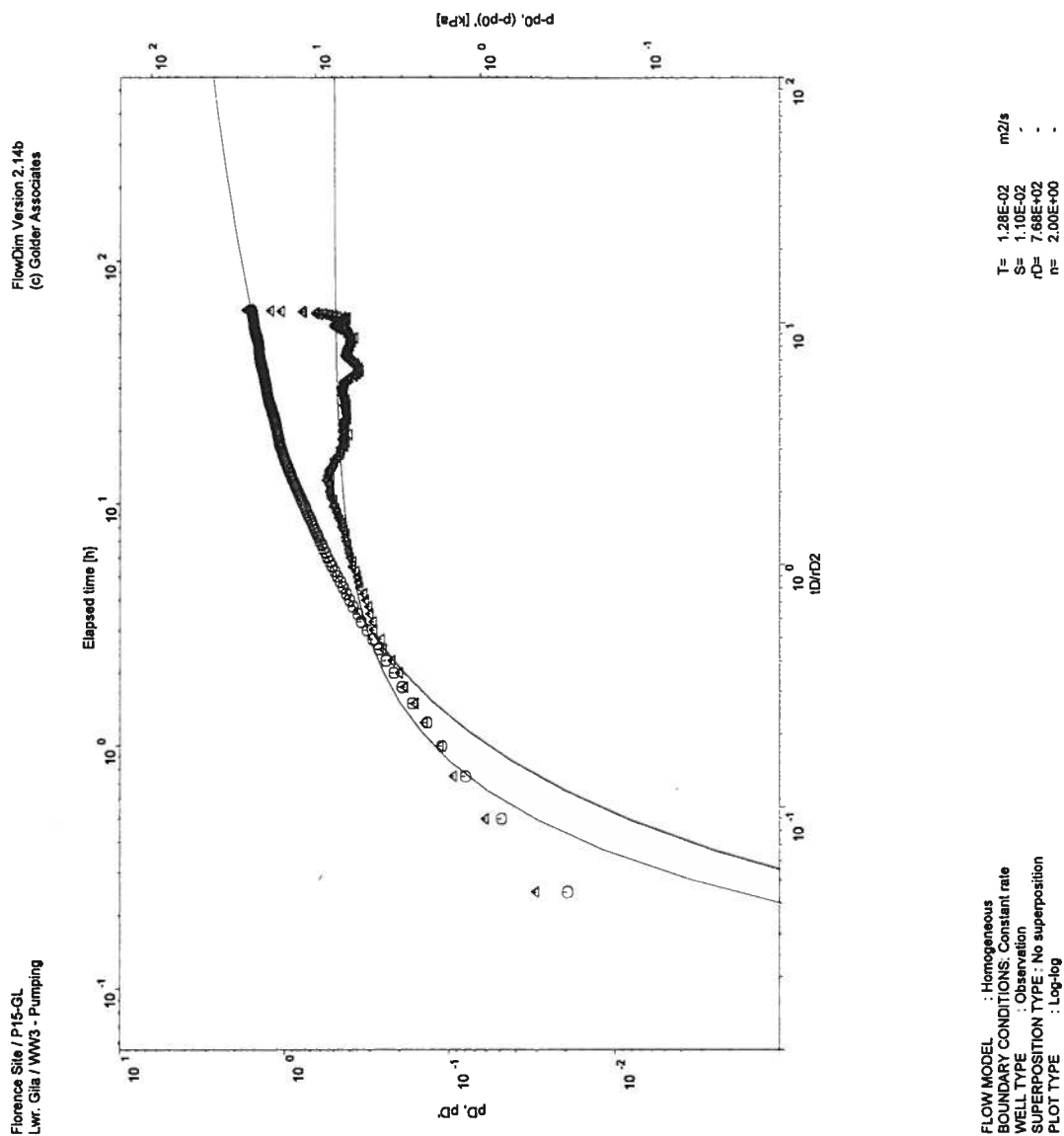


Figure 31R P15-GL FlowDim™ Analysis Log-Log Plot

Hydraulic Conductivity Calculation for a Cylindrical Source

Well Name:	012-O
Sink Radius:	0.2 m
Sink Screened Interval:	211.23 m
Pseudo-Transmissivity:	4.36E-05 m ² /sec
Pseudo-Storage:	1.70E-05
Distance to Sink:	304.9 m
Anisotropy Ratio:	1.00

Pseudo-Spherical Radius:

$r_{sw} = 15.17 \text{ m}$

Hydraulic Conductivity: $2.87\text{E-}06 \text{ m/sec} = 0.81 \text{ ft/day}$

Specific Storage: $2.77\text{E-}09 \text{ 1/m} = 8.46\text{E-}10 \text{ 1/ft}$

Figure 31S O12-O (3D) FlowDim™ Analysis Summary

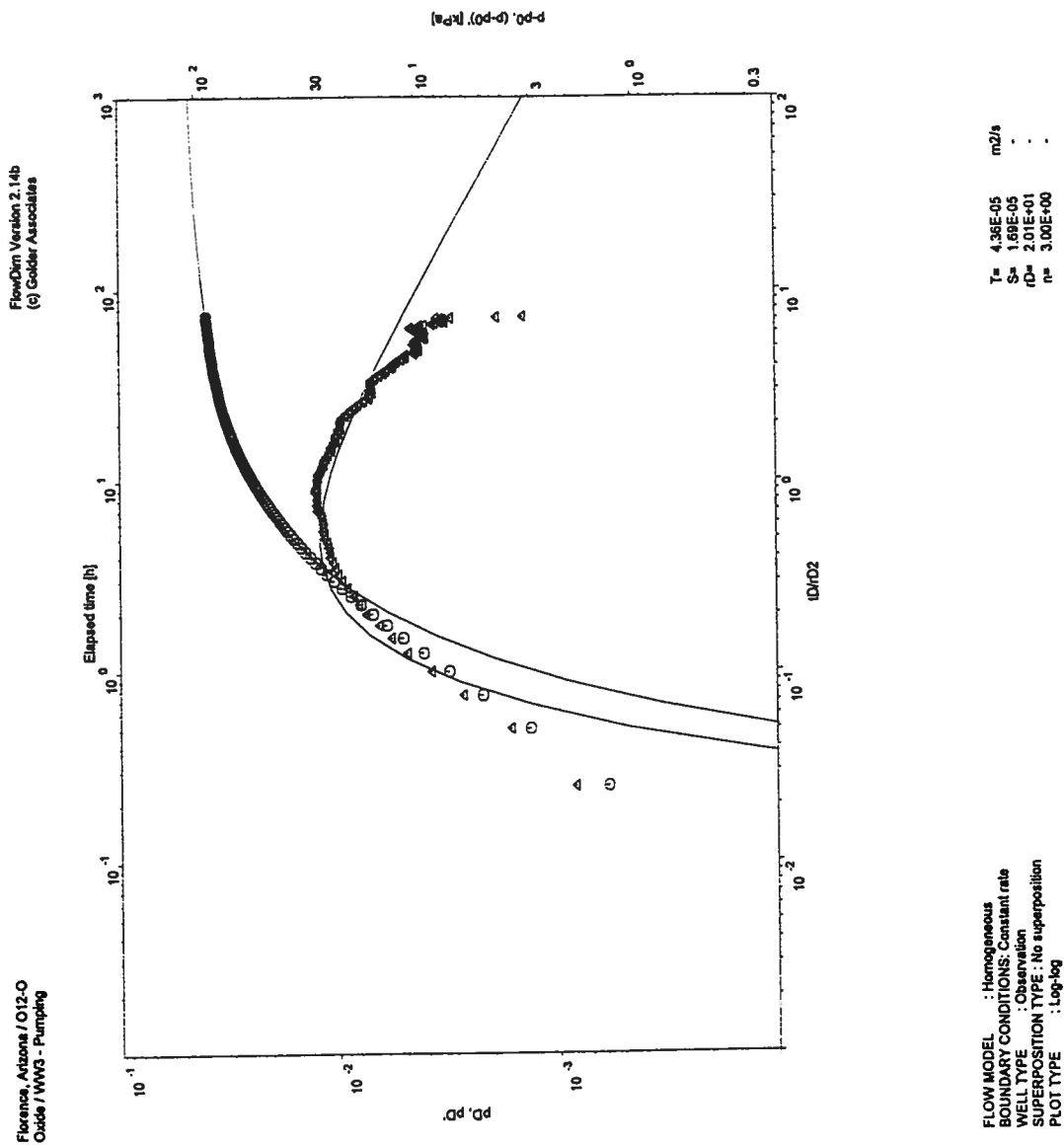


Figure 31T O12-O (3D) FlowDim™ Analysis Log-Log Plot

Hydraulic Conductivity Calculation for a Cylindrical Source

Well Name:	O12-GL
Sink Radius:	0.2 m
Sink Screened Interval:	211.23 m
Pseudo-Transmissivity:	5.36E-05 m ² /sec
Pseudo-Storage:	2.90E-05
Distance to Sink:	807.8 m
Anisotropy Ratio:	1.00

Pseudo-Spherical Radius:

$r_{sw} = 15.17 \text{ m}$

Hydraulic Conductivity: $3.53\text{E-}06 \text{ m/sec} = 1.00 \text{ ft/day}$

Specific Storage: $4.64\text{E-}09 \text{ 1/m} = 1.42\text{E-}09 \text{ 1/ft}$

Figure 31U O12-GL (3D) FlowDim™ Analysis Summary

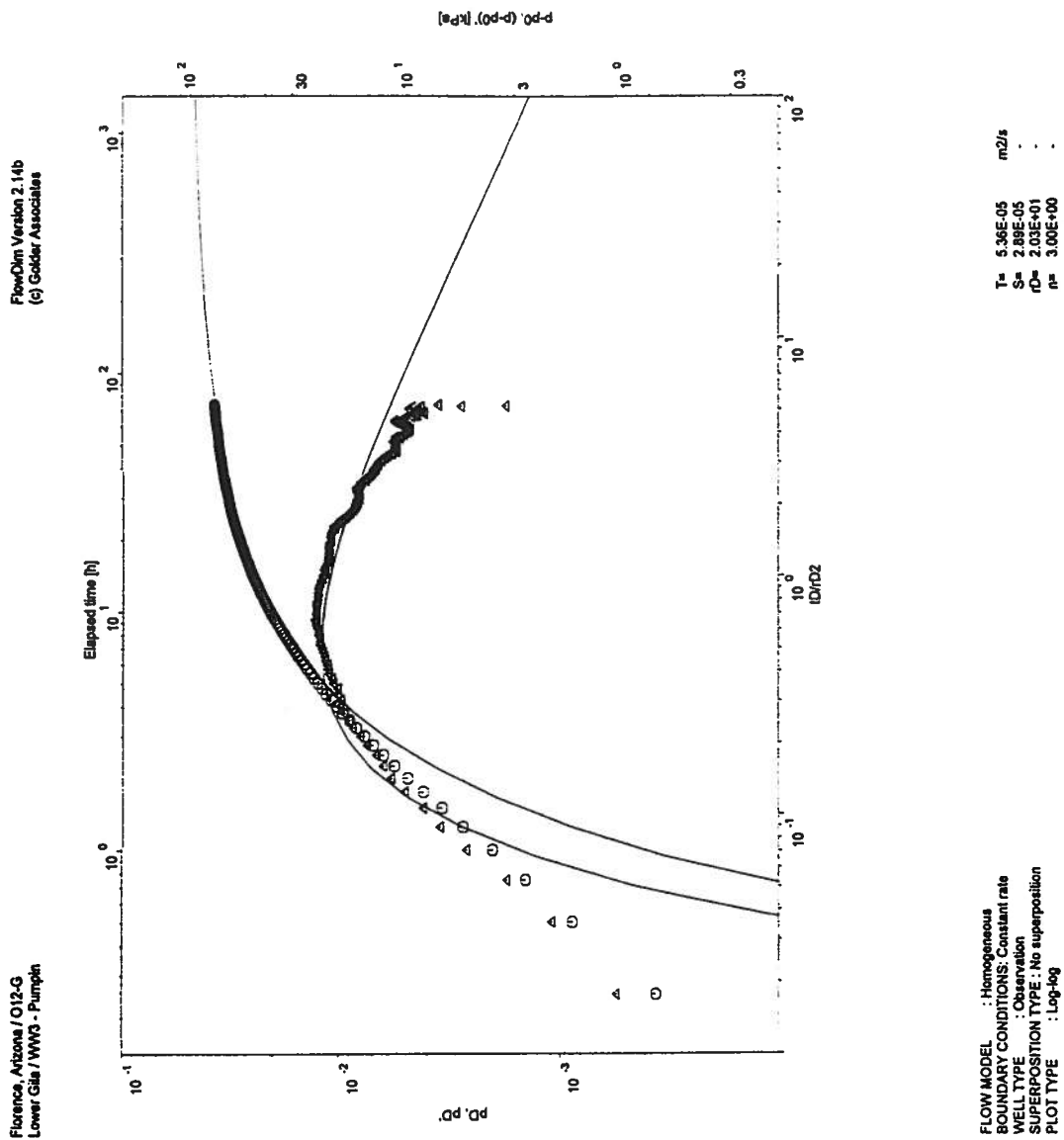


Figure 31V O12-GL (3D) FlowDim™ Analysis Log-Log Plot

Hydraulic Conductivity Calculation for a Cylindrical Source

Well Name:	O3-GL
Sink Radius:	0.2 m
Sink Screened Interval:	211-23 m
Pseudo-Transmissivity:	9.55E-05 m ² /sec
Pseudo-Storage:	5.50E-05
Distance to Sink:	308.2 m
Anisotropy Ratio:	1.00

Pseudo-Spherical Radius:

$r_{sw} = 15.17 \text{ m}$

Hydraulic Conductivity: $6.30\text{E-}06 \text{ m/sec} = 1.78 \text{ ft/day}$

Specific Storage: $8.78\text{E-}09 \text{ 1/m} = 2.68\text{E-}09 \text{ 1/ft}$

Figure 31W O3-GL (3D) FlowDim™ Analysis Summary

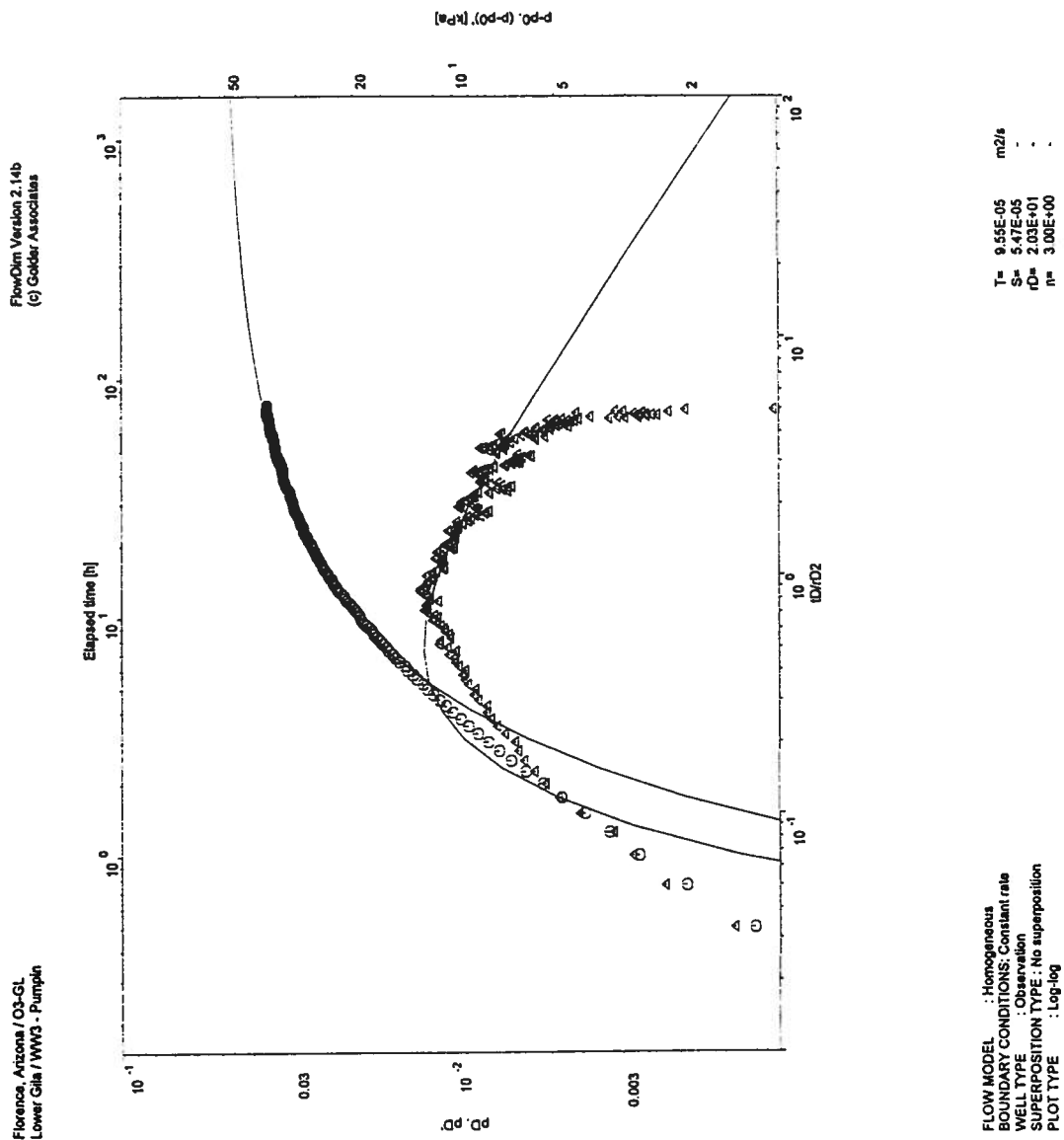


Figure 31X O3-GL (3D) FlowDim™ Analysis Log-Log Plot

Hydraulic Conductivity Calculation for a Cylindrical Source

Well Name:	M14-GL
Sink Radius:	0.2 m
Sink Screened Interval:	211.23 m
Pseudo-Transmissivity:	$7.33\text{E-}05$ m ² /sec
Pseudo-Storage:	$4.10\text{E-}05$
Distance to Sink:	418.7 m
Anisotropy Ratio:	1.00

Pseudo-Spherical Radius:

$r_{sw} = 15.17$ m

Hydraulic Conductivity: $4.83\text{E-}06$ m/sec = 1.37 ft/day

Specific Storage: $3.55\text{E-}09$ 1/m = $1.08\text{E-}09$ 1/ft

Figure 31Y M14-GL (3D) FlowDim™ Analysis Summary

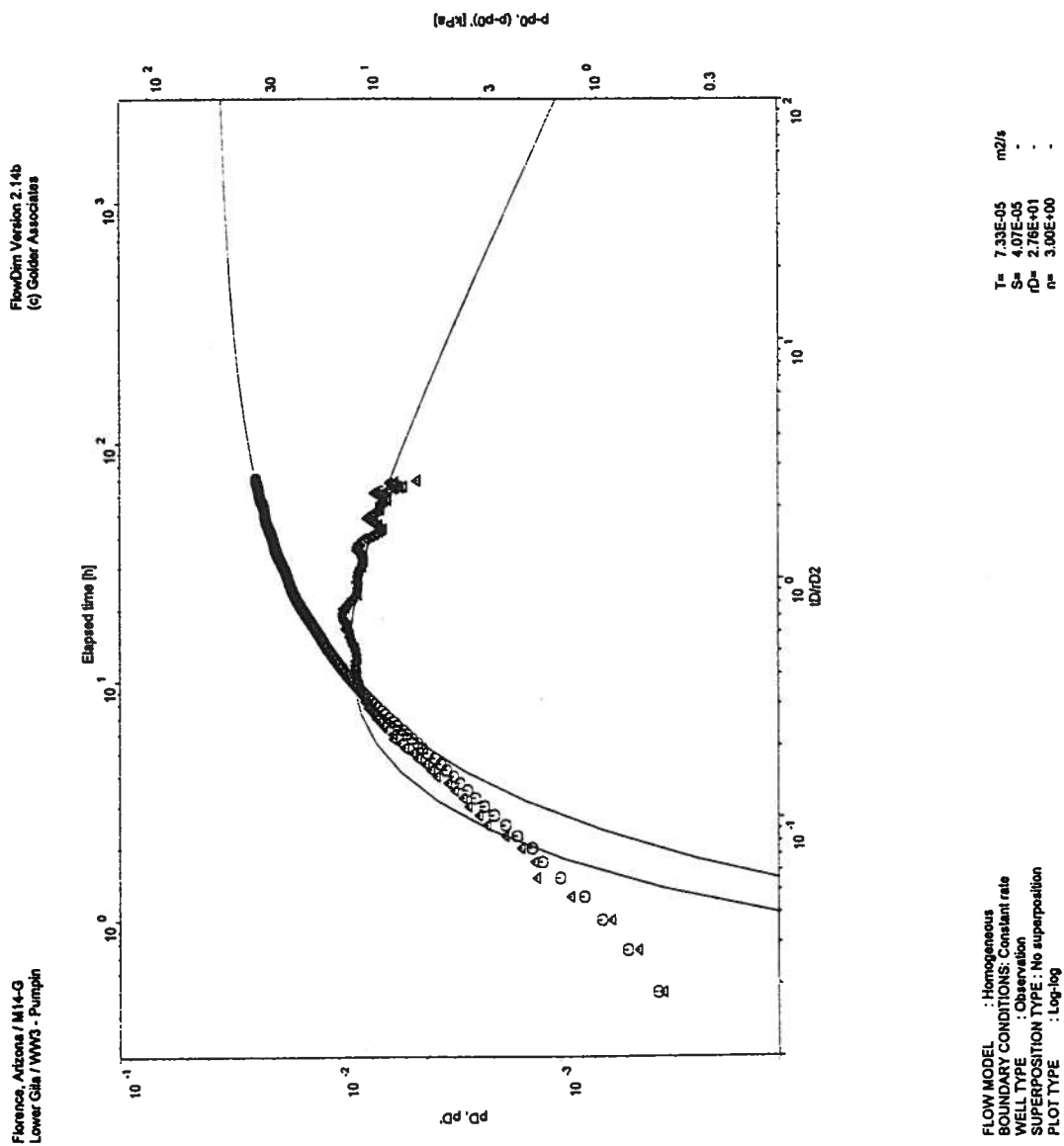


Figure 31Z M14-GL (3D) FlowDim™ Analysis Log-Log Plot

Hydraulic Conductivity Calculation for a Cylindrical Source

Well Name:	O19-O
Sink Radius:	10.2 m
Sink Screened Interval:	211.23 m
Pseudo-Transmissivity:	1.09E-04 m ² /sec
Pseudo-Storage:	4.30E-05
Distance to Sink:	566.7 m
Anisotropy Ratio:	1.00

Pseudo-Spherical Radius:

$r_{sw} = 15.17 \text{ m}$

Hydraulic Conductivity: $7.19\text{E-}06 \text{ m/sec} = 2.04 \text{ ft/day}$

Specific Storage: $2.03\text{E-}09 \text{ 1/m} = 6.19\text{E-}10 \text{ 1/ft}$

Figure 31AA O19-O (3D) FlowDim™ Analysis Summary



Hydraulic Conductivity Calculation for a Cylindrical Source

Well Name:	O19-GL
Sink Radius:	0.2 m
Sink Screened Interval:	2.1123 m
Pseudo-Transmissivity:	1.29E-04 m ² /sec
Pseudo-Storage:	2.10E-05
Distance to Sink:	564.9 m
Anisotropy Ratio:	1.00

Pseudo-Spherical Radius:

$r_{sw} = 15.17 \text{ m}$

Hydraulic Conductivity: $8.50\text{E-}06 \text{ m/sec} = 2.41 \text{ ft/day}$

Specific Storage: $9.98\text{E-}10 \text{ 1/m} = 3.04\text{E-}10 \text{ 1/ft}$

Figure 31CC O19-GL (3D) FlowDim™ Analysis Summary

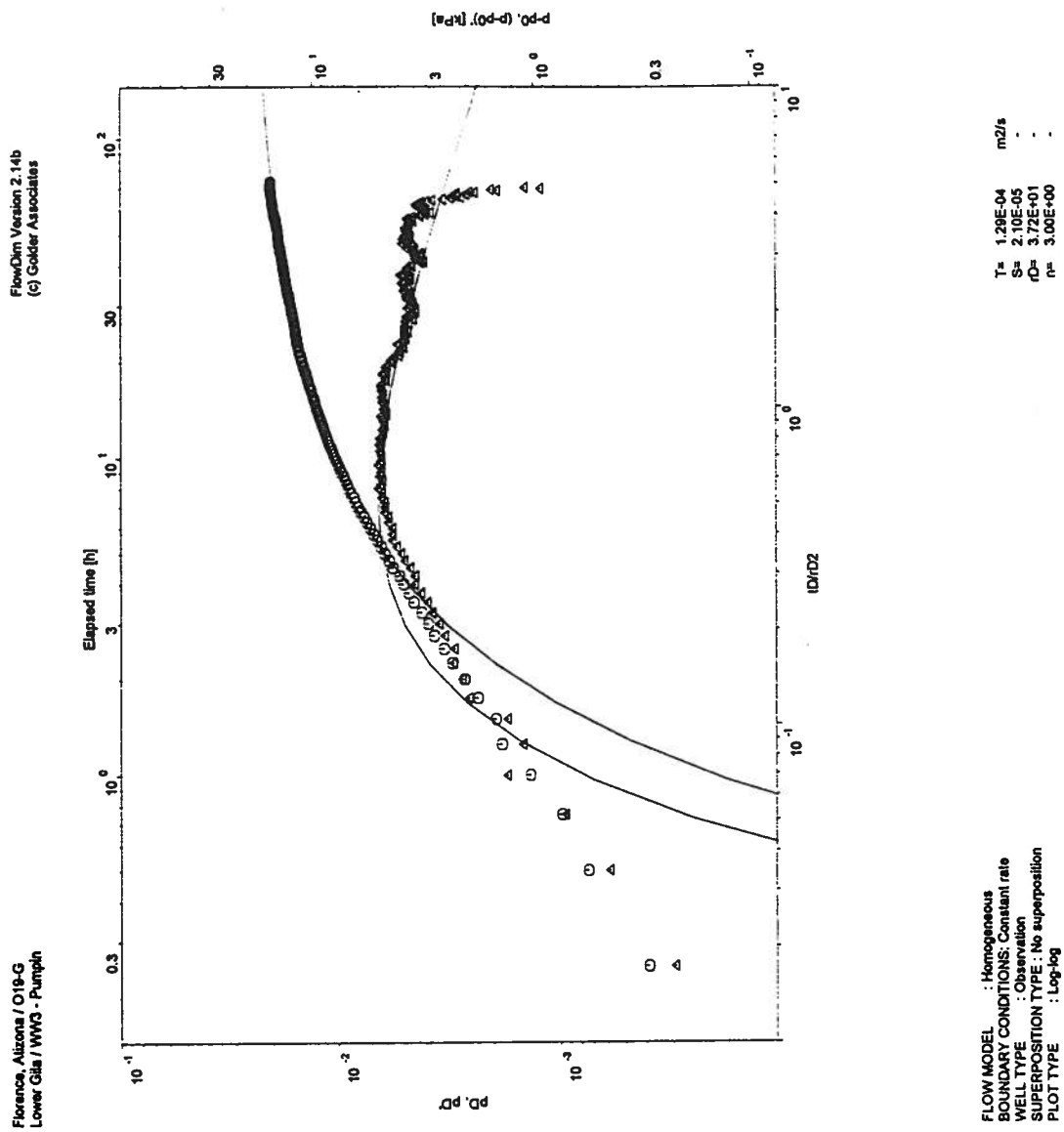


Figure 31DD O19-GL (3D) FlowDim™ Analysis Log-Log Plot

AIR SHAFT

Hydraulic Conductivity Calculation for a Cylindrical Source

Well Name:	AIR SHAFT
Sink Radius:	0.2 m
Sink Screened Interval:	211.23 m
Pseudo-Transmissivity:	$1.04\text{E-}04$ m ² /sec
Pseudo-Storage:	$7.40\text{E-}05$
Distance to Sink:	522.2 m
Anisotropy Ratio:	1.00

Pseudo-Spherical Radius:

$r_{sw} = 15.17$ m

Hydraulic Conductivity: $6.86\text{E-}06$ m/sec = 1.94 ft/day

Specific Storage: $4.12\text{E-}09$ 1/m = $1.25\text{E-}09$ 1/ft

Figure 31EE *AIR SHAFT (3D)* FlowDim™ Analysis Summary

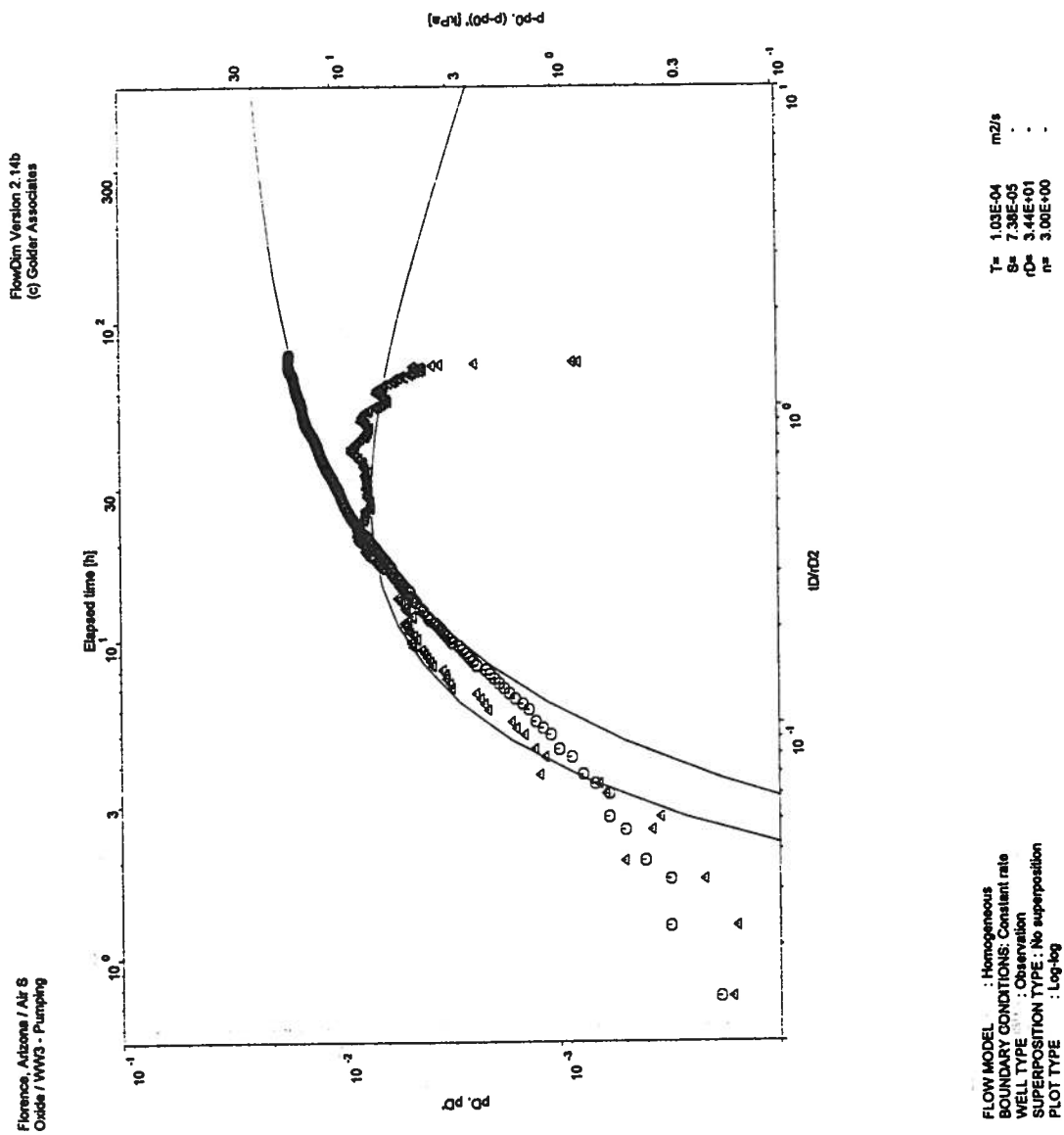


Figure 31FF *AIR SHAFT (3D)* FlowDim™ Analysis Log-Log Plot